Remote control of JAK-STAT signaling through caveolae mechanics

Satish Kailasam Mani

université PARIS-SACLAY

Contrôle à distance de la mechano-signalisation JAK/STAT par les cavéoles

Remote control of JAK/STAT signaling through caveolae mechanics

Thèse de doctorat de l'université Paris-Saclay

École doctorale n°568 : Signalisations et réseaux intégratifs en biologie (Biosigne)
Spécialité de doctorat : aspects moléculaires et cellulaires de la biologie
Unité de recherche : Dynamique et mécanique membranaires de la signalisation intracellulaire (UMR3666/U1143)
Référent : Faculté de médecine

Thèse présentée et soutenue à L'Institut Curie, le 10/12/2021, par

Satish KAILASAM MANI

Composition du Jury

Dr. Philippe CHAVRIER DR-CE, Institut Curie	Président
Asst. prof. Carsten HANSEN University of Edinburgh	Rapporteur & Examinateur
Prof. Jacob PIEHLER University of Osnabrück	Rapporteur & Examinateur
Dr. Lydia DANGLOT CR1, Institut de Psychiatrie et Neurosciences de Paris (IPNP)	Examinatrice

Direction de la thèse

Dr. Christophe LAMAZE DR1, Institut Curie	Directeur de thèse
Dr. Cedric BLOUIN CRCN, Institut Curie	Co-Directeur de thèse

Thèse de doctorat

NNT : 2021UPASL102

"Humility is the surest sign of strength"

- Thomas Merton

ACKNOWLEDGEMENTS

''Focus on the journey, not the destination''… While it applies to all aspects of life in general, being at the culmination of some of the most important (and memorable) years of my scientific career and looking back, I realize that my path towards this point has been filled with some of the most amazing and kind individuals who have helped me overcome obstacles at various points and to whom I would like to offer my humble gratitude.

There's an adage in Indian philosophy that goes by *''Matha, pitha, guru, deivam''* (mother, father, teacher and then only god) which generally translates to respecting and considering your parents and teacher above anything else. Staying true to that, I would like to start by thanking my beautiful family – Amma, Appa, my brother Charan and my beloved wife Nandita. As overprotective as my parents can be at times (cue the Christmas incident that my lab members might recall: D), I can never be thankful enough to my parents for all the support they provided and the sacrifices that they have endured to get me to where I am today. A person whom I have always looked up to and who I aspire to be (but terribly fail) is my brother, Charan and I'm really lucky to have an elder brother such as him who, apart from being a role model of sorts, takes my side always and cares for me more than himself. I feel blessed to have someone like my wife Nandita, who perfectly completes me and has been my pillar over the years. She plays a vital role in maintaining my sanity for the past couple of months and I'm indebted for all the support and understanding that she has offered me. I would also like to thank my second parents (my in-laws) who have been supportive as well.

It goes without saying that this journey wouldn't have been possible without the immense help of my supervisor, Dr. Christophe LAMAZE. I still remember the day I nervously sat for a skype interview with him (back in 2016) for a master's dissertation in

the lab. The excitement and encouragement he showed during the discussion was contagious and something that inspired me. I feel really fortunate to have had a supervisor such as him, who is open and welcoming to new ideas and more importantly believed in my ability to troubleshoot and overcome barriers when things didn't go as planned. I cannot be thankful enough for all that I have learned under his guidance (both professionally and personally) and I'm really grateful for his support throughout my PhD years.

As important a supervisor or a project is, the lab atmosphere plays an equally important role in defining a PhD career and in this regard, I feel fortunate to have been surrounded by outstanding and kind individuals whom I will cherish throughout my life. I would like to start by thanking WeiWei, who welcomed me into the lab and under whose guidance, I spent the initial days of my research. Soft-spoken like me, she played an integral role in helping me get over the intimidation of being away from home for the first time. Very rarely in life, you meet people who are of the same wavelength and mindset as you and this brings me to my brother from another mother – Massi (bhaijaan). Ranging from quirky jokes to philosophical meaningful conversations, the amount of things that we share similar views on is quite astonishing to the level that we both would have been the world's happiest couple if married. Jokes apart, I feel grateful to have encountered an individual such as him and whom I will remember dearly. I say the same for Estelle, whose kindness knows no bounds. Be it offering me a ride during disruptions in the RER B line or the pain au chocolat in the morning whenever I stay the night in the lab, she is one of the sweetest and kindest souls I have come to know.

As many in the lab would agree, things wouldn't run as smoothly without the 'two pillars' of the lab – Christine and Cedric. It was definitely a welcome surprise for me to find a fellow geek in Christine and being my office neighbor, I'm really thankful to her

for all the scientific discussions and help in troubleshooting. Not to mention the engaging discussions on movie plot details (especially the MCU) and gaming advices and recommendations. I'm also grateful to Cedric, the 'chota boss' (junior boss) of the lab, for adopting me towards the latter stage of my PhD. The past few months would have been difficult without his help and I'm really thankful for all his support. I would like to thank Melissa for her ever cheerful presence and more importantly, for awakening the foodie in me by suggesting various cuisines for lunch. I thank Nicolas for laying the foundation of this project and forming an integral part of this thesis and also for his 'refined' sense of humor which served as a stress-buster on hard days. Not forgetting to thank Carlos, our very own spanish chatterbox who likes his fictitious abs more than anything, for introducing me to some fine charcuterie. I'm also thankful to the multi-talented Joanna, ''chocolate is life'' Manon and Vibha who secretly considers the microscopy room as her second home for sharing their experience and help in various aspects. I would also like to thank Changting and Cristian for the good rapport and friendship that we mutually share.

I extend my thanks to our unit director Dr. Ludger JOHANNES for valuable inputs during lab meetings and other members in the lab: Christian, who offers advice on any research topic I approach him with; Ewan for the engaging coffee talks on the dismal life of researchers in general and accompanying me for an interesting semester of French course at the mairie; Alison, who is full of interesting anecdotes and whom I enjoy listening to; Valerie for helping me with whatever I ask her and taking care of the lab resources; and the three new additions to the lab – Debarpan, Akhil and Pamela – who remind me of how I started and the importance of staying curious in science. I would also like to thank past members of the lab whom I had the privilege to engage with: Dhiraj, Stephanie, Daniela, Thomas and Alena.

This thesis would not be complete without the help of our collaborators and I sincerely thank everyone who contributed to this work. I would like to thank Dr. Gregory GIANNONE for hosting me in his lab at IINS, Bordeaux and Dr. Olivier ROSSIER for helping me with single particle tracking experiments. I would also like to thank Filipe for taking time out and teaching me the stretch experiments. dSTORM imaging constitutes an integral part of this work and I extend my sincere thanks to Dr. Cataldo SCHIETROMA from Abbelight™ who took personal interest in the project despite a commercial collaboration and was kind enough to educate me on the intricacies of single molecule localization microscopy (SMLM). In science, a beautiful image has no value if it's not properly analyzed. In this regard, I would like to thank our collaborators Dr. Ivan Robert NABI, Dr. Ghassan HAMARNEH, Ismail KHATER and Ben CARDOEN from Simon Fraser University in Vancouver, Canada for performing 3D SMLM network analysis on our dSTORM data and for the numerous insightful discussions regarding the analysis.

I also offer my sincere gratitude to Dr. Carsten Gram HANSEN, Prof. Jacob PIEHLER, Dr. Lydia DANGLOT, Dr. Philippe CHAVRIER and Dr. Karim BENIHOUD for accepting to be a part of my defense jury. I would like to additionally thank Dr. Carsten Gram HANSEN and Prof. Jacob PIEHLER for the critical reading of my thesis manuscript and suggesting valuable inputs.

As with many things in life, there will be people who indirectly facilitate or make our work easier and I feel that it is important to recognize their contribution. In this regard, I thank all the members of the Laverie for providing and restocking glasswares and basic buffers needed for daily research. I also thank the members the Nikon Imaging center of Institut Curie for maintaining the microscopes, as well as for training me in their proper use and the RPPA platform for performing RPPA and the corresponding data analysis.

I would like to conclude by stating that this is definitely not an exhaustive list of people whom I acknowledge and that I sincerely thank everyone I have encountered and not mentioned here, who have helped me grow into the person I am today and guided me to places that matter.

TABLE OF CONTENTS

LIST OF ABBREVIATIONS

AT1R: Angiotensin 1 receptor

ATP: Adenosine tri-phosphate

BAR: Bin-Amphiphysin-Rvs

BRCA: Breast cancer gene

Ca^{+2}: Calcium

Cav1: Caveolin-1

Cav2: Caveolin-2

Cav3: Caveolin-3

CBM: caveolin binding motif

CD: Circular dichroism

CIE: Clathrin independent endocytosis

CIS: Cytokine-inducible SH2 domain protein

COPII: Coat protein complex II

CRY2: Cryptochrome 2

CSD: Caveolin scaffolding domain

CSFR: Colony stimulating factor receptors

CTD: C-terminal domain

DBD: DNA-binding domain

DGC: Dystrophin-glycoprotein complex

DMD: Duchenne muscular dystrophy

DNA: Deoxy-ribonucleic acid

DR: Disordered region

ECD: Ecto-domain

ECM: Extra-cellular matrix

EGFR: Epidermal growth factor receptor

EHDs: Eps-15 homology domain containing proteins

EM: Electron microscopy

EMT: Epithelial to mesenchymal transition

eNOS: Endothelial nitric oxide synthase

ER: Endoplasmic reticulum

ERES: ER exit site

ERK: Extracellular signal regulated kinase

FAs: Focal adhesions

FBP17: Formin binding protein 17

FERM: Band-4.1, ezrin, radixin, moesin

FLN: Filamins

FNIII: FIbronectin type-III

FPALM: Fluorescence photoactivation localization microscopy

GAS: Growth arrest specific

GDP: Guanosine di-phosphate

GEF: Guanine nucleotide exchange factor

GFP: Green fluorescent protein

GM3: Mono-sialo-dihexosyl-ganglioside

GPCRs: G-protein coupled receptors

GPI: Glycosyl-phosphatidylinositol

GRB: Growth factor receptor-bond protein

GTP: Guanosine tri-phospahate

GTPase: Guanosine tri-phospahatase

HD: Huntington's disease

HDACs: Histone deacetylates

HER2: Human epidermal growth factor receptor 2

HGPS: Hutchinson-Gilford progeria syndrome

HR: Helical region

IFN: Interferon

IFNAR: Interferon-alpha receptor

IFNGR: Interferon-gamma receptor

IL-6: Interleukin-6

ILDs: Interstitial lung diseases

IMD: Intra-membrane domain

IRS: Insulin receptor substrate

JAK: Janus kinase

JH: JAK homology

JNK: JUN N-terminal kinase

LDL: Low-density lipoprotein

LGMD: Limb Girdle Muscular Dystrophy

LIM: Lin-11, Isl-1, and Mec-3

LMPG: Lyso-myrsitoyl-phosphatidyl-glycerol

LOV: Light oxygen voltage

LPPG: Lyso-palmitoyl-phosphatidyl-glycerol

MPT: Multi-proximity threshold

MSCs: Mechanosensitive ion channels

MURC: muscle-related coiled-coil protein

NA: Numerical aperture

NLS: Nuclear localization signal

NMR: Nuclear magnetic resonance

NO: Nitric oxide

NPF: Asn-Pro-Phe

NTD: N-terminal domain

Pacsin: Protein kinase C and casein kinase substrate in neurons protein

PALM: Photoactivated localization microscopy

PC: Phosphatidylcholine

PEST: Proline glutamic acid Serine Threonine

PI3K: Phosphatidyl-inositol 3 Kinase

PIAS: Protein inhibitor of activated STAT

PM: Plasma membrane

PR: Proline rich

PRKCDBP: Protein kinase C delta-binding protein

PRMT1: Protein arginine methyl-transferase 1

PS: Phosphatidylserine

PSF: Point spread function

PtdIns: Phosphatidyl Inositol

PTPs: Protein tyrosine phosphatases

PTRF: Polymerase I and transcript release factor

PV1: Plasmalemmal vesicle protein 1

RESOLFT: Reversible saturable optical fluorescence transitions

RNA: Ribonucleic acid

RTKs: Receptor tyrosine kinases

SB: Src-binding domain

SD: Substrate domain

SDPR: Serum-deprivation-response protein

SH3: Src-homology 3

SIM: Structured illumination microscopy

SMLM: Single molecule localization microscopy

SOCS: Suppressor of cytokine signaling

SOS: Son of sevenless

SR: Serine rich

SRP: Signal recognition particle

STAT: Signal transduction and activators of transcription

STED: Stimulated emission depletion

STORM: Stochastic optical reconstruction microscopy

SUVs: Small unilamellar vesicles

TAD: Transcriptional activation domains

TAZ: Transcriptional coactivator with PDZ-binding motif

TEAD: TEA domain

TGF: Transforming growth factor

TRP: Transient receptor potential

TWIST1: Twist-related protein 1

TYK2: Tyrosine Kinase 2

VAV: Vav guanine nucleotide exchange factor

VEGF: Vascular endothelial growth factor

v-src: Viral tyrosine kinase

WAS: Wiscott Aldrich syndrome protein

YAP: Yes associated protein 1

LIST OF FIGURES

LIST OF TABLES

THESIS SUMMARY

The plasma membrane of most eukaryotic cells possess specialized invaginated lipid nanodomains called caveolae. Like clathrin coated pits, caveolae possess a characteristic coat composed of a suite of essential proteins including caveolins and cavins [Parton and Simons 2007, Parton and del Pozo 2013, Lamaze et al. 2017]. In addition to being implicated in important cellular functions such as transcytosis, lipid homeostasis, endocytosis and signaling, caveolae have been recently shown to demonstrate a protective role in maintaining the integrity of the plasma membrane under conditions of mechanical stress [Sinha et al. 2011]. The caveolar pits act as 'membrane reservoirs' that can flatten out by disassembling their coat and thereby buffer the membrane tension variations resulting from mechanical stress. Following caveolae flattening, caveolins and the caveolar coat proteins are released and this event has been hypothesized to be involved in downstream signal transduction [Nassoy and Lamaze 2012]. The goal of my thesis work was to unravel the precise control of signaling by caveolae mechanics. Here we tried to dissect mechanotransduction through caveolae by elucidating the molecular events underlying the control of JAK-STAT signaling through disassembly of caveolae. Using state-of-the-art super resolution imaging combined with machine-learning network analysis, we show that in response to mechanical stress, caveolae disassemble into so-called smaller scaffolds (also known as non-caveolar caveolin-1 (Cav1) which display increased mobility at the plasma membrane. In addition, we found that Cav-1 negatively regulates JAK1 kinase dependent STAT3 phosphorylation. Furthermore, we revealed the interaction between Cav1 and JAK1 which increases upon an increase in mechanical stress and is mediated by the caveolin scaffolding domain (CSD). Taken together, our results demonstrate that caveolae can act as mechano-signaling

organelles with an ability to remotely control downstream signal transduction from the plasma membrane.

RÉSUMÉ DE LA THÈSE

La membrane plasmique de la plupart des cellules eucaryotes possède des nanodomaines lipidiques invaginés spécialisés appelés cavéoles. Comme les puits recouverts de clathrine, les cavéoles possèdent un manteau caractéristique composé de protéines essentielles comprenant les cavéolines et les cavines [Parton et Simons 2007, Parton et del Pozo 2013, Lamaze et. al 2017]. En plus d'être impliquées dans des fonctions cellulaires importantes telles que la transcytose, l'homéostasie lipidique, l'endocytose et la signalisation, le rôle protecteur des cavéoles dans le maintien de l'intégrité de la membrane plasmique dans des conditions de stress mécanique a récemment été démontré [Sinha et al. 2011]. Les cavéoles agissent comme des « réservoirs membranaires » qui peuvent s'aplatir en démantelant leur manteau protéique et ainsi amortir les variations de tension membranaire résultant des contraintes mécaniques. Après l'aplatissement des cavéoles, cavéolines et leurs protéines d'enveloppe sont libérées et cet événement a été supposé être impliqué dans la transduction du signal en aval [Nassoy et Lamaze 2012]. Le but de mon travail de thèse était de décrypter le contrôle précis de la signalisation par la mécanique des cavéoles. Nous avons donc essayé de disséquer la mécanotransduction cavéolaire en élucidant les événements moléculaires sous-jacents au contrôle de la signalisation JAK-STAT par le désassemblage des cavéoles. En combinant l'imagerie à super résolution à l'analyse de réseaux par apprentissage automatique (machine learning), nous montrons qu'en réponse à un stress mécanique, les cavéoles se fragmentent en assemblages plus petits (également appelés cavéoline-1 (Cav1) non cavéolaires) qui présentent une augmentation de leur mobilité au niveau de la membrane plasmique. En outre, nous avons constaté que Cav-1 régule négativement la

phosphorylation de STAT3 dépendante de la kinase JAK1. De plus, nous avons observé l'interaction entre Cav1 et JAK1 qui augmente lors d'un stress mécanique plus important et qui est médiée par le domaine d'échafaudage de la cavéoline (CSD). L'ensemble de nos résultats démontrent que les cavéoles peuvent agir comme des organites de mécano-signalisation avec la capacité de contrôler à distance la transduction du signal en aval de la membrane plasmique.

PART I

INTRODUCTION

- **Chapter 1: MECHANICS OF CELLS AND TISSUES**
- **Chapter 2: CAVEOLAE - SPECIALIZED PLASMA MEMBRANE NANODOMAINS**
- **Chapter 3: JAK/STAT PATHWAY – 'JACK OF ALL SIGNALING PATHWAYS'**

CHAPTER 1: MECHANICS OF CELLS AND TISSUES

Most decisions that we make in everyday life are based on our ability to probe the mechanical properties of materials and to measure the forces applied on us. We determine ripeness of fruits in part by squeezing them, make inferences about a person by the firmness of their handshake and base our affinity towards certain things by whether they are soft or sticky. These sensory abilities depend on our capacity to simultaneously be aware of stress (force/area) and strain (deformation) when we judge how an object feels or how hard we are pushed or pulled. Likewise, cells appear to be equally sensitive to information about force, stiffness and adhesivity. The range of force and stiffness to which different cell types respond are as individual as their responses to chemical stimuli. It has long been hypothesized that the physical properties of cells are important for their biological function. Over a century ago in 1917, mathematical biologist D'Arcy Wentworth Thompson in his book 'On growth and form', proposed that life forms were envisioned to reflect physics and mathematical principles [Thompson et al. 1917].

Although the importance of mechanical forces in understanding cell and tissue functions was appreciated by embryologists in the 1800s and early 1900s, the molecular biology revolution from the 1960s onwards pushed much of this aside as cell biologists focused on genes and proteins to understand why cells behave the way they do. However, interest in the physics of cells has since been rekindled by evidence from a wide range of studies demonstrating that external forces applied to a cell and the resistance that the extracellular matrix (ECM) exerts on cell-derived forces could generate signals that are as potent as those of chemical stimuli to direct cell growth, survival, differentiation, and function [Ainsworth et al. 2008]. A few examples that demonstrate the importance of forces in preserving biological function are the effects

of shear stress in modulating the morphology and signaling of vascular endothelial cells, loss of bone or muscle mass when gravitational forces are reduced and the ability to promote axonal elongation by applying micro-forces to the tips of the neuronal growth cone [Pita-Thomas et al. 2015]. Hence, a detailed quantitative characterization of the mechanical properties of the cells is required to understand how these forces are transmitted and transduced throughout the cell.

1.1 Force sensing and transduction

Cells may be self-sustaining units of life, but they do not live in isolation. They survive by receiving and processing external information (signals) such as those that pertain to nutrient availability, temperature changes or variations in light levels. In most cases, individual cells receive such signals simultaneously and integrate the information received into a unified action plan. Most signals that cells respond to are chemical in nature. For example, prokaryotes have sensors (receptors) that help them detect nutrients and thereby navigate toward food sources. In multicellular organisms, the many types of chemical signals that cells use include growth factors, hormones, neurotransmitters, and extracellular matrix components.

Cells also possess the ability to respond to mechanical stimuli. Mechanobiology refers to the study of how physical forces (mechanical stimuli) affect cells and tissues, as well as how cell function is controlled by these stimuli by mechanosensing (for e.g. through changes in protein conformation in response to stress). Based on the origin of the force in and on cells, it can be classified into two groups: exogenous and endogenous. Exogenous forces include gravity, compression, stretch, strain, fluid shear, etc. while the latter includes osmotic pressure and cytoskeletal forces. The cellular processes of transducing mechanical signals either through contractile elements of the cells or by converting it into biochemical signals is referred to as **mechanotransduction**. In the

past, research in mechanotransduction was often focused on sensory cells, such as skin cells that respond to touch and hair cells (for e.g. in the inner ear) which have specific cellular structures (ion channels that open/close in response to applied forces) that help transduce mechanical inputs into biochemical signals. Subsequent research has expanded to include diverse cell types such as myocytes, endothelial cells and vascular smooth muscle cells, which show that mechanotransduction is involved in a broad range of cellular functions and not just in a subset of specialized cells and tissues.

At the cellular level, the ECM that surrounds the cell and the linked cytoskeleton act as primary factors in facilitating mechanotransduction and are suggested to transmit local stresses over long distances [Ingber et al. 2005, Wang et al. 2005, Chen et al. 2008]. The manner in which mechanical stimuli are transmitted into the cell is dependent on the coordinated activity of mechanosensors and the subsequent signal integration is influenced by resting tension levels within the cell, which are set by the cytoskeletal system [Chen et al. 2003, Polte et al. 2004, Ingber et al. 2006]. The adaptive cytoskeleton is identical to dense sol-gel networks, which have monomers in solution and polymers coexisting in equilibrium. This characteristic allows the cytoskeleton to deform through assembly or disassembly of its filaments in response to an applied force and shift through different physical forms (i.e. phase transitions) in the absence of a biochemical mechanism [Trepat et al. 2007].

The ability of the cell to modulate its stiffness is vital for maintaining the balance of forces with its surroundings. This determines the elastic nature of the cytoskeleton and so in turn affects a diverse range of cellular processes [Tee et al. 2009]. Currently three models have been widely proposed for the regulation of cytoskeletal stiffness by force:

- Tensegrity: The Tensegrity model is the more predominant model that is often associated with mechanosignaling. According to this model, pre-existing tension

within the architecture of both the cytoskeleton and the extracellular matrix (ECM) determines cytoskeletal rigidity upon the application of load (stress), such that stress is proportional to rigidity (Figure 1A). This model assumes that the cytoskeleton acts as a network of tensed cables interspersed by soft cellular material [Ingber et al. 1993, Ingber et al. 2003, Wirtz et al. 2009]. These cables tense and pull in response to an applied force in order to regain cellular stability.

- Semi-flexible chain: On the assumption that the acto-myosin filaments are distributed uniformly throughout the cell, this model states that the filaments are non-linearly elastic (similar to cytosol) and stiffen under stress. Hence, acto-myosin filaments can be defined as semi-flexible structures, which are suggested to respond to force isotopically i.e. uniformly throughout their structure irrespective of the directionality of the force applied (Figure 1B) [Gardel et al. 2004, Storm et al. 2005, Koenderink et al. 2009].
- Dipole polarization: On a similar assumption that the acto-myosin filaments are distributed uniformly throughout the cell, this model states that upon the application of force, the elastic filaments form dipoles. These dipoles propagate force through the cytoskeletal network through polarization and subsequent pulling on the filaments in direction-dependent manner (Figure 1C). Hence, acto-myosin filaments are suggested to respond to force anisotropically i.e. differentially throughout their structure dependent on the direction of the force applied [Zemel et al. 2006, Zemel et al. 2009].

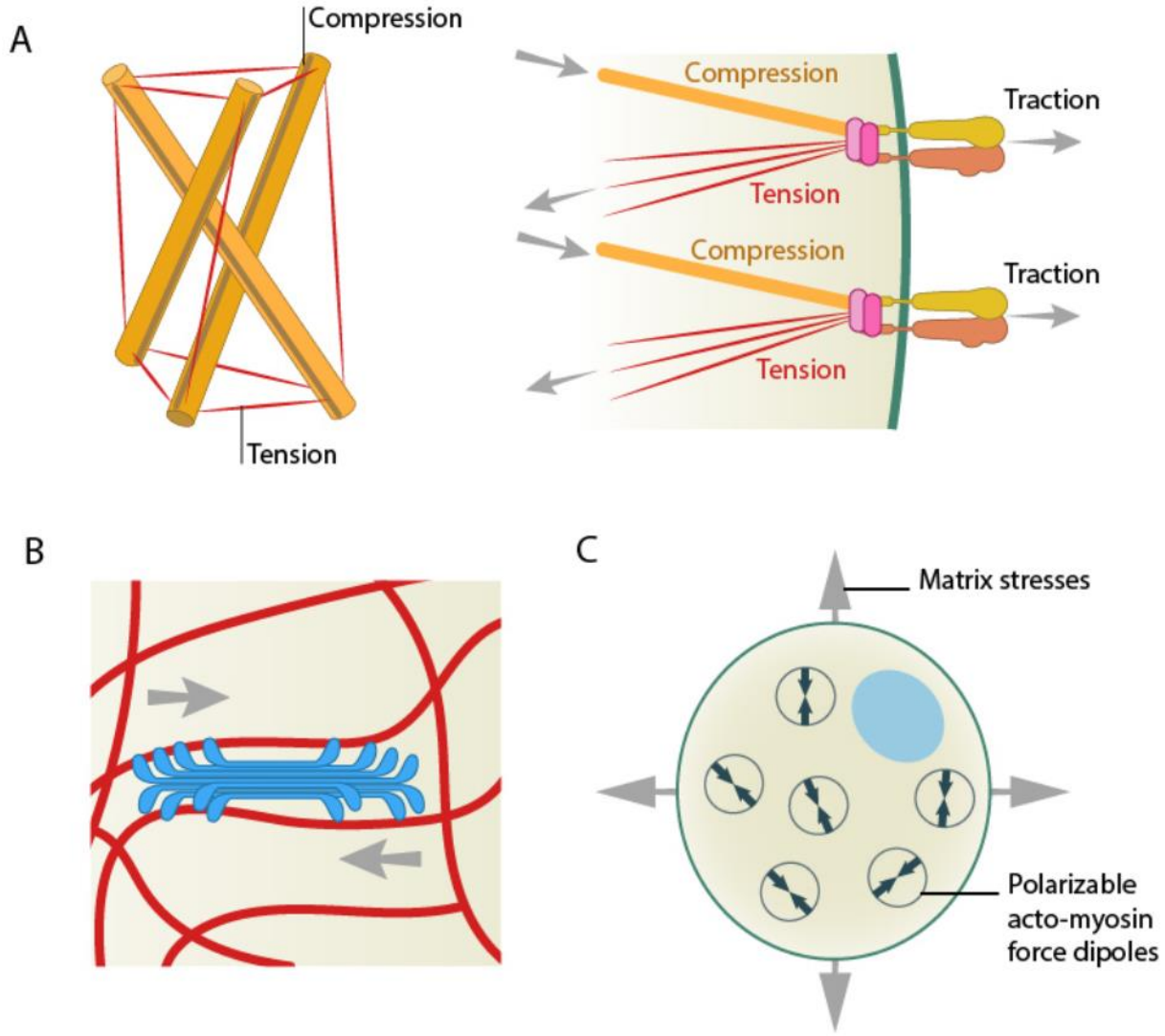

Figure 1: Models for force-induced modulation of cytoskeletal stiffness

(A) Tensegrity model: (Top left) A simplified version with compression struts and tensed cables demonstrating that stress levels regulate cytoskeletal rigidity. (Top right) In the cellular context, microtubules (gold) apply compression on cell-matrix adhesions (represented by actin linking modules in pink and integrin dimers) while the actin filaments (red) experience the cellular tension and hence stiffen accordingly. **(B)** Semiflexible chain model is represented by the flexible actin cables (red) that locally rigidify at points of stress application i.e. myosin (blue bundle) contraction. **(C)** Dipole polarization model: Formation of contractile actomyosin dipoles is symbolically represented by the arrow pairs. According to this model, they freely orient in response to applied stress as experienced at a particular point. [From www.mechanobio.info]

1.2 Mediators of mechanotransduction:

Mechanosensation requires by definition an element that responds to an applied force, without necessarily being triggered by a specific chemical stimulus. In general, the application of force on an object can result in two different outcomes depending on whether the object is attached to another structure or not. If unattached to anything else, an applied force will result in acceleration as seen in the case of free flowing cells in the blood stream. With the exception of such freely suspended cells, most cells are in contact with one another or with the ECM to form tissues. If an object, such as the cell, is attached to another structure or surface, an applied force results in stress which can lead to a mechanical distortion, presented as a morphological and/or structural change (Figure 2A).

Bioactive molecules have extended and contracted forms, structural rearrangements, and nanoscale variations in their motion in living systems [Ingber et al. 1997, Khan et al. 1997]. In this regard, mechanosensory molecules (mechanosensors) have a broad set of structural regions or motifs that can be altered over a range of mechanical forces [Vogel et al. 2006, Vogel and Sheetz 2006]. In addition to the cytoskeleton itself acting as a mechanosensor (as discussed in section 1.1), others include ECM molecules, transmembrane proteins, proteins at the membrane-phospholipid interface, elements of the nuclear matrix, chromatin, and the lipid bilayer itself (Figure 2B). Below, we discuss a few examples of well-known mediators of force transduction.

1.2.1 Mechanosensitive ion channels (MSCs):

Mechanosensitive ion channels (MSCs) form a special group of mechanosensors that can serve as both sensors and effectors as they modify the electrical potential of the cell and mediate a flux of ions across the plasma membrane (PM). They are directly

A

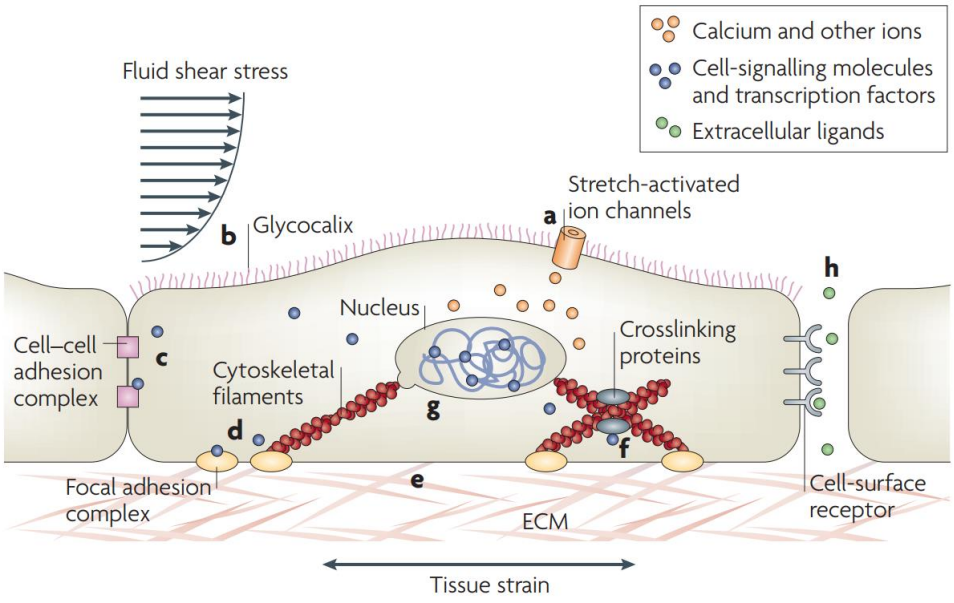

B

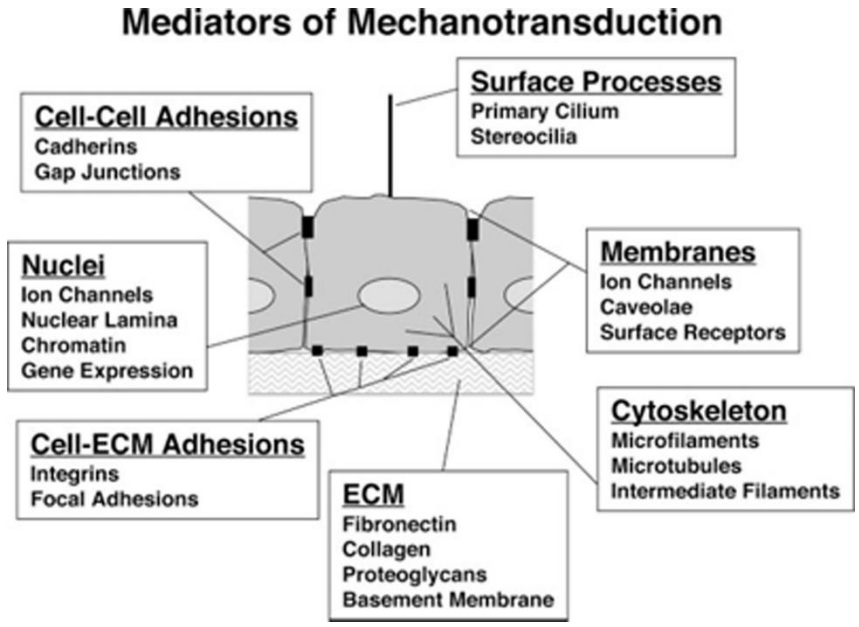

Figure 2: Mediators of cellular mechanotransduction

(A and B) Many molecules, cellular components, and extracellular structures have been shown to contribute to mechano-chemical transduction. These transduction elements include ECM, cell-ECM, and cell-cell adhesions, membrane components, specialized surface processes, cytoskeletal filaments, and nuclear structures. It is still not yet entirely understood how cells orchestrate all these transduction mechanisms in the context of living tissue anatomy to produce a concerted response to mechanical signals [From Ingber et al. 2006, Jaalouk and Lammerding 2009].

activated by stresses applied to the lipid bilayer or its associated non-membrane components and transduce external mechanical force into electrical and/or chemical signals. MSCs appear to be present in all types of animal cells, including red blood cells [Vandorpe et al. 2010]. Below are a few examples of some well-known mechanosensitive ion channels:

TRP channels: Transient receptor potential (TRP) channels are present in all cellular membranes with the exception of the nuclear envelope and mitochondria and play an essential role in the influx of Ca^{+2}, Mg^{+2} and trace metal ions, thereby modulating the membrane potential [Nilius et al. 2011]. For example, shear stress and force applied directly to the cell–matrix or cell–cell adhesions locally activate TRP channels by interacting with adhesion molecules such as integrins. Subsequent Ca^{+2} influx affects cell–matrix and cell–cell adhesion turnover by regulating cytoskeletal contractility.

2P domain K^+ channels: The six classes of 2P domain K^+ channels are mechano-gated and the transmembrane segments (along with some COOH-terminal tail fragments) play an essential role in the mechanosensitivity [Patel et al. 1998, Patel et al. 2001, Enyedi et al. 2010, Mirkovic et al. 2012]. Mechanical force may be transmitted directly to the channel via tension from the lipid bilayer or possibly by direct mechanical links to the cytoskeleton. The opening of these channels by membrane stretch hyperpolarizes thereby decreasing neuronal excitability [Honore et al. 2007].

Piezo channels: Piezo proteins are pore-forming subunits of ion channels that allow positively charged ions, including calcium, to flow into the cell in response to mechanical stimuli. Most vertebrates possess two isoforms, Piezo1 and Piezo2 and are very large proteins (2521 and 2752 amino acids for human Piezo1 and human

Piezo2 respectively) with more than 14 predicted transmembrane domains per subunit [Coste et al. 2010]. Piezo proteins form tetramers to generate functional channels [Xiao et al. 2010]. Piezos comply with the many requirements for truly mechanically activated ion channels, as they are pore-forming subunits, confer mechanically-activated currents when expressed in a heterologous system, and are essential for mechanical responses in many cells [Coste et al. 2012]. However, the intrinsic mechanosensing ability of Piezos are yet to be demonstrated as evidence that Piezos undergo mechically-induced (rather than spontaneous or chemically-induced) openings in a purified lipid bilayer is lacking.

A global knockout of Piezo1 in mouse is lethal during midgestation, owing at least in part to disrupted development of the vasculature system [Li et al. 2014, Ranade et al. 2014]. Consistent with these phenotypes, Piezo1 senses shear stress and cell volume in red blood cells and vascular endothelial cells, and mediates stretch-activated currents in other flow-sensitive cells, including renal epithelial and bladder urothelial cells [Peyronnet et al. 2013, Miyamoto et al. 2014]. In addition, the involvement of Piezo1 in cell motility may explain the link between increased Piezo1-mediated activity in the breast cancer line MCF-7 and reduced survival rates in patients with increased Piezo1 mRNA levels in the primary tumor [Li et al. 2014]. Similar to Piezo1, a global knockout of Piezo2 in mouse is lethal, with pups dying at birth [Ranade et al. 2014]. Several tissue-specific conditional knockout lines have shown that Piezo2 mediates responses to light, but not harsh mechanical touch [Maksimovic et al. 2014, Woo et al. 2014]. Intriguingly, the primarily sensory-specific roles of Piezo2 have not yet been reconciled with the lethal phenotype of the global knockout, indicating that there must be additional functions not yet identified.

1.2.2 Intracellular mechanosensitive proteins:

p130Cas: p130Cas acts as a primary force-sensor and is involved in various cellular events such as migration, survival, transformation, and invasion. The domains of p130Cas include Src-homology 3 (SH3) domain, the proline-rich region (PR), the substrate domain (SD), the serine-rich region (SR), the Src-binding domain (SB), and the C-terminal region. The mechanical stretch experienced by the cell, such as shear stress from blood flow, or cytoskeletal stretch in spreading cells, extends p130Cas and increases exposure of the YxxP repeats within the p130Cas substrate binding domain, structurally priming these sites for tyrosine phosphorylation [Sawada et al. 2006]. Crk adaptor proteins then bind the phospho-tyrosine residues within the YxxP motifs and link p130Cas to downstream effectors. This process of signal transduction brings about changes in the actin cytoskeleton to facilitate cell motility for migration and invasion [Brugnera et al. 2002, Gustavsson et al. 2004, Radha et al. 2011]. In addition, p130Cas functions as a mechanosensor via interaction with integrins. The generally short non-catalytic cytoplasmic domains of integrins associate with adaptor proteins, including p130Cas, to transduce outside-in signaling from the ECM [Giancotti et al. 1999].

Filamin: Filamins (FLN) are conserved, modular, multi-domain cytoplasmic proteins that serve as mechanosensors. In non-muscle cells, filamins colocalize with F-actin along the leading edge and along stress fibers at the cell cortex. Filamins are also enriched at the trailing ends of mature focal adhesions and concentrates in adhesion sites in response to force application [Glogauer et al. 1998, Stossel et al. 2001, Nakamura et al. 2011]. Filamins provide a mechanical link between the ECM, the plasma membrane, and the actin cytoskeleton and are involved in cross-linking and anchoring actin filaments, regulating actin cytoskeleton remodeling, stabilizing

the plasma membrane, thereby contributing to the mechanical stability of the cell cortex [Nakamura et al. 2007, Razinia et al. 2012]. In addition, filamins are important for tuning cellular responses to ECM stiffness and other mechanical forces [Gehler et al. 2009].

Zyxin: Zyxin is a member of the LIM domain protein family that has been implicated in the modulation of cell adhesion and motility, and might have mechanosensing roles in integrin-mediated responses to force. LIM domain proteins possess two distinct motifs: a proline-rich N-terminal region containing an unclear export signaling sequence and a C-terminal region consisting of three LIM domains (termed by the initials of Lin-11, Isl-1, and Mec-3) [Beckerle et al. 1997, Smith et al. 2014]. Zyxin mainly localizes to focal adhesions (FAs), but it may translocate to actin stress fibers in response to certain stimuli and cause a relaxation of cytoskeletal stress allowing zyxin to dissociate from FAs into the cytosol. In addition, zyxin possesses an N-terminal nuclear transport signal and has been postulated to shuttle between focal adhesion sites and the cell nucleus as a way of mediating protein expression changes that accompany cellular mechano-transduction [Nix et al. 1997, Hervy et al. 2006, Wang et al. 2019, Sun et al. 2020].

1.2.3 Membrane mechanosensors:

Here we discuss a couple of mechanosensitive proteins and structures at the plasma membrane that usually link the outer extracellular membrane with intracellular structures such as the cytoskeleton or initiate a signaling cascade in response to mechanical stimuli.

Integrins: Integrins are expressed on almost all cell types in a widely varying pattern. They enable adhesion, proliferation, and migration of cells by recognizing binding motifs in extracellular matrix proteins. Of all the mechanosensors, integrins not only

sense the mechanical stimuli, but is also the only one that presents specificity for ligands. Structural and molecular studies have indicated that integrin adhesions associate with the actin cytoskeleton. As transmembrane linkers between the cytoskeleton and the ECM, they are able to recruit a large variety of proteins and influence signaling pathways bi-directionally, affecting regulation of gene expression and cell survival [Geiger et al. 2009, Geiger et al. 2011, Schiller et al. 2013]. In combination with downstream intracellular mechanosensitive proteins such as talin and vinculin, integrins play an important role in mediating a plethora of signaling cascades involved in regulating cell polarity, adhesion, survival and migration [Schwartz et al. 2002, Hu et al. 2013, Massou et al. 2020].

Primary Cilium: The primary cilium is observed in many cell types including renal tubular epithelia where it functions both as a mechanosensor and a chemosensor. The primary cilium has a so-called 9 + 0 axoneme, which refers to its nine peripherally located microtubule pairs and the absence of the central microtubule pair seen in 9 + 2 cilia [Poole et al. 1997]. In renal tubular epithelia, the primary cilium acts as a flow sensor using proteins polycystin 1 and 2. Fluid shear force or direct bending of the primary cilium causes a calcium (Ca^{+2}) influx, which can spread from the stimulated cells to its neighbors by diffusion of a second messenger through gap junctions, leading to the downstream physiological effects [Praetorius et al. 2003]. Similarly, in chondrocytes, the primary cilium plays a role of detection and transmission of mechanical stimulation, where mechanical loading bends the primary cilium and activates Ca^{+2} influx. In addition, the primary cilium also serves as a mediator of many signaling pathways that are involved in mechanotransduction in the chondrocyte, including integrins and ion channels [Muhammad et al. 2012, Nguyen et al. 2013].

G-protein coupled receptors: In addition to neuro-hormonal signaling, G-protein coupled receptors (GPCRs) have been demonstrated to play a role in mechanotransduction. The Gq/11-coupled angiotensin II AT1 receptor (AT1R) was the first GPCR claimed to be a mechanosensor in cardiac cells and smooth muscle cells [Zou et al. 2004]. Mechanical stress such as an increase of intravascular pressure, exerts a stretch force on the membrane leading to depolarization of the membrane potential and also induces conformational changes and activates GPCRs. This causes an increase in the probability of opening of voltage-gated calcium channels, resulting in calcium entry and an elevation of the free intracellular Ca^{+2} concentration leading to force development, cell shortening and vasoconstriction [Mederos y Shnitzler et al. 2008, Voets et al. 2009, Hu et al. 2021].

1.3 Clinical relevance of mechanosensing:

A common denominator of many mechanobiology diseases is a disruption in the force transmission between the ECM, the cytoskeleton and the interior of the nucleus. Cellular mechanosensing is often based on force-induced conformational changes in mechanosensitive proteins that are subjected to molecular forces. In addition to the defects that affect cellular structure and organization, mutations in proteins that are involved in the downstream signaling pathways can also cause impaired mechanotransduction. In general, any changes in cellular/extracellular structure, the mechanosensing process itself or in subsequent downstream signaling pathways can result in altered and abnormal mechanotransduction and lead to disease (Table 1). Identifying the molecular events that are involved in normal and defective mechanotransduction will help us better understand the underlying disease mechanisms and normal cellular function leading to revised therapeutic approaches for these diseases (Figure 3). The following sections offer a few examples of how

mutations or modifications that impair mechanotransduction and cellular sensitivity to mechanical stress could be implicated in a wide spectrum of diseases.

1.3.1 Cardiac hypertrophy

More than 400 different mutations affecting 9 separate sarcomeric genes encoding actin, α-tropomyosin, troponin, titin and, most commonly, β-myosin heavy chain have been identified in patients with cardiomyopathy [Barry et al. 2008]. Stress-sensitive cellular components such as MSCs at the cell membrane, integrins and integrin-associated proteins, sarcomeric proteins and cell surface receptors (such as GPCRs) act as mechanosensors and activate multiple cellular signaling pathways that trigger the expression of hypertrophic genes and cause an increase in myocyte length/width. This allows the heart to adapt to prolonged changes in the mechanical workload with an increase in cardiac myocyte size (hypertrophy) and modification of the surrounding ECM, referred to as cardiac remodeling. [Heineke et al. 2006, Barry et al. 2008, Perestrelo et al. 2021]. The cardiac hypertrophic response is often categorized into physiological or pathological hypertrophy. Physiological hypertrophy, which arises as a consequence of aerobic exercise or pregnancy, is characterized by the addition of sarcomeres in series and in parallel, resulting in increased cardiac wall thickness and chamber dimensions to accommodate the elevated load. In contrast, pathological hypertrophy is caused by abnormal changes in the cardiac workload, for example through hypertension, aortic stenosis, myocardial infarction or by congenital defects that are due to mutations in genes that encode sarcomeric proteins [McMullen and Jennings 2007]. Several lines of evidence suggest that hypertrophy can further destabilizecardiac mechanics, as hypertrophic tissue is often characterized by

Table 1: Diseases associated with defects in mechanotransduction

Disease	Primary cells/tissues affected
Deafness	Hair cells in the inner ear
Arteriosclerosis	Endothelial and smooth muscle cells
Muscular dystrophies and cardiomyopathies	Myocytes, endothelial cells and fibroblasts
Osteoporosis	Osteoblasts
Axial myopia and glaucoma	Optic neurons and fibroblasts
Polycystic kidney disease	Epithelial cells
Asthma and lung dysfunction	Endothelial cells and alveolar tissue
Premature ageing (HGPS)	Multiple cell types and tissues
Developmental disorders	Multiple cell types and tissues
Cancer	Multiple cell types and tissues
Potential immune system disorders	Leukocytes
Potential central nervous system disorders	Neurons

[From Jaalouk and Lammerding 2009]

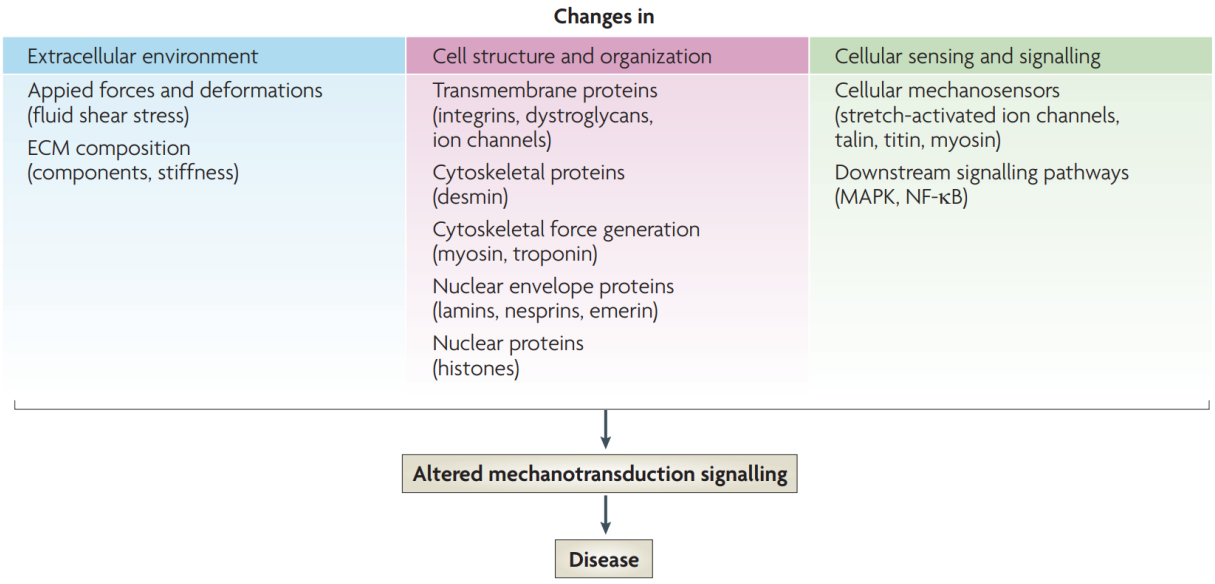

Figure 3: Unifying characteristics of mechanotransduction disorders

Altered cellular mechanotransduction signaling can be caused by changes in the extracellular environment such ad variations in the mechanical forces or deformations that are experienced by the tissue, or changes in extracellular matrix (ECM) composition that affect its stiffness and biochemical properties or the elements of the mechanotransduction process itself. Changes in cellular structure and organization often result from inherited or de novo mutations in proteins that are part of the force-generating machinery, the cytoskeletal network or the nuclear envelope and interior. This also includes transmembrane proteins that are involved in cell–cell or ECM–cell adhesion. Abnormal function of these proteins can alter the intracellular force distribution and thus mechanotransduction signaling [From Jaalouk and Lammerding 2009].

impaired contractility and relaxation dynamics. In addition, the cellular program that is responsible for pathological hypertrophy, results in the re-expression of genes that are normally associated with the embryonic myocardium. This causes disorganized cellular structure, impaired calcium dynamics and increased interstitial fibrosis, worsening the mechanical imbalance between cardiac function and hemodynamic load [Palmer et al. 2005].

1.3.2 Muscular dystrophy

In muscle cells, the sarcomeres protect the cell membrane from excessive stress by transmitting the force generated to the ECM through a specialized protein complex at the plasma membrane consisting of dystrophin and the dystrophin-associated protein complex. Mutations in the dystrophin gene disrupt force transmission between the cytoskeleton and the ECM resulting in Duchenne muscular dystrophy, a case of progressive muscle degeneration [Heydemann et al. 2007]. Importantly, the disruption of cytoskeletal–ECM coupling not only renders cells more susceptible to membrane damage, but also causes aberrant activation of MAPK extracellular signal regulated kinase 1 (ERK1) and ERK2 signaling in response to stretch [Kumar et al. 2004]. In addition, stress-induced rupture of the fragile plasma membrane allows influx of extracellular calcium causing abnormal muscle contraction thereby resulting in physical damage of the cytoskeleton and subsequently leading to loss of muscle cells [Claflin et al. 2008]. Dystrophin is also involved in the fluid shear-stress-mediated dilation of arteries in endothelial cells. For example, endothelial cells from dystrophin-deficient mice demonstrate impaired mechanotransduction in response to fluid shear stress, resulting in reduced dilation of arteries and vascular density in cardiac muscles further contributing to the progressive loss of muscle [Loufrani et al. 2004].

Similarly, mutations in the cytoskeletal proteins such as desmin, titin and myosin, which are important sarcomere components, result in disorganized sarcomeres and perturbed cellular mechanics. This results in impaired force generation and altered cytoskeletal stiffness affecting the relaxation dynamics of myocytes. The deleterious effects of these mutations can result from direct changes in intracellular force distribution and/or generation due to ultrastructural disorganization, but can also arise from downstream effects of altered cellular mechanosensing, as myosin and titin can function as mechanosensors [Hoshijima et al. 2006, Greenberg et al. 2016, van der Pijl et al. 2018]. Recent findings that muscular dystrophies can arise from mutations in nuclear envelope proteins (such as lamins A and C, emerin or nesprins) further highlight the importance of error-free force transmission and mechanotransduction. Cells from model animals suffering from Emery–Dreifuss muscular dystrophy are characterized by decreased nuclear stiffness, increased nuclear fragility and impaired activation of mechanosensitive genes resulting in decreased viability of cells subjected to repetitive strain [Lammerding et al. 2004].

1.3.3 Development and premature ageing

There is mounting evidence that mechanotransduction plays a crucial role in development [Hove et al. 2003, Moore et al. 2005, Lecuit et al. 2007, Kreig et al. 2008]. A classic example is Kartagener's syndrome, which is characterized by a left-right reversal of the primary visceral organs. In early mammalian embryos, left-right patterning is dictated by cilia-driven leftward fluid flow during gestation, which - through mechanotransduction signaling - differentially induces expression of a transforming growth factor (TGF)-family molecule called nodal, in addition to a cascade of other factors in the left side of the embryo. Mutations in the dynein motor proteins block cilia motion in the epithelium of a midline node in the embryo

thereby preventing the leftward fluid flow, the absence of which results in random left–right patterning leading to Kartagener's syndrome.

Perturbed mechanotransduction can also underlie several diseases that are not traditionally approached from a biophysical perspective. One such example is Hutchinson-Gilford progeria syndrome (HGPS), a progeroid disorder that is caused by mutations in the gene encoding lamin A. Patients with HGPS appear normal at birth, but die in their early teens mainly due to arteriosclerosis [Al-Shali et al. 2004, Tran et al. 2020]. Mechanotransduction in vascular cells in response to fluid shear stress and strain from vessel expansion is a crucial protective mechanism against arteriosclerosis and can mediate apoptosis, proliferation and ECM secretion in healthy vascular smooth muscle cells [Davies et al. 1995, Zhou et al. 2014]. Analysis of vascular tissue from patients and mouse models with HGPS have revealed extensive loss of vascular smooth muscle cells and an unusual susceptibility to hemodynamic stress [Stehbens et al. 2001, Capell et al. 2007]. In addition, fibroblasts from patients with HGPS show decreased viability when subjected to repetitive mechanical strain suggesting that cells from patients with HGPS lack the strain-induced proliferation response that is seen in cells from healthy controls [Verstraeten et al. 2008].

1.3.4 Cancer

In the past decade, a wealth of knowledge on ECM mechanics, ECM remodeling and the resultant disturbance in cytoskeletal tension and mechanotransduction signaling have provided new insights into factors that can promote malignant transformation, tumorigenesis and metastasis [Huang et al. 2005, Wolf et al. 2007, Suresh et al. 2007]. In addition to genetic mutations and increased oncogene activity, cytoskeletal reorganizations (such as those induced by changes in the force

generated by the acto–myosin apparatus of the cell) play a pivotal role in the development of invasive phenotypes of tumor cells. The Rho family of GTPases are key regulators of cytoskeletal tension and although studies on Rho activity in tumors have yielded contradictory results (some supporting the notion that tumors have increased Rho activity thereby exhibiting more cytoskeletal tension whereas others reported decreased Rho activity in solid tumors), it has become apparent that cytoskeletal tension significantly impacts signaling pathways that are implicated in cancer progression [Clark et al. 2000, Sahai et al. 2002, Horiuchi et al. 2003, Lozano et al. 2003, Sahai et al. 2003, Burridge et al. 2004, Burridge et al. 2016, Messal et al. 2019].

Several studies have shown that ECM stiffness influences cytoskeletal tension in tumors [Paszek et al. 2005, Huang et al. 2005, Deville et al. 2019]. Tumors are generally much stiffer than the surrounding normal tissue and simultaneous changes in tissue stiffness, tumor growth and/or elevated interstitial fluid pressure together affect the physical environment of cancerous cells inside tumors and the adjacent normal cells [Sarntinoranont et al. 2003, Wu et al. 2013]. Matrix stiffness (exogenous force) and cytoskeletal tension (endogenous force) cooperate in a 'mechano-circuit' that modulates phenotypic transformations in tumors by coupling the mechanosensing role of integrins in relaying external physical cues to Rho and ERK signaling pathways (Figure 4). As an example, higher ECM stiffness disrupts normal epithelial cell polarity causing mammary epithelial cells to fill the cystic lumens in breast cancer [Paszek et al. 2005]. Hence, an altered physical environment can modulate the fate of these cells through mechanotransduction [Mierke 2019].

With the exception of hematopoietic cells, all cells are dependent on their ability to adhere to a solid substrate for normal cell-cycle progression and survival. However, cancer cells lose this dependency as they develop a metastatic phenotype [Huang et al. 1999, Wang et al. 2000, Hanahan and Weinberg 2011]. This hallmark of metastatic cells i.e their ability to break through the basal lamina, infiltrate blood vessels, extravasate and form new tumors, requires precise biomechanical interactions and adaptations between the cancer cell and its extracellular environment. Metastatic cells can be distinguished from noninvasive cancer cells and normal cells by reduced cytoskeletal stiffness and increased deformability [Guck et al. 2005, Suresh et al. 2007, Cross et al. 2007]. Cell deformability has been proposed to strongly correlate with the passage time through narrow pores and with increased metastatic potential in mouse melanoma cells [Ochalek et al. 1998, Xiao et al. 2018]. Hence, increased cellular and nuclear deformability can enable the passage of metastatic cancer cells through size-limiting pores and blood vessels, resulting in enhanced metastasis.

Clearly, cancer is not exclusively caused by defective mechanotransduction signaling, as several other factors including deregulation of cell cycle control, defects in DNA-damage repair, suppression of apoptosis and altered adhesion and/or migration contribute to this multifaceted disease. However, many of the cellular functions that are involved in tumorigenesis and metastasis are modulated by mechanotransduction. Hence, altered mechanotransduction signaling may be an important component in tumor formation and metastatic progression.

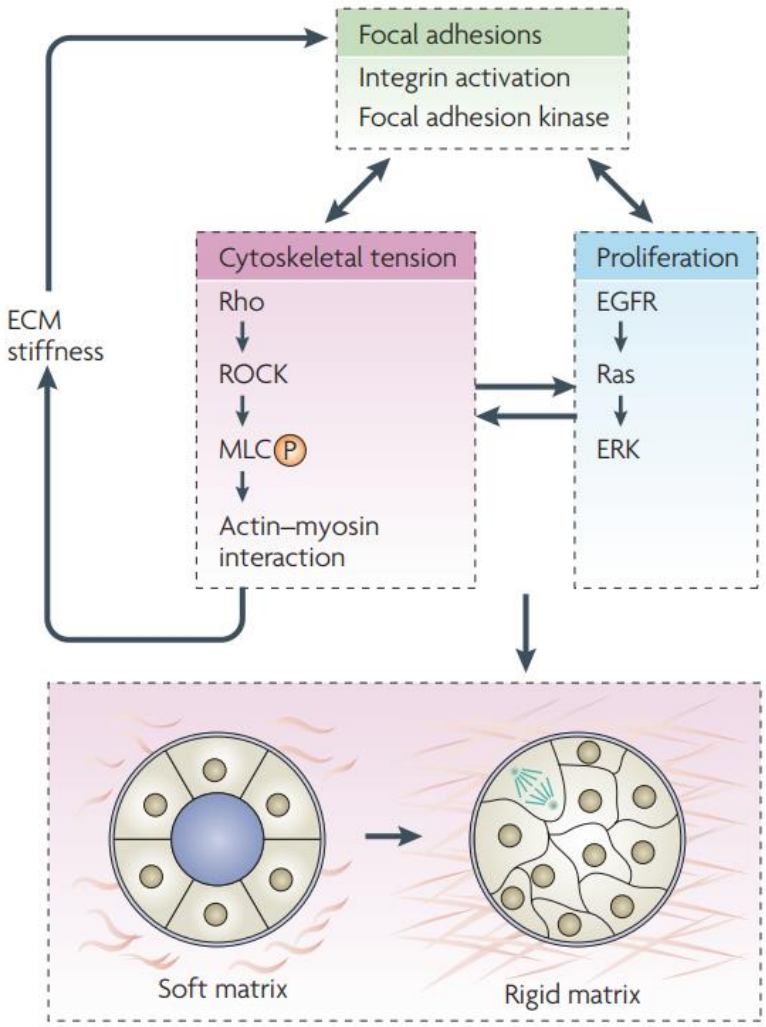

Figure 4: Mechanotransduction in cancer cells

An illustration of how increased extracellular matrix (ECM) stiffness and altered cytoskeletal tension can contribute to tumor formation. Increased ECM stiffness can arise from fibrosis or in response to increased cytoskeletal tension. The increased ECM stiffness is sensed by focal adhesions and activates integrins and focal adhesion kinase, thereby promoting focal adhesion assembly and stimulating the Rho–ROCK pathway. ROCK activation increases cytoskeletal tension by increasing myosin light chain (MLC) phosphorylation, which can result in further increases in ECM stiffness due to cellular mechanotransduction signaling, completing a self-enforcing (positive) feedback loop. Crosstalk between the Rho–ROCK pathway and the epidermal growth-factor receptor (EGFR)–Ras–ERK pathway results in increased proliferation. In breast cancer cells, the combined action of increased contractility and proliferation, triggered by increased ECM stiffness, may drive the undifferentiated and proliferative phenotype of mammary epithelial cancer cells and result in tumor formation [From Jaalouk and Lammerding 2009].

In contrast to the level of understanding of how specific chemical stimuli transduce signals within cells, our knowledge of how cells sense force and respond to various degree, duration and direction of force is very scarce. One of the challenges in understanding cellular response to forces is that there is not yet a universally accepted or fully described instance of a cellular component that responds specifically to a particular type of force. Lack of precise molecular mechanisms of force sensing leaves open the possibility that what is interpreted as a purely mechanical stimulus might, in fact, be a chemical stimulus that coincides with the force application. In this regard, as an example of cellular structures that can sense and transduce forces, our lab demonstrated that nanodomains at the plasma membrane termed caveolae can act as mechanosensors and transduce the mechanical stimuli in addition to buffering physical stresses applied on the membrane [Sinha et al. 2011].

CHAPTER 2:
CAVEOLAE - SPECIALIZED PLASMA MEMBRANE NANODOMAINS

In 1953, cell biologist George Palade - who at that time made extensive use of the electron microscope to visualize the cellular architecture – observed that the plasma membrane of the continuous endothelium of heart was riddled with invaginations of regular shape and size and called them *plasmalemmal vesicles* [Palade et al. 1953]. The appearance of these invaginations were remarkable: intricate, uniformly flask/bulb-shaped and occurred either singly or self-associated to form a cluster. Two years later, Japanese electron microscopist Eichi Yamada observed similar structures in the basolateral face of gall bladder epithelium and coined the term *'caveolae intracellulares'* due to the resemblance of these structures to 'little caves' [Yamada et al. 1955].

The history of research on caveolae can be broadly categorized into phases, each yielding important contributions to our understanding of the various facets of caveolae.

The electron microscopy phase: During the course of four decades from Palade's initial description in 1953 until the 1990s, the majority of studies on caveolae were driven by electron microscopy on a purely morphological basis due to lack of a molecular marker. The presence of caveolae was documented in most cell types including endothelial cells [Simionescu et al. 1972, Simionescu et al. 1975], smooth muscle cells [Somlyo et al. 1971, Forbes et al. 1979] and fibroblasts [Bretscher et al. 1977]. Although caveolae were initially described as non-coated membrane invaginations (due to the absence of the characteristic fuzziness observed in clathrin-coated pits), advancements in the electron microscopy (particularly freeze fracture and metal-replica electron microscopy) later revealed striated filaments on the cytoplasmic

face of caveolae [Solmyo et al. 1971, Montesano et al. 1982, Peters et al. 1985, Izumi et al. 1989, Anderson et al. 1991] suggesting the presence of a unique characteristic coat.

The molecular biology phase: The first breakthrough came in the year 1992, when the Anderson lab identified a 22kd substrate for v-src tyrosine kinase that decorated the striated filaments indicating the molecule's presence in the caveolar coat and thereby named the protein 'Caveolin' [Rothberg et al. 1992]. The discovery of caveolin-1 (Cav1) as a defining molecular marker for caveolae triggered numerous biochemical and cell biology studies in the following years, linking the protein to several potential binding partners involved in cell signaling [Li et al. 1996, Song et al. 1996, Garcia-Cardena et al. 1997, Couet et al. 1997, Nystrom et al. 1999].

The genetics phase: The early 2000s saw the generation of *CAV1*$^{-/-}$ knockout mice which surprisingly obfuscated the knowledge gained through cell biology and biochemical studies on the many roles of caveolae. The groups of Michael Lisanti and Teymuras Kurzchalia independently reported that mice lacking Cav1 (and thereby caveolae) were apparently healthy, had no major developmental defects and were able to reproduce normally [Drab et al. 2001, Razani et al. 2001]. However, despite the near-normalcy of the *CAV1*-knockout mice, they did exhibit an array of less-obvious phenotypes such as vascular abnormalities, lipodystrophy, muscle dystrophy and fat-related metabolic dysfunctions. These genetic data showed that caveolae are important for the normal function of blood vessels, muscle and fat tissue where they are the most abundant.

Given the contrasting data, one cannot escape the conclusion that either caveolae are not crucial regulators of signaling pathways or that compensatory mechanisms exist in the absence of caveolae. A thorough understanding of the molecular mechanisms

involved in the assembly of caveolae and its interactions with functionally significant partners could help resolve this conundrum and thereby shed light on the actual roles of caveolae at the different scales.

2.1 Molecular architecture and composition of caveolae:

2.1.1 Structure:

Caveolae are 50-100nm wide invaginations at the plasma membrane and show a characteristic flask/bulb shape morphology when visualized through transmission electron microscopy. However, caveolae appear as open cups or craters with a wide opening rather than a constricted neck in cryo-fixed preparations [Richter et al. 2008, Schlormann et al. 2010]. In connective tissues such as those of the endothelium, caveolae possess a unique specialized structure at the neck region called the stomatal diaphragm generated by the transmembrane protein PV1 [Stan et al. 2004, Stan et al. 2005]. Although transmission electron micrographs of caveolae do not exhibit an obvious electron dense coat, techniques like freeze fracture EM and deep-etch cryo-EM have revealed the clear presence of a coat structure on the cytoplasmic face of caveolae (Figure 5). Interestingly, unlike clathrin-coated pits which possess a uniform lattice coat structure, the caveolar coat seems to vary between cell/tissue types sporting a spiked coat or striations running around the caveolar bulb [Peters et al. 1985, Rothberg et al. 1992, Nixon et al. 2007, Richter et al. 2008]. Another unique feature of caveolae are their ability to form complex higher-order structures in addition to existing as single well defined units. Termed caveolae clusters or rosettes, these higher order structures represent multiple caveolae connected to the plasma membrane through a single neck and have been reported to be regulated by the formin-binding protein FBP17 [Yeow et al. 2017, Echarri et al. 2019].

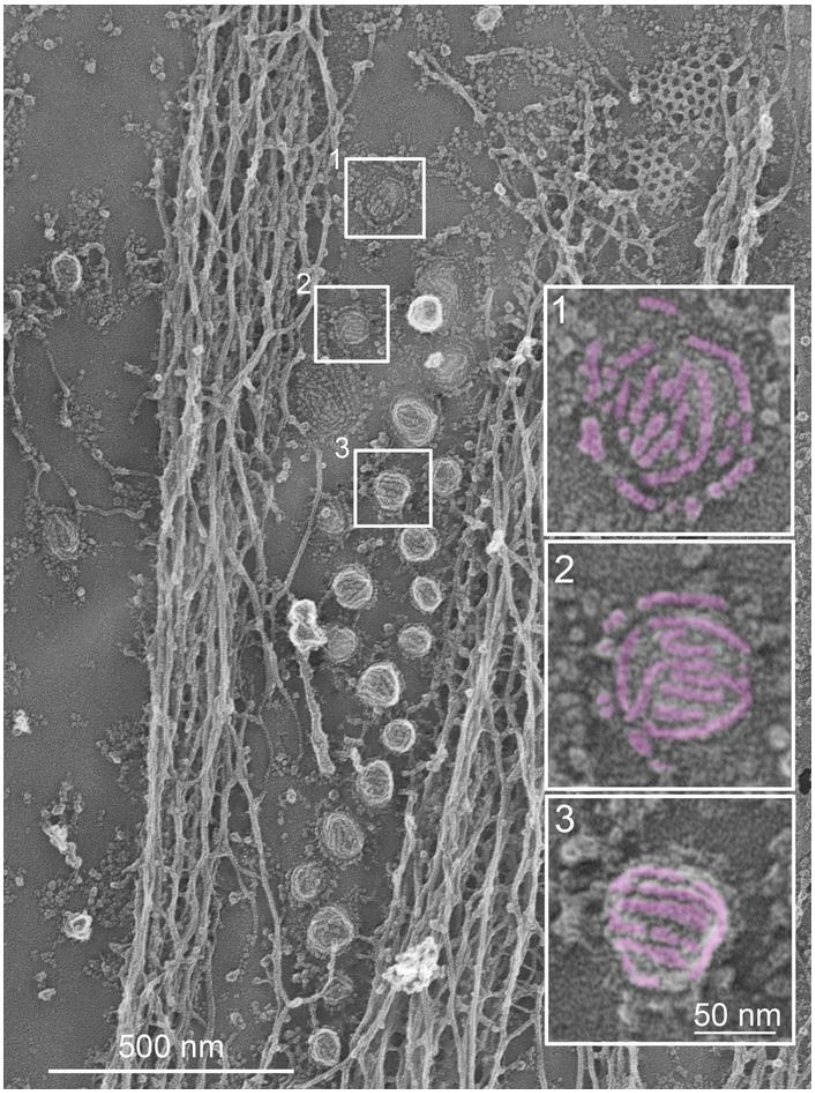

Figure 5. Visualization of the caveolar coat at the plasma membrane of myotubes
Survey view of the cytoplasmic surface of an unroofed myotube obtained using platinum replica electron microscopy. Different types of caveolae structures are apparent, ranging from flat **(1)**, circular **(2)**, to fully budded **(3)** along with the actin cytoskeleton. [From Lamaze et al. 2017]

2.1.2 Composition:

Caveolae possess a characteristic coat that is composed of a suite of proteins and lipids each of which have specific roles and are required for caveolae formation and stability (Table 2). In this chapter, we take a closer look at each of these components in detail and discuss their proposed functions. The protein components required for the formation of a *bona fide* caveolae can be divided into two classes:

Core structural proteins – Caveolins and cavins

Key accessory proteins - EHDs and pacsins

2.1.2.1 Caveolins:

Caveolins are the most abundant proteins found in caveolae, and it has been demonstrated that they are necessary to promote and stabilize the high degree of membrane curvature found in caveolae [Fra et al. 1995, Lipardi et al. 1998, Drab et al. 2001, Walser et al. 2012]. Caveolin is an integral membrane protein and vertebrates express three isoforms – caveolin 1 (20.5 kDa), caveolin 2 (16.8 kDa) and caveolin 3 (17.2 kDa). Cav1 and Cav2 are abundant in non-muscle cells whereas Cav3 is predominantly expressed in striated muscle cells such as skeletal muscle cells and in some smooth muscle cells [Way et al. 1995, Tang et al. 1996, Song et al. 1996]. Cav1 and Cav3 share a high degree of sequence similarity (52%) whereas Cav2 possesses a significantly lower sequence similarity with Cav1 and Cav3 (29% and 32% respectively) [Root et al. 2019]. Consequently, Cav1 and Cav3 are indispensable for the formation of caveolae as ablation of the proteins in the respective cell types results in loss of caveolae [Drab et al. 2001, Galbiati et al. 2001]. In contrast, loss of Cav2 has no apparent effect on caveolae formation *in vivo* but might be important for caveolae formation in certain cell types such as LNCaP and MDCK cells [Razani et al. 2002, Lahtinen et al. 2003, Sowa et al. 2003]. The

Table 2: List of caveolae components

Name other names	**Gene name** (human)	**Properties**
Caveolin-1 VIP21 Caveolin	CAV1	Integral membrane protein with hairpin topology Oligomeric Cholesterol binding, palmitoylated Localizes to caveola bulb Essential for caveola formation in non-muscle cells
Caveolin-2	CAV2	Integral membrane protein with hairpin topology Forms a complex with CAV1 Not essential for caveola formation
Caveolin-3 M-caveolin	CAV3	Integral membrane protein with hairpin topology Essential for caveola formation in muscle cells
Cavin1 PTRF CGL4 FKSG13	CAVIN1	Peripheral membrane protein Oligomeric Binds phosphatidylserine and *PtdIns*(4,5)P_2 Localizes to caveola bulb Essential for caveola formation in mammalian cells and tissues Recruits cavin2, cavin3 and cavin4 to caveolae
Cavin2 SDPR SDR PS-p68	CAVIN2	Peripheral membrane protein Oligomerizes with cavin1 Binds phosphatidylserine Not essential for caveola formation in all tissues but plays a role in sculpting caveolae Role in endothelial eNOS regulation
Cavin3 SRBC HSRBC PRKCDBP	CAVIN3	Peripheral membrane protein Oligomerizes with cavin1 Binds phosphatidylserine Not essential for caveola formation Role in trafficking of caveolae

Cavin4 MURC	CAVIN4	Muscle-specific Peripheral membrane protein Binds phosphatidylserine and *PtdIns*(4,5)P_2 Not essential for caveola formation Promotes Rho/ROCK signaling
EHD2 (EH Domain containing 2) PAST2	EHD2	ATPase forming ring around neck of caveolae Inhibits endocytosis Binds phosphatidylserine and/or *PtdIns*(4,5)P_2 Not required for caveola formation but for caveola stabilization, formation of caveolae clusters, and neck morphology working together with EHD1 and EHD4
PACSIN2 Syndapin II (SDPII)	PACSIN2	BAR domain protein Required for formation of caveolae Mediates dynamin binding and recruitment to caveolae
PACSIN3 Syndapin III (SDPIII)	PACSIN3	BAR domain protein Muscle-specific Localizes to neck region of caveolae Required for caveola formation in muscle with loss leading to flattened caveolae
ROR1 (Receptor tyrosine kinase-like orphan receptor 1) NTRKR1 dJ537F10.1	ROR1	Transmembrane protein Binds CAV1 and cavin1 through distinct sites in cytoplasmic tail to facilitate caveola formation May not be essential in all tissues

From Parton et al. 2018

hallmark feature of caveolins is that unlike most integral membrane proteins, it does not have a transmembrane orientation. Instead, it is postulated to adopt an unusual hairpin topology where the N- and C-termini face the cytoplasmic side of the plasma membrane whereas the hydrophobic central domain adopts an intramembrane loop conformation (Figure 6) [Dupree et al. 1993, Sargiocomo et al. 1993, Monier et al. 1995 and Sargiocomo et al. 1995]. Caveolins possess 4 distinct structural domains - the N-terminal domain; the caveolin scaffolding domain; the intra-membrane domain and the C-terminal domain (Figure 6).

N-terminal domain (NTD): The molecular mass variation between the three caveolin isoforms arises from differing lengths of the NTD (Cav1: 81 residues; Cav2: 66 residues; and Cav3: 54 residues). The NTD is known to facilitate many critical functions of caveolins as it harbors several important phosphorylation sites (Ser5, Tyr14, Ser36, Ser80) and has been implicated in many protein-protein interactions [Li et al. 1996, Schlegel et al. 2001, Vainonen et al. 2004, Mir et al. 2007, Parr et al. 2007]. Several studies performing circular dichroism (CD) spectroscopy on full length and fragmented NTD of Cav1 in aqueous buffer or in the presence of SUVs (small unilamellar vesicles), yielded a CD spectrum indicative of a mostly disordered or random coil formation [Fernandez et al. 2002, Schroeder et al. 2011]. The presence of SUVs did not induce any secondary structure which suggesting that these fragments did not interact with the membrane. NMR (nuclear magnetic resonance) chemical shift data from a functional Cav1 construct reconstituted in LMPG (lyso-myristoyl-phosphatidyl-glycerol) micelles and full length Cav3 reconstituted in LPPG (lyso-palmitoyl-phosphatidyl-glycerol) micelles revealed that residues 62-80 were dynamic and unstructured at physiological pH, consistent with previous CD studies. However, lowering the pH to approx. 5 resulted in increased

helicity of the NTD and caused it to associate with the micelle suggesting that acidic conditions might enable the NTD to adopt secondary structures [Machleidt et al. 2000, Plucinsky et al. 2015, Kim et al. 2016].

Caveolin scaffolding domain (CSD): The CSD has been reported to be functionally important for many aspects of caveolin behavior including interaction with signaling proteins (most notably the endothelial nitric oxide synthase; eNOS), cholesterol binding and oligomerization [Sargiocomo et al. 1993, Sargiocomo et al. 1995, Lisanti et al. 1994, Ju et al. 1997, Okamoto et al. 1998, Carman et al. 1999, Roy et al. 1999]. The length of the CSD is identical for each isoform (20 amino acids) with a particularly high homology between Cav1 and Cav3. CD spectroscopy studies utilizing constructs containing both the NTD and the CSD indicated significant levels of helicity in the CSD region [Fernandez et al. 2002]. Although computational analyses by several groups supported the presence of helical content in the CSD, these studies reported contrasting results regarding the presence of α-helix and β-strands in the CSD [Spisni et al. 2005, Parton et al. 2006, Ariotti et al. 2015]. In an attempt to clarify this discordance in the computation based structural insights, a longer construct of Cav1 and Cav3 encompassing the CSD in tandem with the IMD were reconstituted in LMPG and LPPG micelles respectively, and subjected to NMR chemical shift indexing. This revealed a helical stretch from residues 87-107 for Cav1 and residues 55-80 for Cav3 (analogous to the Cav1 residues). These findings suggest that the degree of helical content observed in the CSD was consistent only when sufficient flanking residues were present. [Rui et al. 2014, Plucinsky et al. 2015, Kim et al. 2016]. The CSD has been proposed to interact with a conserved domain in its effector proteins, referred to as the caveolin binding domain (CBM). Interestingly, a recent bioinformatic study of putative CBMs refute the possibility of

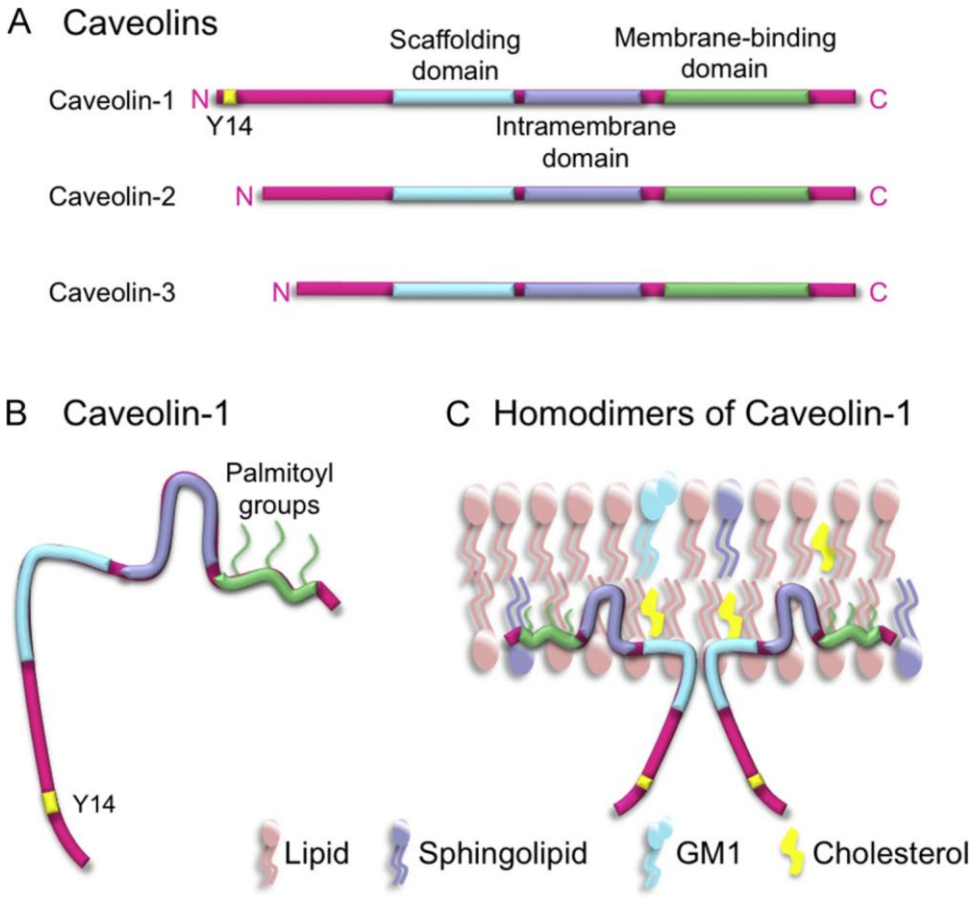

Figure 6: Caveolin isoforms and domains

(A) Schematic presentation of the caveolin family of proteins. **(B)** The tertiary structure of Caveolin-1 shows its functional domains: the membrane binding domain (α-helix), the intramembrane domain (most probably formed by two α-helixes) and the scaffolding domain including a cholesterol binding motif and a β-sheet organized region involved in the homooligomerization of Caveolin-1 molecules. **(C)** Topology of Caveolin-1 in the plasma membrane showing a homooligomer of Caveolin-1 molecules. [From Fiala and Minguet 2018]

of a CSD-CBM interaction (discussed later in section 2.3.4).

Intra-membrane domain (IMD): The IMD has been postulated to adopt the characteristic hairpin or U-conformation that is thought to facilitate interaction with the lipid bilayer thereby inducing and stabilizing the membrane curvature required for caveolae formation [Monier et al. 1995]. Computational studies predicted the presence of two α-helices between residues 97-107 and 112-130 separated by a 4-residue un-structured break [Spisni et al. 2005, Parton et al. 2006]. CD spectroscopy studies were in agreement with the computational analyses suggesting a helix-break-helix structure for the IMD [Lee et al. 2012]. The break was reported to be the intra-membrane turn as mutation of a single conserved residue in the break region - P110 to alanine - resulted in the shifting of the N-terminus to the extracellular space [Aoki et al. 2012]. Taken together, these studies propose a helix-break-helix secondary structure for the IMD with the break region serving as an intra-membrane turn that imparts a wedge-like shape to the caveolin molecules, thereby perturbing the lipid spacing in the inner and outer leaflets of the plasma membrane asymmetrically and inducing membrane curvature [Zimmerberg et al. 2006].

C-Terminal domain (CTD): Similar to the CSD, the length of the CTD is identical between the three isoforms with high sequence homology between Cav1 and Cav3. The CTD has been implicated in several critical functions including membrane trafficking and oligomerization [Rothberg et al. 1992, Song et al. 1997, Machleidt et al. 2000, Schlegel et al. 2000, Razani et al. 2002, Schubert et al. 2002, Mir et al. 2007]. Cav1 has been shown to be palmitoylated at three cysteine residues located in the CTD. However, mutation of these cysteines to serines did not affect proper trafficking of Cav1 to the membrane indicating that palmitoylation may have only a limited impact on the caveolin fold [Dietzen et al. 1995]. Cav2 has also been

reported to be palmitoylated at three cysteine residues [Kwon et al. 2015]. Cav3 has been shown to be heavily palmitoylated, although the exact sites of palmitoylation are unclear since Cav3 contains 9 cysteine residues spread throughout the entire sequence [Galbiati et al. 1999]. Computational, CD spectroscopy and NMR chemical shift studies demonstrate that the CTD has an amphipathic helix that is separated from the second helical region of the IMD by a 3 residue unstructured break region. Similar to P110, a conserved proline in the break region acts as a helix breaker and initiator [Spisni et al. 2005, Parton et al. 2006, Plucinsky et al. 2015].

Ultrastructure of caveolin oligomers: Shortly after synthesis, Cav1 was found to oligomerize and assemble into an 8S complex composed of 7-14 monomers [Monier et al. 1995, Sargiocomo et al. 1995, Fernandez et al. 2005]. While some efforts have been made to characterize the structure of Cav1 monomers, the lack of a 3D structure of Cav1 has limited investigations into understanding the organization of Cav1 molecules in the caveolae. In this regard, a recent study reported the structure of the Cav1 8S complex using single particle electron microscopy [Han et al. 2020]. The Cav1 8S complexes is shown to adopt a toroidal shape with an outer ring structure and a central stalk. It is estimated that approx. 10 Cav1 monomers constitute a Cav1 complex with the N-termini on the outer ring and the C-termini on the central stalk. According to this model, Cav1 monomers are proposed to form wedge-like sections that self-assemble into a disc-shaped complex with the C terminus of Cav1 localized to the center of the complex and the N terminus on the periphery of the disc.

2.1.2.2 Cavins:

In addition to caveolins, the cavin family of proteins has been shown to play a critical part in generation of membrane curvature and caveolae formation [Hill et al. 2008,

Briand et al. 2014]. The Cavin family of proteins are composed of four isoforms in vertebrates: Cavin1 (PTRF), Cavin2 (SDPR), Cavin3 (PRKCDBP), and the muscle-specific isoform Cavin4 (MURC). Cavin1 (also known as Cav-p60, BBP), was first identified as a factor involved in transcription termination, receiving the official name polymerase I and transcript release factor (PTRF) [Jansa et al. 1998]. It displays a relatively broad expression profile and like Cav1, is crucial for the formation of mature budded caveolae. Cavin2 (also known as PS-p68, SDR) was first identified through its abundance and high affinity for phosphatidylserine (PS) in platelets (Burgener et al. 1990). It was later described as a protein induced upon serum deprivation and hence was named serum-deprivation-response protein (SDPR) (Gustincichet et al. 1993). Cavin3 was first discovered for its function as an adaptor for protein kinase Cd homologous to SDPR and named SDPR-related gene product that binds to C-kinase (SRBC) but is now referred to as protein kinase C delta-binding protein (PRKCDBP) [Izumi et al. 1997]. Cavin4 was initially identified in muscle, and was named muscle-related coiled-coil protein (MURC) [Ogata et al., 2008].

All cavins possess a conserved sequence and α-helical secondary structure element within two domains called helical region HR1 and HR2 (Gustincich et al. 1999; Kovtun et al. 2014). In addition, three disordered regions (DR) - DR1, DR2 and DR3 – separate the two helical regions HR1 and HR2 (Figure 7). These are not well conserved at the sequence level but share a highly acidic sequence profile and predicted disordered secondary structure [Tillu et al. 2018, Tillu et al. 2021]. The DR regions also house PEST motifs suggesting post-translational modifications and subsequent degradation might be important for regulating cavin turnover and to maintain homeostasis and function [Breen et al. 2012]. One of the characteristic

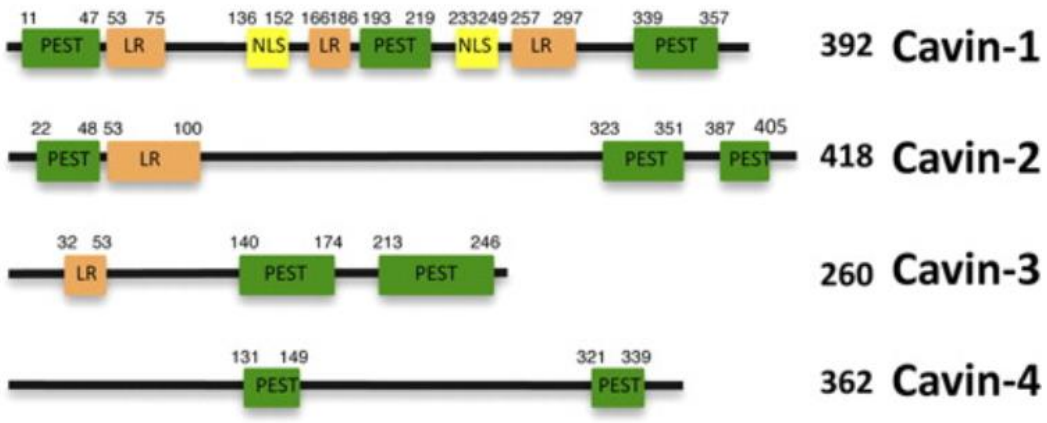

Figure 7: The cavin family of proteins
Domain structure of cavin proteins in mouse. Putative PEST domains (green), leucine-rich regions (LR; orange), and nuclear localization sequences (NLS; yellow) are shown with amino acid numbers indicated. [From Bastiani et al. 2009]

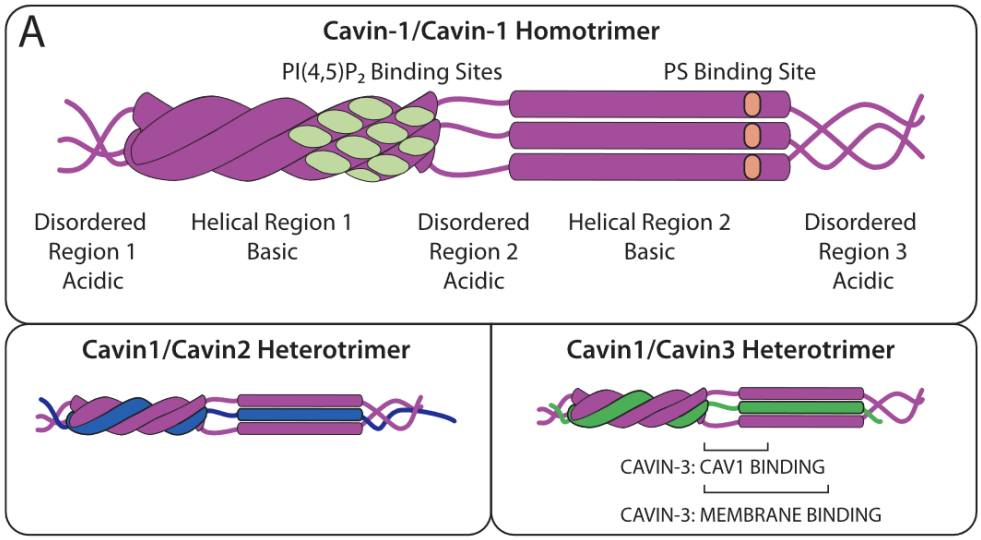

Figure 8: Association of cavin monomers
(A) cavins are cytosolic proteins with three disordered regions (DR1, DR2, DR3) alternating with two helical regions (HR1 and HR2). Two Cavin-1s homo- and hetero-trimerize with a cavin1, cavin2, or cavin3 monomer via an extended coiled-coil structure in HR1, which drives HR2 to generate a helical structure. Cavin1 has membrane-binding sites, including a PtdIns (4,5) bisphosphate [PI (4,5) P_2]-binding site composed of four basic regions in close proximity on HR1 and a phosphatidylserine (PS)-binding basic site on HR2 [From Busija et al. 2017].

feature of cavins is their ability to associate into higher order homo- or hetero-oligomers independent of caveolins or membrane (Figure 8) [Bastiani et al. 2009, Hansen et al. 2009, Gambin et al. 2014, Kovtun et al. 2014]. In vitro expression of various cavins resulted in the formation of protein complexes containing on average 50 cavin monomers which is thought to represent the 60S-size cavin complex reported previously [Hayer et al. 2010, Ludwig et al. 2013, Gambin et al. 2014]. Interestingly, despite similarities in homo-oligomerization tendencies in various cavins, only cavin1 homo-oligomers have the ability to engage with caveolins at the plasma membrane and trigger caveolar formation. This is in agreement with studies of *PTRF*-knockout animals, which show a complete loss of caveolae in all tissues. All other cavins require cavin-1 for incorporation into the caveolar coat [Hill et al. 2008, Liu et al., 2008, Bastiani et al. 2009, Hansen et al. 2013]. To summarize, the life cycle of cavins start with initial trimerisation through the HR1 domain and subsequent assembly into cytoplasmic cavin homo- or hetero-oligomers. These oligomers can bind negatively charged membranes but become stably associated with the PM only in the presence of caveolins [Kovtun et al. 2015]. The recruitment of cavins at these localized PM nanodomains will further increase the local concentration of the negatively charged lipids, facilitating membrane curvature and formation of the distinctive caveola bud [Bastiani et al. 2009, Hansen et al. 2009]. In addition, certain stimuli, such as membrane stretching or cholesterol depletion, can lead to flattening of caveolae and the release of cavins back into the cytoplasmic pool [Liu and Pilch 2008, McMahon et al. 2019].

2.1.2.3 Eps-15 homology domain containing protein 2 (EHD2):

EHD2 is a dimeric ATPase and has been shown to tubulate liposomes in vitro by oligomerizing in evenly shaped rings of varying size around the tubules [Daumke

et al. 2007]. Structurally, EHD2 consists of a membrane-binding interface that is slightly curved, which is thought to be essential for its membrane-bending capacity. EHD2 consists of a central G-domain which only displays binding specificity for ATP, and ATP hydrolysis is important for the oligomerization of EHD2 dimers. This is crucial for the normal function of EHD2 because removal of domains corresponding to ATP-hydrolysis and EHD2 oligomerization abolishes protein binding in a cellular setting. EHD2 also contains an NPF-motif (a three amino acid Asn-Pro-Phe chain that is known to bind to the EH-domain pocket) in a flexible linker at the side of the protein dimer that may be involved in protein-protein interactions. NPF-motifs are found in many proteins involved in endocytic transport and targeting. EHD2 also contains an EH-domain, which is known to interact with the NPF-motif facilitating dimer formation and subsequent oligomerization. While this interaction has been shown to be important for the endocytic targeting in EHD1, it might not be important in the case of EHD2 as removal of the EH-domain from EHD2 does not affect its binding to intracellular structures [Daumke et al. 2007].

It has been suggested that EHD2 is localized to the neck of the caveolae [Moren et al. 2012, Stoeber et al. 2012, Ludwig et al. 2013]. This localization appears to be logical, as it is known that EHD2 oligomerizes in a ring structure and belongs to the dynamin-like protein superfamily [Daumke et al. 2007]. Initially, EHD2 was thought to be important for scission of caveolae because of its ability to tubulate membranes. However, several studies now point towards a function in stabilizing caveolae at the plasma membrane. PtdIns (4,5) P_2 has been shown to be present in caveolae and also important for the localization of EHD2 to the membrane. More importantly, pharmacologic inhibition of a phospholipase involved in the conversion of PtdIns 4P to PtdIns (4,5) P_2, reduces membrane localization of EHD2

[Fujita et al. 2009, Simone et al. 2013]. PtdIns (4,5) P_2 may serve as a determinant of caveolar localization, and EHD2 specification and binding may be dependent on other residues in its membrane-interaction domains [Hoernke et al. 2017, Yeow et al. 2017].

2.1.2.4 Pacsins:

Pacsins (protein kinase C and casein kinase substrate in neurons proteins) or syndapins include three paralogs (Pacsin-1, Pacsin-2 and Pacsin-3) and each member contains an F-BAR domain and an SH3 domain [Modregger et al. 2000]. The SH3 domain binds to dynamin and the actin-nucleating protein N-WASP [Itoh et al. 2005, Tsujita et al. 2006]. Pacsin-1/syndapin-I is implicated in synaptic vesicle recycling in the brain and Pacsin-3/syndapin-3 expression is specific to muscles while Pacsin-2/syndapin-2 is expressed ubiquitously [Qualmann et al. 1999].

Knockdown of pacsin-2/syndapin-2 in cultured cells causes a loss of morphological caveolae and genetic ablation of pacsin-3/syndapin-3, the muscle-enriched member of the pacsin/syndapin family, in mice causes a loss of muscle caveolae [Hansen et al. 2011, Senju et al. 2011, Koch et al. 2012, Seemann et al. 2017]. These findings suggest that the pacsins, which contain membrane-sculpting F-BAR domains, are crucial for the membrane deformation required for caveolae formation. Caveolins, cavins, and pacsins all possess membrane-sculpting activity and a coordinated action of all these proteins is required for efficient caveola formation in vertebrate cells. Pacsins have also been proposed to play an important role in recruiting dynamin-II to caveolae by binding to EHD proteins [Senju et al. 2011]. Interestingly, pacsins may be enriched close to the neck of the caveolae rather than around the caveolae bulb consistent with the proximity of these potential interacting proteins [Seemann et al. 2017].

2.1.2.5 Lipids:

Caveolae represent a specialized lipid domain and detailed quantitative lipid analyses of purified caveolae have shown an enrichment of cholesterol, sphingomyelin and specific glycosphingolipids, such as the ganglioside GM3, relative to the bulk plasma membrane [Ortegren et al. 2004]. Moreover, the core protein components of the caveolar coat show specific lipid-binding properties. Cav-1 binds cholesterol and is palmitoylated [Dietzen et al. 1995, Murata et al. 1995]. Importantly, peptides derived from caveolin reorganize lipids when incorporated into liposomes with particular specificity for cholesterol, PtdIns (4,5) P2 and phosphatidylserine suggesting that oligomers of caveolin could generate a specific lipid environment [Wanaski et al. 2003]. Cavin proteins possess a PtdIns (4,5) P_2 binding site in the HR1 domain and show phosphatidylserine-binding activity. The high concentration of these lipid-binding proteins within caveolae (~140–150 caveolins and ~50 cavins per caveolae) can therefore facilitate the generation of a lipid domain enriched in these specific lipids.

The importance of lipids in caveolae formation and stability cannot be overlooked. It has long been known that cholesterol depletion causes flattening of caveolae leading to the dissociation of caveolar coat proteins from the membrane [Rothberg et al. 1992, Hill et al. 2008, Breen et al. 2012]. In addition, recent reports demonstrate the importance of phosphatidylserine in caveolae formation [Hirama et al. 2017]. Perhaps the most convincing report highlighting the importance of lipids in caveolae formation comes from the study of caveolae in the blood-brain barrier. Generally, the blood-brain barrier maintains a high impermeability and shows a very low density of caveolae. Genetic ablation of the lipid flippase Mfsd2a, which is responsible for transporting long-chain unsaturated fatty acid–containing

phospholipid species from the outer to the inner cytoplasmic leaflet of the endothelial cell plasma membrane, causes the appearance of caveolae and increases vascular permeability [Andreone et al. 2017]. This finding suggests that, in the normal blood-brain barrier, specific polyunsaturated fatty acid containing phospholipids in the cytoplasmic leaflet of the plasma membrane create an inhibitory environment for caveolae formation.

2.2 Biogenesis of caveolae:

As with any cellular process, caveolae formation requires the coordinated action of key proteins and lipids detailed above that act in synergy to generate the flask-shaped domain at the plasma membrane. The assembly of a mature caveolae at the plasma membrane is determined by three distinct molecular layers: a stable integral membrane scaffold composed of Cav1/Cav3 (and Cav2) tightly bound to cholesterol; a lipid nanodomain enriched in cholesterol, phospholipids and sphingolipids; and a peripheral protein scaffold on the cytoplasmic face composed of the cavin family of proteins.

2.2.1 Trafficking of caveolin

The Cav1 monomer is co-translationally inserted into the endoplasmic reticulum (ER) membrane in a signal recognition particle (SRP)-dependent manner. Following this, the Cav1 monomers oligomerize and assemble into 8S complexes which form the basic unit of the caveolar coat [Monier et al. 1995, Sargiocomo et al. 1995, Fernandez et al. 2002]. The presence of a diacidic $_{67}$DFE$_{69}$ residue enables rapid accumulation of the 8S complex at the ER exit sites (ERES) followed by COPII-dependent export to the Golgi complex. On reaching the Golgi apparatus, a second round of oligomerization converts the 8S complexes into 70S complexes which then undergoes conformational changes and associates with cholesterol

[Hayer et al. 2010]. The formation of a higher-order 70S complex is characterized by a loss of diffusional mobility of Cav1 and Cav2 at the Golgi (but not at the ER). Exit from the Golgi complex is accelerated by cholesterol addition and slowed by cholesterol depletion, suggesting a facilitating role of cholesterol in Golgi exit [Pol et al. 2005]. This **integral membrane scaffold** of caveolins exit through the medial golgi complex in discrete vesicular carriers together with glycosyl-phosphatidyl inositol (GPI)-anchored proteins to the plasma membrane [Tagawa et al. 2005], although Cav1 does not seem to be required for efficient delivery of GPI-anchored protein (Figure 9).

2.2.2 Generation of specialized lipid nanodomains

Two mutually exclusive models have been proposed for the generation of a specialized lipid environment for caveolae [Parton et al. 2020]. The first model is based on curvature driven concentration of lipids of specific molecular shape. It is well known that the vast number of lipid species differ in their effective molecular shape depending on their headgroups or acyl chains and can be classified as being cylindrical, cone-shaped or inverted cone-shaped lipid molecule. Specifically, cone or inverted cone-shaped lipid molecules induce negative membrane curvature (bulging in away from the cytoplasm) and positive membrane curvature (bulging out into the cytoplasm) respectively [Zimmerberg and Koslov 2006, McMahon and Boucrot 2015]. Caveolae possess regions of both negative curvature (neck region) and positive curvature (bulb region) and it has been proposed that this difference in curvatures could drive the localization of specific lipid species resulting in specialized lipid nanodomains. This could also explain the redistribution of lipids in response to flattening of caveolae as the prevailing membrane curvature is lost.

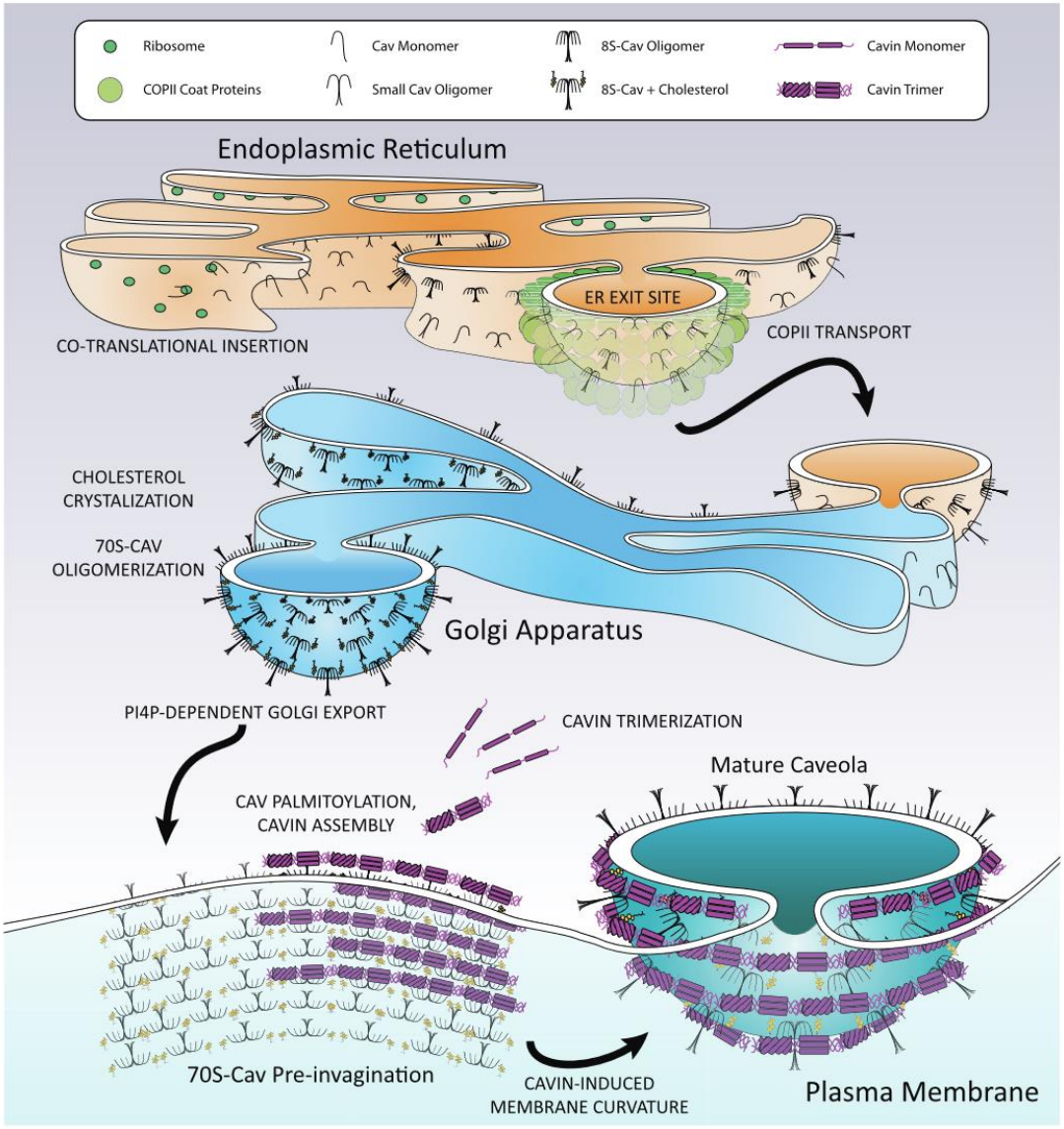

Figure 9: Biosynthetic trafficking of Cav1 and assembly of caveolae

Maturation of caveolae. Cav1 and Cav2 monomers are cotranslationally inserted into the endoplasmic reticulum (ER) membrane and swiftly oligomerized into 8S-Cav oligomers containing 7–14 Cavs. These oligomers are transported to ER exit sites (ERES) within 5 min of synthesis for COPII-dependent transport to the Golgi apparatus 15 min postsynthesis. In the Golgi, cholesterol crystalizes in the membrane and assists in the formation of 70S-Cav complexes composed of 18–25 8S-Cav subunits by ~60 min after synthesis, whereupon 70S-Cav is transported to the PM by four phosphate-adapter protein (FAPP-1, -2)-dependent secretory vesicles. Near or on the PM, palmitoyl acyltransferases palmitoylate 70S-Cav oligomers. Also on the PM, cavin proteins that trimerize in the cytosol gradually aggregate on the 70S-Cav membrane over the course of more than 25 min and assist in membrane curvature. Mature caveolae consist of three layers: a cholesterol and anionic lipid-rich membrane embedded with a palmitoylated 70S-Cav coat, which is surrounded by a striated oligomerized 60S-Cavin coat [From Busija et al. 2017].

The second model involves the inherent lipid/membrane-binding ability of caveolar components and their effect on lipid organization. Quantitative lipid analyses of purified caveolae have shown that cholesterol, specific glycosphingolipids and gangliosides are enriched in caveolae indicating that the major structural components of caveolae have lipid-binding properties [Ortegren et al. 2004]. Cav1 binds cholesterol and is palmitoylated at three cysteine residues in the C-terminal region [Murata et al. 1995, Dietzen et al. 1995]. In addition, peptides derived from caveolin have been shown to reorganize lipids when incorporated into liposomes with a particular specificity for cholesterol, sphingolipids, PtdIns (4,5) P_2 and phosphatidylserine (PS) [Wanaski et al. 2003, Sonnino et al. 2009]. PtdIns (4,5) P_2 and PS are thought to be enriched on the cytoplasmic side of the caveolar membrane [Fujita et al. 2009, Fairn et al. 2011]. In addition, depletion of PS results in reduced caveolae numbers indicating a critical role for PS in maintaining caveolae stability [Hirama et al. 2017]. In addition, cavins have been proposed to bind PtdIns (4,5) P_2 via a basic domain in the HR1 region and PS via a lipid-binding site at the start of HR2. Although a single cavin molecule does not have the necessary affinity to bind PtdIns (4,5) P_2 or PS, it is known that cavins homo- or hetero-oligomerize to form oligomeric lattices which can then sequester these lipid species to facilitate the generation of a lipid nanodomain (Figure 10) [Kovtun et al. 2014, Tillu et al. 2015].

2.2.3 Recruitment of cavins

Newly synthesized cavin molecules remain cytosolic and can either homo/hetero-trimerize and undergo hetero-oligomerization to form 60S complexes [Hill et al. 2008, Liu et al. 2008, Hayer et al. 2010]. The presence of PS and PtdIns (4,5) P_2 binding domains in cavins help in the recruitment of these preformed **peripheral**

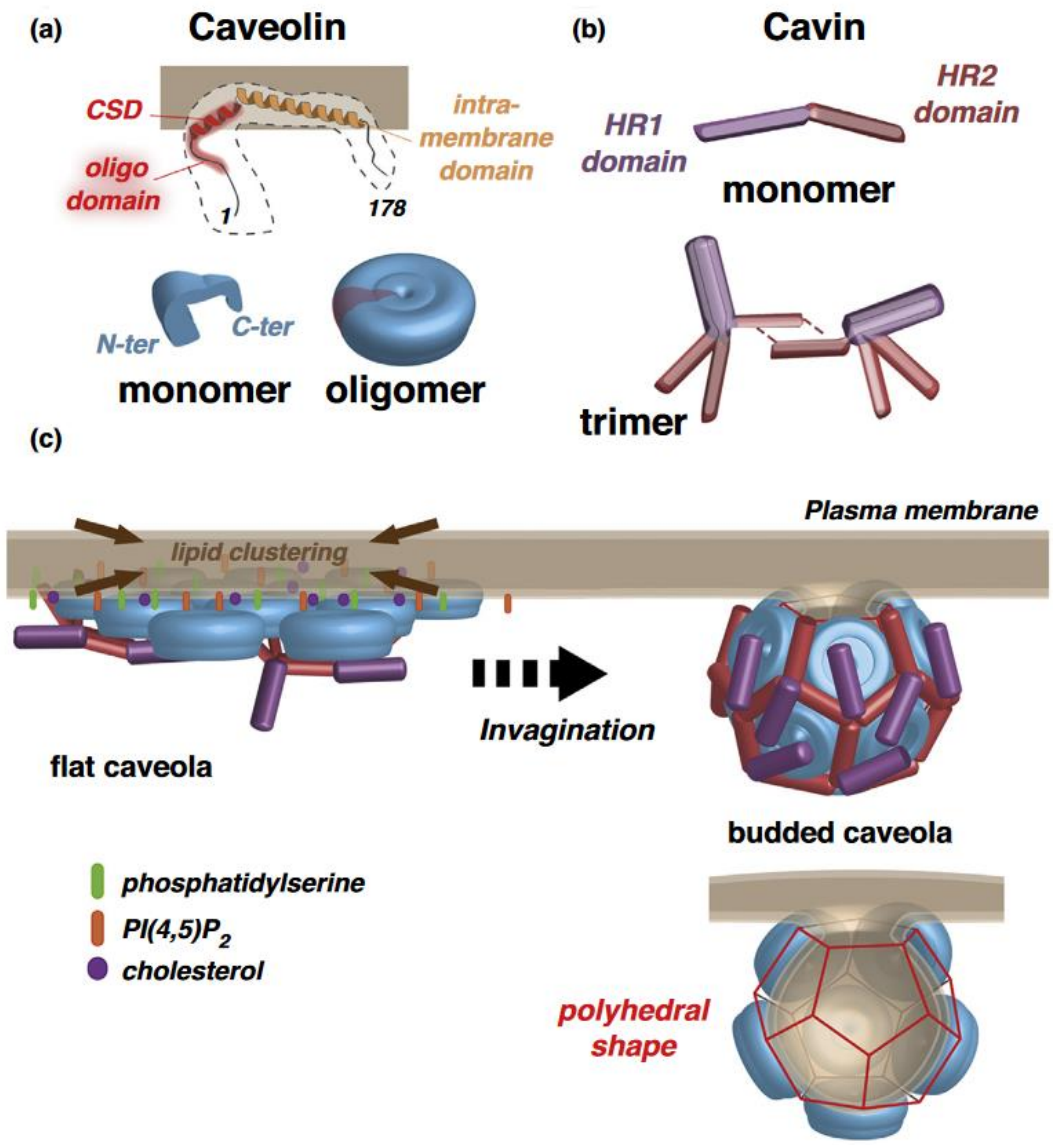

Figure 10: Hypothetical model of caveolae coat assembly and biogenesis
(a) An illustration of Cav1 topology with the different domains and their spatial organization in the plasma membrane. Based on Cav1 monomers may assemble as a disk-shaped oligomer with the C-terminal part oriented toward the center. **(b)** A schematic representation of the helical regions of the HR domains that may form coil-coiled structures. Through interaction between the HR1 domains, cavins can form hetero- or homo-trimers consisting of either three cavin1 or two cavin1 associated with one cavin2 or one cavin3 protein. **(c)** A model for the biogenesis of caveolae at the plasma membrane: Cav1 oligomers cluster specific lipids such as cholesterol, PtdIns (4,5) P2 and phosphatidyl serine thereby facilitating the recruitment of cavin trimers. This is followed by induction of membrane curvature by cavin oligomers through a mechanism that is not yet clearly understood and subsequent formation of a budded caveolae [From Lamaze et al. 2017].

cavin scaffolds to the specialized lipid environment at the plasma membrane generated by the insertion of the 70S caveolin complexes. It has been proposed that the cavin lattice forms a dodecahedron around the disc-shaped caveolin oligomers that float in the underlying membrane and helps induce membrane curvature thereby resulting in the formation of a mature budded caveolae (Figure 11) [Hansen et al. 2009, Kovtun et al. 2015, Ludwig et al. 2016, Stoeber et al. 2016, Tillu et al. 2018].

2.3 Roles of caveolae

2.3.1 Transcytosis:

Two years before Eichi Yamada visualized caveolae in the gall bladder epithelium and coined the term 'caveolae intracellularis' (little caves), George Palade had named them 'plasmalemmal vesicles' owing to their potential involvement in shuttling molecules across the cell [Palade 1953]. Hence, the earliest role attributed to caveolae was that of a specialized form of endocytosis termed transcytosis. Over the ensuing years, several cell biology and electron microscopy studies on endothelial cells reported that caveolae can transcytose LDLs, albumin and insulin, thereby supporting Palade's initial hypothesis that caveolae might be involved in the transcellular movement of molecules [Bruns and Palade 1968, Vasile et al. 1983, Nistor et al. 1986, Ghitescu et al. 1986, Heltianu et al. 1989, Bendayan et al. 1996]. Interestingly, the involvement of caveolae in transcytosis came under scrutiny and was debated following observations of mild phenotypes in *CAV1*$^{-/-}$ mice in addition to the increased rates of albumin efflux from blood vessels in the absence of caveolae [Rosengren et al. 2006, Schubert et al. 2002].

However, subsequent experiments added weight to the suggestion that caveolae do perform transcytosis. Antibodies targeted against aminopeptidase P, a protein

localized in lung endothelial caveolae, can be transported from the blood vessels to the underlying tissue [Oh et al. 2007]. In addition, a specific annexin A1 antibody

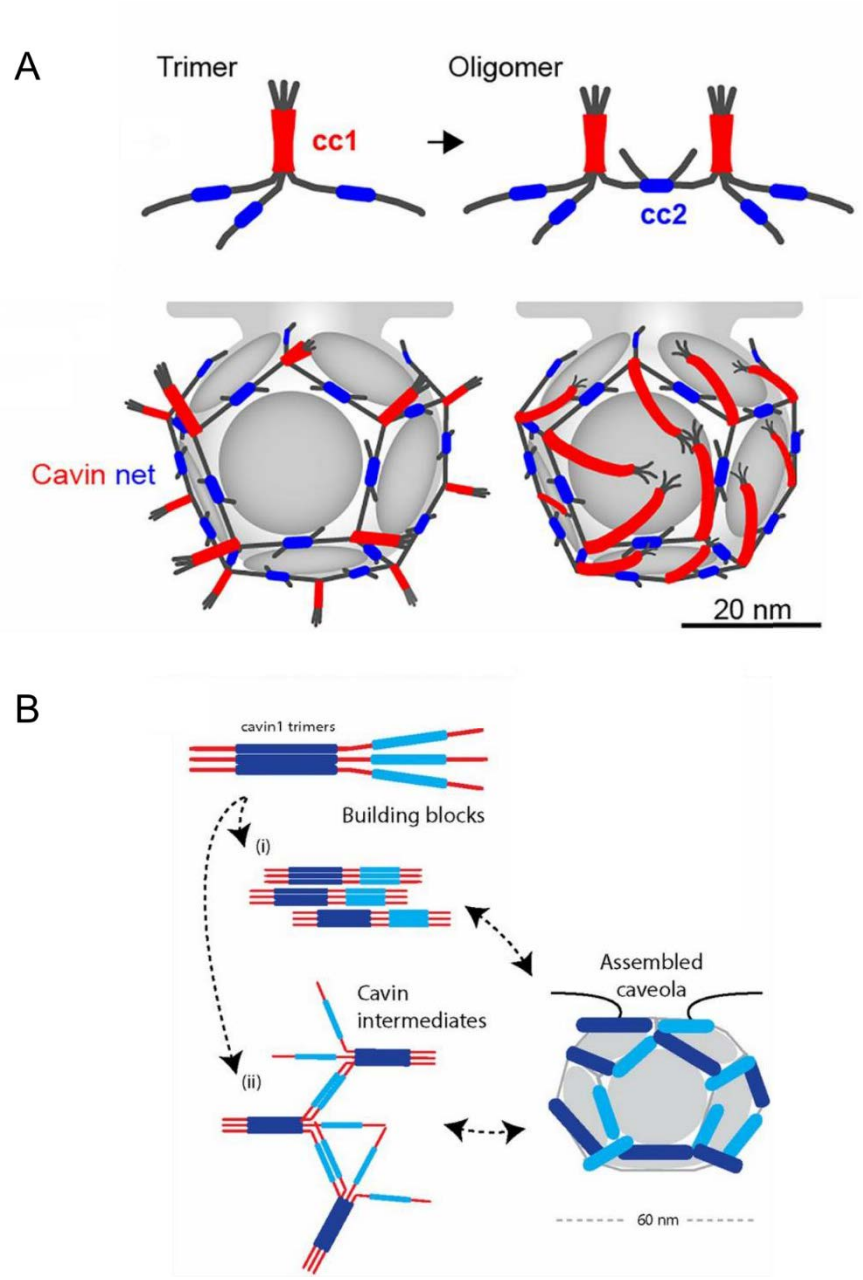

Figure 11: Proposed models for assembly of cavin oligomers
(A) Cavins possess two regions of α-helical structure, termed HR1 (cc1) and HR2 (cc2), which are rich in basic residues. These are linked by disordered acidic sequences DR1–DR3. Cavin1 trimerizes through its N-terminal HR1 domain, and then can form oligomers arranged in a net-like structure. These oligomers organize into striated patterns on the surface of caveolae in cooperation with the CAV1 protein. (B) In the model proposed by Stoeber et al. the cavin trimers form intermolecular

networks via HR2 domain coiled-coil interactions. Alternate mechanisms for intramolecular cavin interactions, such as electrostatic interactions, have also been proposed [Modified from Stoeber et al. 2016 and Parton et al. 2016].

that targets caveolae in the tumor endothelium is rapidly transported across the endothelium and is concentrated in the tumor mass [Oh et al. 2014]. A proposed role for caveolae in transcytosis has been further strengthened by a study focusing on the blood-brain barrier. The blood-brain barrier demonstrates an extremely low rate of transcellular transport and a lack of caveolae due to the absence of certain lipids required for caveolae formation. Interestingly, genetic ablation of a lipid flippase restored these lipids resulting in the formation of caveolae and a corresponding increase in transcellular transport [Andreone et al. 2017]. In addition, several recent studies have clearly demonstrated the importance of caveolae-mediated transcytosis in various biological functions [Ramirez et al. 2019, Bai et al. 2020].

2.3.2 Endocytosis:

Although clathrin mediated endocytosis represents the main pathway for internalization of extracellular ligands and uptake of plasma membrane components, it is now widely accepted that other uptake mechanisms exist in parallel such as caveolae-mediated endocytosis and Clathrin independent endocytosis (CIE) [Doherty and McMahon 2009, Parton et al. 2019]. Over the years, several studies have probed the ability of caveolae to act as endocytic carriers extensively considering and rejecting the views that caveolae are permanently static structures. Although the initial steps leading to pinching off of caveolae from the plasma membrane has been studied in detail, there is contradictory data regarding intracellular trafficking of caveolae putting the idea of caveolae-mediated

endocytosis to debate. In this section, we will look at available data regarding caveolar endocytosis focusing on the factors that may play a role in its internalization [Parton et al. 2020].

Based on electron microscopic observations, caveolae have been described to have varying levels of curvature suggesting that caveolae could be involved in endocytosis operating in parallel with clathrin-mediated endocytosis. In contrast, studies using green-fluorescent protein (GFP) tagged caveolin1 revealed that the exchange of GFP-Cav1 between the plasma membrane and the cytoplasm was low suggesting that caveolae are immobile structures [Van Deurs et al. 2003]. Moreover, overexpression of Cav1 significantly reduces the internalization of autocrine motility factors indicating that Cav1 could be negative regulator of caveolae internalization [Le et al. 2002]. However, Pelkmans and Zerial have shown that a fraction of caveolae are not immobile but are rather dynamic at the plasma membrane. They undergo continuous cycles of fission and fusion with the plasma membrane during which they do not travel long distances and maintain their structural integrity while shuttling between cytoplasm and the cell surface. This phenomenon dubbed 'kiss and run' was also shown to be regulated by serine/threonine kinases [Pelkmans et al. 2002].

It has been reported that budding of caveolae from the plasma membrane is regulated by kinases and phosphatases. Cells treated with tyrosine kinase inhibitor (e.g. genistein) showed reduced internalization of caveolae suggesting the involvement of proteins regulated by tyrosine phosphorylation [Pelkmans et al. 2002]. Interestingly, caveolin 1 (Cav1) was first described as a substrate of viral tyrosine kinase (v-src) and the cellular homologue of this kinase (c-src) has been shown to phosphorylate Cav1 at Tyr14 residue and bind the scaffolding domain

(CSD) of Cav1 [Glenny et al. 1989, Galbiati et al. 1999, Lee et al. 2000]. Furthermore, in endothelial cells, binding of albumin with its receptor gp60 (which is localized in caveolae) induces tyrosine phosphorylation of both gp60 and Cav1 and treatment of these cells with tyrosine kinase inhibitors prevented gp60-activated vesicle formation and albumin endocytosis. These data suggest that phosphorylation of Cav1 is that first step in caveolar internalization [Tiruppati et al. 1997]. In addition, src-induced phosphorylation on Tyr19 residue of caveolin 2 strictly colocalized with phospho-cav1 (TyrP14) suggesting that simultaneous phosphorylation of Cav1 and Cav2 might be important in the internalization of caveolae [Lee et al. 2002].

The role of GTP-binding protein dynamin in the fission and internalization of clathrin-coated pits has been extensively studied. As a result, when dynamin was found to be also recruited to caveolar membranes, it was naturally considered to play an important role in the endocytosis of caveolae [Oh et al. 1998, Henley et al. 1998]. However, it was later reported that dynamin is not a permanent component of caveolae and that association of dynamin with caveolae is a transient event [Pelkmans et al. 2002]. Predescu et al. found a very strong association of intersectin and dynamin in endothelial cells indicating that intersectin may serve as a scaffolding protein to recruit and sequester dynamin in order to achieve the high local concentration required for collar formation [Predescu et al. 2003]. As in the case of clathrin-mediated endocytosis, following hydrolysis of GTP, dynamin constricts the neck of caveolae triggering its fission and internalization from the plasma membrane. The cytoskeleton also plays an important role in the steady state distribution of caveolae. The cortical actin cytoskeleton interacts with caveolae/Cav1 (with the help of proteins such as EHDs and filamin A) and confines them to the cell surface acting as a simple barrier to the detachment of caveolae in

the absence of an endocytic stimulus [Muriel et al. 2011]. Following internalization, microtubules serve as tracks for the transport of Cav1 enriched vesicles thought the cytoplasm [Mundy et al. 2002, Hertzog et al. 2012]. Caveolae have also been reported to be actively internalized during cell division [Boucrot et al. 2011]. Despite these studies, caveolae-mediated endocytosis is still debated due to the lack of a cargo molecule found inside or uptaken through caveolae. Moreover, a recent study reports that bulk PM proteins are excluded from caveolae further questioning the role of caveolae in endocytosis [Shvets et al. 2015].

2.3.3 Mechanoprotection:

Early observations of abnormally high density of caveolae specifically in cells and tissues that are subjected to physiological stress (such as adipocytes, muscle cells, endothelial cells etc.) had long led to the hypothesis that caveolae might play a mechanoprotective role in shielding the PM from physical stress. In the mid 1970s, a couple of studies suggested that caveolae could act as 'membrane reservoirs' that would open and flatten to prevent rupture of the PM. This was based on the observations of opening of caveolar neck and a subsequent increase in the effective cell surface area from stretching smooth muscle cells [Dulhunty et al. 1975, Prescott and Brightman 1976, Gabella and Blundell 1978].

A landmark study from Sinha et al. confirmed the above hypothesis by demonstrating that stretching of plasma membrane causes flattening of caveolae (in an ATP- and actin-independent manner) thereby buffering the membrane tension variations resulting from mechanical stress. Considering the implications of Cav1/caveolae in mechanotransduction at the vascular endothelium [Rizzo et al. 1998, Rizzo et al, 2003, Yu et al. 2006], it was hypothesized that upon caveolar flattening, the caveolar coat proteins could be released which in turn might

participate in downstream signal transduction (Figure 12) [Sinha et al. 2011, Nassoy and Lamaze 2012, Gambin et al. 2014]. In this regard, we recently showed that EHD2 is released upon mechanical stress induced caveolae disassembly and translocates to the nucleus where it regulates gene transcription [Torrino et al. 2018] (also refer Annexe - I). This ability of caveolae to act as a spring or membrane reservoir that can be deformed in order to prevent membrane damage underlies many of the disease conditions associated with loss of caveolae, such as muscular dystrophies. For example, our lab recently reported that myotubes from patients having mutations in the *CAV3* gene (specifically P28L and R26Q) have abnormally low levels of caveolae at the PM and subsequently demonstrate impaired IL6/STAT3 signaling pathway resulting in constitutive activation and increased expression of muscle genes [Dewullf et al. 2019]. In addition, myotubes with defective caveolae are more susceptible to damage and zebrafish lacking the muscle-specific isoform of cavin1 or expressing dominant-acting mutants of Cav3 suffer increased membrane damage when subjected to excessive muscle activity [Sinha et al. 2011, Lo et al. 2015]. In a similar study, mechanical stress on endothelial cells induced through pharmacological stimulation of cardiac output or increased blood flow was shown to cause disassembly of endothelial caveolae. In addition, the endothelial cells were more susceptible to acute plasma membrane damage in the absence of caveolae [Cheng et al. 2015]. Cav3 levels and caveolae density are increased in Duchenne muscular dystrophy suggesting that caveolae may be upregulated to compensate for loss of other structural components of the sarcolemma [Repetto et al. 1999]. Recent findings that polymorphisms in CAV1 and CAV2 are associated with glaucoma and that loss of Cav1 is associated with increased susceptibility to PM damage upon experimental elevations of intraocular pressure indicate that the mechanoprotective roles of caveolae may be even more

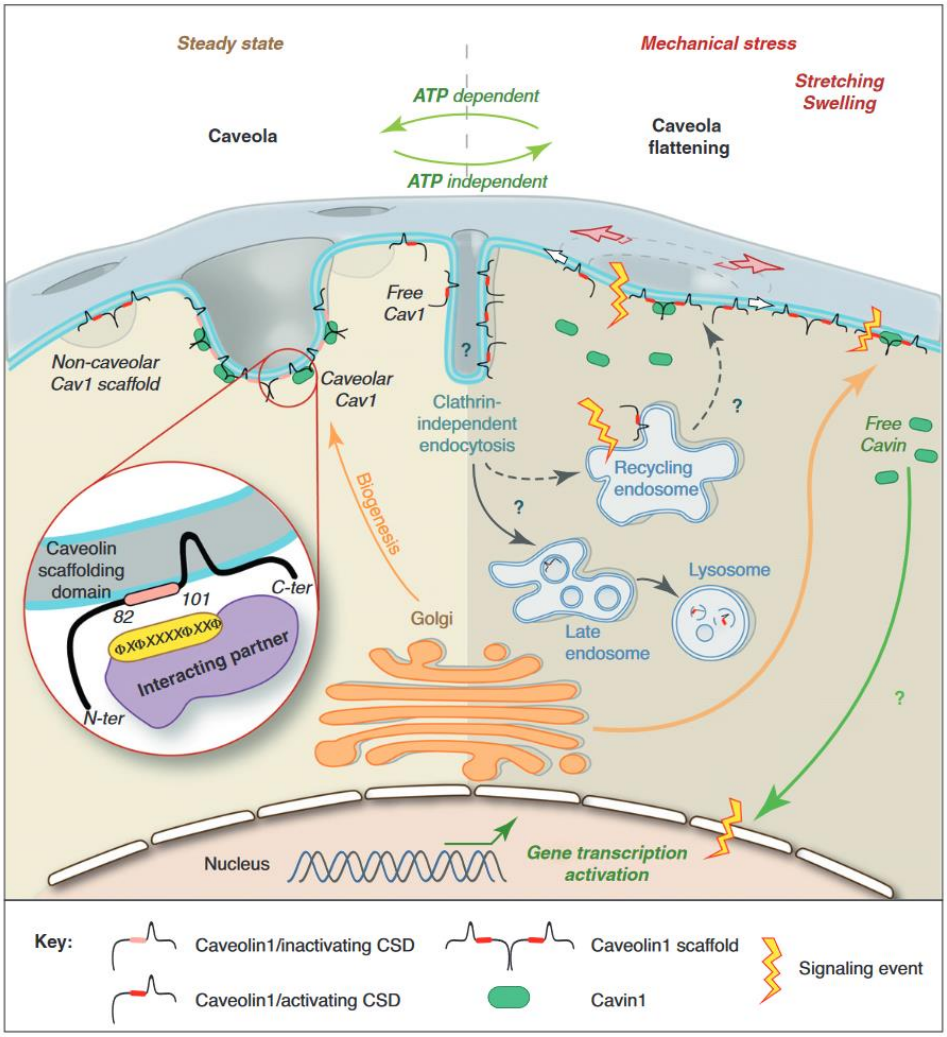

Figure 12: Molecular and cellular consequences of caveolar flattening induced by mechanical stress - Upon acute mechanical stress (hypo-osmotic swelling or stretching), caveolae flatten out in the plasma membrane to provide additional membrane and buffer membrane tension. Caveolar flattening releases Cav1 and Cavin-1 from the caveolar structure, increasing the amount of freely diffusing Cav1 and Cavin-1 at the plasma membrane. On the removal of the force, Cavin-1 and Cav1 rapidly reassemble into caveolae in an ATP-dependent process. This cycle represents the primary cell response to acute mechanical stress. Non-caveolar Cav1 is likely to be internalized by a clathrin-independent pathway that remains to be characterized. Endocytosed Cav1 becomes detectable in late endosomes (LE) and lysosomes, where it is degraded. It can also accumulate in the recycling endosome. Another possibility is that the released Cavins (green arrow) activate cellular processes to induce caveolar biogenesis, thereby increasing membrane reservoir size. Caveolar flattening can modulate mechanosignaling by several non-mutually exclusive mechanisms (lightning arrows). Released Cav1 and Cavins may interfere with the organization and dynamics of membrane microdomains and associated signaling molecules at the plasma membrane and endosomes. Gene transcription may be activated as a result of the nuclear translocation of released Cavins. Magnification shows insertion of Cav1 and the Cav1 scaffolding domain (CSD) into the caveolar structure [From Nassoy and Lamaze 2012].

widespread than previously thought [Elliott et al. 2016]. The majority of studies investigating mechanoprotective roles of caveolae have compared wild-type cells and tissues with cells or tissues lacking Cav1, Cav3, or cavin1. However, it is now known that these proteins show reciprocal regulation at the level of the transcription and translation (e.g. loss of Cav1 decreases levels of Cavin1).

Moreover, a recent study reported that the Hippo pathway which is a well known mechanotransducing pathway, is involved in regulating the expression of caveolar components. Yes associated protein 1 (YAP) and Transcriptional coactivator with PDZ-binding motif (TAZ), the major transcriptional mediators of the hippo pathway have been shown to regulate the expression of Cav1 and cavin1 through the TEA domain (TEAD). Interestingly, caveolae-deficient cells exhibit increased YAP/TAZ-TEAD activity suggesting feedback regulation between caveolar components and the hippo pathway in the context of cellular responses to mechanical stimuli [Rausch et al. 2019]. In another study, mice lacking pacsin3/syndapin3 were generated in order to address the specific role of the caveolae invagination itself. Skeletal muscle from these animals showed wild-type levels of Cav3 and cavin1 but a striking loss of caveolae. Unlike wild-type mice, PACSIN3 knockout mice showed excessive muscle damage including necrotic fibers and inflammation when subjected to physical exercise [Seemann et al. 2017]. The similarity of the phenotypes to those associated with Cav3 associated muscle disease provides further evidence for the model of caveolae flattening acting to protect muscle fibers against abrupt tear forces.

2.3.4 Signal transduction:

The idea that caveolae can play a vital role in regulation of signal transduction first

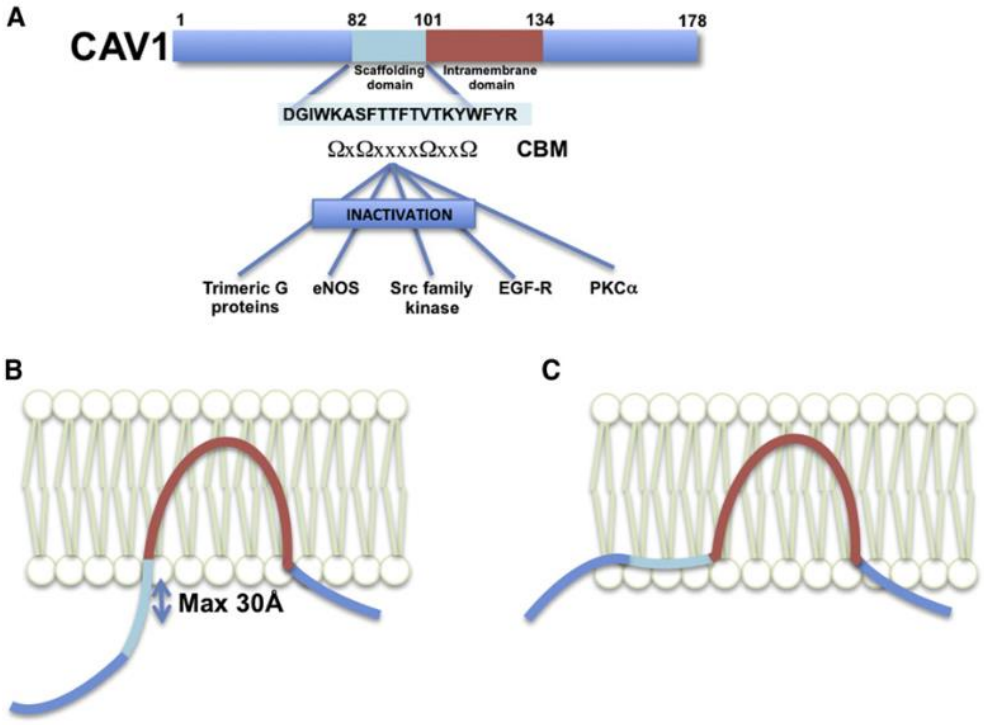

Figure 13: The caveolin signaling hypothesis

(A) an illustration of the caveolin signaling hypothesis as originally proposed by Okamoto et al. with some key interacting partners highlighted. The sequence of the caveolin-1 scaffolding domain (CSD) and the consensus caveolin-binding motif (CBM) are shown. (B and C) Two models for association of caveolin with the membrane bilayer. In the first model (B) the CSD is exposed in an extended conformation, allowing interactions with signaling proteins. In the second model (C), the CSD forms part of an amphipathic cholesterol-binding in-plane helix, and is an alternative model proposed by Kirkham et al. [From Collins et al. 2012]

arose from studies showing enrichment of numerous signaling proteins in detergent insoluble complexes prepared from cells and tissues [Sargiacomo et al. 1993]. Shortly after, the exclusivity of these biochemically defined complexes to caveolae was rejected as similar complexes were isolated from cells lacking caveolae, questioning the role of caveolae in signaling [Fra et al. 1994]. However, the proposed role of caveolae as signaling platforms was further strengthened when evidence for direct interactions between caveolin and numerous signaling proteins was reported as described below.

Signaling through caveolins: Li et al. were the first to show that a synthetic peptide matching the amino acid sequence between residues 80 and 101 of Cav1 inhibited Src kinase activity. Moreover, a GST fusion protein containing amino acids 61–101 of caveolin 1 preferentially interacts with inactive Src. The sequence between residues 80–101 was named the caveolin 1 scaffolding domain (CSD) [Li et al. 1996]. Phage-display screening identified a number of peptides with specificity for the scaffolding domains of Cav1 and Cav3, but not Cav2 (Figure 13). This motif, termed the caveolin binding motif (CBM) has two consensus sequences φXφXXXφ and φXXXXφXφ, where φ is aromatic [Couet et al. 1997]. A number of proteins that interact with Cav1 and Cav3 have been proposed to contain the CBM motif [Collins et al. 2012]. Perhaps the best example of caveolin mediated signal regulation is that of the endothelial nitric oxide (NO) pathway. Endothelial nitric oxide synthase (eNOS) interacts with Cav1 and is hyperactivated in cells/animals lacking Cav1. Moreover, its activity can be selectively modulated *in vitro* and *in vivo* by peptides corresponding to the caveolin scaffolding domain. Cells or animals treated with these peptides show striking functional effects, convincingly supporting the direct

interaction model for the caveolin signaling hypothesis [Garcia-Cardena et al. 1997, Sowa et al. 2001, Reese et al. 2013, Bernatchez 2020].

Despite the wealth of studies that outline a role for caveolin in signal regulation, the notion of caveolin signaling hypothesis has been a subject of controversy for a couple of reasons. Structural analysis of the putative CBMs in around 40 interaction partners of Cav1 suggest that the CBM is not exposed at the surface and is therefore unlikely to be available for interaction. The analysis also revealed no consensus structural motifs among these linear CBMs [Byrne et al. 2012, Collins et al. 2012]. Moreover, putative CBMs were also found to be extremely common in organisms lacking caveolins questioning the specificity of the caveolin signaling mechanism. In addition, there are also doubts about the accessibility of the CSD in caveolin. This highly amphipathic region of caveolin juxtaposes the putative hairpin intramembrane domain, and some studies suggest that this amphipathic region is at least partially buried within the bilayer denying interaction with cytoplasmic proteins [Kirkham et al. 2008]. As a result, precisely how caveolins regulate signaling is still unclear and requires further investigation.

Signaling through cavins: The demonstration that cavins are released upon caveolae flattening as a result of disassembly of their coat structure led to the natural hypothesis that the released cavins could play a role in transducing signal from the plasma membrane into the cell. Cavin1 (originally termed polymerase transcript release factor) was first identified as a regulator of ribosomal RNA transcription in the nucleus [Jansa et al. 1998]. Recent studies in adipocytes provide evidence for nuclear translocation of cavin1 following phosphorylation by insulin. Moreover, loss of cavin1 leads to an imbalance in ribosomal production with an excess of ribosomal proteins, causing nuclear stress and activation of p53 [Liu &

Pilch 2016]. The muscle-specific cavin isoform cavin4 dissociates from surface caveolae in response to hypo-osmotic shock induced caveolae flattening and accumulates in the nucleus in the absence of cavin1 [Lo et al. 2015]. Other non-caveolar roles of released cavins have been reported including regulation of lipolysis through phosphorylation of cavin1 [Aboulaich et al. 2011]. Since cavins are known to form homo- and hetero-trimeric sub-complexes, there may be a range of downstream targets regulated by distinct combinations of cavins [Gambin et al. 2014, Tillu et al. 2015]. More recently, cavin3 was shown to be released upon UV-light induced caveolae disassembly and function together with BRCA1 in multiple cancer related pathways [McMahon et al. 2021].

2.3.5 Lipid regulation:

Phenotypes in mice and humans lacking caveolae components (Cav1 or Cavin1) include lipodystrophy, and adipocyte dysfunction pointing to a role in the regulation of lipid trafficking, storage, and/or metabolism [Kim et al. 2008, Rajab et al. 2010]. *CAV1*$^{-/-}$ null mice lack efficient lipid droplet formation in hepatocytes during liver regeneration, leading to decreased survival after partial hepatectomy [Fernandez et al. 2006]. In addition, they have small adipocytes, are resistant to diet induced obesity and are insulin resistant [Razani et al. 2002]. The small size of adipocytes has been attributed to the dramatic decrease in cell surface phospholipid species such as phosphatidylserine and lysophospholipids suggesting a functional role on lipid droplet expandability [Blouin et al. 2010]. Cavin1 has been shown to play a direct role in the regulation of lipolysis and ribosome synthesis required for adipocyte maturation [Aboulaich et al. 2011, Liu and Pilch 2016].

Caveolae have also been implicated in glycosphingolipid transport and glycosphingolipids regulate caveolae formation and endocytosis [Singh et al. 2003, Sharma et al. 2004, Singh et al. 2010, Shvets et al. 2015]. GM3 is enriched in caveolae, and increasing levels of GM3 upregulate levels of Cav1 [Prinetti et al. 2010]. These studies emphasize a close relationship between caveolae and specific lipid species. Cholesterol has also been demonstrated to be pivotal for caveolae formation and integrity, and while depletion of cholesterol has been shown to cause loss of caveolae morphology and turnover of cavin2 [Rothberg et al. 1992, Hailstones et al. 1998, Breen et al. 2012], caveolae are in turn thought to be important for maintenance of the cholesterol balance in the cell [Ikonen & Parton 2000]. In some mammalian cells, such as many types of neurons, caveolae are absent, but Cav1 still plays an important role. For example, striatal neurons lack caveolae but express Cav1, which in these cells regulates cholesterol trafficking and functionally interacts with mutant Huntington's disease (HD) protein [Trushina et al. 2006].

Loss or overexpression of caveolar components affects membrane lipid properties including the degree of lipid order and the diffusion of lipids and lipid-anchored proteins in the membrane [Gaus et al. 2006, Hoffmann et al. 2010, Chaudhary et al. 2014]. At the level of PM, caveolae influence the nano-clustering of lipids, most prominently PS and PC and the nanoscale organization of lipid based signaling molecules. This effect is thought to be dependent on caveolar curvature as similar effects were observed upon flattening of caveolae suggesting that disassembly of caveolae can lead to significant changes in the bulk PM, influencing the organization of signaling domains [Hirama et al. 2017a, 2017b]. Loss of caveolae also results in the loss of spatial organization of GTP- and GDP-bound forms of H-

ras nanoclusters, whose formation is dependent on specific lipid nanoclusters [Prior et al. 2003, Ariotti et al. 2014]. These data suggest that caveolae are necessary for the organization of particular lipids at the PM and reveal a mechanism by which caveolae can impact signal transduction processes without directly interacting with membrane proteins.

2.4 Caveolinopathies: Caveolae and relationship to disease

A breakthrough contribution to our understanding of the importance of caveolae (caveolins and cavins) in the context of whole animal physiology was the generation of caveolin null mice. Given the diverse attributes of the caveolin proteins and their widespread tissue distributions, it was remarkably surprising that all of the caveolin deficient mouse models generated (Cav1 null, Cav2 null, Cav3 null, and Cav1/3 double knockout mice) were viable and fertile. In this chapter, we discuss our current understanding regarding the phenotypic characteristic of each of the aforementioned caveolin null mouse and how these relate to physiological processes and the pathogenesis of human diseases.

2.4.1 Caveolin-1:

Cav1 null mice have a complete absence of morphologically identifiable caveolae in all tissues and cell types that normally express Cav1 while retaining identifiable caveolae in tissues that normally express Cav3 (i.e., skeletal and cardiac myocytes). Therefore, the Cav1 null mouse unequivocally demonstrates its essential role in caveolar biogenesis in non-muscle cells [Drab et al. 2001, Razani et al. 2001]. Interestingly, Cav1 ablation results in loss of the Cav2 protein (by approx. 90%) in all Cav1 expressing tissues. It has been reported that this reduction in Cav2 protein levels is a result of its destabilization and subsequent proteasomal degradation,

rather than altered transcriptional regulation [Razani et al. 2002]. Hence it is important to consider that Cav1 null mice are essentially Cav2 deficient as well for the phenotypic characterization of Cav1-deficient mice.

Cancer: Cav1 was initially identified as a major substrate for tyrosine phosphorylation in Rous sarcoma virus-transformed chicken embryonic fibroblasts, suggesting that it may be a target for inactivation during oncogenesis [Glenney et al. 1989]. The discovery of caveolin binding motifs within cellular kinases involved in cancer and subsequent mapping of the Cav1 to a tumor suppressor locus (7q31) that is often deleted in most cancers, initiated several studies that further supported a role for caveolin 1 as a tumor suppressor. Several human breast cancer cell lines display decreased Cav1 expression levels compared to benign mammary epithelial cells. Re-expression of Cav1 in most of these cell lines was sufficient to decrease their proliferation highlighting the important role of Cav1 in breast cancer [Engelman et al. 1997, Fiucci et al. 2002]. Analysis of human breast cancer samples revealed that up to 16% of these cancers have a *CAV1* gene point mutation (P132L), with the majority of the mutations being found in invasive carcinomas. It was reported that the Cav1 (P132L) mutant is mislocalized and retained in the Golgi apparatus of cancerous cells. Furthermore, co-expression of the P132L mutant along with the wild-type Cav-1 cDNA resulted in the retention of the wild-type Cav1 protein in the Golgi, indicating that the P132L mutant promotes retention of wild-type Cav1 rendering it inactive in cells [Hayashi et al. 2001].

Although no specific mutations have been identified in the *CAV1* gene in prostate cancers, it has been shown to be upregulated in many primary prostate tumors and metastatic prostate cells (Table 3) [Yang et al. 1998]. Although the expression of Cav1 appears to be associated with the development of metastatic prostate cancer,

the role Cav1 plays in malignant progression remains controversial as it directly contradicts the tumor suppressing role in other cancers. One explanation for this dual behavior is the conversion of Cav1 from an integral membrane protein to a luminal secretory protein through phosphorylation of Cav1 at Ser80 within the ER. It is thought that phosphorylation at this site alters its membrane topology resulting in the regulated secretion of Cav1 from human prostate cancer cells that, in turn can stimulate cancer cell growth in an autocrine/paracrine manner [Tahir et al. 2001, Wu et al. 2002].

Vascular abnormalities: Studies of Cav1 null mice demonstrated its importance in the negative regulation of nitric oxide (NO) production via modulation of eNOS activity. It has been proposed that Cav1 within caveolae binds and inhibits membrane-bound eNOS via the CSD, thereby preventing the synthesis of NO [Li et al. 1996, Michel et al. 1997]. NO production leads to Src-mediated phosphorylation of Cav1 at Tyr14, promoting further eNOS binding in a negative feedback loop. Dysregulation of NO is associated with vascular disease, which has been invoked as an explanation for the cardiovascular phenotypes observed in Cav1 null mice [Zhao et al. 2002, Kolluru et al. 2010].

Angiogenesis is one of the hallmark features of tumorigenesis and essential for tumor growth. In vitro studies have demonstrated that Cav1 expression positively correlates with capillary tubule formation [Griffoni et al. 2000, Liu et al. 2002]. Histopathological and ultrastructural examination of melanoma tumors in Cav1 null mice showed that there was a decrease in blood vessel density and incomplete formation of capillaries along with a total absence of identifiable endothelial cell caveolae. These data indicate that loss of Cav1 can retard tumor growth via diminished angiogenic response [Woodman et al. 2003].

2.4.2 Caveolin-2:

Cav2 null mice were generated by targeted disruption of exons 1 and 2 of the murine *CAV2* gene [Razani et al. 2002]. Characterization of these mice clearly demonstrated that Cav2 is not necessary for caveolae formation or the proper membrane localization of Cav1. Moreover, Cav2 plays no observable role in the pathogenesis of several phenotypes described in the Cav1 null mouse (i.e., vascular dysfunction and lipid imbalance). However, Cav2 null mice display marked lung pathology, similar to that described in Cav1 null mice [Drab et al. 2001, Razani et al. 2001].

Interstitial lung diseases: Histopathological examination of lung specimens from Cav2 null mice revealed alveolar hyper-cellularity due to an increase in endothelial cell number and septal thickening due to an increase in extracellular matrix (ECM) depo-sition [Razani et al. 2002]. One physiological consequence of these pulmonary abnormalities was severe exercise intolerance, manifested by the early onset of exhaustion in Cav1 null mice during a swimming test [Drab et al. 2001]. These pathological abnormalities are analogous to the interstitial lung diseases (ILDs) in humans which are all similarly characterized by progressive, irreversible fibrosis and severely compromised gas exchange [Mazzoccoli et al. 2003].

2.4.3 Caveolin-3:

Characterization of *CAV3* knockout mice showed that they lack muscle cell caveolae yet maintain normal levels of Cav1 and Cav2 expression as well as normal caveolae in non-muscle tissue [Galbiati et al. 2001, Hassan et al. 2004]. Cav3 null mice exhibit muscle degeneration and mild myopathic changes similar to those observed in patients with Limb Girdle Muscular Dystrophy (LGMD-1C). Further characterization

revealed that they also develop a cardiomyopathic phenotype similar to that described above in Cav1 null animals.

Muscular dystrophy: The term muscular dystrophy (MD) refers to a broad range of phenotypically identical myopathies characterized by progressive muscle degeneration and replacement with fibrous connective tissue. The most common and severe form of MD is Duchenne (DMD) caused by a variety of mutations in the dystrophin gene, resulting in a deficiency of the protein product and loss of function of the dystrophin-glycoprotein complex (DGC). The DGC spans the muscle sarcolemma linking the cortical cytoskeleton with the extracellular matrix [Hoffman et al. 1989, Sciandra et al. 2003]. Dystrophin and several members of the DGC including α-sarcoglycan and β-dystroglycan co-immunoprecipitates with Cav3 in cultured mouse myocytes. Patient samples of DMD show that there is both an upregulation of Cav3 expression as well as an increase in the number and size of caveolae at the sarcolemma [Bonilla et al. 1981, Repetto et al. 1991]. Moreover, manual overexpression Cav3 in mice resulted in a severe DMD phenotype suggesting strictly regulated caveolin-3 expression in the pathogenesis of MD. However, it was not until the identification of two mutations in the human *CAV3* gene resulting in an autosomal-dominant form of limb-girdle MD (LGMD-1C), that the specific role of Cav3 in muscular pathogenesis was realized [McNally et al. 1998, Minetti et al. 2002].

LGMD-1C, linked to a missense mutation (P104L) in the membrane-spanning region and a deletion in the *CAV3* gene that removes residues 63–65 in the scaffolding domain. These two mutations result in a severe (approx. 95%) reduction of Cav3 expression in muscle tissue and a concomitant loss of sarcolemmal caveolae [Minetti et al. 2002]. The LGMD-1C Cav3 mutant protein forms unstable

aggregates with the wild-type Cav3 protein resulting in the intracellular retention of both wild-type and mutant Cav3 proteins at the level of the Golgi and leads to their ubiquitination and proteasomal degradation [Galbiati et al. 2000]. Additional studies have shown that dysferlin, a skeletal muscle membrane protein whose deficiency causes Miyoshi myopathy (MM) and limb-girdle muscular dystrophy type 2B (LGMD-2B), is mislocalized in skeletal muscle biopsies taken from LGMD-1C patients. Dysferlin contains Cav3 binding motifs and co-immunoprecipitates with Cav3 from normal skeletal muscle, suggesting that its interaction with Cav3 may serve an important function that remains undetermined [Matsuda et al. 2001]. It has also been reported that four previously identified missense mutations (R26Q, A45T, A45V, and P104L) in the *CAV3* gene is responsible for the pathogenesis of Rippling muscle disease (RMD) [Betz et al. 2001]. In addition, our lab recently demonstrated that patient myotubes bearing the CAV3 P28L and R26Q mutations display significantly reduced levels of caveolae at the plasma membrane and are therefore unable to buffer an increase in membrane tension induced by mechanical stress. This in turn correlates to impaired regulation of the IL6/STAT3 signaling pathway leading to its constitutive hyperactivation and increased expression of muscle genes [Dewulf et al. 2019].

2.5 Caveolae at the nanoscale

In keeping with the proverb 'seeing is believing', biologists have always seeked to visualize the processes that allow cells to maintain homeostasis and react to various environmental cues, both at the molecular level and in intact living specimens. The single-lens optical microscope and the simple compound microscope, first described in the 17th century by Anton van Leeuwenhoek and Robert Hooke respectively,

facilitated early observations of microscopic living organisms. Since then, a vast number of technological advancements and manufacturing breakthroughs have led to significantly advanced microscope designs facilitating dramatically improved image quality with minimal aberration, thereby making subcellular investigations possible.

2.5.1 The diffraction barrier:

Despite these advancements, glass based optical lenses used in current microscopes are still hampered by an ultimate limit in optical resolution imposed by the diffraction of light. In an imaging process through an optical microscope, light rays from each point on the object converge to a single point at the image plane. However, the diffraction of wave-like light prevents exact convergence of the rays, thereby causing an otherwise sharp point on the object to blur into a finite-sized spot referred to as the point-spread function (PSF). When imaging in the visible light spectrum ($\lambda \approx 550$ nm), an objective lens with a numerical aperture (NA) of 1.40 yields a PSF with a lateral diameter of ~200 nm and an axial diameter of ~500 nm. This is referred to as the Abbe's diffraction barrier or diffraction limit.

2.5.2 Beyond the barrier:

While the diffraction limit of optical resolution does not affect imaging at the tissue or organ level, most sub-cellular structures are smaller than the wavelength of light and hence pose an obstacle for elucidating biological processes at the cellular and molecular scale. This was overcome with the advent of techniques that enable imaging at sub-diffraction limit resolution without compromising non-invasiveness and biomolecular specificity. The so-called 'Super-resolution' or resolution beyond the diffraction limit has conventionally been achieved by two approaches - spatially patterned excitation and single molecule imaging. In the case of spatially patterned

excitation, sub-diffraction-limit features are introduced in the excitation pattern, which subsequently enables nanoscopic information read out. These include techniques such as stimulated emission depletion (STED), structured illumination microscopy (SIM) and reversible saturable optical fluorescence transitions (RESOLFT) [Hell et al. 1994, Gustafsson 2000, Hell 2005]. The second approach, as the name suggests, involves determining the precise localization of each fluorophore that stains the target of interest. Techniques such as stochastic optical reconstruction microscopy (STORM), photoactivated localization microscopy (PALM) and fluorescence photoactivation localization microscopy (FPALM) utilize this approach [Betzig et al. 2006, Hess et al. 2006, Bates et al. 2007]. In this section, we will focus on single molecule localization microscopy (SMLM).

2.5.3 Single molecule localization microscopy (SMLM):

In a conventional wide-field microscope, all of the individual fluorescent probe molecules emit light at the same time. As described above, diffraction causes these individual molecules to appear as a spot of ~200-300 nm in diameter. As a result, molecules closer than this spot size overlap and cannot be easily distinguished. By taking advantage of the different energy states that a fluorescent molecule undergoes, it was made possible to switch 'ON' only a small number of random sub-population of fluorophores in each frame of acquisition thereby helping pinpoint the precise localization of individual molecules that stain sub-microscopic structures. In SMLM, the total density of emitted molecules in each frame of acquisition is significantly lowered to a point at which detections from neighbouring fluorophores do not overlap so that their locations can be recorded with sub-diffraction precision (Figure 14). For example, two neighbouring molecules that would otherwise be recognized as a single spot if imaged simultaneously can be

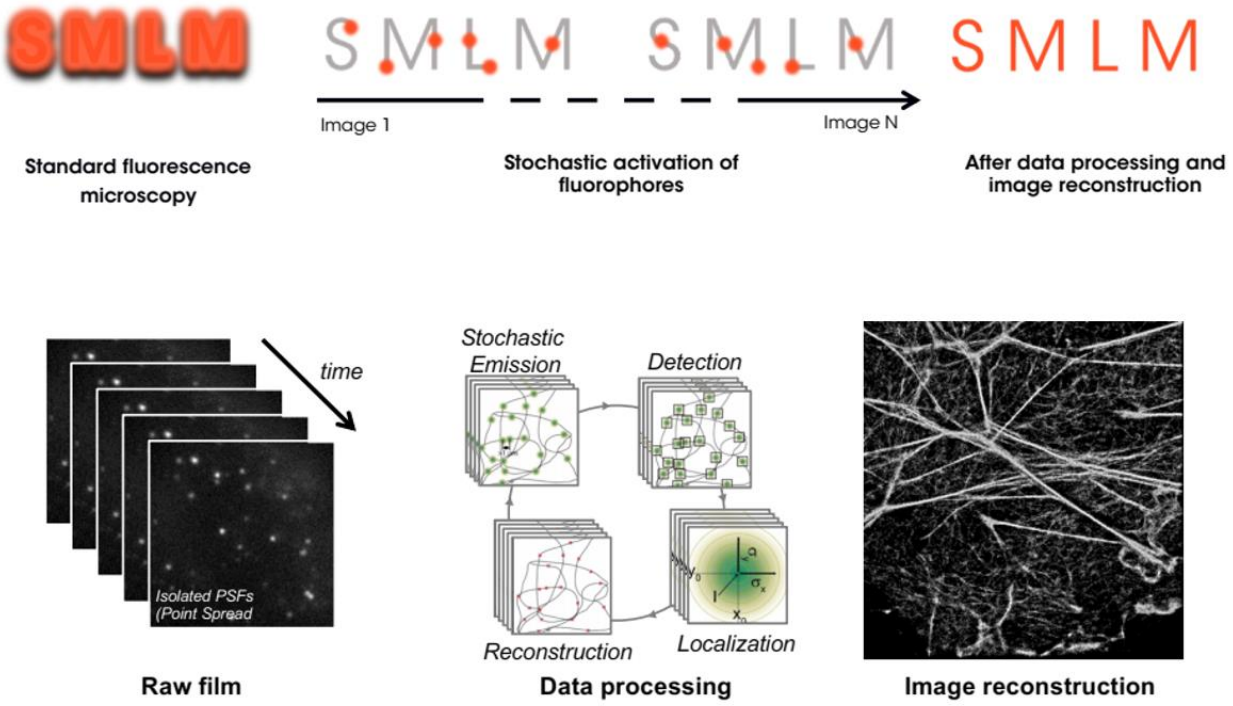

Figure 14: Principle of single molecule localization microscopy
SMLM relies on the ability to randomly activate only a subset of fluorescent molecules to distinguish them spatially. By repeating the process in consecutive image acquisitions, accumulated raw data are processed to detect single molecules with a nanometric precision (down to 10 nm). Data quantification and analysis are then performed to resolve either structures or dynamics at the nanoscale level. To reconstruct a nanoscopy image, each molecule is detected and localized by specialized algorithms. [From www.abbelight.com]

made to blink such that their locations are recorded in different frames [Hell et al. 2015]. However, in order to acquire the locations of enough molecules to generate a sufficiently detailed image, SMLM techniques typically require acquisition of hundreds of thousands of frames [Lelek et al. 2021].

2.5.4 STORMing the caves

Caveolae, with a size ranging between 60-100 nm are well below the limit of resolution of conventional fluorescence microscopes and hence most of our knowledge regarding the ultra-structure of caveolae have been from EM studies.

What EM offers in resolution, it lacks in the ability to differentially stain specific structures simultaneously for functional studies. Moreover, recent reports suggest the existence of subpopulations of Cav1 oligomers at the PM called 'scaffolds' that are not discernable through conventional fluorescence microscopy or EM techniques [Khater et al. 2018]. In this study, the authors use multi-proximity threshold (MPT) network analysis to define three distinct sub-populations of non-caveolar Cav1 (S1A, S1B and S2) in addition to *bona fide* caveolae. The smallest of these are the S1A scaffolds which are proposed to correspond to the previously identified ~14–15 Cav1 homo-oligomers [Monier et al. 1995, Sargiocomo et al. 1995]. Based on modularity analysis, the S1A scaffolds are suggested to dimerize and result in S1B scaffolds. In addition, S1A scaffolds combine to form both S1B dimers and the larger hemispherical S2 scaffold structures. On the other hand, caveolae modules are proposed to correspond in size to S1B and not S1A modules suggesting that caveolae formation may be a two-step process in which S1A scaffolds first combine to form dimers that then interact to form budded caveolae (Figure 15). In this regard, super-resolution techniques provide a solution in

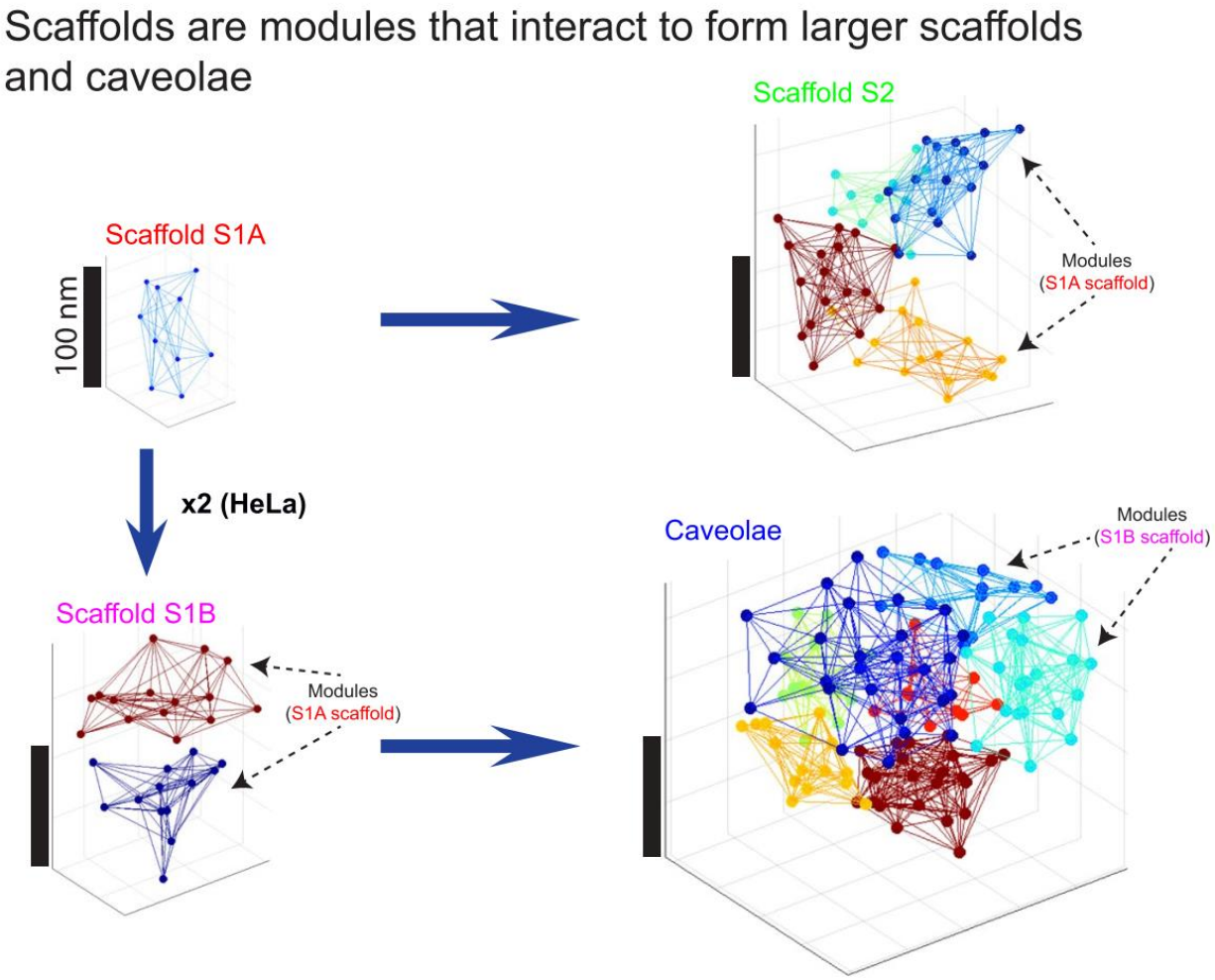

Figure 15: Organization of the 4 classes of Cav1 clusters
Modular interaction of Cav1 S1A scaffolds forms larger scaffolds and caveolae. Based on the modular analysis of blobs, S1A scaffolds are stable primitive structures that are used to build up more complex, modular S1B and S2 scaffolds. S1B scaffolds correspond to S1A dimers and are used to generate budded caveolae [From Khater et al. 2019].

obtaining nanometer resolution while staining caveolae specific proteins and also help to distinguish between the various populations of Cav1 reported. Several studies have taken advantage of nanoscopy techniques to study caveolae [Gabor et al. 2013, Wong et al. 2013, Fernandez et al. 2017, Yang et al. 2017]. While these studies have attempted to provide ultrastructural details, we still lack convincing nanoscopic visualization of caveolae on par with EM. We sought to address this aspect by utilizing a proprietary technique of Abbelight™ that combines 3D STORM and spectral demixing to enable nanoscopic visualization of caveolae and caveolar scaffolds for precise quantitative studies. Spectral demixing enables simultaneous multicolor acquisition using a robust ratiometric approach to spectrally separate thecontribution of far-red dyes [Lampe et al. 2015]. In addition, to realize 3D STORM, we used an astigmatic lens with HiLo illumination for precise localization of caveolae-specific molecules in the three-dimensional space.

2.6 Controlling caveolae assembly/disassembly using light

Living organisms have evolved a variety of photosensitive proteins, called photoreceptors or photosensors, to counteract light-related damage as well as to align with and harvest light. Often, these photoreceptors have distinct “dark/ground” and “light/activated” states which confer different functions to adapt to a light stimulus. Optogenetics, as the name suggests is a biological technique that exploits the information carrying property of light to control genetically encoded lightsensitive proteins, which in turn can influence diverse functions of cells. Optognetics was first conceived in the field of neuroscience due to the need to manipulate individual components of the brain (such as inactivation of neurons of just one type while leaving the others unaltered). This would require a technique that would require both spatial

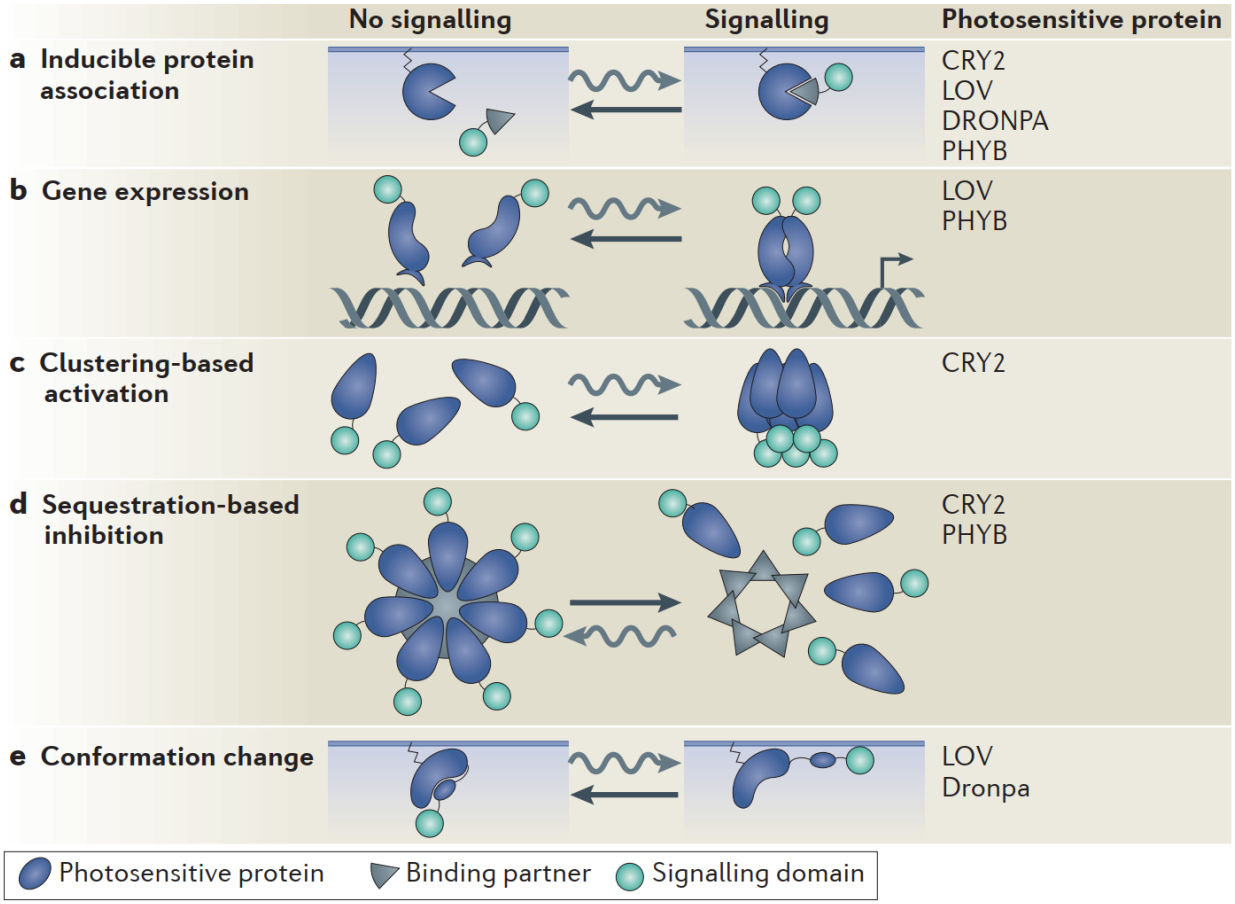

Figure 16: Different strategies of optogenetic manipulations
Optogenetically stimulated signals can be induced in various ways (the photosensitive proteins that have been used for each approach are listed). System reversion occurs either in the dark or can be stimulated with light depending on the system used. a) Heterodimerization is used to recruit a signalling domain to its substrate, which is commonly located on the plasma membrane. b) Homo-dimerization and hetero-dimerization techniques recruit transcriptional activators or other DNA-modifying proteins to the DNA to initiate the expression of a gene of interest. c) CRYPTOCHROME 2 (CRY2) naturally clusters when it is activated. By fusing CRY2 with signalling domains, the activities of which depend on domain density, signaling can be activated with light. d) Alternatively, signalling can be inhibited by sequestering a signalling protein away from its site of action. Proteins can be sequestered in cytosolic clusters or recruited to compartments away from their downstream effectors or upstream activators. e) Conformational changes in the photosensitive protein can expose a concealed signalling domain or relieve a protein from an allosterically autoinhibited state. [From Tischer and Weiner 2014]

and temporal resolution. While pharmacological and genetic manipulations can be specific to cells with certain expression profiles and provide spatial resolution to some extent, they lack the temporal precision on the timescale of neural coding and signaling. As a result of these needs, the first genetically engineered light-sensitive proteins were reported in 2002 when a yeast-two-hybrid system was coupled with photosensitive domains to create a light-regulated transcription system in yeast [Shimizu-Sato et al. 2002]. That same year, the discovery of light-gated ion channels was published [Nagel et al. 2002, Nagel et al. 2003]. Since then, light has been used to perturb and control a variety of cellular functions using different approaches (Figure 16) [Tischer and Weiner 2014, Liu and Tucker, 2017].

Strategies for light-based control of proteins utilize photosensory proteins and domains - molecules that undergo conformational changes upon photoexcitation. These can be broadly classified into two major classes. A first approach relies on manipulating protein subcellular localization wherein target proteins can be brought into proximity with their effectors/substrates, or alternatively tethered or sequestered at subcellular locations away from their effectors, resulting in stimulation or inhibition of activity. A second photo-control approach relies on triggering molecular changes within a target protein that are independent of subcellular localization. In this class of tools, light-induced conformational changes within photosensory domains lead to changes in the activity of the target proteins through clustering, complementation, steric, or allosteric mechanisms.

2.6.1 Lighting up the caves

As discussed in section 5.1 b, we sought to control the assembly and disassembly of caveolae in a localized and reversible manner. In this section, I will focus on the

description of the different optogenetic modules that were utilized to realize our objective.

The Cryptochrome 2 protein: Cryptochrome 2 (CRY2) is a blue light (405–488nm) sensitive protein from *A. thaliana*. Exposure to blue light induces two changes: the light-sensitive CRY2 protein homo-oligomerizes [Bugaj et al. 2013] and binds to its binding partner, CIB1 (Cryptochrome-Interacting Basic helix-loop-helix 1) [Mas et al. 2000], both processes taking place within seconds [Kennedy et al. 2010]. In the dark, CRY2 activated with blue light returns to its initial state within approx. 5 minutes. More recently, a new CRY2-derived optogenetic module, 'CRY2olig', which induces reversible protein oligomerization in response to blue light was reported [Taslimi et al. 2014]. This module facilitates light-induced co-clustering, that can be used to reversibly control diverse cellular processes with spatial and temporal resolution.

The LOV domains: The Light Oxygen Voltage (LOV) sensory domains from several different organisms have been used as optogenetic tools. They are all sensitive to blue light (440–473nm) and differ in how each one uses the light-induced conformational change to regulate cellular processes. One approach directly fuses the LOV domain to an effector protein and relies on the light-induced conformational change in the LOV domain to relieve the autoinhibition [Wu et al. 2009]. In some LOV systems, the LOV domains heterodimerize with natural or engineered binding partners [Strickland et al. 2012] whereas in other systems the domains homodimerize [Wang et al. 2012, Motta-Mena et al. 2014]. A recently reported LOV domain based system is LOVTRAP (LOV2 Trap and Release of Protein), an optogenetic approach capable of repeated and reversible control of protein activity with precise kinetics. The module is based upon a small protein

named Zdark (Zdk), that binds selectively to the dark state of LOV2, a photo-sensor domain from Avena sativa phototropin 1 [Wang et al. 2016].

CHAPTER 3: JAK/STAT PATHWAY – 'JACK OF ALL SIGNALING PATHWAYS'

Cellular fate is mainly decided by the intracellular signaling pathways that control mechanisms involved in phenotypical differentiation. This becomes even more significant in the case of cancer cells that rely upon a vast, complicated, and inter-connected network of signaling pathways for their survival and proliferation. Signaling pathways are mostly activated through cell membrane receptors that are triggered by different ligands, initiating cascades responsible for controlling phenotypical outcomes, e.g., proliferation, or apoptosis. For instance, receptor tyrosine kinases (RTKs, including epidermal growth factor receptor or EGFR, and human epidermal growth factor receptor 2 or HER2) and cytokine receptors are among the most important cell surface receptors that activate these signaling cascades. In addition to the diversity of the signaling pathways, these pathways are not completely independent, and are engaged in signaling "cross-talk." Janus tyrosine kinases (JAKs) and signal transducers and activators of transcription (STATs) - the major proteins of the JAK/STAT pathway - have been proposed to play a pivotal role in this inter-pathway crosstalk and recent research has led to the elucidation of a key role of JAK/STAT signaling pathway in a wide variety of biological processes such as hematopoiesis, innate and adaptive immune function, cell proliferation, differentiation, migration and apoptosis [Igaz et al. 2001; O'Shea et al. 2002; Villarino et al. 2017]. Furthermore, IFN-activated JAK/STAT signaling has been implicated in the pathogenesis of several biological disorders such as diabetes, obesity, autoimmune and inflammatory diseases and cancer [Zaidi & Merlino 2011, Benci et al. 2016]. Initiation of JAK/STAT signaling begins with the activation of JAK by binding of a ligand/cytokine such as growth factors, interferons, or interleukins to specific transmembrane receptors. Of all the

cytokines, interferon-mediated activation of JAK/STAT signaling is the most extensively studied.

3.1 Interferons:

Interferons were discovered in 1957 by British bacteriologist Alick Isaacs and Swiss microbiologist Jean Lindenmann as founding members of the cytokine family [Isaacs et al. 1957, Kisseleva et al. 2002]. Subsequently, this family of proteins was found to stimulate cellular networks that regulate resistance to viral infections, enhance immune responses, and modulate cell survival and death. There are three distinct interferon (IFN) families. The Type-I IFN family encodes 13 partially homologous IFNα subtypes in humans (14 in mice), a single IFNβ and several poorly defined single gene products (IFNε, IFNτ, IFNκ, IFNω, IFNδ and IFNζ) [Pestka et al. 2004]. The Type-II IFN family consists of a single member, IFNγ, that is predominantly produced in T cells and natural killer (NK) cells, and can affect cell types that express the IFNγ receptor (IFNγR) [Schoenborn et al. 2007, Lamaze and Blouin 2013]. The-Type-III IFN family consists of IFNλ1, IFNλ2, IFNλ3 (also known as IL-29, IL-28A and IL-28B, respectively) and IFNλ4, which demonstrate restricted activity, as the expression of their receptor is largely restricted to epithelial cell surfaces [Witte et al. 2010, Prokunina-Olsson et al. 2013, O'Brien et al. 2014]. After binding to high-affinity receptors, IFNs initiate a signaling cascade through signaling proteins that can also be activated by other cytokines.

All IFNs adopt α-helical structures with unique up-up-down-down topology [Walter et al. 2004]. Each IFN consists of six secondary structural elements denoted A-F, of which helices A, C, D, and F form an anti-parallel four helix bundle. The α-helices of the Type-I IFNs are long, straight, and essentially parallel to one another. All 16 IFNs adopt identical α-helical structure despite considerable sequence diversity. In contrast to Type-I IFNs, Type-III IFNs are comprised of shorter helices that contain several kinks,

which form a more compact bundle. Unlike monomeric Type- I and Type-III IFNs, Type-II IFNγ adopts an intercalated dimer structure, where helices E and F from one chain are "swapped" with the other subunit of the dimer. Therefore, each family of IFNs adopt a distinct α-helical scaffold to regulate engagement of their cellular receptors [Senda et al. 1995, Karpusas et al. 1997, Ouyang et al. 2012, Piehler et al. 2014].

3.2 Interferon receptors:

Cytokine receptors can activate JAK/STAT pathway through a plethora of combinations of different JAK and STAT family members highlighting the versatile nature of this pathway. The receptors in this family that are linked to JAK activation could be categorized as interferon (IFN) receptors, interleukin (IL) receptors and colony stimulating factor receptors (CSFRs). All Type-I IFNs bind a common cell-surface receptor known as the Type-I IFN receptor (IFNAR) [Pestka et al. 1987 and Pestka et al. 2004]. Type-II IFN-γ binds a different cell-surface receptor known as the IFNγ receptor (IFNGR) [Pestka et al.1997, Bach et al. 1997]. Likewise, Type-III IFNs bind yet another type of cell-surface receptor, which is composed of two chains, IFNλR1 (also known as IL-28 receptor-α, IL-28Rα) and IL-10Rβ [Kotenko 2003]. Both Type-I IFN receptor and the Type-II IFN receptor have multi-chain structures, which are composed of at least two distinct subunits - IFNAR1 and IFNAR2, and IFNGR1 and IFNGR2 respectively. Each of these receptor subunits interacts with a member of the JAK family. In the case of the Type-I IFN receptor, the IFNAR1 subunit is constitutively associated with tyrosine kinase 2 (TYK2), whereas IFNAR2 is associated with JAK1. In the case of the Type-II IFN receptor, the IFNGR1 subunit associates with JAK1, whereas IFNGR2 is constitutively associated with JAK2 [Darnell et al.1994, Ihle et al. 1995, Platanias et al. 2003, Chen et al. 2004]. In order to stay within the scope of our study, we will focus the discussion specifically on Type-I IFN receptors.

3.2.1 Type-I IFN receptor complex formation

The Type-I IFN receptor complex is distinct from both the Type-II and Type-III receptor complexes. The ectodomain (ECD) of the high-affinity subunit IFNAR2 is composed of two fibronectin type-III (FNIII)-like subdomains referred to as D1 and D2 respectively while the low-affinity receptor chain IFNAR1 consists of four FNIII-like subdomains referred to as SD1–SD4 [Uze et al. 1990, Novick et al. 1994]. IFNs initially bind the IFNAR2 receptor which then leads to the association of IFNAR1 to the IFN/IFNAR2 complex. IFNAR1 and IFNAR2 bind orthogonally on opposing sides of the IFN ligand that is characteristic of cytokine–receptor complexes. The IFNAR2-IFN interface is formed between the D1 subdomain of IFNAR2 and regions of helices A, E and the A–B loop of IFN. On the other hand, the IFNAR1–IFN interface involves contacts between helices B, C, and D of the IFN molecule and subdomains SD1-SD3 of IFNAR1 [Roisman et al. 2005, Akabayov et al. 2010, Thomas et al. 2011]. Binding of IFN ligand to IFNAR1 results in a conformational change that allows the ligand molecule to sit at the hinge between SD2 and SD3 with the long axis of the helical bundle lying perpendicular to the IFNAR1 receptor chain (Figure 17a). This facilitates efficient capping of top of the IFN molecule by SD1. While the IFNAR1 SD1-SD3 domains form an IFN-binding module, the SD4 domain is attached to SD3 by a flexible linker that allows the SD4 domain to adopt multiple conformations, even when bound to IFN [Li et al. 2008]. The stability of the IFN/IFNAR1/IFNAR2 interaction controls the number of transient open/closed binding events, thereby influencing the signaling strength. As a result, the stability of the IFN/IFNAR2 and IFN/IFNAR1 interactions regulates signaling [Walter 2020]. Formation of this ternary complex enables the juxtaposition of JAK1 and TYK2 (Figure 17b), leading to repositioning of their respective pseudokinase domains thereby relieving the self-

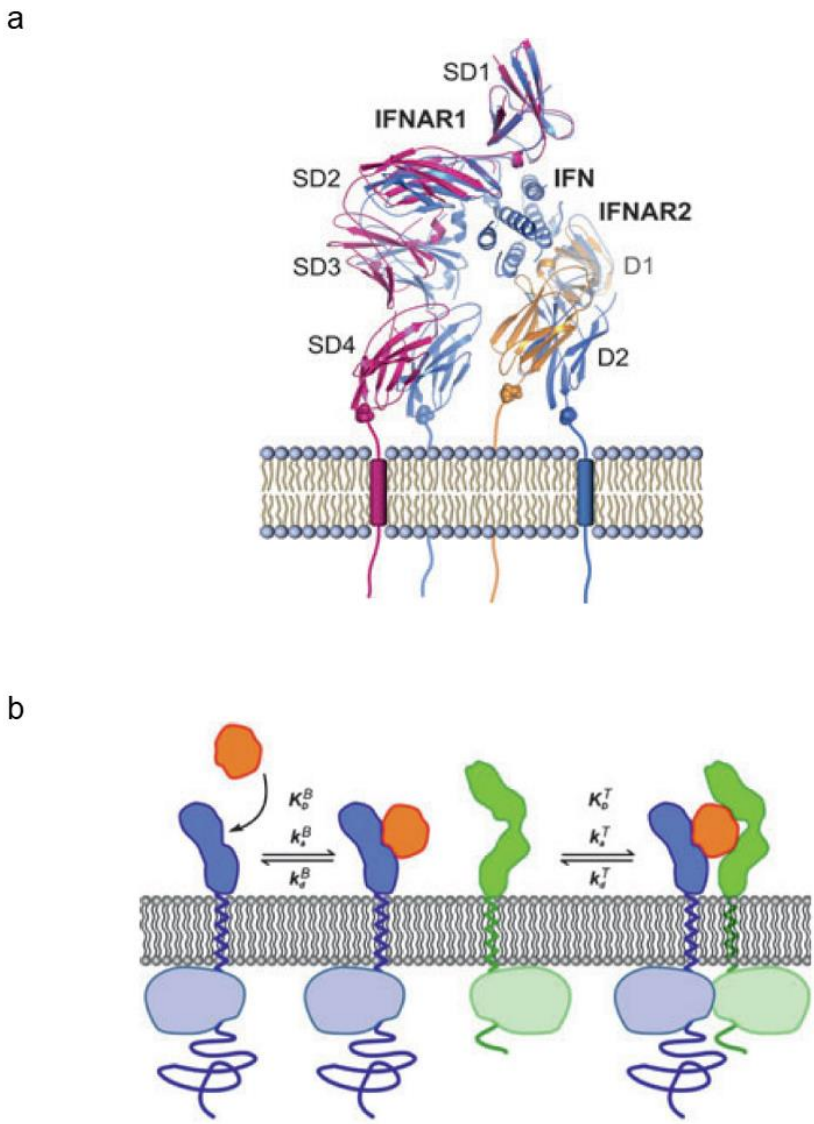

Figure 17. Structure and dynamics of IFN-IFNAR ternary complex formation.
(a) Ligand-induced conformational changes in IFNAR (based on a comparison of unbound and bound structures). The bound conformation is in blue. The domains of IFNAR1(SD1-4) and IFNAR2 (D1, D2) are illustrated. **(b)** Two-step assembly of the ternary IFN-receptor complex in the plasma membrane (orange, IFN; blue, IFNAR2; green, IFNAR1): rapid and high-affinity binding of IFN to IFNAR2 is followed by recruitment of IFNAR1 into the ternary complex. The dynamic equilibrium between binary and ternary complexes depends on the dissociation constant K_D^T and concentrations of the receptor subunits. K_a^B: binding affinity of IFN to IFNAR2; K_D^T: binding affinity of IFN to IFNAR1 [From Piehler et al., 2012].

inhibition imposed by the JH1/JH2 domains of JAK1 and activation of subsequent downstream cascade as described in later sections [Babon et al. 2014].

3.2.2 Receptor organization at the PM:

Since the initial postulation of the fluid mosaic model of the PM in 1972 by Jonathan Singer and Garth Nicolson, decades of research have led to the conclusion that the plasma membrane displays non-random protein distribution (lateral organization) which is a prerequisite for several key cellular processes such as cell signaling and cell adhesion. In most cases, protein function is directly coupled to the lateral organization by clustering of proteins in functional membrane domains or separating them in different domains. Moreover, the formation of these protein domains occurs over a broad range of length scales and is highly dynamic [Garcia-Parajo et al. 2014]. Recent advancements in super-resolution microscopy have enabled nanoscopic investigations of proteins at the PM. One such study demonstrated that overexpressed IFNAR1 and IFNAR2 partially co-clustered in nanoscale domains and were frequently found in the vicinity of actin structures [Wilmes et al. 2012]. In addition, another study confirmed the confinement of the receptor chains at physiological density in the cortical actin meshwork using quantum dot tracking and localization microscopy [You et al. 2016]. In summary, these studies provide insights into the nanoscale partitioning of IFNAR chains that are confined in actin-dependent nanodomains at the PM.

3.3 Janus Kinases (JAKs):

There are a total of four members in the JAK family of non-receptor tyrosine kinases - JAK1, JAK2, JAK3, and TYK2 - which are ubiquitously expressed except JAK3 whose

expression is restricted to hematopoietic cells and is highly regulated during cell development [Wilks et al. 1989, Firmbach-Kraft et al. 1990, Kisseleva et al. 2002, Levy et al. 2002, O'Shea et al. 2002]. At the cellular level, JAKs are predominantly found in the cytosol when expressed in the absence of cytokine receptors, but localize to endosomes and the PM in the presence of their cognate receptors [Ragimbeau et al. 2003, Hofmann et al. 2004]. The link between JAKs and cytokine signaling was first demonstrated using mutant cell lines that lacked TYK2. Naturally, these cell lines lacked responsiveness to IFNs and expression of TYK2 in these mutant cell lines restored IFN signaling [Velazquez et al. 1992].

3.3.1 Structure of JAKs

JAKs range in size from 120 to 140 kDa and due to their large size and consequent difficulties in purifying them, the full three-dimensional structures of JAKs have not yet been resolved. Seven JAK homology (JH) domains have been predicted, numbered from the carboxyl to the amino terminus. The JH1 domain at the carboxyl terminus has all the features of a typical eukaryotic tyrosine kinase domain. Adjacent to the JH1 domain is a catalytically inactive pseudokinase or kinase-like domain (JH2) [Manning et al. 2002]. This tandem architecture of kinase domains is a hallmark of JAK kinases and gives them their name as they are two-faced just like the Roman god Janus (Figure 18). Although the pseudokinase domain lacks catalytic activity, it has an essential regulatory function as mutations within this domain abrogate kinase activity [Chen et al. 2000, Saharinen et al. 2000]. The amino terminus of JAKs contains an SH2-like domain (JH3-JH4) and a FERM (Band-4.1, ezrin, radixin, moesin) homology domain (JH6-JH7). The FERM domain is implicated in mediating interactions with transmembrane proteins such as cytokine

receptors. In addition, the FERM domain has been reported to bind the kinase domain and positively regulate catalytic activity [Zhou et al. 2001].

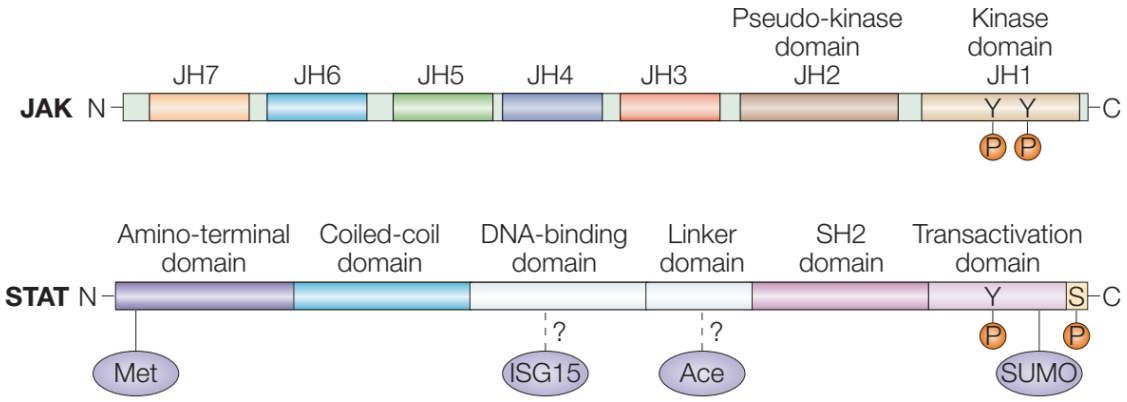

Figure 18: General structure of JAKs and STATs
The domains JH1–JH7 are based on sequence similarity of four known JAKs. JH1 is the kinase domain, which contains two tyrosines that can be phosphorylated after ligand stimulation. JH2 is the pseudo-kinase domain. The JH6 and JH7 domains mediate the binding of JAKs to receptors. The activity of STATs can be regulated by protein modification, including tyrosine and serine phosphorylation, methylation (Met), sumoylation(SUMO), ISGylation (ISG15) and acetylation (Ace). The modification sites of ISGylation and acetylation has not been identified.

3.3.2 Role in intracellular crosstalk

The pivotal role of JAKs in intracellular signaling is not limited to the JAK/STAT pathway. Over the years, crosstalk between JAKs and other well-known signaling pathways has been documented. For example, in myeloproliferative disorders, activation of two major signaling pathways - PI3K/Akt and Ras/Raf/MAPK/ERK - were found to be mediated through JAK2. It is proposed that JAK2-mediated ERK activation is regulated through Ras and via SH2-domain containing transforming protein (SHC), growth factor receptor-bond protein (GRB), and son of sevenless (SOS) proteins [Fernandez-Perez et al. 2013, Spolski et al. 2014]. In addition, activation of PI3K has been suggested to take place via phosphorylation of Insulin

Receptor Substrate 1/2 (IRS1/2) [Vansaun et al. 2013]. Other members of the JAK family are involved in the activation of the catalytic subunit (p110) of PI3K, and MAPKs via phosphorylation of Vav Guanine Nucleotide Exchange Factor (VAV) or other guanine-nucleotide-exchange factors (GEFs) [Platanias et al. 2005]. Multiple studies have reported direct activation of focal adhesion kinases (FAKs) through JAK2 [Zhu et al. 1998, Swiatek-Machado et al. 2012, Zheng et al. 2014]. Furthermore, JAK1 was identified as an interacting partner of paxillin and has been reported to be involved in the assembly of invadosomes [Petropoulos et al. 2016]

3.3.3 Activation

Unlike Receptor Tyrosine Kinases (RTKs), cytokine receptors do not possess an intrinsic kinase domain, and therefore rely on the JAK family of kinases to transfer the extracellular signals to the cytoplasmic components of the cascade [Babon et al. 2014]. JAKs associate with cytoplasmic domains of cytokine receptors via JAK binding sites that are located close to the membrane and form a complex that is equivalent in function to RTKs [Behrmann et al. 2004]. As stated above, members of the JAK family are composed of seven different JAK homology (JH) domains. JH1 and JH2 form the kinase and pseudo-kinase domains respectively while the N-terminus half of all four members is made up of the FERM domain (JH5, JH6, JH7) and the Src-homology 2 (SH2) domain (JH3 and JH4). The FERM and the SH2 domains facilitate binding of JAK to the cytoplasmic tail of cytokine receptors [LaFave et al. 2012, Wallweber et al. 2014]. Binding of a ligand to a cytokine receptor (for e.g. binding of IFNα to IFNAR) reorients the receptor/JAK dimers, which brings the JAKs close enough to transphosphorylate the partner JAK in the dimer at JH1. Activated JAKs in turn, phosphorylate the residues on the cytoplasmic tail of the cytokine receptor to create docking sites for recruitment of downstream

proteins with SH2 domains, e.g., STAT family of proteins (Figure 19) [LaFave et al. 2012]. Although it has been demonstrated that different cytokine receptors have preferences for a specific JAK family protein that is used as a signaling effector, there are cases where in the absence of the specific JAK family member, other proteins in the family have taken over [Ghoreschi et al. 2009, Morris et al. 2018].

3.4 Signal transducers and activators of transcription (STATs):

There are a total of seven members in the mammalian STAT family (STAT1, STAT2, STAT3, STAT4, STAT5a, STAT5b, and STAT6). They range in size from 750 to 900 amino acids and feature several conserved domains. Upon ligand binding, receptor-associated JAKs become activated (refer JAK activation) leading to the phosphorylation of a specific receptor tyrosine residues [Mertens et al. 2006]. These receptor phosphotyrosyine residues direct the SH2-dependent recruitment of specific STATs, which in turn become JAK substrates. Activated STATs are released from the receptor as they reorient into an antiparallel dimer, where the SH2 domain of one STAT binds a highly conserved C-terminal phosphorylated tyrosine residue of the other STAT. These activated STAT dimers translocate to the nucleus and bind to specific enhancer elements. [Shuai et al. 2003, Rawlings et al. 2004, Platanias et al. 2005, Bousoik et al. 2018]

3.4.1 Structure of STATs

Biochemical, genetic, and structural studies have identified seven conserved STAT domains, including the amino-terminal (NH2), coiled-coil, DNA-binding (DBD), linker (Lk), SH2, tyrosine activation (Y), and transcriptional activation domains (TAD). The NH2 domain (approx. 125 residues) is a structurally independent moiety that directs homotypic dimerization of inactive STATs and is also implicated in nuclear import and export [Mertens et al. 2006]. The adjacent coiled-coil domain (residues

135–315) consists of a four-a-helix bundle that protrudes laterally from the core structure and provides a large hydrophilic surface and binds regulators. The DNA-binding domain (residues 320–480) consists of a b-barrel immunoglobulin fold that directs binding to the growth arrest specific (GAS) family of enhancers. The adjacent linker domain (residues 480–580) ensures appropriate conformation between the DNA-binding and dimerization domains. The SH2 domain (residues 575–680) is the most highly conserved domain between the members of the STAT family as it is crucial for receptor recruitment and dimerization. The tyrosine activation domain (residue 700 onwards) is positioned directly adjacent to the SH2 domain, precluding self-association. The remaining carboxyl-terminal residues vary considerably among STAT family members and constitute the TAD. This diversity enables STATs to associate with distinct transcriptional regulators (Figure 18).

3.4.2 Recruitment and translocation to nucleus

As stated above, inactive/latent STATs exist in the cytoplasm. Following activation of JAKs through ligand binding, a highly conserved C-terminal tyrosine residue is phosphorylated, enabling STATs to form stable homodimers or heterodimers with other STAT proteins via SH2 domain interactions. The STAT dimers then translocate into the nucleus, where they act as transcription factors. Although most STATs form homodimers, formation of heterodimers (including STAT1/2, STAT1/3, and STAT5a/b) have also been reported [Subramaniam et al. 2001]. STAT1 has been reported to exist as pre-formed homodimers, and phosphorylation induces a conformational change (anti-parallel to parallel conformation) which is suggested to be true for other STATs as well [Mertens et al. 2006]. While translocation between cytoplasm and nucleus is a common intracellular occurrence, the nuclear envelope presents a barrier preventing free diffusion of large molecules (more than 40–60

kDa in molecular weight). As a result, STATs require a specific transport receptor called importins for facilitated transport into the nucleus [Hulsmann et al. 2012]. Following translocation to the nucleus, STATs initiate and regulate transcription by binding specific sites in the promoters of IFN-stimulated genes (ISGs) (Figure 19) [Darnell et al. 1994, Chen et al. 2004].

3.4.3 Serine phosphorylation of STATs

Although phosphorylation of tyrosine residues in STATs by activated JAKs is a crucial step for the formation of the various STAT complexes and their translocation into the nucleus, several other events that either involve modification of STATs or their interaction with other proteins that function as transcriptional coactivators are also important for optimal IFN-regulated gene transcription. One such modification is the serine phosphorylation of STATs. All STATs (with the exception of STAT2) have at least one serine residue in their TAD that is phosphorylated [Decker et al. 2000]. Conserved phosphorylation sites included Ser727 in STAT1 and STAT3, Ser721 in STAT4, Ser725 in STAT5a, Ser730 in STAT5b and Ser756 in STAT6. In addition, STAT1 and STAT5 possess at least one additional serine phosphorylation site in their TAD - Ser708 and Ser779 respectively [Wang et al. 2000]. Both Type-I and Type-II IFNs induce phosphorylation of STAT1 and STAT3 on Ser727, which is located in their C-terminal domain. Ser727 phosphorylation is not required for proper translocation to the nucleus or for their binding to the promoters of ISGs, but it is essential for full transcriptional activation [Wen et al. 1995, Wen et al. 1997]. One kinase that interacts with STAT1 and regulates Ser727 phosphorylation in response to either Type-I or Type-II IFNs is a member of the protein kinase C (PKC) family, PKC-δ [Uddin et al. 2002, Deb et al. 2003, Kristof et al. 2003]. Moreover, recent research suggests that additional IFN-dependent serine kinases such as

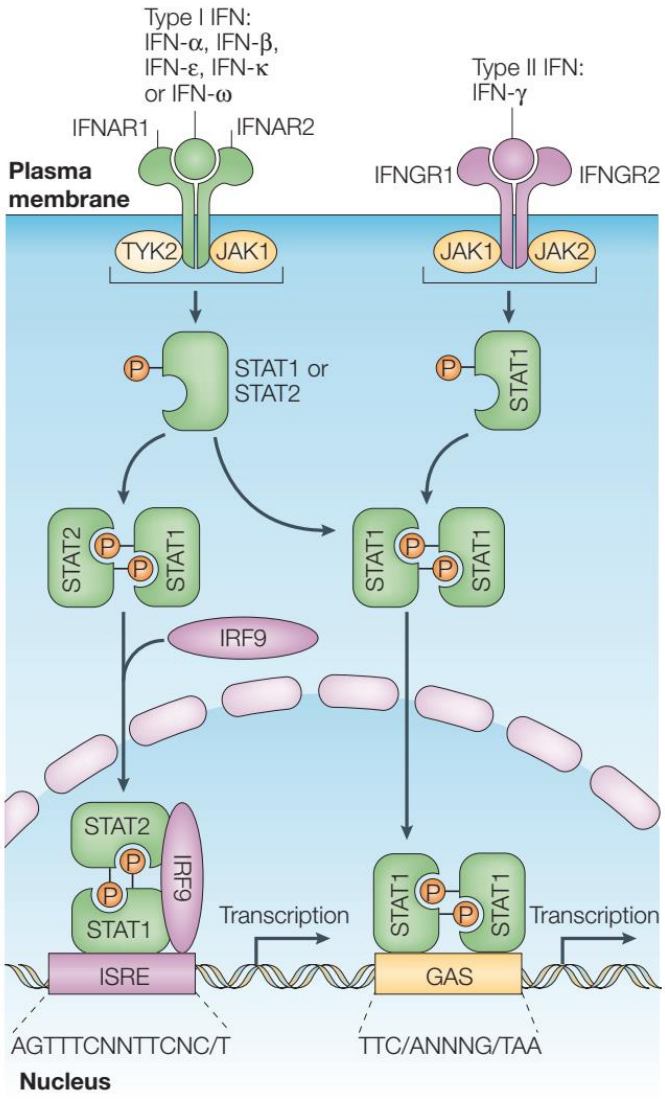

Figure 19: Activation of JAK-STAT pathway by Type-I and Type-II IFNs

All Type-I interferons (IFNs) bind a common receptor known as the Type-I IFN receptor. The Type-I IFN receptor is composed of two subunits, IFNAR1 and IFNAR2, both of which are associated with the Janus activated kinases (JAKs) - tyrosine kinase 2 (TYK2) and JAK1, respectively. The only Type-II IFN, IFN-γ, binds a distinct cell-surface receptor known as the Type-II IFN receptor. This receptor is also composed of two subunits, IFNGR1 and IFNGR2, which are associated with JAK1 and JAK2, respectively. Activation of the JAKs that are associated with the Type-I IFN receptor results in tyrosine phosphorylation of STAT2 (signal transducer and activator of transcription 2) and STAT1 leading to the formation of STAT1–STAT2–IRF9 (IFN-regulatory factor 9) complexes. These complexes translocate to the nucleus and bind IFN-stimulated response elements (ISREs) in DNA to initiate gene transcription. Both Type-I and Type-II IFNs also induce the formation of STAT1–STAT1 homodimers that translocate to the nucleus and bind GAS (IFN-γ-activated site) elements that are present in the promoter of certain ISGs, thereby initiating the transcription of genes. [From Platanias et al. 2005].

extracellular signal-regulated protein kinase (ERK), p38 and JUN N-terminal kinase(JNK) might be activated in a cell-type-restricted manner and that are involved in the regulation of STAT1 Ser727 phosphorylation.

3.5 Regulation of interferon-induced JAK/STAT pathway

As discussed earlier, JAK/STAT is a key signaling pathway that controls a multitude of critical cellular processes in response to extracellular stimuli. Therefore, a tight regulation is essential to prevent unwanted responses leading to dramatic consequences at the whole organism level. In this regard, several regulatory mechanisms have been setup at each level of the signaling pathway to ensure correct signal activation, termination and desensitization. Recent studies have shown that JAK/STAT signaling can be regulated at many steps through distinct mechanisms. Key regulators include the suppressor of cytokine signaling (SOCS) proteins and the recently discovered protein inhibitor of activated STAT (PIAS) family, as well as various protein tyrosine phosphatases (PTPs). The modulation of JAKs and STATs by various protein modifications and the cross-talk between different JAK/STAT pathways and other cellular signaling pathways provide additional levels of regulation that might be crucial.

3.5.1 Regulation at the level of IFNARs:

Apart from the fact that the different IFN types use distinct transmembrane receptors for signal transduction, the ability of cells to respond to cytokines is absolutely dependent on the presentation of the required receptor components on the cell surface. As a result, the distribution of IFN receptor components at the PM is strictly regulated and the different types of IFN have either widespread or cell/tissue-specific functions based on the presentation of their receptors at the cell surface of target cells. As stated above, in order to avoid the development of

uncontrolled signaling leading to inflammation and lethality, the levels of IFN receptors at the PM are regulated through various mechanisms. These include the induction of ligand-induced receptor downregulation, ubiquitination and proteolytic receptor degradation. Moreover, both clathrin-mediated and clathrin-independent endocytosis have been demonstrated to be involved in the regulation of IFN receptor levels on the surface of target cells. Blocking clathrin-mediated endocytosis of IFNAR using the dominant negative mutant DynK44A or a siRNA against the clathrin heavy chain resulted in drastic reduction of STAT1 and STAT2 phosphorylation levels induced by IFN-α but not by IFN-γ [Marchetti et al. 2006, Zanin et al. 2021]. To complicate the matter further, the mechanisms of regulation vary between the two receptors and also upon the ligand stimulus. At steady state, the decay of IFNAR1 has been shown to be more pronounced than that seen for IFNAR2 in certain cell types, reflecting differential regulation of the two receptors [Marijanovic et al. 2007].

3.5.2 Regulation at the level of JAKs:

JAKs are mainly regulated at the post-translational level through various mechanisms as discussed below.

3.5.2.1 Regulation by SOCS

SOCS proteins are the most thoroughly studied regulators of JAK–STAT signaling. The SOCS family of proteins consists of eight members: CIS (cytokine-inducible SH2 domain protein) and SOCS1–SOCS7 [Hilton et al. 1998, Hilton et al. 1999]. All members of the SOCS family contain an SH2 domain, which is flanked by a variable amino-terminal domain and a carboxy-terminal SOCS box (Figure 20) [Kile et al. 2002]. SOCS proteins are generally expressed at low levels in unstimulated cells and become rapidly induced by cytokines, thereby

inhibiting JAK–STAT signaling and forming a classic negative-feedback loop [Greenhalgh et al. 2001]. SOCS1 has been shown to inhibit Type-I IFN signaling not via a direct interaction with IFNAR1 but rather through an interaction with the IFNAR1 associated kinase Tyk2 [Piganis et al. 2011]. However, SOCS3-mediated inhibition of JAKs requires binding of SOCS3 to the activated receptor [Nicholson et al. 1999, Sasaki et al. 2000]. Interestingly, it has been recently reported that that cavin1 interacts with SOCS3 and that proper localization of SOCS3 to the plasma membrane is cavin1 dependent. Deletion of SOCS3 was shown to significantly abrogate the expression of cavin1 and cav1 proteins, thereby reducing caveolae numbers in endothelial cells. More importantly, depletion of cavin1 resulted in enhanced cytokine-stimulated STAT3 phosphorylation and abolished SOCS3-dependent inhibition of IL-6 signaling by cAMP suggesting a new mechanism linking SOCS3-mediated inhibition of cytokine signaling to cavin1 mediated localization at the plasma membrane [Williams et al. 2018]. On the other hand, rather than acting on JAKs, CIS seems to inhibit STAT activation by competing with STATs for binding to the receptor docking sites [Yoshimura et al. 1998]. Finally, SOCS proteins have also been implicated in the degradation of signaling proteins through the ubiquitin-proteasome pathway. The SOCS box binds to elongins B and C, which are known components of ubiquitin E3 ligase complex and can target signaling proteins for degradation [Kamura et al. 1998, Zhang et al. 1999].

3.5.2.2 Regulation by tyrosine phosphatases

Several protein tyrosine phosphatases (PTPs) have been suggested to regulate JAKs, including SHP1, SHP2, CD45, PTP1B and T-cell PTP (TCPTP). SHP1 and SHP2 are SH2-domain-containing PTPs. Genetic and mutation studies have

indicated that SHP1 and SHP2 have a role in the dephosphorylation of JAK1 and JAK2 thereby preventing activation of JAKs and the subsequent downstream cascade [Neel et al. 1993, Kingmuller et al. 1995]. CD45 is a receptor PTP that can directly bind and dephosphorylate all JAKs as enhanced JAK phosphorylation is observed in $CD45^{-/-}$ cells [Irie-Sasaki et al. 2001]. PTP1B and TCPTP, which are two highly related PTPs, have also been suggested to dephosphorylate JAKs (Table 4). JAK2 and TYK2, but not JAK1, serve as substrates of PTP1B whereas JAK1 and JAK3 are dephosphorylated by TCPTP [Myers et al. 2001, Simoncic et al. 2002].

3.5.3 Regulation at the level of STATs:

3.5.3.1 Regulation by PIAS

The mammalian PIAS family consists of four members: PIAS1, PIAS3, PIASX and PIASY. In addition, splice variants of PIAS proteins also exist. For example, PIAS3β contains a small insertion of 39 amino acids that is absent from PIAS3 [Liu et al. 1998]. The most highly conserved domain of the PIAS family is a RING-finger-like zinc-binding domain (RLD) in the central part of PIAS (Figure 20). After cytokine stimulation, PIAS1, PIAS3 and PIASX interact with STAT1, STAT3 and STAT4, respectively. In addition, PIASY has also been shown to be associated with STAT1 [Chung et al. 1997]. The PIAS–STAT interaction is cytokine dependent and PIAS proteins do not interact with STATs in unstimulated cells. The cytokine dependency of the interaction might be explained by the finding that PIAS1 can bind to the dimeric, but not the monomeric, form of STAT1 [Liao et al. 2000]. Each member of the PIAS family has been shown to inhibit STAT-mediated gene activation. PIAS1 and PIAS3 can inhibit the DNA-binding activity of STAT1 and STAT3, respectively. In contrast, PIASX and PIASY can inhibit STAT4 and STAT1-

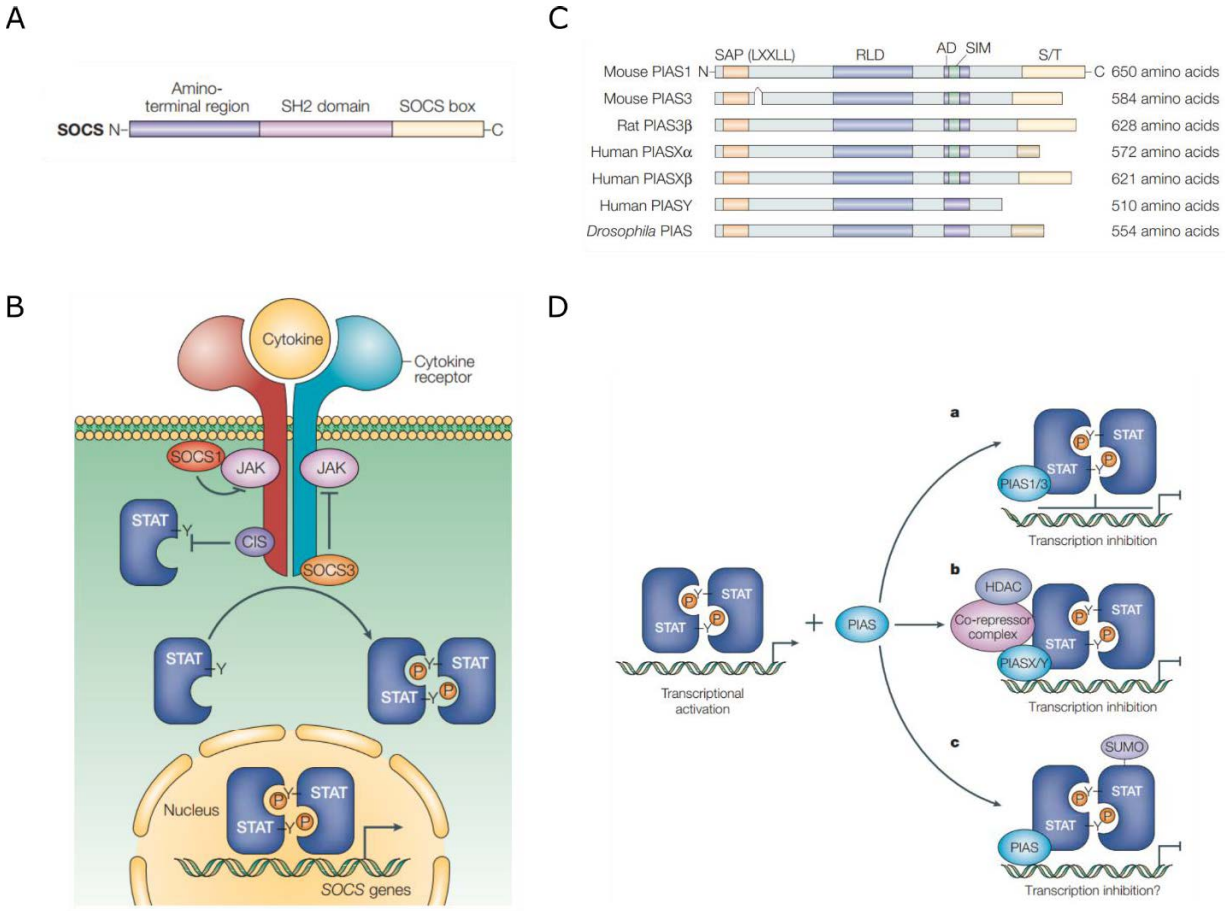

Figure 20: SOCS and PIAS family of JAK-STAT regulators

(A) Domain structure of suppressor of cytokine signalling (SOCS) proteins. The SOCS family of proteins has eight members: cytokine-inducible SRC homology 2 (SH2) domain protein (CIS) and SOCS1–SOCS7. SOCS proteins contain an SH2 domain that is flanked by a variable amino-terminal domain and a carboxy-terminal SOCS box. The SOCS box can bind to elongins B and C, which are known components of an ubiquitin E3 ligase complex. (B) Inhibition of the Janus kinase (JAK)–signal transducer and activator of transcription (STAT)-signalling pathway by SOCS proteins through distinct mechanisms. SOCS1 binds directly to tyrosine-phosphorylated JAKs through the SH2 domain, resulting in the inhibition of kinase activity. SOCS3 inhibits JAKs through binding to the receptor. By contrast, CIS does not affect the activity of JAKs. Instead, CIS inhibits STATs by competing with STATs for docking sites on the receptor. (C) The different members of the PIAS family (D) Proposed mechanisms for inhibiting the JAK–STAT pathway by PIAS proteins: a) PIAS1 and PIAS3 block the DNA-binding activity of STAT dimers. b) PIASX and PIASY might act as transcriptional co-repressors of STAT by recruiting other co-repressor proteins such as histone deacetylase (HDAC). c) PIAS proteins can promote the conjugation of small ubiquitin-related modifier (SUMO) to STAT1. [From Shuai et al. 2003]

dependent transcription without affecting the DNA-binding activity of STAT4 and STAT1 (Table 4). PIAS proteins have also been shown to interact with histone deacetylates (HDACs) indicating that they can function as transcriptional co-repressors of STATs, possibly by recruiting HDACs and other co-repressor molecules [Liu et al. 2001, Arora et al. 2003].

3.5.3.2 Regulation by tyrosine phosphatases

STATs can also be inactivated by PTPs in both the cytoplasm and the nucleus. SHP2 interacts with and can directly dephosphorylate STAT5 in the cytoplasm. Interestingly, SHP2 is also reported to be involved in the dephosphorylation of STAT1 at both tyrosine and serine residues [Chen et al. 2003]. In addition, PTP1B has also been implicated in the dephosphorylation of STAT5, however whether STAT5 is a physiological substrate of PTP1B remains to be established. The nuclear isoform of TCPTP called TC45 has been identified to dephosphorylate STAT1. In addition to TC45, SHP2 is also involved in the nuclear dephosphorylation of STAT1 [ten Hoeve et al. 2002, Wu et al. 2002].

3.5.3.3 Regulation by protein modifications

STATs can be post-translationally modified by phosphorylation, methylation, ubiquitination and sumoylation, the most important of which is tyrosine phosphorylation [Schindler et al. 1992, Shuai et al. 1992]. Tyrosine phosphorylation functions as a switch to activate STATs and it has been shown that tyrosine phosphorylated STAT1 needs to be dephosphorylated to leave the nucleus, indicating a role for tyrosine phosphorylation in the nuclear retention of STAT1 [McBride et al. 2000, Meyer et al. 2003]. STAT1 can be methylated on

Arg31 by protein arginine methyl-transferase 1 (PRMT1), which has also been found to be associated with the IFN-α/β receptor. The arginine methylation of STAT1 occurs constitutively, independent of tyrosine or serine phosphorylation. Methylation of STAT1 increases its DNA-binding activity, possibly due to inhibition of the interaction of PIAS1 with non-methylated STAT1. Whether other STATs are also regulated by protein methylation remains to be determined [Altschuler et al. 1999, Mowen et al. 2001]. STATs can also be post-translationally modified by ubiquitin and ubiquitin-related molecules. Poly-ubiquitination of STAT1 has been described, although it seems that this does not have an important role in regulating STAT1 activity [Kim et al. 1996]. It has been shown that STAT1 can be sumoylated on Lys703, which is strongly enhanced by PIAS proteins. In addition, treatment with IFNγ induces STAT1 sumoylation [Rogers et al. 2003]. However, the potential role of STAT1 sumoylation is under debate due to contradictory findings and further studies are required to clarify whether sumoylation has a role in regulating STAT function under physiological conditions [Song et al. 2006].

3.6 The JAK/STAT pathway and cancer

Early evidence that JAK/STAT signaling is activated in solid tumors was derived from cancer cell lines demonstrating tyrosine phosphorylation and nuclear localization of STATs, indicative of STAT activation. A relationship between JAK/STAT activation and prognosis has been observed in many of these tumor types. In general, activation of STAT3 or STAT5 is associated with a worse prognosis although in breast cancer and colorectal cancer, it appears to be associated with more favorable outcomes. On the other hand, activation of STAT1, is generally associated with better outcomes across all tumor types. In order for solid tumors to enlarge, cancer cells must not only

Table 3: Specificity in the negative regulation of JAK–STAT signalling

Inhibitor	Target
JAK PTPs	***JAKs***
SHP1	JAK2, JAK1
SHP2	JAK1
CD45	JAK1, JAK2, JAK3, TYK2
PTP1B	JAK2, TYK2
TCPTP	JAK1, JAK3
Cytoplasmic STAT PTPs	***STATs***
SHP2	STAT5
PTP1B	STAT5
TCPTP	STAT1, STAT3
Nuclear STAT PTPs	***STATs***
SHP2	STAT1
TCPTP	STAT1, STAT3
PIAS proteins	***STATs***
PIAS1	STAT1
PIAS3	STAT3
PIASX	STAT4
PIASY	STAT1

JAK, Janus-family kinase; PIAS, protein inhibitor of activated STAT; PTP, protein tyrosine phosphatase; SHP, SH2-domain-containing PTP; STAT, signal transducer and activator of transcription; TCPTP, T-cell PTP; TYK, tyrosine kinase 2. [From Shuai et al. 2003]

proliferate but also adapt to and alter their microenvironment. Genes controlled by activation of the JAK-STAT pathway have roles in both of these aspects of the malignant phenotype. STAT3 facilitates cell cycle progression (and thereby cell proliferation) by promoting transcription of positive regulators such as cyclin D2 and downregulating transcription of CDK inhibitors such as p21. In contrast, STAT5 activates transcription of Bcl-x to produce the anti-apoptotic protein Bcl-xL thereby conferring protection from apoptosis.

Angiogenesis is required for tumor growth, with a key role played by vascular endothelial growth factor (VEGF). STAT3 binds to the VEGF promoter and induces VEGF expression thereby promoting vasculogenesis. A key feature in the interaction of malignant cells with the tumor microenvironment is their ability to suppress antitumor immune responses. Activation of STAT1 by interferons promotes immune surveillance and antitumor immunity, partly by upregulating MHC class I-mediated antigen presentation by tumor cells. In contrast, STAT3 and STAT5 signaling in immune cells appears to suppress antitumor immunity. JAK/STAT activation contributes to acquisition of properties required for tumor invasion and metastasis. This is in part mediated by activation of epithelial to mesenchymal transition (EMT) involved in embryonic development. The transcription factor TWIST1 is a key regulator of the induction of EMT. STAT3 is required for TWIST1 expression, as abrogation of STAT3 activity reduces its expression [Cho et al. 2013]. In addition, STAT3 can activate transcription of matrix-degrading enzymes such as matrix metalloproteinase-2 (MMP-2) facilitating extravasation of metastatic cells.

Although STAT activation has now been observed in a wide range of tumor types, in many cases the associations between JAK/STAT activation and corresponding outcomes do not indicate whether the observed JAK/STAT activation has a causal role

in the diseases. Despite this, inhibiting JAK/STAT is already seen as a therapeutical means for diseases such as cancer, for e.g. with the development of state-of-the-art pharmacological inhibtors called Jakinibs [Kontzias et al. 2012, Gadina et al. 2020].

PART II

RESULTS

- OBJECTIVES AND SUMMARY
- ARTICLE:
  REMOTE CONTROL OF JAK/STAT SIGNALING THROUGH CAVEOALE MECHANICS

OBJECTIVES AND SUMMARY

As discussed in chapter 1, cell mechanics plays an important role in regulating several key biological processes required for maintaining homeostasis. A number of proteins and cellular structures localized in different regions within the cell have been implicated in transducing the external mechanical stimuli to the inside of the cell thereby acting as mechanotransducers. Our lab had earlier demonstrated that caveolae, which are 50-100 nm coated invaginations in the PM, could facilitate mechanoprotection by flattening out upon membrane tension increase induced by a mechanical stress, thereby providing additional plasma membrane surface in order to prevent cell rupture [Sinha et al. 2011]. Since caveolae have long been associated with intracellular signaling, our lab hypothesized that the mechano-dependent cycle of caveolae disassembly/reassembly could constitute a mechanical switch for signaling pathways [Nassoy & Lamaze 2012]. In this regard, we recently showed that EHD2 present at the caveolar neck could translocate to the nucleus upon release due to mechanical stress induced caveolae disassembly [Torrino et al. 2018]. Subsequently, considering the ability of Cav1 to modulate the activity of signaling molecules, through this present work, we sought to investigate if the mechanical disassembly of caveolae modulates major signaling pathways. Using high throughput screening we identified JAK-STAT as a signaling pathway that is modulated by caveolae mechanics. Therefore, the aim of this study is to elucidate the molecular mechanisms underlying the control of JAK-STAT signaling by caveolae mechanics.

In agreement with the high throughput screening results, biochemical assay and cell imaging confirmed that IFN-α-induced STAT3 activation is decreased upon cell stretching in a Cav1-dependent manner. Immunoprecipitation experiments revealed that Cav1 interacts with JAK1 - a key effector of the JAK-STAT signaling pathway –

indicating that the reduced STAT3 activation observed upon mechanical stress could be mediated by this interaction. In line with this, we noticed that Cav1-JAK1 interaction is increased upon rise in membrane tension induced by mechanical stress. In the caveolae field, it has been proposed that Cav1 modulates signaling molecules via direct binding and inhibition through its caveolin scaffolding domain (CSD). Despite the idea being controverted, we demonstrate that the Cav1 CSD has a prominent role in the Cav1-mediated JAK-STAT control. This is further confirmed by the fact that point mutations in the CSD (F92A/V94A) which prevents Cav1 interaction with its effectors, abolishes the negative effect of Cav1 on STAT3 activation. In order to better understand the dynamics of the Cav1-JAK1 interaction, we performed single particle tracking PALM (sptPALM) of Cav1 and JAK1 under conditions of mechanical stress. We observed that single Cav1 molecules display increased diffusion while single JAK1 molecules are immobilized upon increase in membrane tension. Furthermore, 3D STORM coupled with SMLM network analysis revealed that caveolae disassemble into non-caveolar Cav1 scaffolds (described in section 2.5.4) upon conditions of increased membrane tension. This indicates that the immobilization of single JAK1 molecules could be a result of interaction with the efflux of non-caveolar Cav1 scaffolds upon caveolae disassembly. Consistent with this hypothesis, interaction analysis revealed a higher affinity for Cav1 scaffolds to interact with JAK1.

The detailed results of this work are presented below, in the form of an article in preparation for submission.

Remote Control of JAK-STAT Signaling through Caveolae Mechanics

Satish Kailasam Mani[1§], Nicolas Tardif[1§], Olivier Rossier[2,3], Richard Ruez[1#], Melissa Dewulf[1], Ismail Khater[4], Ghassan Hamarneh[4], Ivan Robert Nabi[4], Grégory Gianonne[2,3], Cédric M. Blouin[1*] and Christophe Lamaze[1*]

[1] Institut Curie, PSL Research University, CNRS UMR3666, INSERM U1143, 75005 Paris, France

[2] Interdisciplinary Institute for Neuroscience, UMR 5297, University of Bordeaux, France.

[3] Interdisciplinary Institute for Neuroscience, UMR 5297, CNRS, Bordeaux, France.

[4] Department of Cellular and Physiological Sciences, University of British Columbia, Vancouver, Canada

[#] Current position: Translational validation scientist at ImaBiotech

* Corresponding authors: christophe.lamaze@curie.fr, cedric.blouin@curie.fr

[§] equal contribution

Abstract:

Caveolae are small invaginated nanodomains of the plasma membrane that have been classically involved in membrane trafficking and signaling. These multifunctional organelles were recently shown to play a key role as mechano-sensors that adapt the cell response to mechanical stress. Here, we investigated the role of caveolae mechanics in the control of the JAK-STAT signaling pathway. Single molecule imaging experiments revealed that caveolae disassembly induced by mechanical stress led to a drastic increase of caveolin-1 diffusion at the plasma membrane. This promoted the direct interaction of the caveolin-1 scaffolding domain with the tyrosine kinase JAK1, which strongly impaired its catalytic activity. Consequently, the activation by IFN-α of the JAK1 downstream effector STAT3 was inhibited. These results therefore establish caveolae as mechano-signaling hubs that remotely couple the sensing of membrane tension variations to the regulation of intracellular signaling through the release of freely diffusing caveolin-1 at the plasma membrane.

Introduction:

Caveolae are specialized budded pits that were first identified through electron microscopy (EM) over 60 years ago at the plasma membrane (PM) of epithelial and endothelial cells [Palade et al. 1953, Yamada et al. 1955]. Caveolae have been documented in numerous types of cells, with a particular abundance in adipocytes, endothelial and muscle cells contrasting with complete absence in lymphocytes and neurons. In transmission electron micrographs, caveolae appear as 50-80 nm diameter flask/bulb shaped structures attached to the PM mostly as single units and more rarely clustered in 'rosettes' [Lamaze et al. 2017, Parton et al. 2020a, Parton et al. 2020b]. The caveolin family of proteins consist of three isoforms – caveolin-1 (Cav1), caveolin-2 (Cav2) and caveolin-3 (Cav3) – of which Cav1 and Cav3 are the core structural

components that are necessary for the assembly of a *bona fide* caveola in non-muscle and muscle cells, respectively [Rothberg et al. 1992, Way and Parton 1995, Scherer et al. 1996]. Although caveolae were initially described as non-coated invaginations based on the absence of the characteristic fuzziness observed in clathrin-coated pits, more sophisticated electron microscopy such as freeze fracture and metal-replica electron microscopy later revealed striated filaments on the cytoplasmic face of caveolae suggesting the presence of a unique characteristic coat [Solmyo et al. 1971, Montesano et al. 1982, Peters et al. 1985, Izumi et al. 1989, Anderson et al. 1991]. The composition and organization of the caveolar coat were finally revealed with the identification of the cavin family of cytosolic proteins (cavin1 – cavin4). Cavin1, first identified in 2004 [Aboulaich et al. 2004], is essential for caveolae morphogenesis in all cell types while cavin4 expression is restricted to muscle cells [Hill et al. 2008, Liu and Pilch 2008, Liu et al. 2008, Bastiani et al. 2009]. Recent single particle electron microscopy and X-ray crystallography studies have provided further insights into the potential structure and organization of the Cav1 8S complex and the stoichiometry of the characteristic striated coat observed on the outer cytoplasmic side of caveolae. The Cav1 8S complexes have been proposed to adopt a toroidal shape with an outer ring structure and a central stalk [Han et al. 2020]. It is estimated that approx. 10 Cav1 monomers constitute a Cav1 complex with the N-termini on the outer ring and the C-termini on the central stalk. In addition, it has been estimated that 150-200 Cav1 monomers associate with 50-60 cavins organized as trimers to form a budded caveola [Rothberg et al. 1992, Qualmann et al. 1999, Aboulaich et al. 2004, Daumke et al. 2007, Hill et al. 2008, Hansen et al. 2011, Ludwig et al., 2013, Gambin et al., 2013, Kovtun et al. 2014, Stoeber et al., 2016]. Several accessory proteins including EHD2, pacsin2/syndapin2 (pacsin3/syndapin3 in muscle cells), filamin A and dynamin2 have also been localized at the neck of caveolae. Although caveolae accessory proteins are

less well characterized, they have been proposed to facilitate interactions with the actin cytoskeleton and to contribute to the stability and dynamics of caveolae at the PM [Oh et al. 1998, Sverdlov et al. 2009, Hansen et al. 2011, Senju et al. 2011, Moren et al. 2012, Seemann et al. 2017, Torrino et al. 2018].

Since their discovery, caveolae have been extensively studied and postulated to be involved in key biological processes including transcytosis [Ghitescu et al. 1986, Oh et al. 2007, Oh et al. 2014, Andreone et al. 2017, Ramirez et al. 2019, Bai et al. 2020], endocytosis [Montesano et al. 1982, Simionescu et al. 1982, Tiruppati et al. 1997, Pelkmans et al. 2002, Boucrot et al. 2011], lipid homeostasis [Cohen et al. 2004, Blouin et al. 2010, Pilch et al. 2011] and signal transduction [Anderson et al. 1993, Sargiocomo et al. 1993, Lisanti et al. 1994]. Mutations or impaired expression of caveolins and cavins have been associated with several human diseases including lipodystrophy, vascular dysfunction, cancer and muscle dystrophies [Lamaze and Torrino 2015, Lamaze et al., 2017, Singh and Lamaze, 2020].

Despite exhibiting multifaceted functions, the discovery of Cav1 as a defining marker for caveolae initially led to extensive implications in intracellular signal transduction [Cheng and Nichols 2016]. The idea that caveolae can play a vital role in regulation of signal transduction first arose from studies showing enrichment of numerous signaling proteins in detergent-insoluble complexes prepared from cells and tissues [Sargiacomo et al. 1993]. While several growth factors, signaling receptors and kinases have been proposed to localize in caveolae such as endothelial nitric oxide synthase (eNOS), insulin receptor, EGFR, src-like kinases, H-ras and K-ras [Li et al. 1996, Song et al. 1996, Couet et al. 1997, Garcia-cadena et al. 1997, Nystrom et al. 1999], it is important to note that most of these studies were based on the overexpression of both

cargos and Cav1 possibly leading to localization artefacts. The localization/sequestration of signaling molecules and receptors in caveolae could take place through various mutually inclusive means. It is known that PM protein function is directly coupled to the lateral organization by clustering of proteins in functional membrane domains or separating them in different domains [Nicolson 2014, Sezgin et al. 2017, Jacobson et al. 2019]. The formation of these protein domains occurs over a broad range of length scales and is highly dynamic [Garcia-Parajo et al. 2014, Blouin et al. 2016]. Owing to the strong affinity of Cav1 for cholesterol and sphingolipids, caveolae can modulate the local lipid composition and thereby the nanoscale organization of the PM [Parton et al. 2020]. As a result, caveolae can function as nanodomains themselves to confine signaling effectors locally at the PM [Ariotti et al. 2014, Parton et al. 2020].

In addition, it has been proposed that Cav1 can also cluster proteins in caveolae by direct interaction through the caveolin scaffolding domain (CSD) [Li et al. 1996]. A number of proteins that interact with Cav1 and Cav3 have been proposed to contain a consensus motif referred to as the caveolin binding motif (CBM) [Lisanti et al. 1995, Okamoto et al. 1998, Collins et al. 2012]. Despite the wealth of studies that outline a role for caveolin in signal regulation, the notion of caveolin signaling hypothesis has been a subject of controversy for a couple of reasons. Structural *in silico* analysis of the putative CBM suggest that it is not exposed at the surface and is therefore unlikely to be available for interaction [Byrne et al. 2012, Collins et al. 2012]. Moreover, putative CBMs were also found in organisms lacking caveolins questioning the specificity of the caveolin signaling mechanism. In addition, there are also doubts regarding the accessibility of the CSD as some studies suggest that the CSD is at least partially buried within the bilayer denying interaction with cytoplasmic proteins [Kirkham et al. 2008].

As a result, precisely how caveolins regulate signaling is still controverted and requires further investigation.

In 2011, our lab demonstrated a novel role for caveolae in mechano-protection where in response to mechanical stress, caveolae flatten out to protect the PM from rupture by providing additional membrane stored in their invagination so as to buffer the resulting membrane tension variations [Sinha et al. 2011]. The essential role of caveolae in cell mechano-protection was confirmed in several cell types *in vitro* and *in vivo* (Lo et al., 2015, Elliot et al. 2016, Lim et al., 2017, Parton 2018, Del Pozo et al. 2021). It has been hypothesized that the classical functions of caveolae including signaling should be reconsidered through their new function in cell mechanics [Nassoy and Lamaze 2012, Cheng and Nichols 2016]. Indeed, upon flattening, caveolins and caveolar coat proteins are likely to be released which in turn could modulate intracellular processes. In this context, we demonstrated that EHD2 which localizes at the neck region of caveolae, is released upon caveolae disassembly in response to increased membrane tension and translocates to the nucleus where it regulates gene transcription [Torrino et al. 2018]. More recently, cavin3 was shown to be released upon UV-light induced caveolae disassembly and function together with BRCA1 in multiple cancer related pathways [McMahon et al. 2021].

Here, we revisited the role of caveolae on intracellular signaling by investigating the effects of the mechano-dependent cycle of caveolae disassembly/reassembly on cell signaling. We performed high-throughput reverse phase protein array (RPPA) analysis on cells subjected to mechanical stress and identified the janus kinase/signal transducers and activators of transcription (JAK/STAT) signaling pathway to be directly regulated by caveolae mechanics. We found that in response to mechanical stress,

caveolae rapidly disassembled into smaller assemblies called scaffolds. The pool of released Cav1 scaffolds was found to diffuse rapidly in the PM and to directly interact with JAK1 outside of caveolae via Cav1-CSD. As a result, JAK1 catalytic activity was inhibited as shown by the lack of JAK-STAT activation by interferon-α (IFN-α). Upon stress release, JAK-STAT activation by IFN-α resumed to normal levels. Altogether, our study provides a new mechanism by which caveolae regulate mechanosignaling in a remote manner outside of caveolae.

Results:

Several signaling pathways are controlled by caveolae under mechanical stress

We were interested in determining whether the mechano-dependent cycle of caveolae disassembly/reassembly may constitute a mechanical switch by which caveolae and /or caveolins could partake in modulating some signaling pathways in response to mechanical stress [Nassoy and Lamaze 2012, Lamaze et al. 2017]. To this end, we performed a high-throughput screening experiment utilizing the reverse phase protein array (RPPA) – a miniaturized dot-blot technology for proteomic analysis allowing the analysis of protein expression, post-translational modifications and identification of activated or altered signaling pathways [Boellner et al. 2015]. The RPPA analysis was performed on wild-type (WT) and Cav1 knockout (*CAV1*$^{-/-}$) Mouse Lung Endothelial Cells (MLEC) subjected to uniaxial stretching. The above experiment was also performed under conditions of IFN-α activation so as to analyze the effect on JAK/STAT pathway (Fig. 1a). Several signaling pathways were affected by uniaxial stretching as exemplified by the stretch dependent activation of MAPK and Akt pathways (Fig.1b). Whereas some signaling pathways such as MAPK were activated by stretch independently from the presence of caveolae, we also observed a significant increase in Akt phosphorylation on Ser473 (pSer473) upon stretch in a Cav1-dependent

manner. Moreover, PKC-α activation (pSer657) was only observed in stretched cells devoid of Cav1 (Fig 1b). These observations reflect the implications of caveolae and/or Cav1 in the mechano-regulation of signaling pathways. The activation of JAK-STAT signaling by IFN-α relies on the ubiquitous IFNAR receptor composed of the two receptor subunits IFNAR1 and IFNAR2. IFN-α binding to IFNAR2 allows the formation of a ternary complex with IFNAR1, where the two IFNAR-associated JAK1 and TYK2 tyrosine kinases are mutually activated by trans-phosphorylation. Subsequent tyrosine phosphorylation of IFNAR-bound STAT molecules (STAT1, STAT2 or STAT3) allows their cytosolic release and their translocation to the nucleus where they induce a transcriptional program specific to IFN-α [Schreiber and Piehler, 2015]. As expected, IFN-α stimulation led to the phosphorylation of STAT3 Tyrosine705 (Tyr705) and STAT1 Tyrosine701 (Tyr701) (Supp Fig.1). Interestingly, under conditions of IFN-α stimulation, the level of STAT3 phosphorylation drastically reduced upon cell stretching in a Cav1-dependent manner whereas STAT1 phosphorylation was not affected (Fig. 1c and 1d). Observations from the RPPA analysis were confirmed by monitoring the phosphorylation levels of STAT1 (pSTAT1) and STAT3 (pSTAT3) in the corresponding cell lines under conditions of stretch and IFN-α stimulation. Western blot analysis in MLEC WT and MLEC *CAV1*$^{-/-}$ cells stimulated with IFN-α under 25% uniaxial stretching revealed a 43% decrease in pSTAT3 levels compared to steady state cells (Fig. 1e). As observed in the RRPA analysis, the level of STAT3 tyrosine phosphorylation remained unchanged in MLEC *CAV1*$^{-/-}$ cells subjected to stretch, indicating that this regulation requires functional caveolae (Fig. 1e). Moreover, the decrease of STAT3 phosphorylation translated into a corresponding defect in STAT3 nuclear translocation in stretched cells (Fig. 1f). These results indicate the involvement of caveolae and/or Cav1 in the modulation of STAT3 phosphorylation levels in response to mechanical stress.

STAT3 inhibition is mediated by interaction of Cav1 with JAK1

Our data indicate that caveolae/Cav1 and mechanical stress can control the activation (i.e. phosphorylation) of STAT3 by IFN-α. We next determined whether this control could occur in unstimulated cells. As expected, in the absence of stimulation by IFN-α, no activation of STAT1 and STAT3 were detected in WT MLEC (Fig. 2a). In contrast, we observed a strong activation of STAT3 (pSTAT3) in unstimulated *CAV1*$^{-/-}$ MLECs whereas the absence of caveolae had no effect on the level of phosphorylated STAT1 (pSTAT1) at steady state. STAT3 is a direct cytosolic downstream effector of JAK1 and TYK2 kinases that are associated with the IFNAR complex [Shuai et al. 2003, Platanias et al. 2005]. Therefore, we monitored pSTAT3 levels in MLEC *CAV1*$^{-/-}$ at steady state and upon IFN-α stimulation after JAK1 siRNA depletion. In the absence of JAK1, we no longer observed IFN-α-induced high levels of pSTAT3 in MLEC *CAV1*$^{-/-}$ (Fig. 2b).

These results led us to hypothesize that the modulation of STAT3 phosphorylation in response to mechanical stress by caveolae/Cav1 could be mediated through interaction of Cav1 with JAK1. Treatment of cells with hypo-osmotic medium (30 mOsm) for 5 minutes increases membrane tension through cell swelling and leads to rapid caveolae disassembly similarly to cell stretching [Sinha et al. 2011]. Endogenous co-immunoprecipitation (Co-IP) of both Cav1 and JAK1 interactors was performed on MLEC WT and MLEC *CAV1*$^{-/-}$ cells subjected to hypo-osmotic shock. At rest, we found that Cav1 indeed interacts with JAK1 and this interaction drastically increases (up to 45%) in response to mechanical stress (Fig. 2c). We also repeated the Co-IP experiment with IFN-α stimulation to determine the impact of increased Cav1-JAK1 interaction on STAT3 phosphorylation. As expected, we observed a significant decrease (upto 35%) in the levels of pSTAT3 in response to hypo-osmotic shock (Fig. 2d). Interestingly, upon returning to iso-osmotic conditions when caveolae have been reassembled to initial numbers (recovery) [Sinha et al. 2011], both the levels of Cav1 interaction with JAK1

and IFN-α-induced STAT3 phosphorylation returned to basal levels measured at rest. These data indicate that the level of Cav1-JAK1 interaction is tuned by the amount of Cav1 released from caveolae that are disassembled to buffer the increase of membrane tension induced by hypo-osmotic shock. Moreover, it shows that the inhibition of STAT3 activation by IFN-α is correlated with the level of Cav1 interaction with JAK1 suggesting that JAK1 inhibition is tuned by the amount of Cav1 that binds to JAK1.

JAK1 inhibition is mediated by the caveolin scaffolding domain

The so-called "caveolin signaling hypothesis" is based on the idea that Cav1 interacts with a select number of signaling effectors through its caveolin scaffolding domain (CSD) mainly to exert an inhibitory effect [Couet et al., 1997b; Garcia-Cardena et al. 1997]. Many of these Cav1-interacting proteins have been shown to possess a consensus motif called the caveolin binding motif (CBM) which has been proposed to be complementary for recognition by the CSD [Lisanti et al. 1995, Byrne et al. 2012, Collins et al. 2012]. Interestingly, JAK1 sequence analysis revealed that it carries 3 putative CBMs – one each is localized in the FERM domain, the pseudokinase domain and the kinase domain of JAK1 [Jasmin et al. 2006]. The phenylalanine 92 (Phe92) and valine 94 (Val94) residues of Cav1 have been proposed to play a key role in the CSD-CBM interaction [Nystrom et al. 1999, Bernatchez et al. 2011, Trane et al. 2014, Meng et al. 2017]. In order to determine whether the interaction between Cav1 and JAK1 is mediated by the CSD, we expressed a Cav1 construct possessing point-mutations at the Phe92 and Val94 residues (Cav1-RFP F92A/V94A) in MLEC *CAV1*$^{-/-}$ cells. JAK1 was not detected in the immunoprecipitated fractions from cells expressing Cav1 F92A/V94A whereas it co-precipitated with Cav1 WT (Fig. 3a). This shows that the interaction between Cav1 and JAK1 requires the CSD Phe92 and Val94 residues.

To further test if the inhibitory role of Cav1 on JAK1 activity was indeed mediated by the CSD, we examined the level of pSTAT3 nuclear translocation induced by IFN-α stimulation in MLEC *CAV1*$^{-/-}$ cells expressing either Cav1 WT or Cav1 F92A/V94A (Fig. 3b). While the nuclear translocation of pSTAT3 occurred normally in non-transfected cells, cells overexpressing Cav1 WT showed defects in pSTAT3 nuclear translocation corroborating the inhibitory role of Cav1 on JAK1 activity. It has been reported that overexpression of Cav1, in addition to golgi sequestration, generates a pool of non-caveolar Cav1 at the plasma membrane presumably due to a stoichiometric imbalance between the number of Cav1 molecules and the other caveolar components required for caveolae assembly [Hayer et al. 2010, Moon et al. 2013]. On the contrary, in cells expressing the F92A/V94A mutated Cav1 CSD, we observed a normal nuclear translocation of pSTAT3 upon IFN-α stimulation, indicating that F92A/V94A Cav1 lost the ability to negatively regulate STAT3 activation, most likely through its inability to interact with JAK1 (Fig. 3a and 3b). In agreement with the insensitivity of STAT1 activation to mechanical stress and caveolae, the nuclear translocation of pSTAT1 induced by IFN-α was not affected irrespective of whether cells express Cav1 WT or Cav1 F92A/V94A (Supp Fig.1).

We further established the role of the Cav1 CSD using two CSD mimicking peptides, a peptide named CavTratin corresponding to the Cav1 CSD (Cav1 ^{82}DGIWKASF**TTF**TVTKYWFYR^{101}) and a dominant negative peptide named CavNoxin (Cav1 ^{82}DGIWKASF**AAA**TVTKYWFYR^{101}) where key amino acids of the CSD are replaced by alanines thereby abolishing its inhibitory effect [Bernatchez et al. 2011]. MLEC WT cells treated with CavTratin showed a significant decrease of pSTAT3 upon IFN-α stimulation, as compared to cells treated with control peptide, showing that the CSD domain is sufficient for the negative regulation of STAT3 activation by Cav1.

Conversely, cells treated with CavNoxin showed a significant increase of IFN-α-induced pSTAT3 (Fig. 3c). These data confirm that increasing the amount of Cav1 that is able to interact with the JAK1 kinase inhibit STAT3 activation whereas the mutated Cav1 CSD peptide relieves the JAK1 inhibition, most likely by competing with endogenous Cav1. To rule out the potential effect of an unknown third-party interactor, we also assessed the effect of CSD binding on the ability of JAK1 to catalyze ATP hydrolysis in a cell free assay. Therefore, we measured the *in vitro* catalytic activity of human recombinant JAK1 by measuring the conversion of ATP to ADP. Increasing concentrations of the control peptide did not affect the catalytic activity of JAK1 as ADP production was maintained. In contrast, JAK1 dependent ADP production significantly decreased in a dose dependent manner when CavTratin was added to the reactional mix (Fig. 3d). Altogether, these data demonstrate that the CSD is crucial for the ability of Cav1 to directly interact with JAK1 and its inhibitory effect toward JAK1 activity.

Mechanical stress drastically increases the diffusion of Cav1 molecules at the plasma membrane

Considering that some *in silico* studies have debated the involvement and the ability of the CSD to facilitate protein interactions with Cav1, it was essential to further understand the possible mechanisms of interaction between Cav1 and JAK1. We have initially hypothesized that the disassembly of caveolae in response to increased membrane tension was likely to release caveolins at the PM and coat proteins into the cytosol [Sinha et al. 2011, Nassoy and Lamaze, 2012]. Indeed, single-molecule fluorescence analysis revealed that changes in membrane tension led to the release of the cavin coat from flattened caveolae as two distinct cavin-1/cavin-2 and cavin-1/cavin-3 cytosolic sub-complexes [Gambin et al., 2014]. In addition, we recently showed that EHD2 is released from caveolae upon an increase in membrane tension

and translocates to the nucleus where it regulates gene transcription [Torrino et al. 2018]. Less is known about the topology of Cav1 oligomers after caveolae flattening. Caveolins could remain organized as a flat caveolar structure, as observed by deep-etch electron microscopy [Sinha et al., 2011], or released as non-caveolar Cav1 oligomers. Indeed, FRAP experiments showed that the mobile fraction of Cav1 was increased upon mechanical stress, suggesting a higher number of Cav1 molecules freely diffusing outside of caveolae [Sinha et al., 2011]. In this regard, we were interested in observing the kinetics and dynamics of Cav1 and JAK1 in response to mechanical stress. In order to monitor the fate of single Cav1 molecules with high spatio-temporal resolution at the PM, we performed single particle tracking (sptPALM) combined with total internal reflection fluorescence microscopy (TIRFM). The use of Cav1 and JAK1 fused with the phospho-switchable mEOS3.2 fluorophore allowed us to track their dynamics by measuring the diffusion coefficient (D) in MLEC *CAV1*$^{-/-}$ cells subjected to hypo-osmotic shock. At rest, the Cav1-mEOS3.2 trajectories remain confined around static Cav1-mEOS3.2 objects, indicating that they are most likely confined within caveolae (Fig. 4a). Under membrane tension increase induced by hypo-osmolarity, we observed dramatic increase in the diffusion of a pool of Cav1 molecules as indicated by the higher diffusion coefficient of Cav1-mEOS3.2 trajectories (Fig. 4b). Importantly, the logarithmic value of the diffusion coefficient (logD) increased with time of exposure to hypo-osmolarity, in agreement with the visualization of Cav1-mEOS3.2 trajectories exploring a wider area (Supp Fig. 3a). Moreover, in cells reintroduced to iso-osmotic conditions following a hypo-osmotic shock (i.e. recovery), the diffusion coefficient of Cav1-mEOS3.2 returns to levels similar to that of resting state, indicating a possible return of Cav1 molecules confined into caveolae during reassembly (Fig. 4c).

Interestingly, the kinetics of JAK1 single molecules followed a completely opposing trend to what was observed for Cav1 molecules. At steady state, the JAK1-mEOS3.2 trajectories were highly diffusive (Fig. 4d). However, upon exposure to hypo-osmotic shock, the diffusivity of JAK1 molecules are drastically reduced contrary to those of the membrane targeting sequence containing the CAAX motif taken as a control for bulk membrane dynamics (CAAX-mEOS3.2) (Supp. Fig. 3b). This might possibly reflect that an initially highly diffusive JAK1 molecule encounters Cav1 upon membrane tension increase (shock). Indeed, the measurement of a similar diffusion coefficient of 0.1 $\mu m^2.s^{-1}$ for both the mobile pool of Cav1 and the immobile pool of JAK1 suggests that these two pools follow a common path when membrane tension is increased (Fig. 4b and 4f). Taken together, the contrasting kinetics of Cav1 and JAK1 molecules suggest that in response to mechanical stress, immobilized Cav1 molecules (presumably in caveolae) are released into the PM as indicated by the higher diffusivity facilitating their encounter with JAK1 molecules and thereby partially immobilizing them. This process is highly dynamic and reversible as indicated by the decrease and increase in the diffusion of Cav1 and JAK1 respectively upon recovery to resting conditions.

Non-caveolar Cav1 interacts with JAK1 to modulate the JAK-STAT pathway

A long-standing objective in the field of caveolae has been to distinguish the roles of caveolae and caveolins in cellular processes [Lamaze et al. 2017, Parton et al. 2020, Pol et al. 2020]. Moreover, in the absence of cavin1, Cav1 is unable to assemble into morphologically distinguishable caveolae and remains as a pool of non-caveolar Cav1 with increased lateral mobility at the plasma membrane [Hill et al., 2008]. In this regard, we sought to investigate if the pool of Cav1 that interacts with JAK1 in response to membrane tension variations is non-caveolar in nature. We used mouse embryonic

fibroblasts (MEF) knocked out for *CAVIN1* and measured the level of STAT3 phosphorylation in unstimulated and IFN-α-stimulated MEF *CAVIN1*$^{-/-}$ cells. As expected, STAT3 was not activated in unstimulated cells (Fig. 5a). Whereas the stimulation of MEF *CAVIN1*$^{-/-}$ cells by IFN-α failed to activate STAT3, the re-expression of cavin1 in these cells restored the IFN-α-induced activation of STAT3 (Fig. 5b). These results indicate that non-caveolar Cav1, the only form of Cav1 present in cells devoid of cavin1, is solely responsible for the inhibition of STAT3 activation by IFN-α. Moreover, treatment of MLEC WT cells with methyl-β-cyclodextrin, which disrupts caveolae by sequestering cholesterol at the plasma membrane, also led to a significant decrease in the level of STAT3 activation by IFN-α (Supp. Fig. 4). Finally, we used MEF *CAVIN1*$^{-/-}$ cells re-expressing varying amounts of Cav1 and found that the level of STAT3 activation was inversely correlated with the amount of non-caveolar Cav1 present in the cells (Fig. 5c).

Nanoscale imaging of non-caveolar Cav1 under mechanical stress

Late advancements in super-resolution microscopy coupled with machine-learning has provided new insights into the nanoscopic organization of several cellular structures [Betzig et al. 1993, Hell et al. 1994, Bowler et al. 2019, Laine et al. 2019, Orré et al. 2021]. We used STochastic Optical Reconstruction Microscopy (STORM) to image endogenous Cav1 or Cavin1 in MLEC cells (Fig. 5d) and were able to observe circular structures with apparent diameter in the range of 50-100 nm consistent with the known size of caveolae (Fig. 5e and Supp Fig. 5a). The disassembly of caveolae upon hypo-osmotic shock is a two-step process where budded caveolae first flatten out before completely disassembling their coat structure. In line with this, the observed diameter of some Cav1 positive structures (presumably flat caveolae) increases as shown with their fluorescent profiles (Fig. 5e). In order to realize multicolor 3D STORM, we resorted

to the use of spectral demixing (Supp. Fig. 5b), that allows multicolor imaging with a single excitation laser, allowing to monitor Cav1 and JAK1 endogenous protein localizations simultaneously (Fig. 5f and Supp Fig. 5b).

Recent reports have proposed that Cav1 could exist as oligomers outside of caveolae in so called 'scaffolds'. These scaffolds have been further classified depending on their size and are suggested to be the building blocks of a *bona fide* caveola [Khater et al. 2019]. This could in part explain the ability of Cav1 to simultaneously interact with effector proteins while also engaging in mechanoprotective roles through caveolae. These subpopulations, classified as S1A, S1B and S2, constitute the building blocks of the final 70S complex that is required for the formation of a budded caveolae. Therefore, we investigated if there are preferential interactions of any of these subpopulations with JAK1 in response to mechanical stress. For this purpose, we resorted to the use of multicolor 3D STORM combined with spectral demixing and machine learning to visualize Cav1 scaffolds/caveolae and their interactions with JAK1 at the nanoscale (Fig. 5f-g and Supp. Fig. 5c-d). This was performed on MLEC WT cells at steady state as well as on cells subjected to a 5-minute hypo-osmotic shock. Furthermore, on measuring the number of caveolae and the different scaffolds per unit area, we noticed a significant increase in the amount of the three scaffold S1A, S1B, S2 populations and a concomitant decrease in the number of caveolae (Fig 5h). Moreover, interaction analysis using the MOSAIC plugin [Shivanandan et al. 2013] revealed a significant increase in the interaction of the S1A and S1B scaffolds with JAK1 in response to hypo-osmotic shock (Fig 5i). These results indicate that in response to mechanical stress, *bona fide* caveolae disassemble into non-caveolar Cav1 scaffolds which are then rapidly diffusing at the PM to interact with JAK1 and regulate signaling through the JAK-STAT pathway.

Discussion

Since the discovery of caveolae in 1953, research over the years have bestowed a variety of roles for caveolae in preserving biological functions [reviewed in Cheng and Nichols 2016, Lamaze et al. 2017, Parton et. al 2020]. Although caveolae were hypothesized to be involved in mechanoprotection by maintaining cellular integrity as early as mid-1970's, it was not until a pioneering study from our lab demonstrating the ability of caveolae to respond to mechanical stress that the field was prompted to revisit its classical functions in the context of cell mechanics [Dulhunty et al. 1975, Prescott and Brightman 1976, Gabella and Blundell 1978, Sinha et al. 2011]. We showed that caveolae can flatten and disassemble in response to membrane tension increase, and hypothesized that caveolar proteins could be released upon stress-induced disassembly [Nassoy and Lamaze 2012]. In this regard, we recently showed that EHD2 which localizes at the neck of caveolae can translocate to the nucleus in response to increase in membrane tension and regulate gene transcription [Torrino et al. 2018]. Cavin1 has been shown to be released from the caveolar coat in response to hypo-osmotic shock and also translocate to the nucleus and dysregulate the p53 pathway upon disruption of caveolae by methyl-β-cyclodextrin [Gambin et al. 2014, Liu and Pilch 2016]. More recently, cavin3 has been shown to interact with BRCA1 and regulate multiple cancer related pathways upon release from caveolae through UV exposure [McMahon et al. 2021]. Considering the established role of caveolae in signaling, we were interested in determining the involvement of stress-induced release of Cav1 in the regulation of intracellular signaling cascades.

High throughput screening revealed that the JAK-STAT signaling pathway was modulated by cell stretching in a Cav1-dependent manner. Using IFN-α induced STAT1 and STAT3 tyrosine phosphorylation levels as readout, we show that Cav1

impairs STAT3 activation in response to mechanical stress. Early studies reported the enrichment of several signaling molecules in detergent-insoluble fractions and the ability of Cav1 to interact with them. Subsequently, Cav1 was proposed to interact with its effectors through the CSD [Li et al. 1996, Couet et al. 1997, Garcia-Cadena et al. 1997, Nystrom et al. 1999]. Moreover, several proteins with a consensus sequence called the caveolin binding motif (CBM) that can bind the CSD have been reported [Couet et al. 1997b]. Sequence analysis of JAK1 reveals three domains that could correspond to putative CBMs: one each in the FERM domain (^{157}YLFAQGQY^{164}), the pseudokinase domain (^{777}WSFGTTLW^{784}) and the kinase domain (^{1065}WSFGVTLH^{1072}). Despite these studies, the concept of CSD-mediated interaction of Cav1 with CBM-containing proteins has been under debate owing to structural studies of the two motifs. The argument is based on the proposal that the CSD, being composed of an amphipathic helix, would be buried in the inner leaflet of the PM and hence would not be available for interaction with the CBM of possible interactors. [Kirkham et al. 2008, Byrne et al. 2012, Collins et al. 2012]. It is also worth noting that the CSD shares primary sequence similarities with the pseudo-substrate domain of SOCS1, which primarily mediates JAK inhibition by SOCS1 [Jasmin et al. 2006, Kershaw et al. 2013]. Nevertheless, with the help of CSD mimicking peptides and point mutations in the Cav1 CSD, we demonstrate that the interaction of Cav1 with JAK1 is indeed mediated by the CSD, thereby inhibiting the catalytic activity of JAK1. In addition, a recent study reported that the deletion of the CSD decreases the level of STAT3 phosphorylation in agreement with our observations [Okada et al. 2019].

More importantly, the level of Cav1-JAK1 interaction is modulated by mechanical stress. We demonstrated that upon an increase in membrane tension induced by hypo-osmotic stress, the interaction between Cav1 and JAK1 drastically increases, leading us to hypothesize that this increased interaction could be due to an efflux of Cav1

molecules released into the plasma membrane from caveolae disassembly. Consequently, we looked at the membrane trajectories of Cav1 and JAK1 molecules under conditions of hypo-osmotic stress and observed opposite diffusion behaviors. The Cav1 particles which were initially restricted to confined domains (presumably within caveolae), shifted to a highly scattered diffusion pattern with progressive increase in membrane tension. In contrast, the JAK1 molecules that were initially highly diffusive at steady state, became partially immobilized upon hypo-osmotic shock. This further suggests the possibility that the highly diffusive pool of Cav1 molecules released in response to mechanical stress could interact with JAK1, thereby limiting their diffusivity and inhibiting its catalytic activity.

The roles attributed to Cav1 cannot be directly conferred to caveolae as Cav1 can also exist as oligomers outside of caveolae (termed non-caveolar Cav1 or scaffolds). Several subclasses of Cav1 oligomers, that act as building blocks of a *bona fide* caveolae have been reported to exist based on super-resolution imaging and network analysis [Khater et al. 2019]. With the help of network analysis and single molecule localization microscopy (SMLM) of cells subjected to hypo-osmotic shock, we found that caveolae disassemble into scaffolds in response to an increase in membrane tension, which then interact with JAK1. The notion of Cav1 scaffolds (but not caveolae) interacting with JAK1 could possibly explain the involvement of CSD in mediating the Cav1-JAK1 interaction. The CSD which might not be accessible in a budded caveolae could be exposed during lipid reorganization and disassembly of caveolae into scaffolds. In line with this view, a recent report suggests that compared to caveolae, the S2 and S1B scaffolds have a CSD that is more exposed and hence more likely to be involved in CSD mediated interactions [Wong et al. 2021].

Altogether, we report a new mechanism by which caveolae control the regulation of JAK-STAT signaling cascade in a remote manner that is outside of the caveolae

structure itself. This remote control is based on the balance between the two populations of caveolar Cav1 and non-caveolar Cav1 (scaffolds) allowing for the fine tuning of the JAK-STAT pathway based on caveolae mechanosensing. We noticed that STAT3 was activated in cells devoid of Cav1 even in the absence of IFN-α. Moreover, Cav1 CSD was seen to interact with JAK1 and inhibit its catalytic activity in the absence of IFN-α. These results indicate that this control is not restricted to IFN-α but could be extended to other cytokines activating JAK1. In this context, the control of IL-6/Stat3 signaling by caveolae mechanosensing that we recently described in human muscle cells is likely to follow the same mechanism [Dewulf et al., 2019]. Another study revealed that proper suppression of JAK-STAT signaling through SOCS3 requires *bona fide* caveolae and stably associated cavin1 [Williams et al. 2018]. Hence, it is possible that the mechanical disassembly of caveolae and the destabilization of cavins complexes could lead to impaired SOCS3 mediated JAK-STAT signal termination. In this regard, the release of free Cav1 and subsequent inhibition of the JAK1 could act as a substitute to impaired SOCS3 activity and prevent aberrant JAK-STAT signaling. Interestingly, the proposed mechanism selectively targets JAK1 dependent STAT3 activation but not STAT1 activation and the molecular basis driving this signal specificity would need further investigation. In addition, the physiological implications of such control of JAK-STAT signaling by caveolae mechanics remains to be studied. STAT3 has known oncogenic properties while STAT1 is seen as a tumor suppressor [Sellier et al. 2013, Koromilas et al. 2013, Zhang et al. 2017]. In addition, the exact role of Cav1 in cancer has long been debated as it seems to possess an ambivalent behavior, with reports suggesting that it has both oncogenic as well as tumor suppressor properties [Goetz et al. 2008, Lamaze and Torrino 2015, Singh and Lamaze 2020]. This new perspective of caveolae functioning as mechano-signaling hubs may play a critical role during tumor growth as mechanical forces encountered by cancer

cells during tumor progression may perturb caveolar dynamics that in turn would impair the fine tuning of the STAT3/STAT1 activation balance through caveolae mechanics.

To conclude, although Cav1 have been shown to bind with and immunoprecipitate several proteins ranging from signaling molecules to membrane receptors, often there has been little convincing evidence for these proteins to be found inside caveolae raising a conundrum of how a signaling molecule can be regulated by caveolae if not present into caveolae. Our results provide a new mechanistic insight into the regulation of cell signaling through caveolae. We show that Cav1 can remotely control signaling molecules outside of caveolae by disintegrating into non-caveolar Cav1 scaffolds in response to mechanical stress which in turn facilitates interaction of these scaffolds with potential effector molecules through the CSD. Taken together, our results demonstrate that caveolae can acts as mechano-signaling hubs with an ability to remotely control downstream signal transduction from the PM.

Materials and Methods:

Antibodies and reagents.

Mouse anti-α-tubulin (Sigma-Aldrich, clone B512, Cat. No: T5168, 1:1000 for WB); mouse anti-CHC (BD Transduction, Cat. No: 610500, 1:5000 for WB); rabbit anti-Cav1 (Cell Signaling Technologies Cat. No: 3238S, 1:1000 for WB, 2-5 µg/condition for IP, 1:50 for dSTORM, 1:150 for IF); mouse anti-Cav1 (BD Transduction, Cat. No: 610407,); mouse anti-PTRF (BD Transduction Cat. No: 611258, 1:1000 for WB); rabbit anti-PTRF (Cat. No: ab48824, Abcam – discontinued, 1:1000 for WB, 1:50 for dSTORM, 1:150 for IF); mouse anti-STAT3 (Cell signaling, clone 124H6, Cat. No: 9139, 1:1000 for WB); rabbit anti-pSTAT3 (Cell signaling technologies, clone D3A7, Cat. No: 9145, 1:1000 for WB, 1:100 for IF); rabbit anti-STAT1 (Cell signaling technologies, Cat. No: 9172, 1:1000 for WB); mouse anti-pSTAT1 (Cell signaling technologies, Cat. No: 9167, 1:1000 for

WB, 1:100 for IF); rabbit anti-JAK1 (Cell signaling technologies, Cat. No: 3332S, 1:1000 for WB). All secondary antibodies were obtained from Jackson Immuno-research and raised in donkey for the corresponding species of origin of primary antibodies irrespective of the conjugate.

Cell lines:

Wild-type and *CAV1*$^{-/-}$ mouse lung endothelial cell lines (MLECs) were characterized by William.C.Sessa's team and kindly provided by Radu.V. Stan (Darthmouth Medical School, NH, USA). They were immortalized using polyomavirus T-antigen and selected according to CD31, VE-Cadherin and PV1 expression. Mouse embryonic fibroblasts (MEFs) expressing low, medium and high levels of Cav1 were kindly provided by Miguel Del Pozo.

Cell culture:

All cells were grown at 37°C under 5% CO_2. WT MLEC and *Cav1*$^{-/-}$ MLEC cell lines were cultured in Endothelial Basal Medium (EBM2, Cat. No: CC-3156, Lonza Biosciences) supplemented with 10% FBS, 4mM glutamine, 5mM sodium pyruvate, 0.01 % penicillin streptomycin (v/v), 0.04% hydrocortisone (v/v), 0.4% hEGF-B (v/v), 0.1% VEGF (v/v), 0.1% R3-IGF-1 (v/v), 0.1% ascorbic acid (v/v), 0.1% hEGF (v/v), 0.1% GA-1000 (v/v), 0.1% heparin (v/v) (EGM2 singlequote, Cat. No: CC-4176, Lonza Biosciences). MLEC cells were tested for expression of VE-Cadherin before each experiment. MEF cells were cultured in DMEM high-glucose GlutaMAX (Cat. No: 10566-016, Thermo Fisher Scientific), supplemented with 10% FBS (v/v), 0.01% penicillin streptomycin (v/v) and 5mM sodium pyruvate.

dSTORM sample preparation:

MLEC WT cells grown on high resolution #1.5 glass coverslips (THOR labs) were washed three times with PHEM solution (60 mM PIPES, 25 mM HEPES, 5 mM EGTA and 2 mM Mg acetate adjusted to pH 6.9 with 1 M KOH) and fixed for 20 min in 4% PFA. They were then washed 3 times in PBS (137 mM NaCl, 2.7 mM KCl, 8 mM Na_2HPO_4, and 2 mM KH_2PO_4). Up to this fixation step, all chemical reagents were pre- warmed at 37°C. The cells were then quenched for auto-fluorescence from PFA in 25mM NH_4Cl for 20 min at RT. The cells were washed in PBS three times before being blocked and permeabilized in blocking buffer (1X PBS / 1% BSA / 0.1% Saponin) for 1 hr at RT. Fixed

cells were incubated for 1 hr at 37°C with the respective primary antibodies diluted in blocking buffer and washed three times with PBS. This was followed by 1 hr incubation at 37°C with corresponding secondary antibodies diluted in blocking buffer, and washed three times with PBS. After immunolabelling, a post-fixation step was performed using PBS with 3.6% formaldehyde for 15 min. The cells were washed in PBS three times and then reduced for 10 min with 25 mM NH_4Cl (Sigma Aldrich, 254134), followed by three additional washes in PBS.

Dual colour dSTORM imaging:

Fluorophores Alexa-Fluor™ 647 (AF647) and CF680 photo switch under reducing and oxygen-free buffer conditions, making them suitable for dSTORM single molecule imaging, which enables the localization of the emitters with sub-diffraction localization precision [Heilemann et al. 2008]. Thanks to their close spectral proximity, AF647 was excited and acquired simultaneously with CF680 in the same dSTORM buffer (Abbelight™ SMART-Kit) using a 640 nm laser (Oxxius), and their respective signals discriminated after single molecule localization using a spectral demixing strategy [Lampe et al. 2015]. To implement spectral demixing dSTORM of JAK1-A647 and Cav1-CF680, we used a dual-view Abbelight™ SAFe360, equipped with two Hamamatsu Fusion sCMOS cameras and mounted on an Olympus Ix83 inverted microscope with a 100X 1.5NA TIRF objective. The SAFe360 uses astigmatic PSF engineering to extract the axial position and achieves quasi-isotropic 3D localization precision, and a long-pass dichroic mirror to split fluorescence from single emitters on the two cameras. Samples were illuminated in HILO at 80% of max laser power and imaged at 50 ms exposure time for 100000 frames. Single molecule localization, drift correction, spectral demixing and data visualization were performed using Abbelight™ NEO software.

RNA interference-mediated silencing.

MLEC WT cells were transfected with small interfering RNAs (siRNAs) using HiPerFect reagent (QIAGEN) according to manufacturer's protocol. Experiments were performed 24 hours after transfection, on validation of silencing efficiency by immunoblot analysis using specific antibodies and normalizing to the total level of α-tubulin used as loading control. 20 nM SMART pool siRNA targeting JAK1 mRNA (Dharmacon, Cat. No: L-040117-00-0005) was used for JAK1 knock down. Control siRNA (QIAGEN, Cat. No:

1022076) was used at the same concentration and served as reference point.

Immunoblotting.

Cells were lysed in sample buffer (62.5 mM Tris-HCl pH 6.0, 2% SDS (v/v), 10% glycerol (v/v), 40 mM DTT and 0.03% phenol red (w/v)). Lysates were analyzed by SDS-PAGE and western blot analysis and immunoblotted with the indicated primary antibodies and HRP-conjugated secondary antibodies. Chemiluminescence signal was revealed using Pierce™ ECL Western Blotting Substrate, SuperSignal West Dura Extended Duration Substrate or SuperSignal West Femto Substrate (Thermo Fisher). Acquisition were performed with the ChemiDoc MP Imaging System (BioRad).

Immunofluorescence.

Transfected MLEC Cav1 KO cells were seeded on 12mm coverslips 24 hours before the pSTAT nuclear translocation assay. After IFNα stimulation, cells were fixed and permeabilized with ice-cold methanol for 15 min at -20°C. Cells are washed with PBS 0.2% BSA (v/v) then sequentially incubated with indicated primary antibody and fluorescence-conjugated secondary antibody in PBS 0.2% BSA (v/v) for 1h at room temperature. Coverslips are mounted in Fluoromount-G mounting medium (eBioscience) supplemented with 2 µg/mL DAPI (Sigma-Aldrich). Pictures were acquired on a Leica DM 6000B inverted epifluoresence microscope equipped with a HCX PL Apo 63X NA 1.40 oil immersion objective and an EMCCD camera (Photometrics CoolSNAP HQ); Camera: CCD 1392x1040; objective 40x or 63x. Quantification of pSTATs nuclear translocation by calculating the nucleocytoplasmic ratio of phospho-STAT1-3 signal (nuclei masks were realized with the DAPI staining) with image J software 1.49a (NIH) and plugins bundle proposed by the McMaster Biophotonics Facility (http://www.macbiohotonics.ca).

Single particle tracking:

MLEC WT cells were transfected using the AMAXA electroporation setup with Cav1-mEOS3.2 and Cav1-GFP 24 hrs prior experiment. Cells were grown in Ringer media and subjected to 30 mOsm hypo-osmotic shock during acquisition. Images were acquired using sensitive EMCCD and Nikon CFI Apo TIRF 100x oil, 1.49NA objective.

Transfection:

For single particle tracking experiment MLEC WT and MLEC Cav1 KO cells were transfected using Lonza AMAXA. Adapted settings for MEFs were provided in the AMAXA setup. Lonza provided specific reagent for AMAXA mice cells transfection. Double transfection of 5 µg of Cav1 mEOS3.2 and 1 µg of Cav1 GFP on 1 million cells was performed 24 hrs prior experiment. For pSTATs nuclear translocation upon Cav1 expression, cells were electroporated using a pulse of 220 V and 975 µF with a Gene Pulser® the BioRad setup.

IFNα stimulation.

Cells were treated with or without 1000 U/ml IFNα at 37°C for the indicated times. For biochemical analysis, cells were washed with PBS and lysed in SDS Sample Buffer 1X. Total lysates were analyzed by SDS-PAGE and Western blot analysis and immunoblotted with the indicated antibodies. Chemiluminescence detection was performed with SuperSignal West Dura Extended Duration Substrate or with SuperSignal West Femto Substrate (Thermo Scientific Life Technologies). Phosphorylated and total forms of the proteins are quantified and normalized to clathrin heavy chain or tubulin levels in the same lysate. Phosphorylated protein over total ratio is determined for each condition.

High Throughput screening.

25 µg/mL fibronectine diluted in NaOH 100 mM pH 8.6 is incubated on a PDMS layer at 37°C. 70k WT MLEC or *Cav1*$^{-/-}$ MLEC cells were seeded and incubated for 4 hours at 37°C in complete MLEC media. Cells were stretched by 25% for 2 minutes then while stretch is maintained, cells media is replaced by stimulation media (EBM-2 no SVF with IFNα 1000 U/ml) for 20 min at 37°C. Cells were washed with PBS and lysed with hot laemmli 1X sample buffer (50 mM Tris pH=6.8, 2% SDS, 5% glycerol, 2mM DTT, 2,5 mM EDTA, 2.5 mM/EGTA, 2.5mM/EGTA, 2x Phosphatase inhibitors (Halt Phosphatase inhibitor cocktail 100x, Perbio, Ref. 78420), Protease inhibitors (Protease inhibitor cocktail, complete MINI EDTA-free, Roche, Ref. 1836170), 1 tablet/5 mL, 4 mM Sodium Orthovanadate, 20 mM Sodium Fluoride).

Co-immunoprecipitations.

Cells were lysed in 1% NP-40 in TNE (10 mM Tris/HCl pH 7.5, 150 mM NaCl, 0.5 mM EDTA) with protease inhibitors cocktail (Roche) for 30 min at 4°C. Cleared lysates (16,000g, 10 min, 4°C) were incubated overnight at 4°C under rotation with 1 µg/ml of the indicated antibody followed by incubation for 1 hr with 25 µl of protein A/G magnetic beads (Thermo Scientific) in the case of endogenous proteins. In the case of tagged proteins, 25 µl GFP-Trap or RFP-Trap beads (Chromotek) were used. After 3 washes in TNE, immunoprecipitated beads were eluted following the manufacturers' instructions.

Osmotic shock and uniaxial stretch.

For osmotic shock, cells were seeded 24 hr before experiment, then complete media was replaced by ten times diluted media for 5 minutes, cells were immediately lysed or hypo-osmotic media was replaced by normal iso-osmotic media (recovery) before lysis. For cell stretch, cells were seeded on a 100 µm thick PDM sheet (12x7 mm) coated with fibronectin 4 hr prior experiment. The PDMS sheet was linearly stretched using a homemade setup motorized (PI, Karlsruhe, Germany). Cells were pre-stretched by 25% for 2 minutes and stretch was maintained during IFNα stimulation.

CSD mimicking peptides

CSD mimicking peptides were synthetized from Biomatik. Control peptide sequence: HHHHHH-RQIKIWFQNRRMKWKKWGIDKASFTTFTVTKYWFRY; CavTratin sequence: HHHHHH-QIKIWFQNRRMKWKKDGIWKASFTTFTVTKY; CavNoxin sequence HHHHH H-RQIKIWFQNRRMKWKKDGIWKASFAAATVTKWYFYR. Cells were treated for 6 hours with 1 µM CSD mimicking peptide resuspended in endothelial basal medium 0.2% PBS/BSA (v/v).

In vitro Kinase activity measurement.

Invitro kinase assay was performed using purified JAK1 (ProQinase 1480-0000-1 JAK1 aa583-1154), RBER-IRStide (ProQinase 0863-0000-1). Kinase reaction was performed in Kinase reaction buffer ([ATP] 100 µM, RBER-IRStide 80 µg/ml, DMSO according to peptide concentration) at 30°C for 1 hr. Measurement of ADP production was performed using Promega ADP-Glo™ Kinase Assay. Luminescence measurement was performed using BMG Labtech FLUOstar Omega plate reader.

Drug treatment

MLEC WT cells were treated 1% with methyl-β-cyclodextrin (w/v) (Sigma Aldrich, Cat. No: C4555) for 20 min and stimulated with 1000 U/ml IFNα at 37°C for 10 min.

References:

Aboulaich, N., Vainonen, J.P., Stralfors, P., and Vener, A. V (2004). Vectorial proteomics reveal targeting, phosphorylation and specific fragmentation of polymerase I and transcript release factor (PTRF) at the surface of caveolae in human adipocytes. Biochem. J. *383*, 237–248.

Anderson, R. G. (1993). Plasmalemmal caveolae and GPI-anchored membrane proteins. *Current opinion in cell biology*, *5*(4), 647-652.

Anderson, R. G., Kamen, B. A., Rothberg, K. G., & Lacey, S. W. (1992). Potocytosis: sequestration and transport of small molecules by caveolae. *Science*, *255*(5043), 410-412.

Ariotti, N., Fernández-Rojo, M.A., Zhou, Y., Hill, M.M., Rodkey, T.L., Inder, K.L., Tanner, L.B., Wenk, M.R., Hancock, J.F., and Parton, R.G. (2014). Caveolae regulate the nanoscale organization of the plasma membrane to remotely control Ras signaling. J. Cell Biol. *204*, 777–792.

Ariotti, N., Rae, J., Leneva, N., Ferguson, C., Loo, D., Okano, S., Hill, M.M., Walser, P., Collins, B.M., and Parton, R.G. (2015). Molecular characterization of caveolin-induced membrane curvature. J. Biol. Chem. *290*, 24875–24890.

Bastiani, M., Liu, L., Hill, M.M., Jedrychowski, M.P., Nixon, S.J., Lo, H.P., Abankwa, D., Luetterforst, R., Fernandez-Rojo, M., Breen, M.R., et al. (2009). MURC/Cavin-4 and cavin family members form tissue-specific caveolar complexes. J. Cell Biol. *185*, 1259–1273.

Beebe, J., Liu, J.-Y., and Zhang, J.-T. (2018). Two decades of research in discovery of anticancer drugs targeting STAT3, how close are we? Pharmacol. Ther.

Bernatchez, P., Sharma, A., Bauer, P.M., Marin, E., and Sessa, W.C. (2011). A noninhbitory mutant of the caveolin1 scaffolding domain enhances eNOS-derived NO synthesis and vasodilation in mice. *121*.

Blouin, C.M., Hamon, Y., Gonnord, P., Boularan, C., Kagan, J., Viaris de Lesegno, C., Ruez, R., Mailfert, S., Bertaux, N., Loew, D., et al. (2016). Glycosylation-Dependent IFN-??R Partitioning in Lipid and Actin Nanodomains Is Critical for JAK Activation. Cell *166*, 920–934.

Boellner S, Becker KF. Reverse Phase Protein Arrays-Quantitative Assessment of Multiple Biomarkers in Biopsies for Clinical Use. *Microarrays (Basel).* 2015;4(2):98-114. Published 2015 Mar 24. doi:10.3390/microarrays4020098

Bowler, M., Kong, D., Sun, S., Nanjundappa, R., Evans, L., Farmer, V., ... & Loncarek, J. (2019). High-resolution characterization of centriole distal appendage morphology and dynamics by correlative STORM and electron microscopy. *Nature communications*, *10*(1), 1-15.

Byrne, D.P., Dart, C., and Rigden, D.J. (2012). Evaluating Caveolin Interactions: Do Proteins Interact with the Caveolin Scaffolding Domain through a Widespread Aromatic Residue-Rich Motif? PLoS One *7*.

Cheng, J.P.X., and Nichols, B.J. (2016). Caveolae: One Function or Many? Trends Cell Biol. *26*, 177–189.

Collins, B.M., Davis, M.J., Hancock, J.F., and Parton, R.G. (2012). Structure-Based Reassessment of the Caveolin Signaling Model: Do Caveolae Regulate Signaling through Caveolin-Protein Interactions? Dev. Cell *23*, 11–20.

Couet, J., Li, S., Okamoto, T., Ikezu, T., and Lisanti, M.P. (1997a). Identification of peptide and protein ligands for the caveolin- scaffolding domain. Implications for the interaction of caveolin with caveolae-associated proteins. J. Biol. Chem. *272*, 6525–6533.

Couet, J., Sargiacomo, M., and Lisanti, M.P. (1997b). Interaction of a receptor tyrosine kinase, EGF-R, with caveolins. Caveolin binding negatively regulates tyrosine and serine/threonine kinase activities. J. Biol. Chem. *272*, 30429–30438.

Elliott MH, Ashpole NE, Gu X, Herrnberger L, McClellan ME, Griffith GL, Reagan AM, Boyce TM, Tanito M, Tamm ER, Stamer WD. Caveolin-1 modulates intraocular pressure: implications for caveolae mechanoprotection in glaucoma. Sci Rep. 2016 Nov 14; 6:37127.

Fujimoto, T. (1993). Calcium pump of the plasma membrane is localized in caveolae. J. Cell Biol. *120*, 1147–1157.

Gabella, G., & Blundell, D. (1978). Effect of stretch and contraction on caveolae of smooth muscle cells. *Cell and tissue research*, *190*(2), 255-271.

Gambin, Y., Ariotti, N., McMahon, K.A., Bastiani, M., Sierecki, E., Kovtun, O., Polinkovsky, M.E., Magenau, A., Jung, W., Okano, S., et al. (2014). Single-molecule analysis reveals self assembly and nanoscale segregation of two distinct cavin subcomplexes on caveolae. Elife *3*, e01434.

Gangadharan, V., Nohe, A., Caplan, J., Czymmek, K., and Duncan, R.L. (2015). Caveolin-1 regulates P2X7 receptor signaling in osteoblasts. Am. J. Physiol. Cell Physiol. *308*, C41-50.

Garcia-Cardena, G. (1997). Dissecting the Interaction between Nitric Oxide Synthase (NOS) and Caveolin. FUNCTIONAL SIGNIFICANCE OF THE NOS CAVEOLIN BINDING DOMAIN IN VIVO. J. Biol. Chem. *272*, 25437–25440.

Goetz, J.G., Lajoie, P., Wiseman, S.M., and Nabi, I.R. (2008). Caveolin-1 in tumor progression: The good, the bad and the ugly. Cancer Metastasis Rev. *27*, 715–735.

Han B, Porta JC, Hanks JL, Peskova Y, Binshtein E, Dryden K, Claxton DP, Mchaourab HS, Karakas E, Ohi MD, Kenworthy AK. Structure and assembly of CAV1 8S complexes revealed by single particle electron microscopy. Sci Adv. 2020 Dec 2;6(49): eabc6185.

Hansen, C.G., Howard, G., and Nichols, B.J. (2011). Pacsin 2 is recruited to caveolae and functions in caveolar biogenesis. J. Cell Sci. *124*, 2777–2785.

Hayer, A., Stoeber, M., Bissig, C., and Helenius, A. (2010). Biogenesis of caveolae: stepwise assembly of large caveolin and cavin complexes. Traffic *11*, 361–382.

Heilemann, M., Van De Linde, S., Schüttpelz, M., Kasper, R., Seefeldt, B., Mukherjee, A., ... & Sauer, M. (2008). Subdiffraction-resolution fluorescence imaging with conventional fluorescent probes. *Angewandte Chemie International Edition*, *47*(33), 6172-6176.

Hill, M.M., Bastiani, M., Luetterforst, R., Kirkham, M., Kirkham, A., Nixon, S.J., Walser, P., Abankwa, D., Oorschot, V.M.J., Martin, S., et al. (2008). PTRF-Cavin, a Conserved Cytoplasmic Protein Required for Caveola Formation and Function. Cell *132*, 113–124.

Hirai, H., Karian, P., and Kikyo, N. (2011). Regulation of embryonic stem cell self-renewal and pluripotency by leukaemia inhibitory factor. Biochem. J. *438*, 11–23.

Hoop, C.L., Sivanandam, V.N., Kodali, R., Srnec, M.N., and van der Wel, P.C.A. (2012). STRUCTURAL CHARACTERIZATION OF THE CAVEOLIN SCAFFOLDING DOMAIN IN ASSOCIATION WITH CHOLESTEROL-RICH MEMBRANES. *51*, 90–99.

Igaz, P., Toth, S., and Falus, A. (2001). Biological and clinical significance of the JAK-STAT pathway; lessons from knockout mice. Inflamm. Res. *50*, 435–441.

Jacobson K, Liu P, Lagerholm BC. The Lateral Organization and Mobility of Plasma Membrane Components. Cell. 2019 May 2;177(4):806-819.

Jasmin, J.F., Mercier, I., Sotgia, F., and Lisanti, M.P. (2006). SOCS proteins and caveolin-1 as negative regulators of endocrine signaling. Trends Endocrinol. Metab. *17*, 150–158.

Kai, F., Laklai, H., and Weaver, V. (2016). Force Matters: Biomechanical Regulation of Cell Invasion and Migration in Disease. Trends Cell Biol. *xx*, 1–12.

Kaptein, A., Paillard, V., and Saunders, M. (1996). Dominant negative stat3 mutant inhibits interleukin-6-induced Jak-STAT signal transduction. J. Biol. Chem. *271*, 5961–5964.

Kershaw, N.J., Murphy, J.M., Lucet, I.S., Nicola, N.A., and Babon, J.J. (2013). Regulation of Janus kinases by SOCS proteins. Biochem. Soc. Trans. *41*, 1042–1047.

Kirkham, M., Nixon, S.J., Howes, M.T., Abi-Rached, L., Wakeham, D.E., Hanzal-Bayer, M., Ferguson, C., Hill, M.M., Fernandez-Rojo, M., Brown, D. a, et al. (2008). Evolutionary analysis and molecular dissection of caveola biogenesis. J. Cell Sci. *121*, 2075–2086.

Koromilas, A.E., and Sexl, V. (2013). The tumor suppressor function of STAT1 in breast cancer. Jak-Stat *2*, e23353.

Laine, R. F., Tosheva, K. L., Gustafsson, N., Gray, R. D., Almada, P., Albrecht, D., ... & Henriques, R. (2019). NanoJ: a high-performance open-source super-resolution microscopy toolbox. *Journal of Physics D: Applied Physics*, *52*(16), 163001.

Lamaze, C., and Torrino, S. (2015). Caveolae and cancer: A new mechanical perspective. Biomed. J. *38*, 367–379.

Lamaze, C., Tardif, N., Dewulf, M., Vassilopoulos, S., and Blouin, C.M. (2017). The caveolae dress code: structure and signaling. Curr. Opin. Cell Biol. *47*, 117–125.

Lampe, A., Tadeus, G., & Schmoranzer, J. (2015). Spectral demixing avoids registration errors and reduces noise in multicolor localization-based super-resolution microscopy. *Methods and applications in fluorescence*, *3*(3), 034006.

Le Lan, C., Neumann, J.-M., and Jamin, N. (2006). Role of the membrane interface on the conformation of the caveolin scaffolding domain: a CD and NMR study. FEBS Lett. *580*, 5301–5305.

Levet, F., Julien, G., Galland, R., Butler, C., Beghin, A., Chazeau, A., ... & Sibarita, J. B. (2019). A tessellation-based colocalization analysis approach for single-molecule localization microscopy. *Nature communications*, *10*(1), 1-12.

Li, S., Okamoto, T., Chun, M., Sargiacomo, M., Casanova, J.E., Hansen, S.H., Nishimoto, I., and Lisanti, M.P. (1995). Evidence for a regulated interaction between heterotrimeric G proteins and caveolin. J. Biol. Chem. *270*, 15693–15701.

Li, S., Couet, J., and Lisanti, M.P. (1996). Src tyrosine kinases, Galpha subunits, and H-Ras share a common membrane-anchored scaffolding protein, caveolin. Caveolin binding negatively regulates the auto-activation of Src tyrosine kinases. J. Biol. Chem. *271*, 29182–29190.

Lim, Y.W., Lo, H.P., Ferguson, C., Martel, N., Giacomotto, J., Gomez, G.A., Yap, A.S., Hall, T.E., and Parton, R.G. (2017). Caveolae Protect Notochord Cells against Catastrophic Mechanical Failure during Development. Curr. Biol. *27*, 1968–1981.e7.

Lisanti, M.P., Tang, Z., Scherer, P.E., Kubler, E., Koleske, A.J., and Sargiacomo, M. (1995). Caveolae, transmembrane signalling and cellular transformation. Mol. Membr. Biol. *12*, 121–124.

Liu, H., Yang, L., Zhang, Q., Mao, L., Jiang, H., and Yang, H. (2016). Probing the structure and dynamics of caveolin-1 in a caveolae-mimicking asymmetric lipid bilayer model. Eur. Biophys. J.

Lo, H.P., Nixon, S.J., Hall, T.E., Cowling, B.S., Ferguson, C., Morgan, G.P., Schieber, N.L., Fernandez-Rojo, M.A., Bastiani, M., Floetenmeyer, M., et al. (2015). The caveolin-Cavin system plays a conserved and critical role in mechanoprotection of skeletal muscle. J. Cell Biol. *210*, 833–849.

Ludwig, A., Howard, G., Mendoza-Topaz, C., Deerinck, T., Mackey, M., Sandin, S., Ellisman, M.H., and Nichols, B.J. (2013). Molecular composition and ultrastructure of the caveolar coat complex. PLoS Biol. *11*, e1001640.

Meng, F., Saxena, S., Liu, Y., Joshi, B., Wong, T.H., Shankar, J., Foster, L.J., Bernatchez, P., and Nabi, I.R. (2017). The phospho–caveolin-1 scaffolding domain dampens force fluctuations in focal adhesions and promotes cancer cell migration. Mol. Biol. Cell *28*, 2190–2201.

Moon, H., Lee, C.S., Inder, K.L., Sharma, S., Choi, E., Black, D.M., Lê Cao, K., Winterford, C., Coward, J.I., Ling, M.T., et al. (2013). PTRF/cavin-1 neutralizes non-caveolar caveolin-1 microdomains in prostate cancer. Oncogene 1–10.

Morén, B., Shah, C., Howes, M.T., Schieber, N.L., McMahon, H.T., Parton, R.G., Daumke, O., and Lundmark, R. (2012). EHD2 regulates caveolar dynamics via ATP-driven targeting and oligomerization. Mol. Biol. Cell *23*, 1316–1329.

Murata, T., Lin, M.I., Stan, R. V., Bauer, P.M., Yu, J., and Sessa, W.C. (2007). Genetic evidence supporting caveolae microdomain regulation of calcium entry in endothelial cells. J. Biol. Chem. *282*, 16631–16643.

Nassoy, P., and Lamaze, C. (2012). Stressing caveolae new role in cell mechanics. Trends Cell Biol. *22*, 381–389.

Nicolson GL. The Fluid-Mosaic Model of Membrane Structure: still relevant to understanding the structure, function and dynamics of biological membranes after more than 40 years. Biochim Biophys Acta. 2014 Jun;1838(6):1451-66.

Nystrom, F.H., Chen, H., Cong, L.N., Li, Y., and Quon, M.J. (1999). Caveolin-1 interacts with the insulin receptor and can differentially modulate insulin signaling in transfected Cos-7 cells and rat adipose cells. Mol. Endocrinol. *13*, 2013–2024.

O'Shea, J.J., Gadina, M., and Schreiber, R.D. (2002). Cytokine signaling in 2002: new surprises in the Jak/Stat pathway. Cell *109 Suppl*, S121-31.

O'Shea, J.J., Schwartz, D.M., Villarino, A. V, Gadina, M., Iain, B., and Laurence, A. (2015). The JAK-STAT Pathway: Impact on Human Disease and Therapeutic Intervention. 311–328.

Okamoto, T., Schlegel, a, Scherer, P.E., and Lisanti, M.P. (1998). Caveolins, a family of scaffolding proteins for organizing "preassembled signaling complexes" at the plasma membrane. J Biol Chem *273*, 5419–5422.

Orré, T., Joly, A., Karatas, Z., Kastberger, B., Cabriel, C., Böttcher, R. T., ... & Giannone, G. (2021). Molecular motion and tridimensional nanoscale localization of kindlin control integrin activation in focal adhesions. *Nature communications*, *12*(1), 1-17.

Palade, G.E. (1953). The fine structure of blood capillaries. J. Appl. Phys. *24*, 1424.

Parton, R.G., and Simons, K. (2007). The multiple faces of caveolae. Nat. Rev. Mol. Cell Biol. *8*, 185–194.

Parton, R.G., Hanzal-Bayer, M., and Hancock, J.F. (2006). Biogenesis of caveolae: a structural model for caveolin-induced domain formation. J. Cell Sci. *119*, 787–796.

Parton RG. Caveolae: Structure, Function, and Relationship to Disease. Annu Rev Cell Dev Biol. 2018 Oct 6; 34:111-136.

Parton RG, Kozlov MM, Ariotti N. Caveolae and lipid sorting: Shaping the cellular response to stress. J Cell Biol. 2020 Apr 6;219(4):e201905071.

Parton RG, Del Pozo MA, Vassilopoulos S, Nabi IR, Le Lay S, Lundmark R, Kenworthy AK, Camus A, Blouin CM, Sessa WC, Lamaze C. Caveolae: The FAQs. Traffic. 2020 Jan;21(1):181-185.

Parton RG, McMahon KA, Wu Y. Caveolae: Formation, dynamics, and function. Curr Opin Cell Biol. 2020 Aug;65:8-16.

Patel, H.H., Murray, F., and Insel, P.A. (2008). Caveolae as organizers of pharmacologically relevant signal transduction molecules. Annu. Rev. Pharmacol. Toxicol. *48*, 359–391.

Platanias, L.C. (2005). Mechanisms of type-I- and type-II-interferon-mediated signalling. Nat. Rev. Immunol. *5*, 375–386.

Pol A, Morales-Paytuví F, Bosch M, Parton RG. Non-caveolar caveolins - duties outside the caves. J Cell Sci. 2020 May 11;133(9):jcs241562.

Prescott, L., and M.W. Brightman. 1976. The sarcolemma of Aplysia smooth muscle in freeze-fracture preparations. *Tissue Cell*. 8:248-258.

Rothberg, K.G., Heuser, J.E., Donzell, W.C., Ying, Y.S., Glenney, J.R., and Anderson, R.G. (1992). Caveolin, a protein component of caveolae membrane coats. Cell *68*, 673–682.

Scherer, P.E., Okamoto, T., Chun, M., Nishimoto, I., Lodish, H.F., and Lisanti, M.P. (1996). Identification,

sequence, and expression of caveolin-2 defines a caveolin gene family. Proc. Natl. Acad. Sci. U. S. A. *93*, 131–135.

Schreiber, G., and Piehler, J. (2015). The molecular basis for functional plasticity in type I interferon signaling. Trends Immunol. *36*, 139–149.

Sezgin, E., Levental, I., Mayor, S. *et al*. The mystery of membrane organization: composition, regulation and roles of lipid rafts. *Nat Rev Mol Cell Biol* **18,** 361–374 (2017).

Shajahan, A.N., Dobbin, Z.C., Hickman, F.E., Dakshanamurthy, S., and Clarke, R. (2012). Tyrosine-phosphorylated caveolin-1 (Tyr-14) increases sensitivity to paclitaxel by inhibiting BCL2 and BCLxL proteins via c-Jun N-terminal Kinase (JNK). J. Biol. Chem. *287*, 17682–17692.

Shivanandan, A., Radenovic, A., & Sbalzarini, I. F. (2013). MosaicIA: an ImageJ/Fiji plugin for spatial pattern and interaction analysis. *BMC bioinformatics*, *14*(1), 1-10.

Singh, V., Lamaze, C. Membrane tension buffering by caveolae: a role in cancer?. *Cancer Metastasis Rev* **39,** 505–517 (2020).

Sinha, B., Köster, D., Ruez, R., Gonnord, P., Bastiani, M., Abankwa, D., Stan, R. V., Butler-Browne, G., Vedie, B., Johannes, L., et al. (2011). Cells respond to mechanical stress by rapid disassembly of caveolae. Cell *144*, 402–413.

Stoeber, M., Schellenberger, P., Siebert, C.A., Leyrat, C., Helenius, A., and Grünewald, K. (2016). Model for the architecture of caveolae based on a flexible, net-like assembly of Cavin1 and Caveolin discs. Proc. Natl. Acad. Sci. U. S. A. 201616838.

Taira, J., Sugishima, M., Kida, Y., Oda, E., Noguchi, M., and Higashimoto, Y. (2011). Caveolin-1 is a competitive inhibitor of heme oxygenase-1 (HO-1) with heme: identification of a minimum sequence in caveolin-1 for binding to HO-1. Biochemistry *50*, 6824–6831.

Trane, A.E., Pavlov, D., Sharma, A., Saqib, U., Lau, K., Van Petegem, F., Minshall, R.D., Roman, L.J., and Bernatchez, P.N. (2014). Deciphering the binding of Caveolin-1 to client protein endothelial nitric-oxide synthase (eNOS): Scaffolding subdomain identification, interaction modeling, and biological significance. J. Biol. Chem. *289*, 13273–13283.

Villarino, A. V, Kanno, Y., and Shea, J.J.O. (2017). Mechanisms and consequences of Jak – STAT signaling in the immune system. *18*.

Way, M., and Parton, R.G. (1995). M-caveolin, a muscle-specific caveolin-related protein. FEBS Lett. *376*, 108–112.

Williams, J.J.L., Alotaiq, N., Mullen, W., Burchmore, R., Liu, L., Baillie, G.S., Schaper, F., Pilch, P.F., and Palmer, T.M. (2018). Interaction of suppressor of cytokine signalling 3 with cavin-1 links SOCS3 function and cavin-1 stability. Nat. Commun. *9*, 168.

Yamada, E. (1955). The fine structure of the gall bladder epithelium of the mouse. J. Biophys. Biochem. Cytol. *1*, 445–458.

Figure 1: Several signaling pathways are controlled by caveolae under mechanical stress

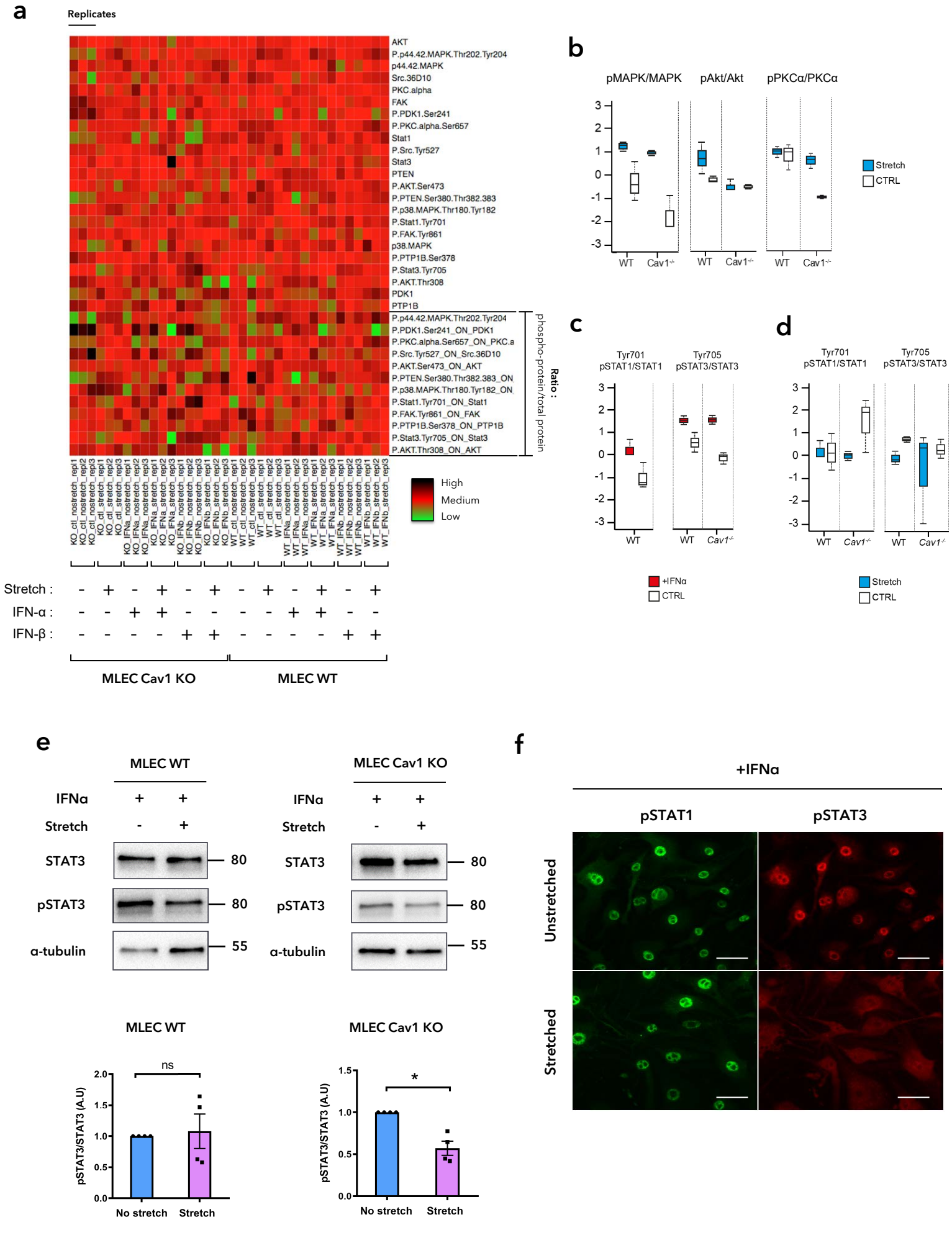

Figure 2: STAT3 inhibition is mediated by interaction of Cav1 with JAK1

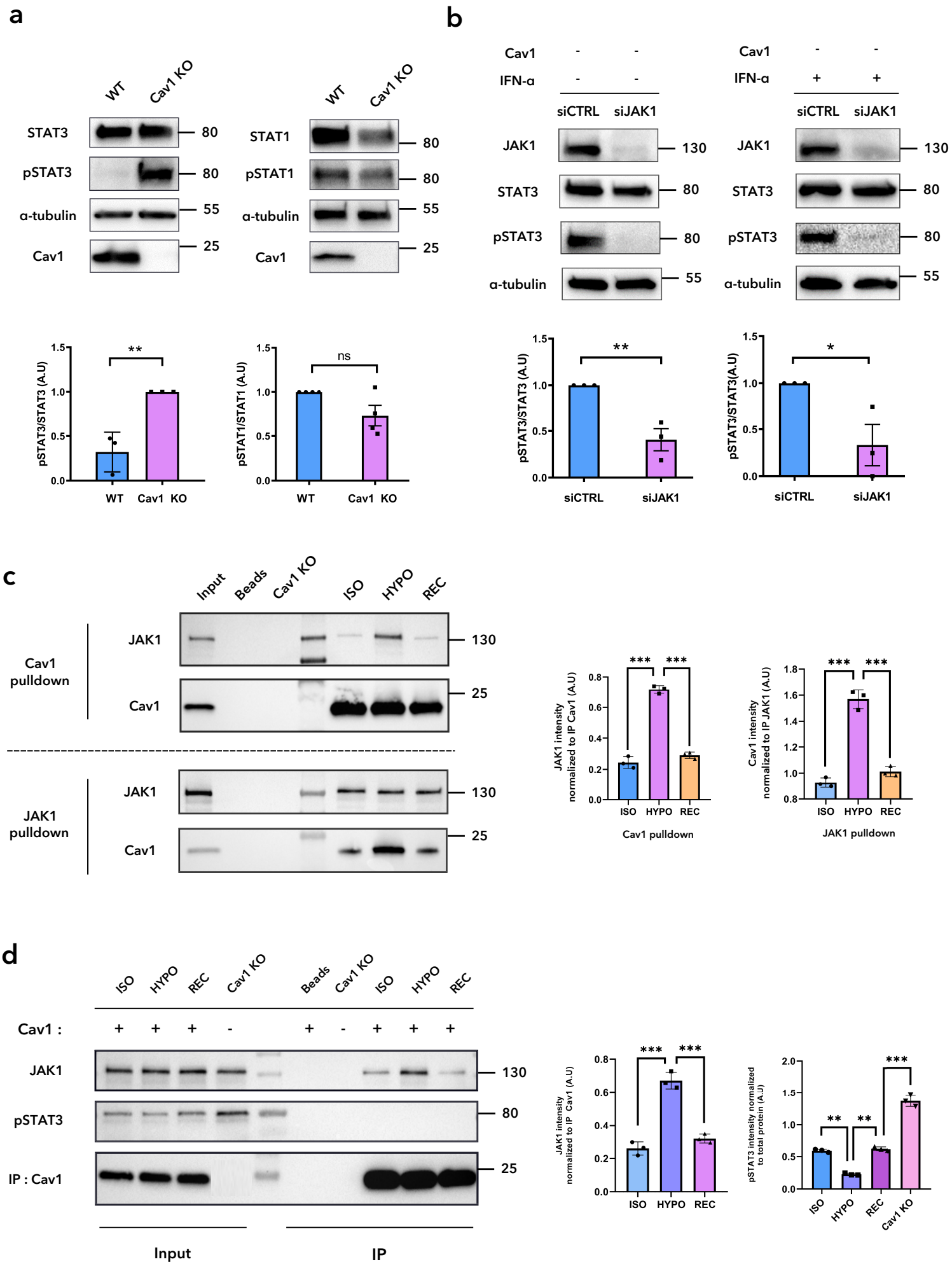

Figure 3: JAK1 inhibition is mediated by the caveolin scaffolding domain

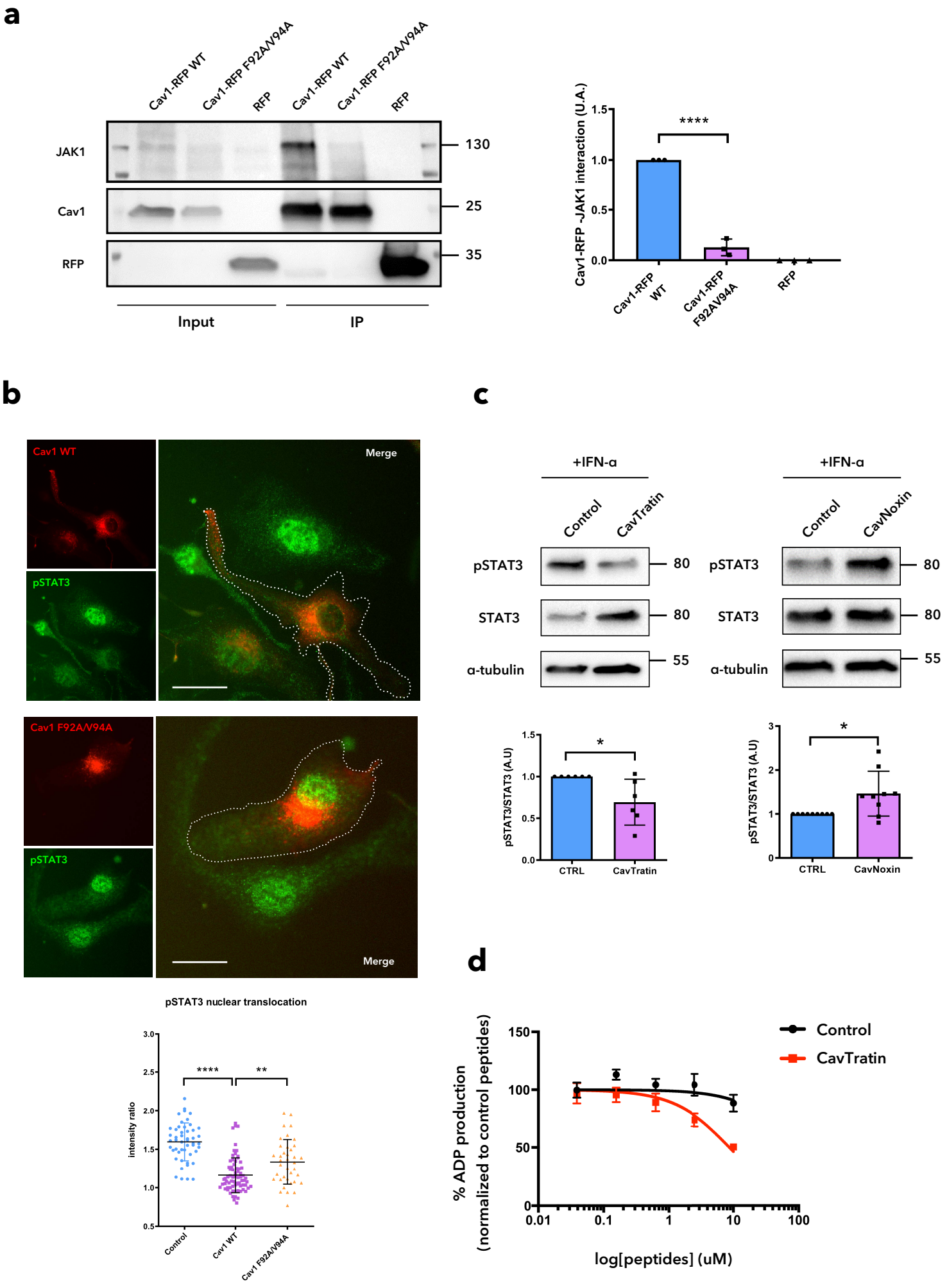

Figure 4: Mechanical stress drastically increases the diffusion of Cav1 molecules at the PM

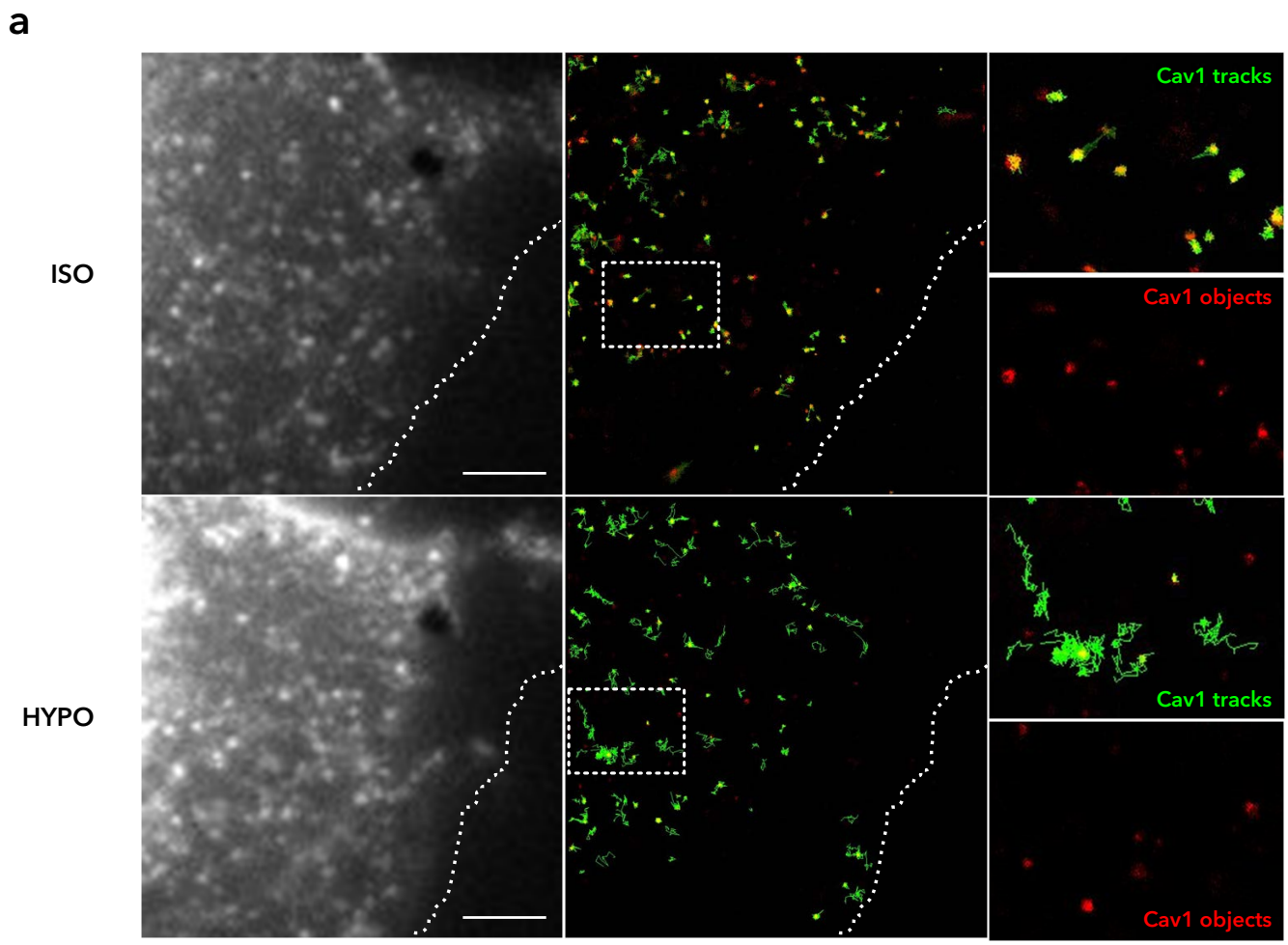

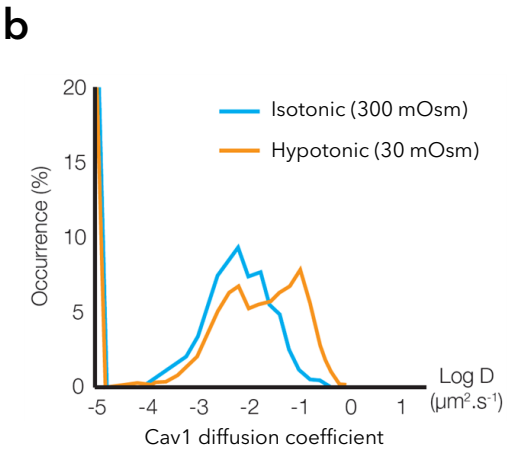

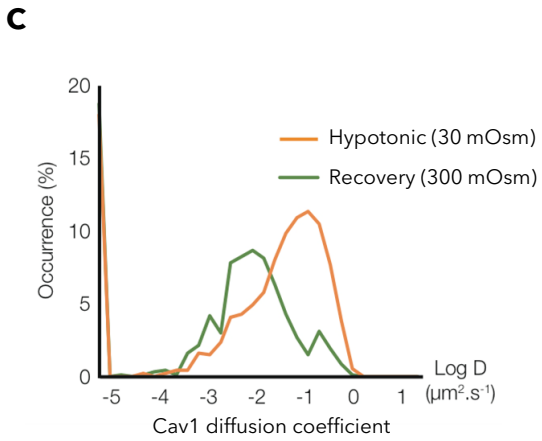

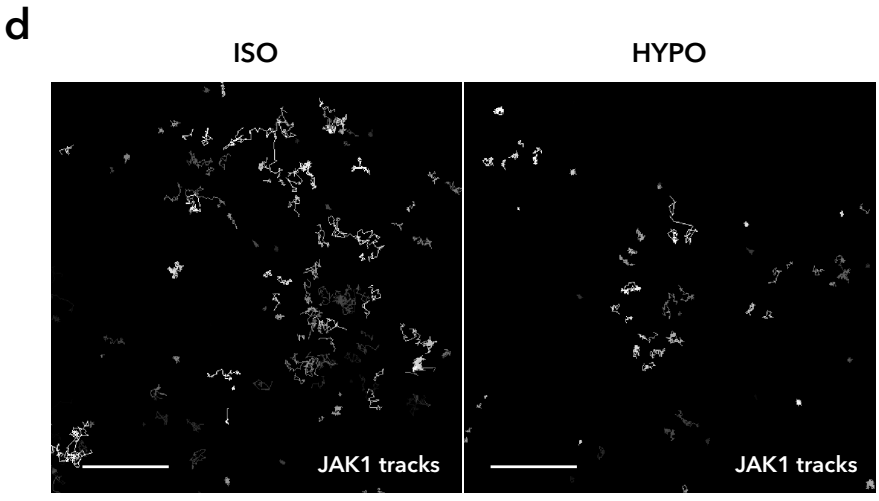

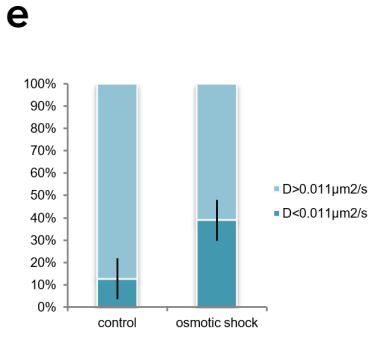

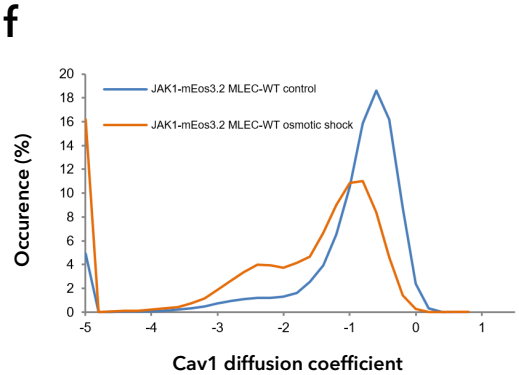

Figure 5: Nanoscale imaging of non-caveolar Cav1 under mechanical stress

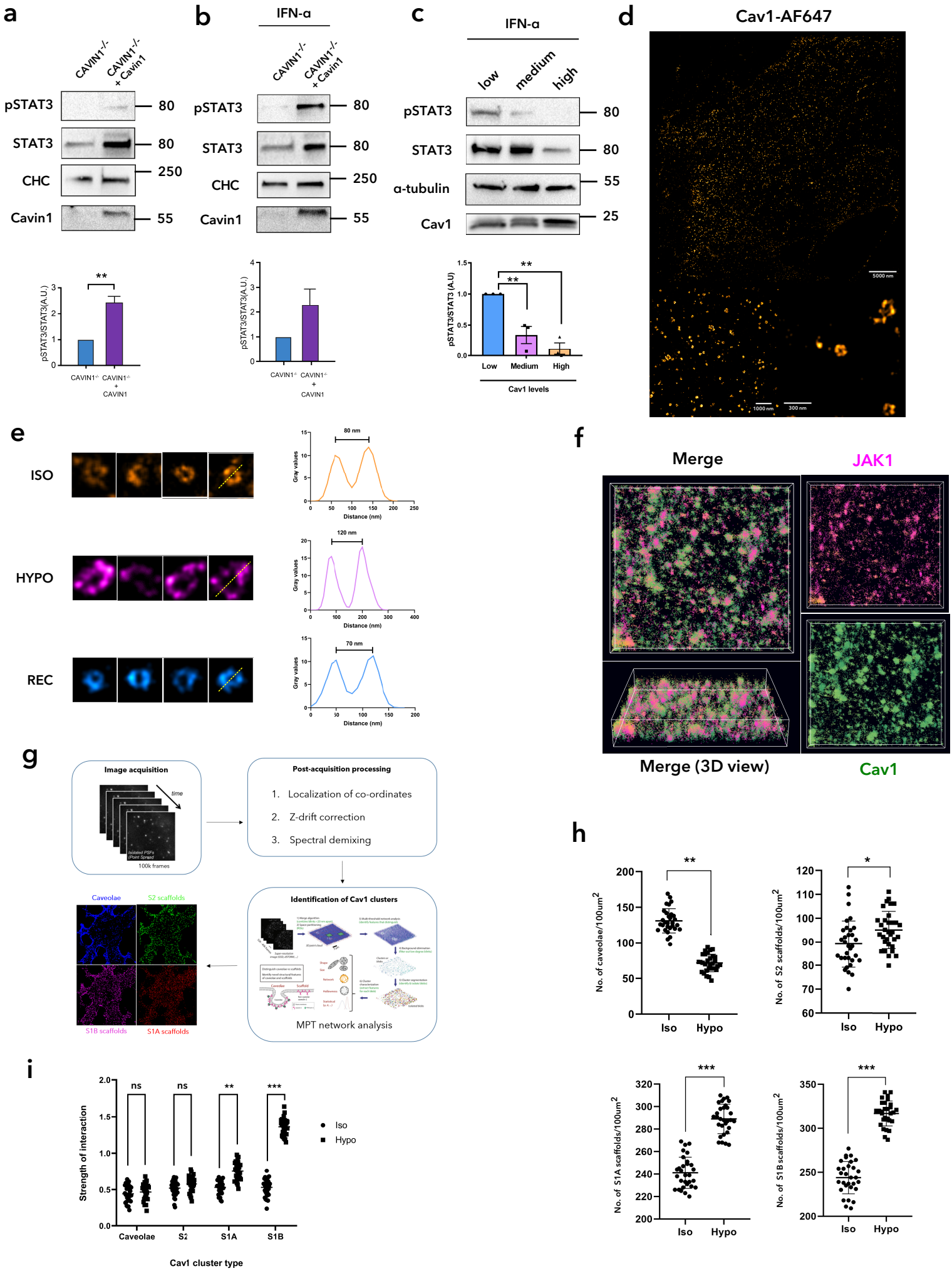

Supp Fig. 1 :

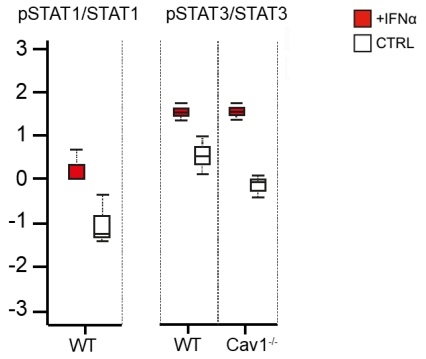

Supp Fig. 2 :

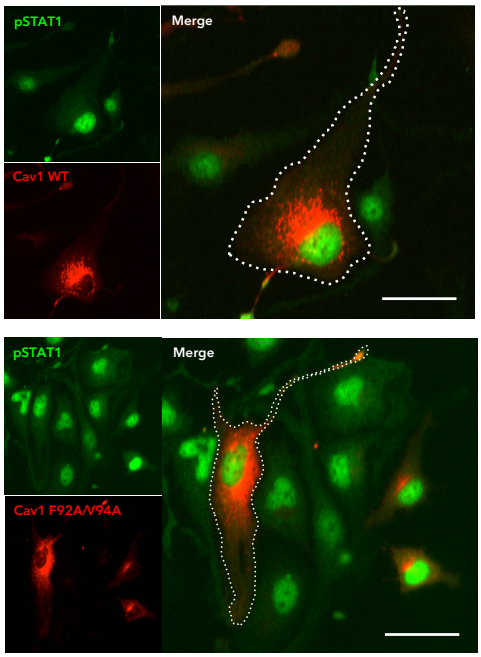

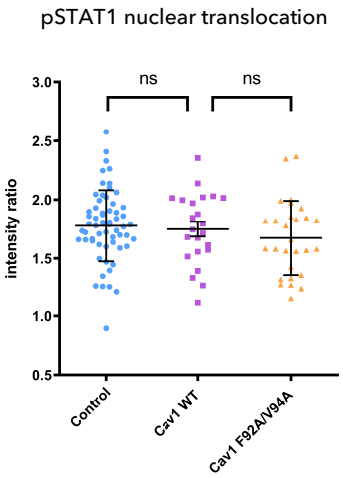

Supp Fig. 3 :

a

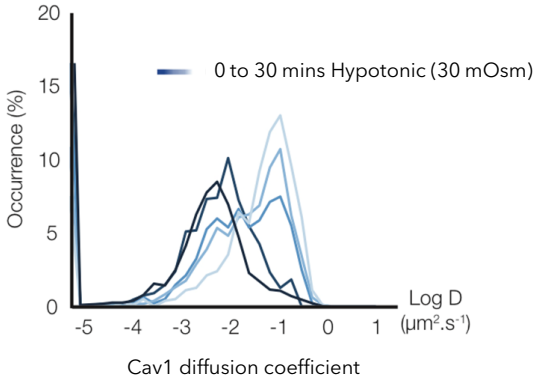

b

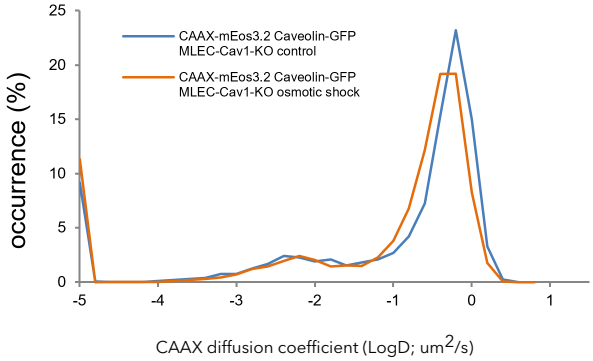

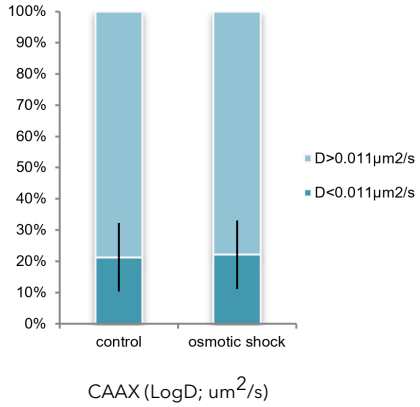

Supp Fig. 4 :

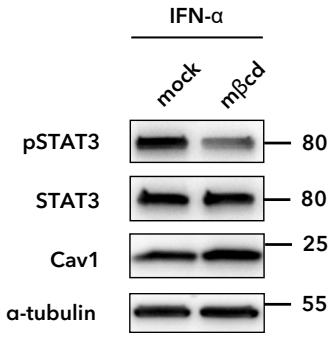

Supp Fig. 5 :

a

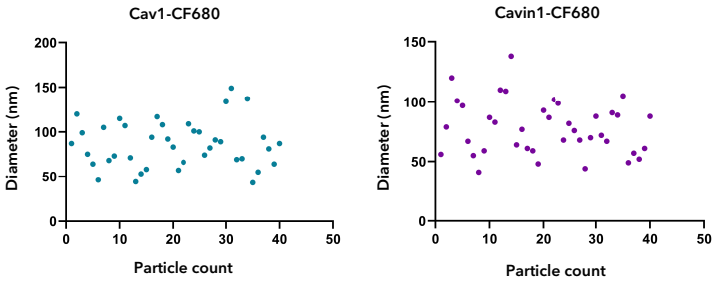

b

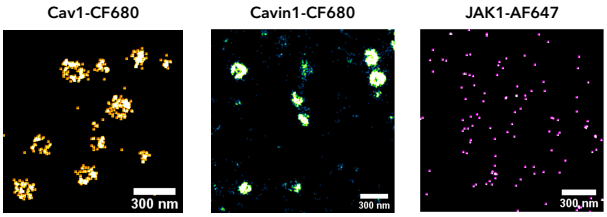

c

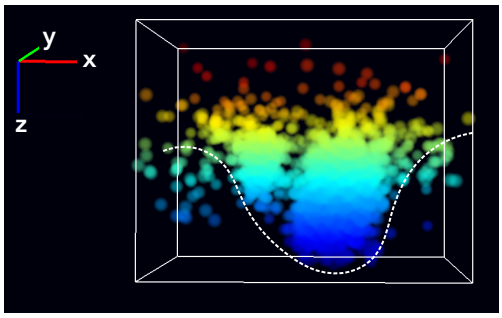

Calibration curves

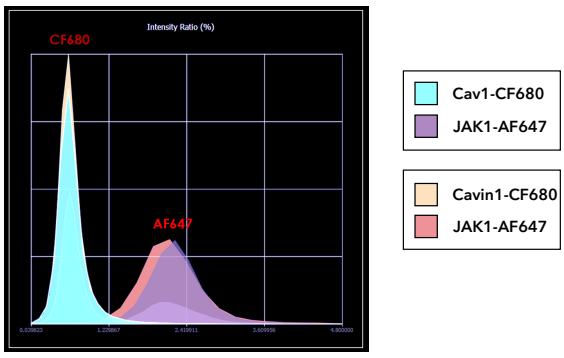

d

Raw image

Post cluster segmentation

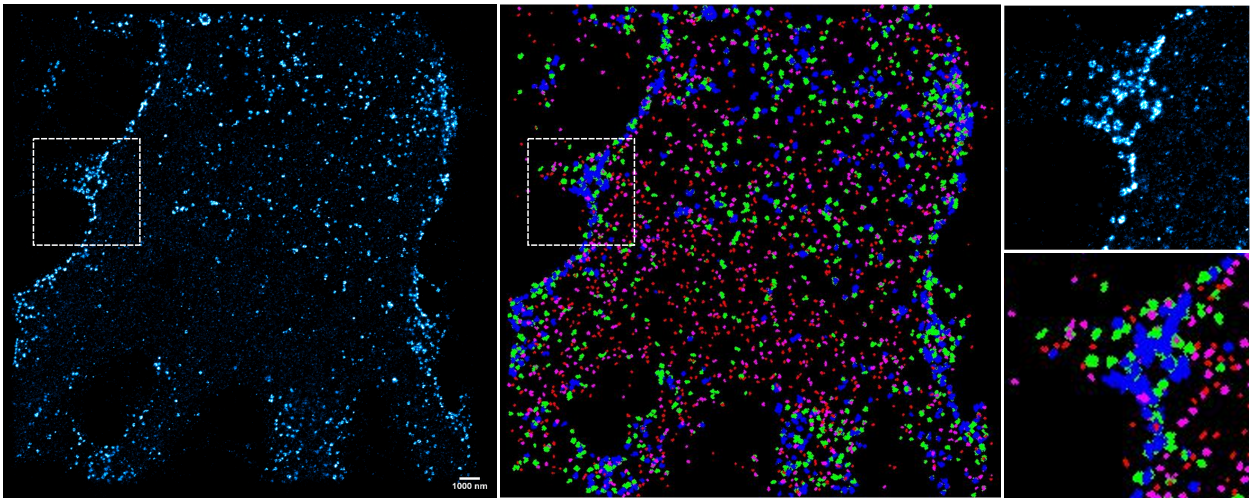

Caveolae S2 scaffolds S1B scaffolds S1A scaffolds

FIGURE LEGENDS

Figure 1: High throughput screening of signaling pathways modulated by caveolae mechanics. (a) Heat map of signaling effectors activation in WT and CAV1$^{-/-}$ MLEC cells under resting condition or uniaxial stretch and treated or not with type I IFN. **(b)** p44/42 MAPK, Akt and PKCα phosphorylation level under resting condition and uniaxial stretch in WT and CAV1$^{-/-}$ MLEC cells. **(c and d)** STAT1 and STAT3 phosphorylation level under type I IFN stimulation (c) and uniaxial stretch (d) in WT and CAV1$^{-/-}$ MLEC cells. **(e)** STAT3 phosphorylation level induced by IFN-α stimulation in WT (left panel) and CAV1$^{-/-}$ (right panel) MLEC cells submitted or not to uniaxial stretch. Representative immunoblot, quantification of signal ratio relative to "no stretch" condition. N=3; Mean value ± SEM; statistics were performed using two tailed unpaired t test; *P<0.05. **(f)** Immunofluorescence images of the nuclear translocation of pSTAT1 (green) and pSTAT3 (red) in WT MLEC cells submitted or not to uniaxial stretch. Scale bar: 5 µm.

Figure 2: Cav1 dependent inhibition of STAT3 activation is mediated through JAK1 interaction. (a) STAT3 (left panel) and STAT1 (right panel) basal phosphorylation level in WT MLEC compared to CAV1$^{-/-}$ MLEC. N=3 (pSTAT3) and N=4 (pSTAT1); Mean value ± SEM. Statistics was performed using two tailed unpaired t test. **P<0,01. **(b)** STAT3 phosphorylation level in CAV1$^{-/-}$ MLEC. upon control (CTRL) or JAK1 siRNA treatment. At steady state (left) or upon IFN-α stimulation (right). **(c)** Immunoprecipitation experiment of endogenous Cav1 and JAK1 in iso-osmotic (ISO), hypo-osmotic (HYPO) and successive hypo-osmotic shock and iso-osmotic condition (REC). Quantification of (JAK1 and Cav1) signal is based on the ratio relative to the corresponding immunoprecipated protein levels. N=3; Mean value ± SEM; statistics were performed using two tailed unpaired t test. **P<0.01; ***P<0. 001. **(d)** Immunoprecipitation experiment of endogenous Cav1 and concomitant STAT3 phosphorylation level in WT MLEC upon IFN-α stimulation in iso-, hypo-osmotic and recovery conditions. Representative immunoblot. N=3; Mean value ± SEM; statistics was performed using two tailed unpaired t test. **P<0.01; ***P<0. 001.

Figure 3: Cav1-JAK1 interaction requires the caveolin scaffolding domain. (a) Representative immunoblot of RFP-trap pull-down experiment performed on CAV1$^{-/-}$

MLEC cells expressing either WT Cav1-RFP or F92A/V94A Cav1-RFP or RFP (left). Quantification of JAK1/Cav1 signal ratio relative to "WT Cav1-RFP" condition (right); N=3; Mean values ± SEM; ****P<0.0001; Statistics were processed using unpaired t-test. **(b)** Wide field immunofluorescence images of nuclear translocation of pSTAT3 (green) of IFN-α stimulated CAV1$^{-/-}$ MLEC expressing either exogenous WT Cav1-RFP or F92A/V94A Cav1-RFP (red). Quantification of nuclear/cytosol pSTAT3 signal ratio in control (CTRL), WT Cav1 and Cav1 F92A/V94A. Mean values ± SEM; **P<0.01, ****P<0.0001; Statistics were processed using unpaired t test. Scale bar: 5 µm **(c)** IFN-α induced STAT3 phosphorylation level of WT MLEC cells upon either control peptide, CavTratin (right) or CavNoxin (left) treatment. N=6 (CavTratin) and N=9 (CavNoxin); Mean values ± SEM; *P<0.05; Statistics were processed using unpaired t test. **(d)** In vitro ADP production via ATP conversion by JAK1 relative to peptide log concentration (µM). Mean values ± SEM. Statistics for (a, b) were processed using standard multi-comparison one-way ANOVA ****P<0,0001, **P<0,01 or using two tailored unpaired t test **P<0,01, *P<0,05.

Figure 4: High resolution analysis of Cav1 diffusion under mechanical stress. (a) Left panel, wide field images of CAV1$^{-/-}$ MLEC expressing Cav1-GFP under iso-osmolarity (300 mOsm) and hypo-osmolarity (30 mOsm). Middle and right panels, Cav1-mEOS3.2 trajectories (green) and Cav1-mEOS3.2 objects (red) acquired using TIRF-sptPALM. Scale bar: 1 µm **(b)** % occurrence relative to log D coefficient of Cav1-mEOS3.2 in iso-osmotic condition (blue) and hypo-osmotic condition (orange). **(c)** % occurrence relative to log D coefficient of Cav1-mEOS3.2 in hypo-osmotic condition (orange) and recovery condition (green). **(d)** Wide field images of CAV1$^{-/-}$ MLEC expressing Cav1-mEOS3.2 under Iso (left) and hypo (right) conditions and the corresponding trajectories. Scale bar: 1 µm (**e)** Quantification of proportion of JAK1-mEOS3.2 molecules with diffusion less (dark blue) or more (light blue) than 0.011 µm^2. **(f)** % occurrence relative to log D coefficient of JAK1-mEOS3.2 (left) in iso-osmotic condition (blue) and hypo-osmotic condition (orange). Quantification (right) of proportion of JAK1-mEOS3.2 molecules with diffusion less (dark blue) or more (light blue) than 0.011 µm^2.

Figure 5: Nanoscale visualization of Cav1 and its fate in response to mechanical stress. (a) STAT3 activation levels in MEF *cavin-1*$^{-/-}$ cells and MEF *cavin-1*$^{-/-}$ cells transfected with cavin-1 (+ cavin-1). Quantification of signal ratio relative to "*cavin-1*$^{-/-}$" condition. N=3; Mean values ± SEM; *P<0.05; Statistics were processed using unpaired t test. **(b)** IFNα induced STAT3 activation in *cavin-1*$^{-/-}$ MEF cells and *cavin-1*$^{-/-}$ MEF cells + cavin-1. Representative immunoblot. Quantification signal ratio relative to "*cavin-1*$^{-/-}$ "condition. N=3; Mean values ± SEM; *P<0.05; Statistics were processed using unpaired t test. **(c)** IFNα induced STAT3 phosphorylation level in *cavin-1*$^{-/-}$ MEF cells with either low, medium or high Cav1 expression. Representative immunoblot. Quantification of signal ratio relative to "low" condition. (a, b, c) mean values ± SEM. Statistics were processed using unpaired t test (a, b) and multi-comparison one-way ANOVA (c). **P<0,01; *P<0,05. (d) 2D dSTORM image of MLEC cell stained for Cav1-AF647 with increasing magnifications. **(e)** Line intensity profiles for Cav1 positive structures from representative 2D dSTORM acquisitions of cells stained for Cav1-AF647 and subjected to ISO, HYPO and REC conditions. **(f)** Visualization of 3D point cloud localizations of Cav1-CF680 and JAK1-AF647 imaged using spectral demixing. **(g)** A schematic workflow of the 3D SMLM analysis. **(h)** Interaction analysis using the MOSAIC suite plugin for FIJI/ImageJ. Mean values ± SEM, statistics were done using unpaired t-test **P<0.01, ***P<0.001. **(i)** Histograms representing the number of caveolae and the three subclasses of non-caveolar Cav1 scaffolds per unit area. Mean values ± SEM, statistics were done using unpaired t-test *P<0.05, **P<0.01, ***P<0.001.

Supplementary Figure 1. STAT1 and STAT3 phosphorylation level under type I IFN stimulation under resting condition in WT and CAV1$^{-/-}$ MLEC cells (data from RPPA analysis).

Supplementary Figure 2. Representative wide-field immunofluorescence images of nuclear translocation of pSTAT1 (green) of IFN-α stimulated CAV1$^{-/-}$ MLEC expressing either exogenous WT Cav1-RFP or F92A/V94A Cav1-RFP (red). Quantification of nuclear/cytosol pSTAT1 signal ratio in control (CTRL), WT Cav1 and Cav1 F92A/V94A. Mean values ± SEM; Statistics were processed using unpaired t test. Scale bar: 5 µm

Supplementary Figure 3. (a) % occurrence relative to log D coefficient of Cav1-mEOS3.2 expressed in CAV1$^{-/-}$ MLEC during hypo-osmotic shock from 0 (dark blue) to 30 min (light blue). (b) % occurrence relative to log D coefficient of CAAX-mEOS3.2 expressed in CAV1$^{-/-}$ MLEC (left) in iso-osmotic condition (blue) and hypo-osmotic condition (orange). Quantification (right) of proportion of CAAX-mEOS3.2 molecules with diffusion less (dark blue) or more (light blue) than 0.011 μm^2.

Supplementary Figure 4. Representative immunoblots for STAT3 phosphorylation level of WT MLEC upon IFNα stimulation for 10 mins and treated or not with 1% mβCD.

Supplementary Figure 5. (a) Estimation of caveolar Cav1 (left) and cavin1 (right) particle sizes from dSTORM acquisitions at steady state (b) Representative images of Cav1-CF680, cavin1-CF680 and JAK1-AF647 acquired through 3D STORM spectral demixing and corresponding calibration curves (bottom panel) for the imaging pairs of Cav1-CF680/JAK1-AF647 and cavin1-CF680/JAK1-AF647. (c) Side-view of 3D point cloud localization depicting the morphology of a *bona fide* budded caveolae. (d) Comparison of raw image and processed image to represent the reliability and integrity of the 3D SMLM network analysis.

PART III

DISCUSSION

- MECHANICAL STRESS MODULATES SEVERAL SIGNALING PATHWAYS THROUGH CAVEOLAE
- NANOSCOPIC VISUALIZATION OF CAVEOLAE AND CAV1 SCAFFOLDS
- CSD MEDIATED REGULATION OF JAK1
- MECHANOTRANSDUCTION THROUGH CAVEOLAE : ROLE IN TUMOR PROGRESSION

1. Mechanical stress modulates several signaling pathways through caveolae

As discussed in the results section of the article manuscript, we sought to determine whether caveolar disassembly in response to mechanical stress had an impact on signaling pathways. We performed RPPA analysis on wild-type (WT) and Cav1 knockout (*CAV1*$^{-/-}$) MLEC cells subjected to uniaxial stretching and found that several signaling pathways were affected by uniaxial stretching in a Cav1 dependent manner including IFN-α induced JAK-STAT pathway (manuscript Fig. 1a and 1b). The specificity of this regulation through caveolae mechanics can be appreciated by the fact that there are pathways affected by stretching in a Cav1-independent manner such as the p44/42 MAPK pathway. We report that Cav1 specifically inhibits STAT3 activation (but not STAT1) by interacting directly with JAK1 through its CSD. Moreover, preliminary FLIM-FRET experiments using IFNAR1-GFP and Cav1-RFP indicate an interaction at steady state (Figure 21). We further tested other pathways that were found in the RPPA analysis to be activated by Cav1 mechanics such as PTEN/Akt and found an increased interaction of Cav1 with PTEN upon hypo-osmotic shock (Figure 22). We indeed plan to further investigate the impact of caveolae mechanics on the PTEN/AKT/PI3K pathway. This suggests that mechanotransduction through Cav1 is not limited to the JAK-STAT pathway and could be generalized to global mechanosignaling. In order to be more critical of our study, the following questions can be raised.

a. How can we explain the specific Cav1-dependent inhibition of STAT3?

As can be seen from manuscript fig. 1c and 1f, while the level of STAT3 tyrosine phosphorylation drastically reduced upon cell stretching in a Cav1-dependent manner, the levels of STAT1 tyrosine phosphorylation was not affected. Considering the fact that IFN-α binding to IFNAR leads to JAK1 and TYK2 cross-activation resulting in the activation of both STAT1 and STAT3, the molecular

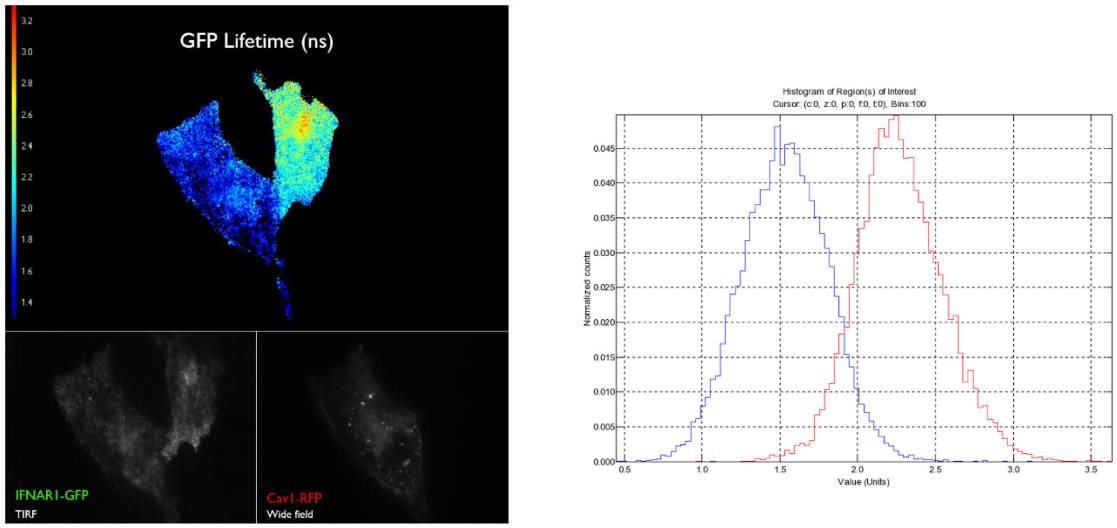

Figure 21: FLIM-FRET between Cav1-RFP and IFNAR1-GFP
Fluorescence lifetime imaging (FLIM) of RPE1 cells expressing IFNAR1-GFP, FRET donor, and Cav1-RFP, FRET acceptor (left) or not (right). Histograms for pixel GFP lifetime for cell expressing both donor-acceptor (blue) and donor only (red).

mechanism driving the specific Cav1-dependent inhibition of STAT3 (but not STAT1) remains to be understood. A logical hypothesis would involve the selective targeting of JAK1 by Cav1 resulting in STAT3 inhibition while TYK2 remains uninhibited and mediates STAT1 activation. It is worth noting that Cav1 does not interact with TYK2 (Figure 22). Nevertheless, there are no evidence of such a JAK specificity for STAT activation. Moreover, JAKs are activated by mutual trans-phosphorylation and therefore, there is a reciprocal interdependency between JAK1 and TYK2. Thus, according to the consensus mechanism of JAK activation, the targeting of one of the two kinases should inevitably prevent the activation of the other one. However, it has been reported that TYK2 plays a restricted role in IFN-α signaling and lack of TYK2 in murine cells does not prevent IFN-α signaling [Shimoda et al. 2000, Majoros et al. 2017]

On the other hand, mechanotransduction through caveolae is not restricted to IFN-α induced JAK-STAT pathway. This process may constitute a general regulatory mechanism for JAK-STAT signaling, irrespective of the receptors or the ligands. In line with this, basal STAT3 activation in *CAV1*$^{-/-}$ MLEC cells and *in vitro* kinase assay indicates that this mechanism directly targets JAK1 regardless of upstream signaling molecules. Hence, it is not unexpected that it can be extended to other cytokines and receptors that use JAK-STAT such as the IL6 pathway. Indeed, our laboratory recently reported that caveolae mechanics also control the IL6/STAT3 pathway through a similar process involving caveolae mechanosensing in the context of muscle physiology suggesting that the muscle specific isoform of Cav3 (that also carries a CSD) behaves similarly to Cav1 and regulate signaling in muscle cells/tissues [Dewulf et al. 2019].

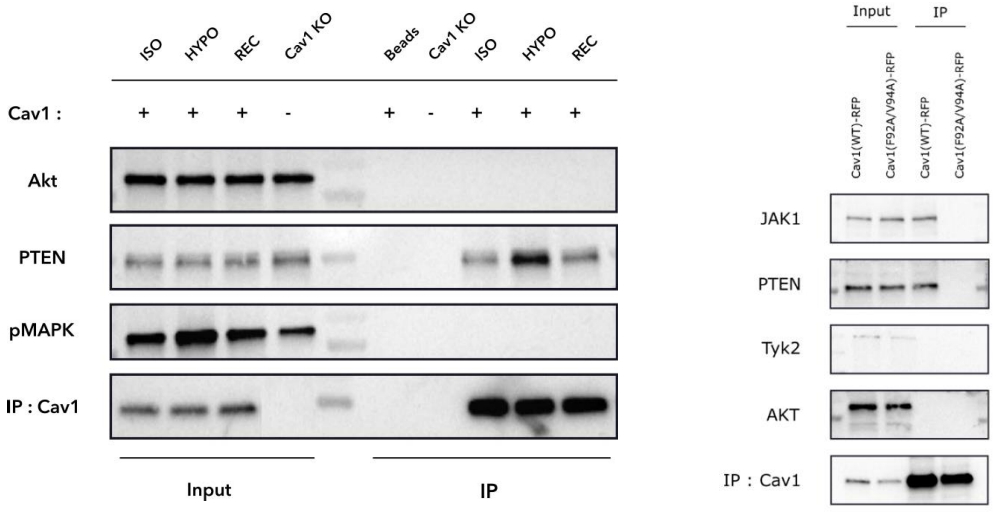

Figure 22: CSD mediated interaction of Cav1 with PTEN
Representative immunoblots showing the increased interaction of Cav1 with PTEN under conditions of hypo-osmotic shock (left panel) and that this interaction is dependent on the CSD (right panel). Experiments performed using MLEC cells.

b. Can the observed immobilization of JAK1 upon hypo-osmotic shock induced membrane stress be strictly credited to the release of Cav1 through caveolae disassembly?

In addition to uni-axial or bi-axial stretching of cells plated on PDMS substrates, modulation of the extracellular osmolarity has been used as an alternative tool to study changes in membrane tension. When cells are exposed to a hypotonic solution, they respond by increasing their volume through water uptake. Fusion of the internal membrane pool with the PM helps to balance the tension as the cell volume increases [Pietuch et al. 2013]. In addition, our lab demonstrated that PM invaginations called caveolae can also help mitigate the concomitant increase in membrane tension by flattening out and disassembling their coat structure [Sinha et al. 2011]. While uni/bi-axial stretching of cells might better simulate physiological cellular stress, it is difficult to integrate with modern techniques such as high-resolution imaging, thereby limiting its versatile use. As a result, osmotic shock has been the go-to choice for studying the effect of membrane tension variations due to its ease of use and integration.

However, osmotic shock has been proposed to have a global effect on the cell, simultaneously affecting the membrane lipid composition, ion channels and the dynamics of several cellular components such as the cytoskeleton and nucleus, in addition to exerting an increased tension at the PM [Di Ciano et al. 2002, Finan and Guilak 2013, Tsai et al. 2019, Zapata-Mercado and Hristova 2021 - Biorxiv]. Moreover, a recent report studying the coupling of membrane tension to cell volume states that the cell recovers from hypo-osmotic shock-induced increase in membrane after several minutes, in agreement with our observations that this effect lasts for at least 15 mins [Sinha et al. 2011, Roffay et al. 2021, Biorxiv]. Therefore, our finding that JAK1 is immobilized at the PM in

response to hypo-osmotic shock due to efflux of 'free' Cav1 from caveolae disassembly comes under question as JAK1 could also be immobilized due to other factors such as changes in the cytoskeleton or lipid reorganization (which in turn could be mediated by Cav1 release). While we have indeed confirmed the direct role of Cav1 in this process through other experiments (as described below), it is nevertheless valuable to be able to strictly modulate the assembly and disassembly of caveolae in a localized and non-invasive manner as it would enable precise functional investigations of caveolar Cav1 and non-caveolar Cav1.

As described earlier in section 2.6, optogenetics facilitates control and modulation of cellular processes with high spatio-temporal resolution using light. This technique involves fusing the target protein of interest to another protein/peptide that changes conformation in response to specific wavelengths of light. Several classes of optogenetic modules have been generated to specific needs such as sequestration away from the site of action, clustering through oligomerization or inactivating the target protein itself [Tischer and Weiner 2014]. Since we were keen in controlling the assembly and disassembly of caveolae with light, we first looked at the possible target proteins that can be manipulated. Caveolins were immediately out of contention as our aim was to investigate their functional role at the PM and manipulating it would be impractical. As a result, we turned to the next two key proteins that are required for a *bona fide* budded caveolae – cavins and EHD2. Since EHD2 stabilizes caveolae at the PM, we tested the effect of its depletion from the PM through optogenetics. As it is known that EHD2 binds PtdIns (4,5) P_2 preferentially at the PM [Simone et al. 2013], we hypothesized that depletion of PM PtdIns (4,5) P_2 would reduce the affinity of EHD2 to bind the PM and hence caveolae. For this

purpose, we utilized the CRY2-OCRL-GFP and CIBN-CAAX optogenetic module which was a kind gift from the lab of Dr. Olof Idevall-Hagren. CRY2 and CIBN have low affinity for each other in the dark state and immediately associate with each other in the presence of blue light (380 to 500 nm). OCRL is a phosphatase that converts PtdIns (4,5) P_2 to PtdIns (4) P. As a result, in the presence of blue light, CRY2-OCRL-GFP is recruited to CIBN-CAAX at the PM leading to depletion of PtdIns (4,5) P_2 and thereby EHD2. While we were able to successfully recruit OCRL to the PM as indicated by the increase in GFP intensity over time (Figure 23), and therefore deplete EHD2, we did not see a decrease in the number of caveolae. Instead, we found that the depletion of EHD2 resulted in a highly diffusive population of caveolae (data not shown) corroborating with the proposed role of EHD2 stabilizing and immobilizing caveolae at the PM.

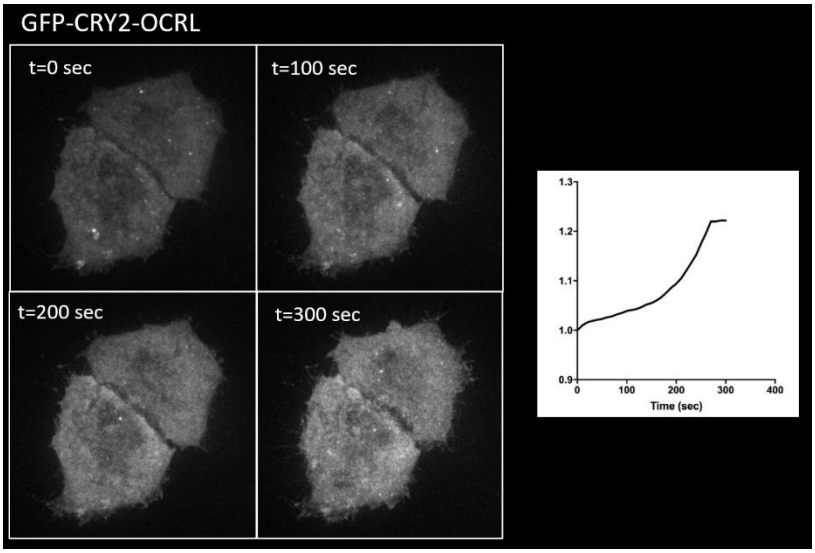

Figure 23: Optogenetic control of EHD2 localization at the PM
Increase of GFP intensity overtime indicating the accumulation of OCRL at the PM (left panel) and the corresponding intensity (right panel) values over a time period. Cells were imaged using TIRF microscope.

Out of the different isoforms of cavins, cavin1 is indispensable for the formation of a budded caveolae [Hill et al. 2008, Liu et al. 2008]. As a result, we next attempted to reversibly sequester cavin1 at the mitochondria and control the availability of cavin1 at the PM thereby modulating caveolae assembly and disassembly in a localized and reversible manner. We decided to use the LOVTRAP optogenetic module for a couple of reasons. Unlike most optogenetic modules, the LOVTRAP system is a photo-dissociative module meaning that the two components (photosensor LOV2 and effector Zdk1) are tightly associated in the dark state and dissociate in the presence of blue light [Wang et al. 2016]. This would facilitate the release of sequestered cavin1 molecules in the light state and hence enable observations of the assembly of caveolae. In addition, the two components of the LOVTRAP system are small in size compared to many other modules and hence minimizes perturbations of the functionality of cavin1. Cavin1-mcherry was fused to Zdk1 and TOMM20 (the outer mitochondrial membrane protein) was fused to LOV2. Both these constructs were co-transfected in HeLa CAVIN1$^{-/-}$ cells. In the dark state, cavin1 will be sequestered in the mitochondria due to the high affinity of Zdk1 to LOV2. Upon blue light illumination, cavin1 will be released from mitochondria and available for the formation of caveolae at the PM.

While we were able to successfully manipulate the sequestration of the control construct expressing just mcherry-Zdk1 (Figure 24), we faced difficulties with cavin1-mcherry-Zdk1. Although cavin1 was sequestered at the mitochondria, it was not released in the presence of blue light (data not shown). Since Cav1 has been reported to be present in the mitochondria [Volonte et al. 2016], the lack of dissociation could probably be due to the formation of a complex with Cav1 at the mitochondrial membrane. Other cellular structures were considered such as ER and Golgi but since these organelles are involved in trafficking of Cav1 to the PM, we

resorted to cytosolic clustering of cavin1 molecules. Work is underway in testing this approach using the CRY2Olig module that enables clustering of target molecules in the dark state and spontaneous dissociation of these clusters upon blue light illumination.

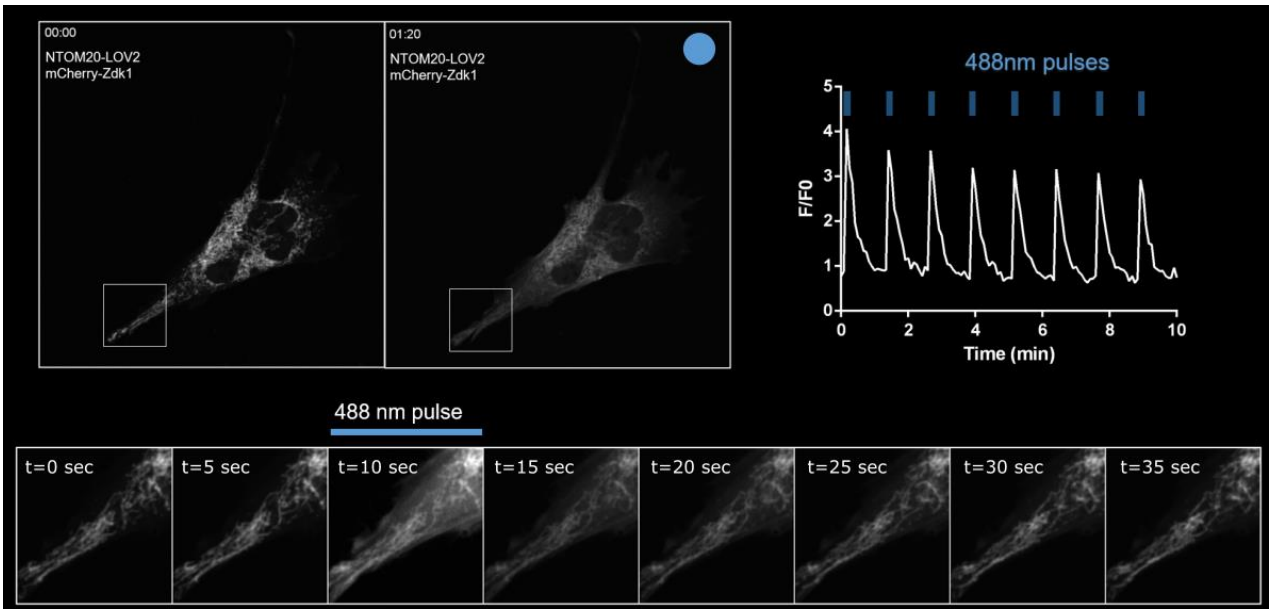

Figure 24: Reversible sequestration of mcherry-Zdk1 at the mitochondria
Representative still images showing sequestration of mCherry-Zdk1 at the mitochondria in the dark state and release upon blue light illumination (top left panel) and the corresponding intensity values over a time period (top right panel). Zoomed inset (bottom panel).

2. Nanoscopic visualization of caveolae and Cav1 scaffolds:

Until recently, electron microscopy and conventional fluorescence microscopy served as the predominant techniques to visualize and investigate caveolae. As described in section 2.1, caveolae range in size from 50-100 nm and hence visualization by conventional fluorescence microscopes are constrained by the inherent resolution limit. As a result, it is not possible to distinguish between a single caveolae or a rosette as both will appear as a single Cav1 positive spot. Although EM might ameliorate this,

it presents another limitation with the inability to stain specific structures simultaneously for functional studies. In addition, recent reports indicate the existence of Cav1 outside of caveolae in oligomeric forms [Khater et al. 2019]. These non-caveolar Cav1 oligomers, termed ''scaffolds'' exist in three subclasses referred to as S1A, S1B and S2 and are proposed to be the building blocks of a mature budded caveolae. Furthermore, it is to be noted that the existence of these scaffolds was suggested through cluster analysis on super-resolution data localizations and are not distinguishable either through EM or conventional fluorescence microscopy. The discovery of non-caveolar Cav1 could explain the inconsistencies in correlating the observed roles for Cav1 to caveolae. For e.g., although Cav1 have been shown to bind with and immunoprecipitate several proteins ranging from signaling molecules to membrane receptors, there has been often little convincing evidence for these proteins to be found inside caveolae raising a conundrum of how a signaling molecule can be regulated by caveolae if not present into caveolae. Our results reconcile these data since we show that Cav1 can remotely control signaling molecules outside of caveolae. As a result, it is important to distinguish the roles of Cav1 from caveolae. Primary to this, is the ability to discern the various subclasses of non-caveolar Cav1 and caveolae simultaneously and at present, super-resolution imaging coupled with machine learning remains the only possible means to do so.

Although the concept of sub-diffraction limit microscopy gained traction in mid-1990s, its applications to studying cellular structures in detail has been more nascent. In recent years, several studies have utilized super-resolution to visualize caveolae [Gabor et al. 2015, Yang et al. 2017, Shreshta et al. 2021]. While some of them report nanoscopic visualization of caveolae in the context of mechanical stress, they mainly focus on morphology and do not provide any functional aspects. In our study, we were interested in determining the fate of caveolar and non-caveolar Cav1 in response to

mechanical stress and its implications (if any) on the inhibition of intracellular signaling. We utilized 3D multicolor STORM with spectral demixing from Abbelight™ SAFe 360 module and the network analysis that Khater et al. used to distinguish Cav1 scaffolds from caveolae.

As described in section 2.5, spectral demixing allows simultaneous acquisition of two or more channels with the use of a single laser. As a result, it is important to calibrate to avoid channel cross-talk. In our study, we performed dual-color 3D STORM with Cav1-CF680/JAK1-AF647 labeling and also cavin1-CF680/JAK1-AF647 labeling and the corresponding calibration curves indicated good separation of peaks for the respective combinations (manuscript supp. Fig. 5b). Both fluorophores (AF647, CF680) photo-switch under reducing and oxygen-free buffer conditions, making them suitable for dSTORM single molecule imaging [Heilemann et al. 2008], and thereby the localization of the emitters with sub-diffraction localization precision. Thanks to their close spectral proximity, AF647 was excited and acquired simultaneously with CF680 in the same dSTORM buffer (Abbelight™ SMART-Kit) using a 640 nm laser, and their respective signals were discriminated after single molecule localization using a ratiometric approach to spectrally separate the contribution of red emitting dyes. The observed particle size for both Cav1 and cavin1 staining fell in the known range of 50-100 nm (manuscript supp. Fig. 5a). While acquisitions of cavin1 staining showed exclusive localization to caveolae-like structures at the PM, Cav1 staining was visible even outside of caveolae-like structures indicating the presence of non-caveolar Cav1 scaffolds. Moreover, cavin1-positive structures (and hence caveolae) were decorated along lines indicating that they are lined along the actin filaments as visualized through EM (Figure 25).

Following the spectral separation of the two channels, we process the corresponding localizations using the 3D SMLM network analysis pipeline outlined in

section 2.5. The reliability of the network analysis (cluster segmentation and identification) in distinguishing the various populations of Cav1 was evaluated by comparing raw images with the corresponding data obtained after cluster identification (manuscript supp. Fig. 5d). We then performed downstream analysis of the processed SMLM data as required. Since the density of the Cav1-positive structures are highly heterogeneous between cells as well as locally within cells, we decided to define random ROIs and calculate the number of Cav1-positive structures per unit area for each cluster-type. We found a decrease in the number of caveolae and a corresponding increase in the number of scaffolds (S1A, S1B and S2) in response to hypo-osmotic shock indicating that caveolae disassembled into non-caveolar Cav1

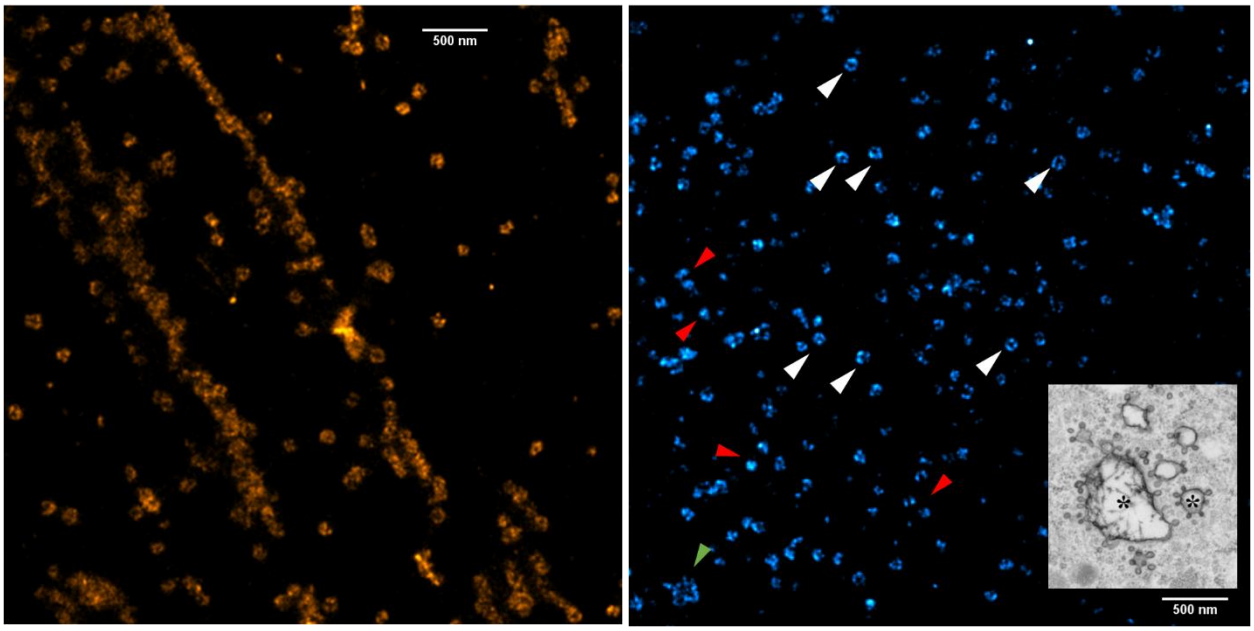

Figure 25: SAFe-STORM imaging of Cavin1 and Cav1
NIH3T3 cells stained for Cavin1-CF680 (left panel) and Cav1-CF680 (right panel) and imaged in the SAFe 360 module. White arrows indicate *bona fide* budded caveolae; red arrows indicate non-caveolar Cav1 scaffolds; green arrows indicate potential rosettes [Inset image from: Parton and Simons 2007].

scaffolds in response to increased membrane tension. Interaction analysis using the MOSAIC suite [Shivanandan et al. 2013] helps measure the probability of localizations from two channels being random or following a pattern which in turn defines the strength of interaction between the two channels. Analysis for each subpopulation of Cav1 clusters with the JAK1 channel revealed that the S1B and S1A scaffolds had a higher affinity for interacting with JAK1 than the S2B scaffolds or caveolae.

As discussed in section 1 above, sptPALM analysis revealed that Cav1 molecules follow an increased diffusion pattern and scanned a wider area in response to hypo-osmotic shock. Considering our finding that caveolae disassemble into scaffolds in response to membrane tension increase, it is reasonable to postulate that the increased diffusion observed through single particle tracking could belong to Cav1 molecules of scaffolds generated from caveolae disassembly. However, this is an indirect inference as we were not able to directly confirm the kinetics of the different scaffolds through single particle tracking. This is due to the fact that the network analysis requires precise, saturated Cav1 localizations for segmenting them into the caveolae or non-caveolar Cav1 classes and this is not feasible with current live-cell super resolution techniques. Since the identification and study of Cav1 scaffolds is relatively new, a better understanding of the dynamics of these Cav1 clusters is required.

3. CSD mediated regulation of JAK1:

During the 1990s, extensive research on the ability of Cav1 to immunopurify a diverse set of proteins led to the inception of the 'caveolin signaling hypothesis', aimed at providing a new perspective to signal regulation at the PM [Lisanti et al. 1995, Couet et al. 1997, Okamoto et al. 1998]. As discussed in section 2.3.4, the central tenet of the model is that signaling proteins can form direct protein-protein interactions with the

scaffolding domain of caveolin (CSD) via a signature peptide sequence, termed the caveolin binding motif (CBM). CBMs were first identified by a phage display screen and were proposed to be hydrophobic and rich in aromatic residues (ΩxΩxxxxΩ or ΩxxxxΩxxΩ or the combined sequence ΩxΩxxxxΩxxΩ, where Ω is a Phe, Tyr or Trp residue and x can be any amino acid) [Couet et al., 1997]. Although a plethora of signaling and non-signaling molecules ranging from cytoplasmic proteins (such as Ras, src-kinases, β-catenin) to regulators of autophagy (such as LC3) has been proposed to interact with Cav1, the idea that Cav1 can mediate interactions via binding to CBMs is however debated upon. The basis for the argument stems from a bioinformatic *in silico* study on CBM-containing proteins and the identification of CBM-containing proteins in cells that lack Cav1 [Chen et al. 2010, Collins et al. 2012].

It has been suggested that for a CBM to be functional, it must either lie in a disordered region or form a common recognition structure for caveolin binding and that it must be exposed and accessible. Previous bioinformatic studies revealed that the CBM adopts a variety of different structures with no consistent conformation and that these motifs are invariably found within structured regions of the proteins and hence inaccessible for binding the CSD [Byrne et al. 2012, Collins et al. 2012]. On the other hand, the CSD has been proposed to be composed of an amphipathic α-helix that is partially embedded in the inner lipid layer of the plasma membrane suggesting that this configuration would not favor CSD interaction with binding partners. In light of these reports, we found that Cav1 inhibits JAK1 catalytic activity by binding through its CSD and that this interaction in modulated by mechanical stress. Moreover, at steady state, there is basal level of interaction between Cav1 and JAK1 which drastically increases in response to mechanical stress and returns to basal levels upon recovery to steady state. These findings raise key questions such as:

a. How is the CSD-CBM interaction justified in light of the contradicting structural studies?

While some computational studies predict that the CSD strictly assumes an α-helix conformation, there are others which propose that the CSD could possess a dynamic secondary structure either partially unstructured or fully helical [Liu et al. 2016]. This dynamic conversion could control the relative position of the CSD with respect to the plasma membrane and facilitate interactions with CBM-containing proteins. Future studies on crystallization of Cav1 could provide a better understanding of the actual structure of the CSD. Moreover, computational studies are *in vitro* and does not consider the physiological context in which the protein exists such as pH, lipid environment etc. As an example, our cell free *in vitro* studies using CSD mimicking peptides demonstrate inhibition of JAK1 catalytic activity as they are likely more accessible. Therefore, structural studies on CSD in the context of lipid environment could provide a better understanding of the changes in domain conformation in response to changes in lipid organization at the PM. In line with this, structural analysis of the CSD inserted in POPC/cholesterol adopts a mixture of β-stranded and α-helical structure while the CSD inserted in DPC micelles adopts a fully helical structure [Le Lan et al. 2006, Hoop et al. 2012]. These studies suggest that although the CSD has been implicated in several functions such as membrane binding, oligomerization and protein interaction, it is important to consider the physiological context and the localization of Cav1 within cells. For e.g., it has been reported that palmitoylation is non-essential for localization of Cav1 in caveolae but that it is critical for the cholesterol trafficking by Cav1 [Uittenbogaard et al. 2000]. Therefore, it seems likely that the Cav1 conformation

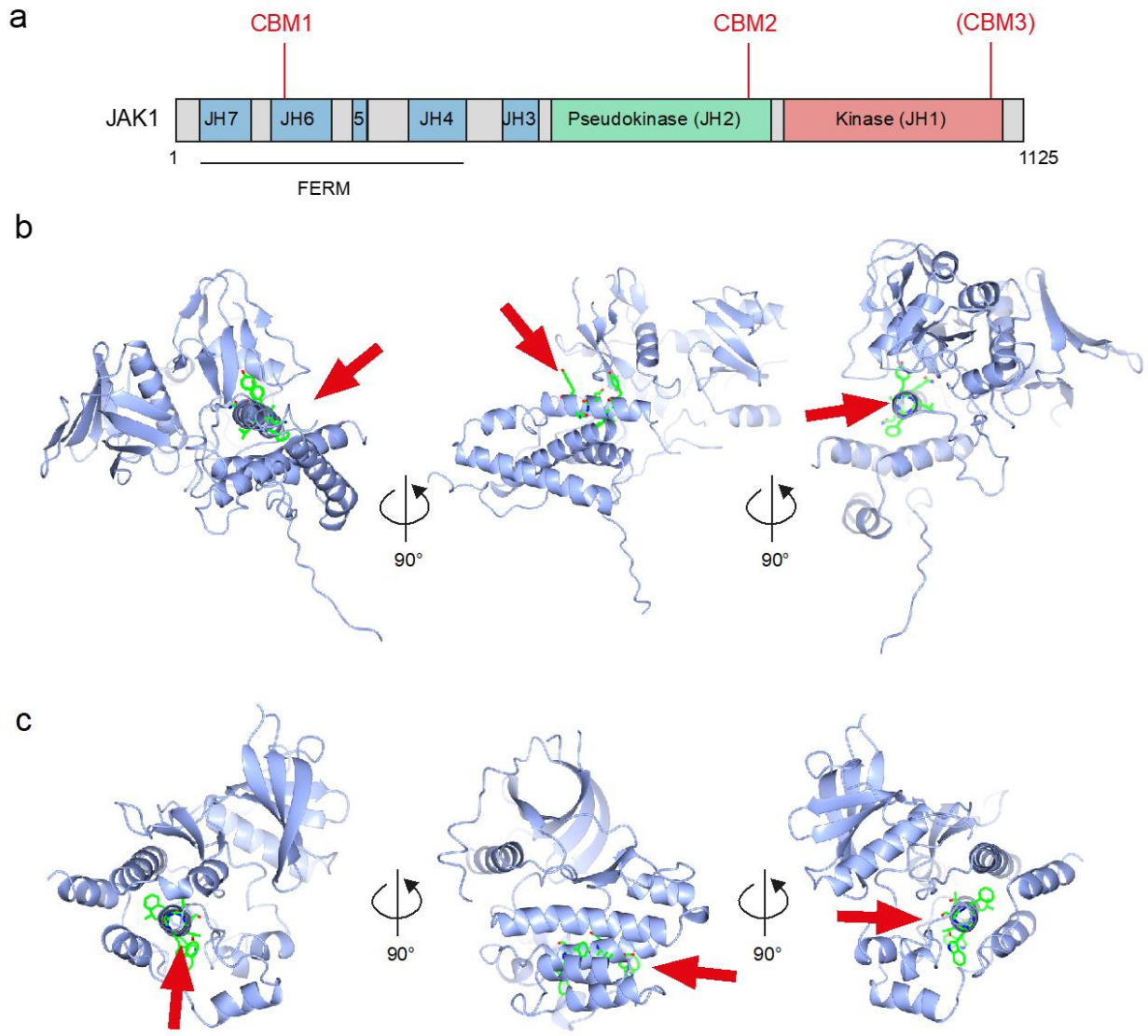

Figure 26: CBM localization on JAK1 structure

(a) Putative CBM localization in JAK1 primary structure. **(b)** CBM1 (highlighted lateral chains, red arrow) localization in the 3D structure of the FERM domain of JAK1 (PDB 5IXI). **(c)** CBM2 (highlighted lateral chains, red arrow) localization in JAK1 pseudokinase 3D structure (PDB 4L00). The pseudokinase and kinase domains are structurally identical. The putative CBM3 has a localization similar to the CBM2 but within the kinase domain.

within caveolae could be significantly different from say, its structure in a cholesterol-bound cytosolic state or in Cav1 scaffolds (refer section 2.5.4).

With respect to the CBM, all JAKs are known to contain putative CBMs. In the case of JAK1, three putative CBMs can be defined in each of its domain – ^{157}YLFAQGQY^{164} in the FERM domain, ^{777}WSFGTTLW^{784} in the pseudokinase domain and ^{1065}WSFGVTLH^{1072} in the JH1 kinase domain (Figure 26). JAK1 CBMs are located on two α-helices that are buried inside JAK1 ternary structure. In order to determine which of the three CBMs of JAK1 are required for interaction with Cav1, we generated a JAK1 construct with point mutation in CBM1 (JAK1-CBM). Pulldown experiments of JAK1-CBM1 in HeLa cells overexpressing Cav1 (to generate an excess of non-caveolar Cav1) revealed that mutations in the CBM1 located in the FERM domain did not affect its ability to interact with Cav1 (Figure 27). This data is consistent with our *in vitro* kinase assay performed using a recombinant JAK1 that contains only the pseudokinase-kinase tandem (i.e. CBM2 & CBM3). This assay revealed that the CBMs in these two domains are sufficient to undergo inhibition of catalytic activity by the CSD mimicking peptide. Moreover, we generated two JAK1 mutants – JAK1-alfa-CBM3stop which contains a stop codon just after CBM3 and JAK1-alfa-ΔCBM3 with a stop codon just before CBM3 – to further determine which of these two CBMs are involved in Cav1 interaction. Preliminary pulldown experiments using these constructs are underway.

b. How can we explain the interaction between Cav1-JAK1 knowing that the lipid environment of caveolae excludes the possibility of bulk membrane protein sequestration in caveolar domains?

A recent study exploring the role of caveolae in intracellular trafficking and the influence of caveolar coat proteins in the local lipid composition reported that bulk

membrane proteins such as transmembrane proteins with cytosolic domains are excluded from caveolae [Shvets et al. 2015]. This exclusion of proteins from caveolar domains can be attributed either to the negative curvature at the neck region or to the association of the caveolar coat complex close to the surface of the bulb. In this regard, the fact that JAK1 is associated with the transmembrane receptor IFNAR2 and that binding of IFN-α leading to the formation of a receptor complex which might not diffuse into caveolar domains, directly contradicts our results regarding interaction between Cav1 and JAK1 at steady state and under IFN-α stimulation. As explained above in section 2, it has been proposed that various subpopulations of Cav1 clusters exist at the plasma membrane in addition to caveolae at steady state.

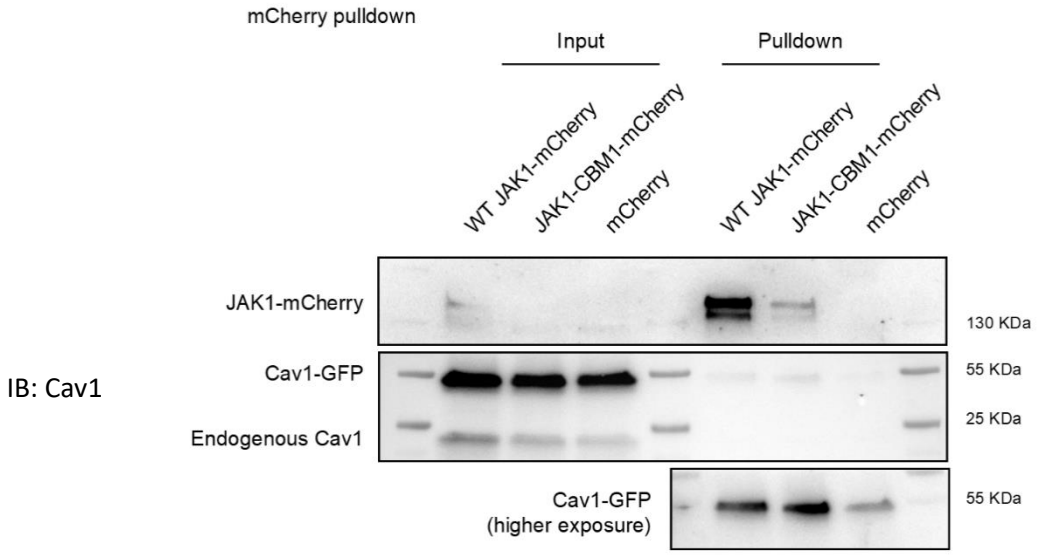

Figure 27: Immunoprecipitation of JAK1 WT and CBM1 mutant constructs
Immunoblot of mCherry pulldown in HeLa cells stably expressing Cav1-GFP and overexpression of either WT-JAK1 or CBM1-mutated JAK1 mCherry constructs.

A recent study by the same group that defined the existence of these scaffolds, investigated the structural impact of the CSD of Cav1 oligomers in mediating protein interactions [Wong et al. 2021]. They report that the S2 and S1B scaffolds in particular might have a tendency to mediate protein interactions through the CSD. Taking this into consideration along with our findings that caveolae disassemble into scaffolds upon mechanical stress, it is reasonable to suggest that JAK1 interacts with the exposed CSD of the non-caveolar Cav1 population at the PM remotely from caveolae. The precise molecular mechanism underlying CSD-mediated inhibition of JAK1 catalytic activity is still unclear. Our results highlight the importance of the CSD in JAK1 inhibition since point mutations in F92 and V94 residues of the CSD fully abolish the inhibitory effect. Whether the F92 or V94 lateral chain sits in an important domain of JAK1 as demonstrated for regulation of eNOS is unknown. Structural studies of the Cav1-JAK1 complex or at least, CSD-JAK1 would bring deeper insights on the molecular mechanism mediating the resulting inhibition. Interestingly, it has been suggested that caveolins may regulate JAK- STAT

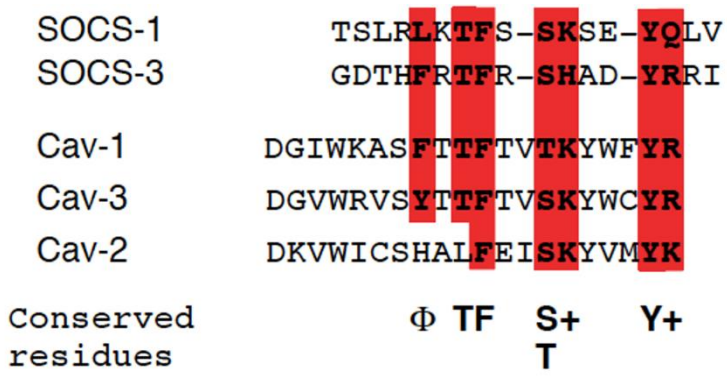

Figure 28. Sequence alignment of SOCS1 and SOCS 3 KIR domain with caveolins
The Cav-1 scaffolding domain shares primary sequence similarities with the SOCS-1 pseudo-substrate domain. The conserved domains are identified by the consensus sequence ΦxTFxxS/T (+) xxxY (+), where Φ is a hydrophobic or aromatic amino acid and (+) is a positively charged residue [Jasmin et al. 2006]

signaling in a way similar to that of SOCS proteins. Sequence alignment revealed that the CSD shares a common motif with the KIR domain of SOCS1 and SOCS3 [Jasmin et al. 2006] (Figure 28). Therefore, one could hypothesize that the CSD could sit in the substrate binding site of JAK1, similar to how SOCS proteins inhibit JAK1. Interestingly, as discussed earlier, PTEN which is proposed to possess a CBM interacts with Cav1 in a CSD dependent manner suggesting that the control of signaling through caveolae mechanics is not restricted to the JAK-STAT pathway.

4. Mechanotransduction through caveolae: Role in tumor progression

Although a number of epidemiological, clinincal, metabolic, genetic and cellular studies have implicated either caveolae or caveolin to be involved in cancer, its exact role remains controversial to date, mainly due to the contrasting data attributing dual roles for caveolae/caveolins in either promoting or suppressing tumor progression [reviewed in Lamaze and Torrino 2015, Martinez-Outschoorn et al. 2015, Vibha and Lamaze 2020]. As explained in Chapter 1, cell mechanics have recently emerged as playing an important role in enabling cells to perceive their microenvironments and respond accordingly. This applies to both normal cells as well as diseased cells such as those in solid tumours which exist in a constantly evolving tissue microenvironment of varying physical forces [Yu et al. 2011, Northcott et al. 2015]. Cells translate these stimuli by mechanotransduction into biochemical signals controlling multiple cellular aspects such as cell growth and differentiation, and modulation of cellular and tissue homeostasis. Considering this, it is worth noting that the plasma membrane of cells that are constantly subjected to various types of mechanical stress (such as endothelial, muscle, adipocytes and fibroblasts) are enriched in caveolae. In 2011, our lab established that budded caveolae can flatten out and act as a buffer against instantaneous changes in membrane tension [Sinha et al. 2011]. The flattening of

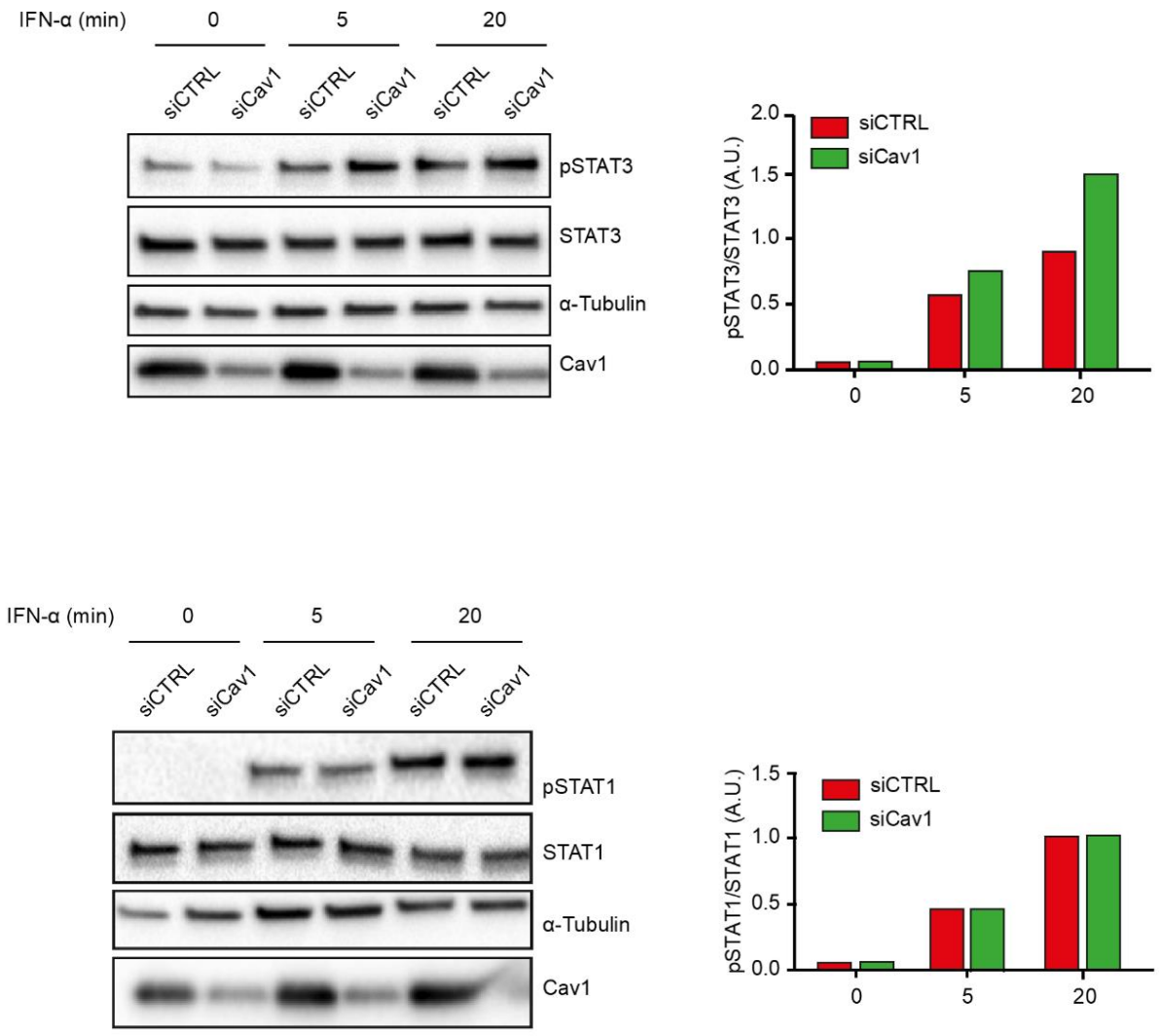

Figure 29. Specific inhibition of STAT3 by Cav1 in human breast cancer cells
Immunoblot of levels of IFN-α-induced STAT3 and STAT1 activation in MCF10A cells upon siCTRL or siCav1 treatment (left). Immunoblot quantification (right). N=1 for both experiments

caveolae is followed by disassembly of the caveolar coat and it was hypothesized that the subsequent release of the caveolar proteins could impact downstream cellular processes [Lamaze and Nassoy, 2012].

As a result, there is now consensus in the caveolae field that the classical roles attributed to caveolae or caveolins should be revisited through this new perspective of mechanics [Parton et al. 2020]. In this regard, we recently demonstrated that EHD2, which localizes at the neck of caveolae, translocates to the nucleus in response to mechanical stress and regulates gene transcription, thereby acting as a mechano-transducer (refer Annexe - I) [Torrino et al. 2018]. It is also worth noting that EHD2 has been implicated in several cancer types with loss of EHD2 leading to tumor metastasis [Yang et al. 2015, Liu et al. 2016, Shen et al. 2020]. Moreover, cavin1 and cavin3 have also been shown to possess mechanotransductive roles [Liu and Pilch 2016, McMahon et al. 2019]. However, the significance of caveolae mechanosensing and mechanotransduction in cancer cells and tumors has not been investigated. A key role of caveolae that is interesting to investigate in the context of mechanical forces associated with tumor growth is signaling. As described above in section 5.3, although several studies have associated caveolae or Cav1 with a broad range of signaling pathways, the exact mechanism of control remains poorly understood. In this study, we report for the first time, a new mechanism by which caveolae could remotely control the regulation of JAK-STAT signaling cascade through a balance between the populations of caveolar Cav1 and non-caveolar Cav1 (scaffolds) allowing for the fine tuning of the JAK-STAT pathway based on caveolae mechanics. As described in section 5.1 above, we found that caveolae mechanics exclusively inhibits JAK1 mediated activation of STAT3 but not STAT1. Considering that STAT3 and STAT1 play oncogenic and tumor suppressor roles respectively, the mechanical forces encountered by cancer

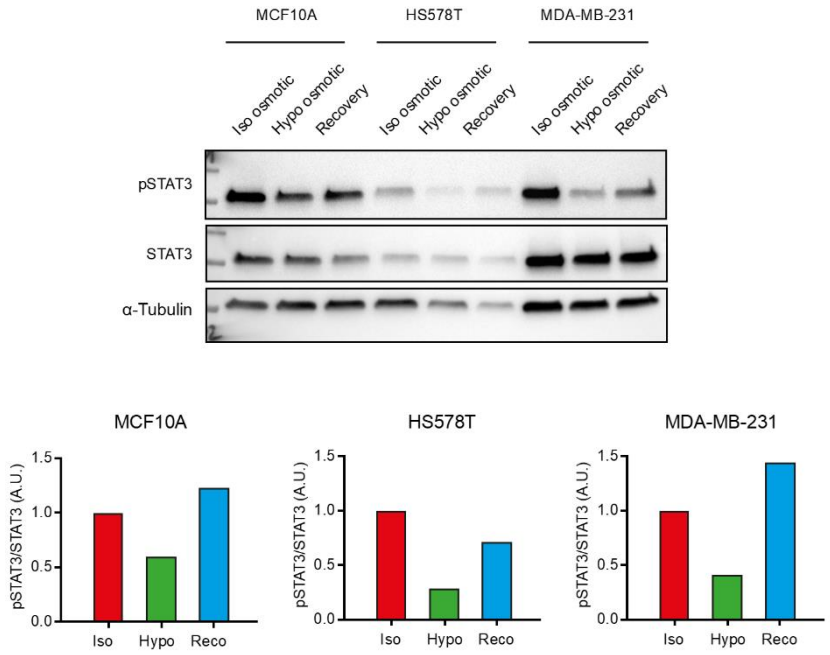

Figure 30: IFN-α-induced STAT3 activation in breast cancer cells upon hypo-osmotic shock
Immunoblot of IFNα-induced STAT3 phosphorylation in breast cancer cell lines (MCF10A, HS578T and MDA-MB-231) upon either steady-state, hypo-osmotic shock or recovery. N=1.

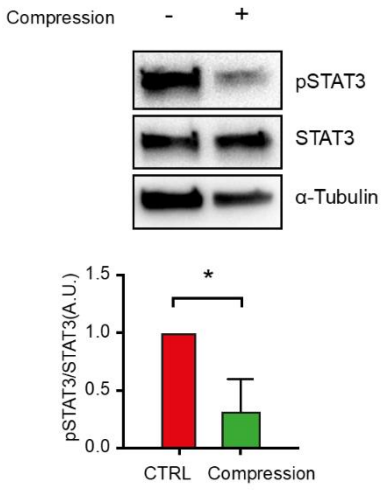

Figure 31: IFN-α-induced STAT3 activation of breast cancer cell under compression
Immunoblot of IFNα-induced STAT3 phosphorylation of breast tumor cells HS578T subjected to compression through encapsulation in alginate spheroids (N=3; unpaired t-test; $p<0.05$).

cells during tumor progression may regulate signal interpretation and modulate the balance of STAT3 or STAT1 activation through caveolae mechanics. This hypothesis is in agreement with the proposed ambivalent roles of Cav1 during tumor progression.

Moreover, any perturbations affecting the integrity of caveolae mechanotransduction may result in an imbalance of STAT3/STAT1 activation. For example, transient suppression of Cav1 in MCF10A breast cancer cells also induces STAT3 activation in response to IFN-α most likely because of the lack of negative regulation of JAK1 by non caveolar Cav1 (Figure 29). In addition, tumor cells subjected to hypo-osmotic shock exhibit this characteristic pSTAT3 inhibition (Figure 30). Considering the fact that MDA-MB-436 cells have defective caveolae as result of almost no expression of EHD2 (refer Annexe – I) [Torrino et al. 2018], it would be interesting to compare the levels of STAT3 activation in these cells with those that have functional caveolae (Hs578T). We also found that non-aggressive tumor cells Hs578T submitted to tumor-like compressive forces by encapsulation [Alessandri et al. 2013] also exhibit the characteristic decrease of IFNα-induced STAT3 activation (Figure 31). Therefore, it is rational to hypothesize that the caveolae-dependent mechanical control of JAK-STAT constitutes a physiological regulatory mechanism of cell proliferation in response mechanical strains generated by cellular microenvironments such as space limitations found in the tumor mass. Hence, an impaired caveolar mechano-response would result in cell growth and other caveolae-related processes.

CONCLUSION

To conclude, although Cav1 have been shown to bind with and immunoprecipitates several proteins ranging from signaling molecules to membrane receptors, often there has been little convincing evidence for these proteins to be found inside caveolae raising a conundrum of how a signaling molecule can be regulated by caveolae if not present inside caveolae. Moreover, with the recent discovery that Cav1 can also exist as oligomers outside of caveolae (termed non-caveolar Cav1 or scaffolds) and the field moving towards a consensus on this view, it is becoming clear that the roles attributed to Cav1 can no longer be directly conferred to caveolae. In this regard, our results provide a new mechanistic insight into the regulation of cell signaling through caveolae. We show that Cav1 can remotely control signaling molecules outside of caveolae by disintegrating into non-caveolar Cav1 scaffolds in response to mechanical stress which in turn facilitates interaction of these scaffolds with potential effector molecules through the CSD. Considering the fact that caveolae excludes bulk membrane proteins and the controversy surrounding the ability of Cav1 CSD to mediate interactions with effector proteins, the notion of Cav1 scaffolds (but not caveolae) interacting with JAK1 could possibly explain the involvement of CSD in mediating the Cav1-JAK1 interaction. The CSD which might not be accessible in a budded caveolae could be exposed during lipid reorganization and disassembly of caveolae into scaffolds. Taken together, our results demonstrate that caveolae can acts as mechano-signaling hubs with an ability to remotely control downstream signal transduction from the PM.

Preliminary results indicate that this regulatory control through caveolae mechanics is not limited to the JAK-STAT pathway. We observed an increased interaction of PTEN with Cav1 upon membrane tension increase. This needs further characterization to

understand the role of caveolae mechanics in the PTEN/AKT/PI3K pathway. Moreover, experiments are underway to further define the CBM domain of JAK1 that interacts with JAK1. As discussed in section 5.1 b, optogenetics provides a means to specifically control the assembly and disassembly of caveolae. Once established, it would serve as a versatile tool to study caveolae mechanics in the context of different cellular functions. Nevertheless, it would indeed be very interesting to utilize the optogenetic module to confirm our results presented in through this study.

ANNEXE - I

JCB Journal of Cell Biology

REPORT

EHD2 is a mechanotransducer connecting caveolae dynamics with gene transcription

Stéphanie Torrino[1,2,3*], Wei-Wei Shen[1,2,3*], Cédric M. Blouin[1,2,3], Satish Kailasam Mani[1,2,3], Christine Viaris de Lesegno[1,2,3], Pierre Bost[4,5], Alexandre Grassart[6], Darius Köster[7], Cesar Augusto Valades-Cruz[2,3,8], Valérie Chambon[2,3,8], Ludger Johannes[2,3,8], Paolo Pierobon[9], Vassili Soumelis[4], Catherine Coirault[10], Stéphane Vassilopoulos[10], and Christophe Lamaze[1,2,3]

Caveolae are small invaginated pits that function as dynamic mechanosensors to buffer tension variations at the plasma membrane. Here we show that under mechanical stress, the EHD2 ATPase is rapidly released from caveolae, SUMOylated, and translocated to the nucleus, where it regulates the transcription of several genes including those coding for caveolae constituents. We also found that EHD2 is required to maintain the caveolae reservoir at the plasma membrane during the variations of membrane tension induced by mechanical stress. Metal-replica electron microscopy of breast cancer cells lacking EHD2 revealed a complete absence of caveolae and a lack of gene regulation under mechanical stress. Expressing EHD2 was sufficient to restore both functions in these cells. Our findings therefore define EHD2 as a central player in mechanotransduction connecting the disassembly of the caveolae reservoir with the regulation of gene transcription under mechanical stress.

Introduction

Cells translate physical stimuli by mechanotransduction into biochemical signals that relay information from the cell surface to the nucleus, where gene expression is regulated. Mechanotransduction controls multiple cellular aspects including, but not limited to, cell growth, shape, or differentiation (Iskratsch et al., 2014). Abnormal cell responses to external and internal mechanical constraints are often associated with human pathologies such as heart diseases, myopathies, and cancer (DuFort et al., 2011). The underlying mechanisms integrating mechanosensing with mechanotransduction remain poorly understood.

Caveolae are 60–80-nm bulb-like plasma membrane invaginations discovered more than 60 years ago (Palade, 1953; Yamada, 1955). Caveolae are generated through tight association of caveolin 1 (Cav1) oligomers, its main structural component, and are stabilized by the assembly of cytoplasmic cavins into a coat-like structure around the caveolae bulb (Gambin et al., 2013; Ludwig et al., 2013; Stoeber et al., 2016). We established a new function of caveolae in mechanosensing and mechanoprotection in endothelial and muscle cells: under increase of membrane tension generated by cell swelling or stretching, caveolae flatten out immediately to provide additional surface area and prevent the rupture of the plasma membrane (Sinha et al., 2011). The central role of caveolae in cell mechanics has been confirmed in vivo (Cheng et al., 2015; Garcia et al., 2017; Lim et al., 2017) and has been extended to the muscle-specific isoform Cav3 (Cheng et al., 2015; Lo et al., 2015) and other cell types (Gervásio et al., 2011; Ariotti et al., 2014).

Here, we reveal that the Eps15 homology domain-containing 2 (EHD2) ATPase is released from mechanically disassembled caveolae and is subsequently translocated to the nucleus to mediate mechanotransduction through gene transcription. EHD2 is also required to maintain the caveolae reservoir at the plasma membrane under membrane tension variations. Thus, EHD2 plays a pivotal role in the cell adaptation to mechanical perturbations by connecting caveolae mechanosensing at the plasma membrane with the regulation of gene transcription.

Results and discussion

EHD2 is rapidly translocated from caveolae to the nucleus upon mechanical stress

The mechanical flattening of caveolae is immediately followed by the disassembly of caveolae and the release of caveolar proteins

[1]Membrane Dynamics and Mechanics of Intracellular Signaling Laboratory, Centre de Recherche, Institut Curie, PSL Research University, Paris, France; [2]Institut National de la Santé et de la Recherche Médicale (INSERM), U1143, Paris, France; [3]Centre National de la Recherche Scientifique, UMR 3666, Paris, France; [4]Laboratoire d'Immunologie Clinique, INSERM U932, Centre de Recherche, Institut Curie, Paris, France; [5]Department of Biology, École Normale Supérieure, PSL Research University, Paris, France; [6]Unité de Pathogénie Microbienne Moléculaire, INSERM 1202, Institut Pasteur, Paris, France; [7]Cell and Developmental Biology, Warwick Medical School Biomedical Sciences, Warwick University, Coventry, UK; [8]Endocytic Trafficking and Intracellular Delivery Laboratory, Centre de Recherche, Institut Curie, PSL Research University, Paris, France; [9]INSERM U932, Institut Curie, PSL Research University, Paris, France; [10]Sorbonne Université, INSERM, Institute of Myology, Centre of Research in Myology, UMRS 974, Paris, France.

*S. Torrino and W.-W. Shen contributed equally to this paper; Correspondence to Christophe Lamaze: christophe.lamaze@curie.fr.

including Cav1 and cavins (Sinha et al., 2011; Gambin et al., 2013). We hypothesized that the release of caveolae components into the cytosol could mediate mechanotransduction events (Nassoy and Lamaze, 2012; Lamaze et al., 2017). We monitored the fate of cavin1 and EHD2 because these two peripheral proteins of caveolae bear nuclear localization signals and can undergo nucleocytoplasmic shuttling (Pekar et al., 2012; Nassar and Parat, 2015). ATP hydrolysis drives EHD2 oligomerization at the neck of caveolae, where it controls their stability through anchoring to the actin cytoskeleton (Morén et al., 2012; Stoeber et al., 2012). Cavin1/PTRF is the first identified member of the cavin family that participates in the formation of the cytoplasmic coat of caveolae (Ludwig et al., 2013; Kovtun et al., 2014).

Under resting conditions, EHD2 was present at the plasma membrane of HeLa cells, where it colocalized with ∼50–60% of Cav1 puncta, as previously shown (Fig. S2 A; Morén et al., 2012; Stoeber et al., 2012). As expected, a fraction of EHD2 was present in the nucleus (Fig. 1 A; Pekar et al., 2012). Repeated cycles of cell stretching and relaxation led to a moderate (≈10%), albeit significant, increase of the EHD2 signal in the nucleus. A fraction of cavin1, which bears two nuclear localization signals, was also present in the nucleus at steady state. No further increase of nuclear cavin1 was measurable upon cyclic stretch (Fig. 1 B). We also followed the intracellular fate of EHD2 under acute disassembly of caveolae induced by hypo-osmotic shock (Sinha et al., 2011). After 5 min of hypo-osmotic shock (Hypo), we measured a significantly higher (≈45%) increase in EHD2 nuclear translocation. In contrast, Cav1 was not translocated to the nucleus upon mechanical stress (Figs. 1 C and S1 A). EHD2 nuclear translocation increased with the hypo-osmotic shock strength (Fig. S1 A). We followed EHD2 dynamics in live cells in 3D with lattice light sheet microscopy (Chen et al., 2014). During the course of the hypo-osmotic shock, the amount of nuclear EHD2 increased rapidly, reaching a plateau in ∼100 s (Fig. S1 C and Video 1). Upon return to iso-osmotic conditions, the caveolae reservoir is rapidly reassembled at the plasma membrane (Sinha et al., 2011). Under this condition (Rec), the amount of nuclear EHD2 decreased to a level slightly below steady state (Figs. 1 C and S1 A).

We quantified the amount of endogenous EHD2 present in the nuclear, cytoplasmic, and membrane fractions of cellular protein extracts from mouse lung endothelial cells (MLECs). At steady state, EHD2 was distributed between the nuclear, cytoplasmic, and membrane fractions of MLEC WT cells having caveolae (Fig. 1 D). Hypo-osmotic shock led again to a significant increase of EHD2 nuclear content and a concomitant decrease in the membrane fractions, whereas the cytoplasmic fraction remained constant. In contrast, the initial distribution of EHD2 was not significantly changed by hypo-osmotic shock in MLEC Cav1$^{-/-}$ cells devoid of caveolae, indicating that functional caveolae were required for EHD2 nuclear translocation induced by mechanical stress (Fig. 1 D). Similarly, a lack of EHD2-mCherry nuclear translocation was observed in HeLa Cav1$^{-/-}$ cells (Fig. S1 B). In these cells, the amount of nuclear EHD2-mCherry was higher, suggesting that the association of EHD2 with caveolae at the plasma membrane prevents its nuclear translocation. Finally, total internal reflection microscopy (TIRF) live-cell imaging showed that dually labeled Cav1 and EHD2 puncta synchronously disappeared from the plasma membrane with the same amplitude under hypo-osmotic shock, implying that EHD2 was released during caveolae disassembly (Fig. S2 A). These observations clearly demonstrate that the mechanical disassembly of caveolae at the plasma membrane results in the translocation of EHD2 to the nucleus.

Mechanical stress results in EHD2 SUMOylation

We next investigated which possible posttranslational modifications of EHD2 could be associated with its mechanical release from caveolae. EHD2 was reported to be SUMOylated by SUMO1 (small ubiquitin-like modifier) on Lys^{315}, which, when mutated, resulted in EHD2 nuclear accumulation (Pekar et al., 2012). Protein SUMOylation has clearly been associated with nucleocytoplasmic transport and the response to different types of stresses, including osmotic stress (Geiss-Friedlander and Melchior, 2007; Enserink, 2015). We first explored the interaction between endogenous EHD2 and SUMO using the proximal ligation assay (PLA; Söderberg et al., 2006). In Hs578T cells, which present substantial amounts of caveolae (see Fig. 5, A–C), PLA confirmed that endogenous EHD2 was SUMOylated by SUMO1 (Fig. S2 B). At steady state, a significant amount of EHD2-SUMO1 was localized in the nucleus and to a lesser extent in the cytoplasm and at the plasma membrane. Hypo-osmotic shock did not increase EHD2 SUMOylation but led to a significant relocation of EHD2-SUMO1 in the nucleus. We also analyzed the possible SUMOylation of EHD2 by SUMO2/3 and found minimal levels of EHD2-SUMO2/3 under resting conditions (Fig. 2 A). Unlike SUMO1, however, hypo-osmotic shock led to a general increase of the cellular amount of EHD2-SUMO2/3, with a significant increase in nuclear EHD2-SUMO2/3 (Fig. 2, A and B). We confirmed EHD2 SUMOylation biochemically by transfecting EHD2-GFP in HeLa cells stably expressing His-SUMO2/3. The amount of EHD2-SUMO2/3, minimal under resting conditions, increased again after hypo-osmotic shock (Fig. 2 C).

We also measured EHD2 SUMOylation after mechanical stress release when the initial number of caveolae has fully recovered. We found a significant decrease of both EHD2-SUMO1 and EHD2-SUMO2/3, especially in the nucleus, suggesting that EHD2 deSUMOylation had occurred (Figs. 2 A and S2 B). Finally, we analyzed the EHD2 SUMOylation deficient mutant KK315-316AA, previously shown to accumulate in the nucleus, implying that EHD2-SUMOylation controlled EHD2 nuclear exit (Pekar et al., 2012). The EHD2-KK315-316AA mutant disappeared synchronously with Cav1 from the plasma membrane under hypo-osmotic shock but was unable to relocate to caveolae after shock release (Fig. S2 A). Finally, no increase in EHD2-SUMOylation was measurable in MLEC Cav1$^{-/-}$ cells (Fig. 2 D), indicating that the pool of EHD2 that is SUMOylated under hypo-osmotic shock is the pool that was initially associated with caveolae at the plasma membrane. Together, these data show that the cycle of EHD2 SUMOylation is controlled by mechanical stress and plays a key role in the nucleocytoplasmic shuttling of EHD2.

EHD2 controls gene transcription under mechanical stress

To address the functional significance of EHD2 nuclear translocation, we used gene set enrichment analysis (GSEA; Subramanian et al., 2005) to compare the transcriptome of Hs578T cells

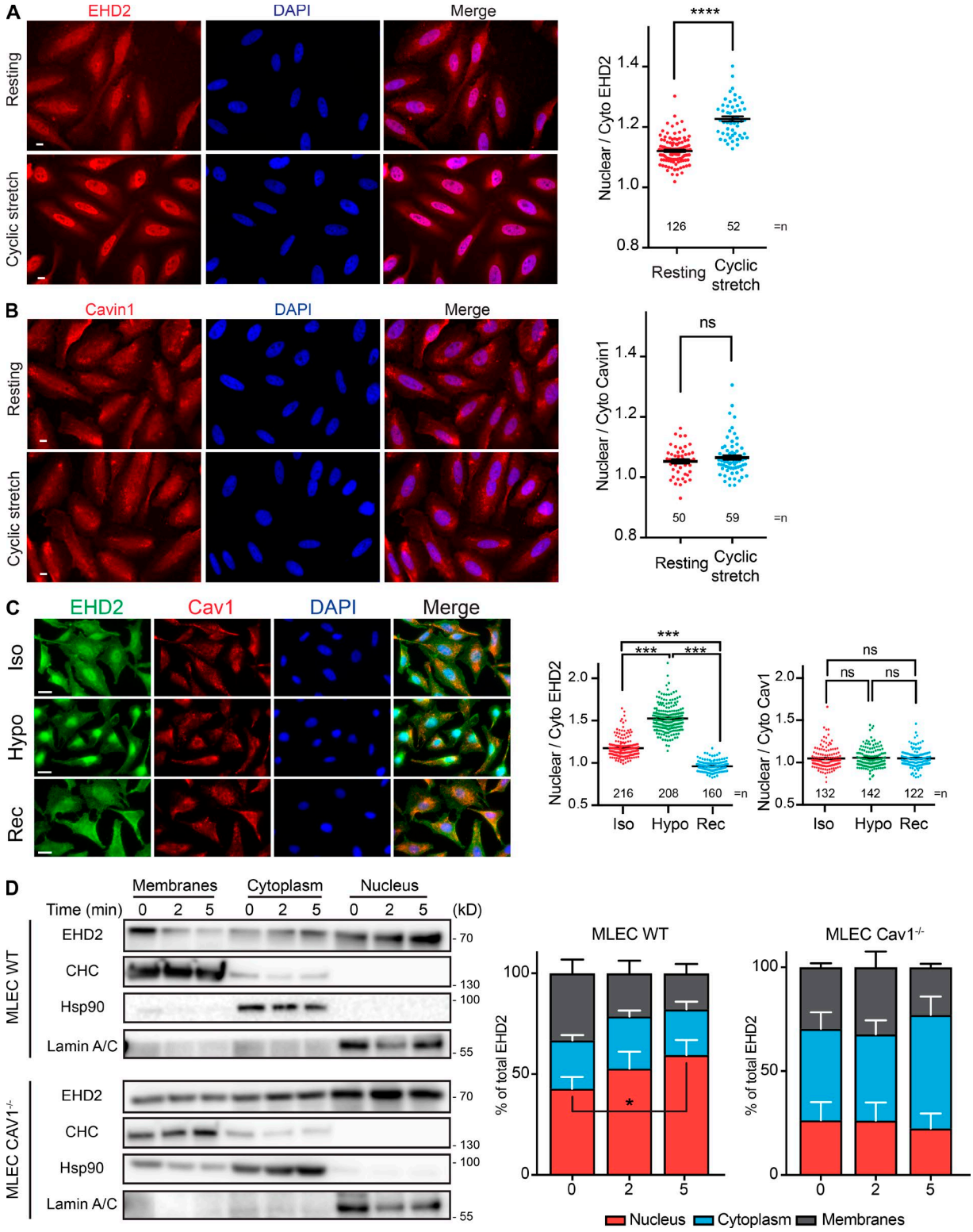

Figure 1. **Mechanical stress induces EHD2 nuclear translocation. (A and B)** Representative wide-field immunofluorescence (left) and quantification (right) of the nuclear translocation of endogenous EHD2 (A) but not cavin1 (B) in HeLa cells after 30 min of cyclic stretch. **(C)** Representative wide-field immunofluorescence (left) and quantification (right) of endogenous EHD2 and Cav1 localization in HeLa cells under resting (Iso), after 5 min of 30 mOsm hypo-osmotic shock (Hypo), and 5 min after return to iso-osmotic conditions (Rec). **(D)** Immunoblot analysis (left) and quantification (right) of equal amounts of nuclear, cytoplasmic and cell membrane extracts after hypo-osmotic shock for the indicated times in MLEC cells having caveolae (WT) or not ($Cav1^{-/-}$). Scale bar = 10 µm; $n \geq 3$ independent experiments; *, $P < 0.05$; ***, $P < 0.001$; ****, $P < 0.0001$; in A and B, two-tailed *t* test; data are representative of three experiments, mean ± SEM; in C, Bonferroni's multiple comparison test; data are mean ± SEM; numbers of cells are indicated on the graphs; in D, Dunn's multiple comparison test; $n = 3$; data are mean ± SEM.

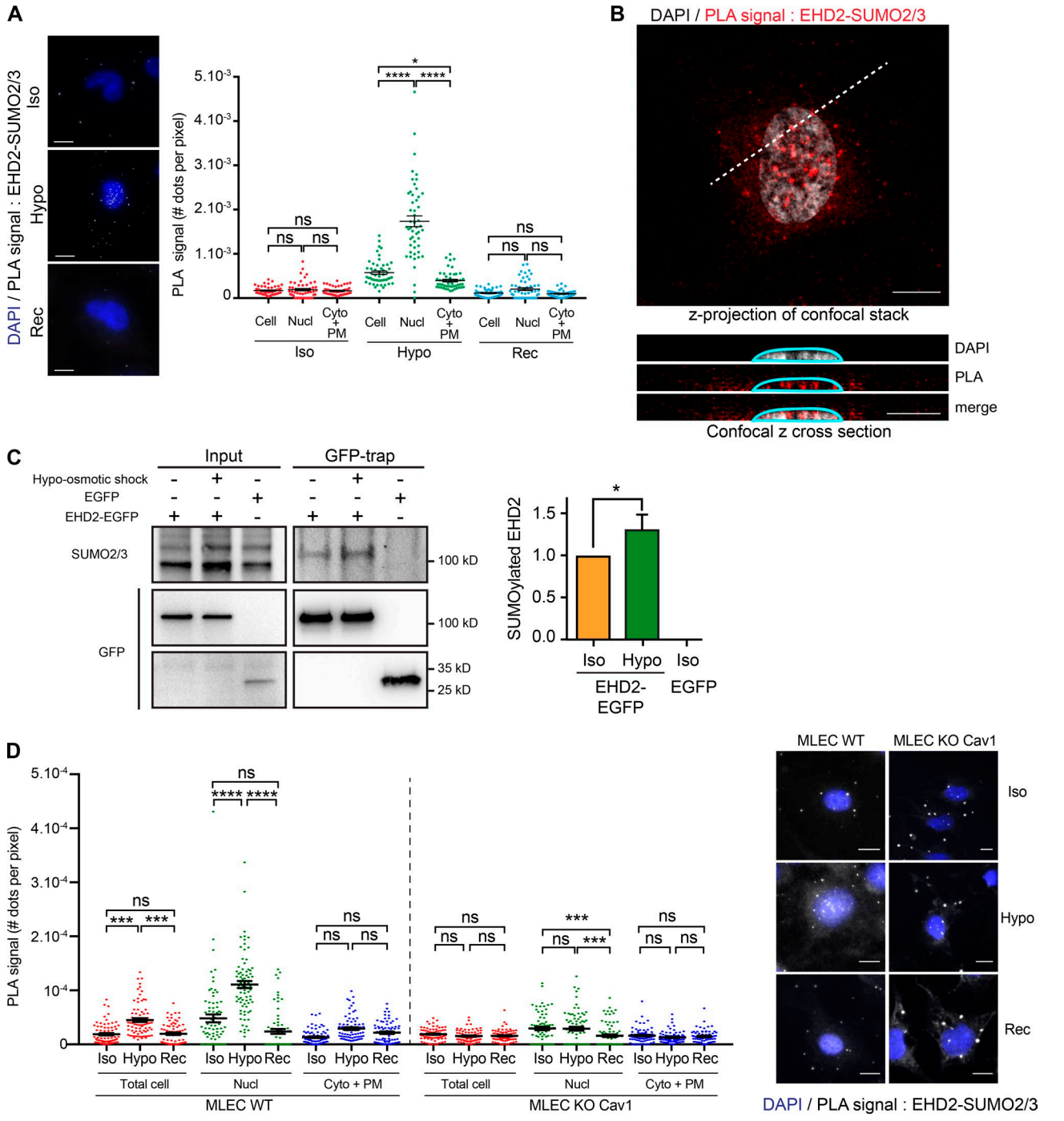

Figure 2. **EHD2 is SUMOylated by SUMO2/3 upon mechanical stress. (A)** Representative wide-field fluorescence (left) and quantification (right) of in situ PLA experiments in Hs578T cells monitoring EHD2 and SUMO2/3 interaction in the whole cell (Cell), the nucleus (Nucl), and the cell minus the nucleus (Cyto + plasma membrane) under resting (Iso, *n* = 51), under hypo-osmotic (Hypo, *n* = 51), and after return to iso-osmotic (Rec, *n* = 50) conditions. **(B)** Representative z-projection (average intensity) of a confocal stack of a PLA experiment monitoring EHD2 and SUMO2/3 interaction (red signal) in MLEC cells 5 min after 30 mOsm hypo-osmotic shock. A confocal z cross section along the dashed line shows localization of PLA spots in the nucleus (DAPI; gray). **(C)** Immunoblot analysis (left) and quantification (right; SUMO2/3 level normalized to GFP) of EGFP-EHD2 SUMOylation by SUMO2/3 in immunoprecipitates from stable HeLa His-SUMO2/3 cells transfected with EHD2-EGFP or EGFP under Iso and Hypo conditions. **(D)** Same PLA experiments as in A performed in MLEC WT (Iso, *n* = 76; Hypo, *n* = 77; Rec, *n* = 72) or Cav1$^{-/-}$ cells (Iso, *n* = 75; Hypo, *n* = 75; Rec, *n* = 75). Scale bar = 10 µm; *, P < 0.05; ***, P < 0.001; ****, P < 0.0001; in A and D, Dunnett's multiple comparison test, data are representative of three experiments, mean ± SEM; in C, repeated measures one-way ANOVA; data are mean ± SEM.

depleted or not from EHD2 and subjected to cyclic stretch for 30 min at 0.5 Hz. GSEA showed that cyclic stretching resulted in the positive enrichment of gene sets involved in hallmark signaling pathways such as TNF-α, K-Ras, and receptor interaction with the extracellular matrix (Fig. 3 A; http://microarrays.curie.fr/). When EHD2 was silenced, the gene set regulation observed under mechanical stress was lost. In addition, distinct gene sets related to cell cycle, cell division, and cell-cycle checkpoints were also

negatively regulated. Although cyclic stretching did not result in major changes in the pattern of gene set enrichment modified by EHD2 silencing, differences in the regulation of gene sets encoding transcription factors and cell division were further shown.

We next measured mRNA levels of caveolae constituents by reverse-transcription quantitative PCR (RT-qPCR) in HeLa cells under mechanical stress. Cyclic stretch led to a significant decrease of caveolae constituent transcripts, i.e., Cav1, Cav2, cavin1, and cavin2, without affecting transcripts of flotillin-1 (Flot1), a related membrane protein assembling microdomains distinct from caveolae at the plasma membrane (Fig. 3 B). Similar data were obtained under hypo-osmotic shock (Fig. S2 C). Importantly, no modification of transcript levels was detected in cells depleted of EHD2 (Figs. 3 B and S2 C), and a siEHD2-resistant variant fully rescued the regulation of caveolae constituent genes in EHD2-depleted cells (Fig. S2 C). The mechanical regulation of caveolae constituent gene transcription by EHD2 was no longer observed in Cav1-depleted cells, confirming that the nuclear translocation of EHD2 and its impact on gene transcription requires the disassembly of functional caveolae (Fig. S2 D). Finally, the repression activity of EHD2 on transcription was mediated by Krüppel-like factor 7 (KLF7) and modulator of KLF7 activity (MOKA; Fig. 3 C), two known partners of EHD2-regulated transcription (Pekar et al., 2012). Interestingly, KLF7 was found to bind to several enhancers of caveolae constituent genes in different cell lines (Fig. S2 E).

EHD2 stabilizes caveolae during membrane tension variations

We next analyzed the role of EHD2 in caveolae dynamics using TIRF and found, as previously published (Morén et al., 2012; Stoeber et al., 2012; Yeow et al., 2017), that EHD2 depletion did not change the number of Cav1 spots present at the plasma membrane under resting conditions. Whereas EHD2 depletion had no effect on the extent of caveolae disassembly under hypo-osmotic shock, the reassembly of caveolae, which normally occurs immediately after the release of mechanical stress, was significantly reduced (Fig. 3 D). Expression of the dominant-negative EHD2-T72A mutant (unable to bind ATP) also reduced caveolae recovery after mechanical stress release. Conversely, expression of wild-type EHD2, EHD2-I157Q constitutively active mutant (with accelerated ATP hydrolysis), or a siEHD2-resistant variant allowed caveolae reassembly (Figs. 3 E and S3 A). Finally, depletion or overexpression of Pacsin2 and filamin A, proteins that link caveolae to the actin cytoskeleton, did not affect the reassembly of caveolae after mechanical stress release (Fig. S3, B and C).

We next examined the role of EHD2 under membrane tension variations by measuring the effective membrane tension using the tether pulling technique as described previously (Sheetz, 2001; Sinha et al., 2011). HeLa cells were first exposed to a 5-min hypo-osmotic shock (150 mOsm) to increase membrane tension, and then to iso-osmolarity for 5 min to allow the return of membrane tension to homeostasis (Rec condition). By recording the mean variations of the tether force ΔF over the initial force F_{iso} measured in isotonic conditions, we found, as expected for cells having functional caveolae (Sinha et al., 2011), that the increase of membrane tension induced by hypo-osmotic shock was buffered, as F_{hypo} remained almost identical to F_{iso} (Fig. 3 F). When cells were depleted of EHD2, there was a slight but not significant increase in membrane tension, in agreement with our finding that EHD2 depletion did not change the extent of caveolae disassembly induced by hypo-osmotic shock (Fig. 3 F). 5 min after return to iso-osmolarity (Rec), the membrane tension of control cells had not yet returned to the initial value measured before stress, as indicated by the negative value of the tether force ΔF. In EHD2-depleted cells, however, we measured a drastically smaller value of membrane tension, indicating a stronger delay in the return to membrane tension homeostasis (Fig. 3 F). We also found that repeated cycles of stretching and relaxation led to a slight but significant decrease of the number of caveolae at the plasma membrane in cells depleted of EHD2 (Fig. 3 G). Altogether, these data indicate that EHD2 is required for maintaining a functional reservoir of caveolae at the plasma membrane, which buffers the variations of membrane tension during mechanical stress.

Loss of EHD2 expression impairs caveolae mechanosensing and gene transcription

Low EHD2 expression was recently reported in several solid tumors (Li et al., 2013; Shi et al., 2015; Yang et al., 2015; Liu et al., 2016). Whether low EHD2 expression was also associated with defects in caveolae stabilization and nuclear translocation was not investigated in those studies. Given the importance of the mechanical microenvironment in tumor progression (DuFort et al., 2011) and the association of Cav1 with tumorogenesis (Goetz et al., 2008; Lamaze and Torrino, 2015), we investigated caveolae mechanics in breast cancer cell lines. We measured EHD2 mRNA levels in several normal and cancerous breast epithelial cell lines and selected Hs578T and MDA-MB-436, two triple-negative basal-like breast cancer cell lines that express high and minimal levels of EHD2 transcripts, respectively. Immunoblot analyses confirmed similar amounts of Cav1 and cavin1 proteins in Hs578T and MDA-MB-436 cells, whereas EHD2 was expressed in Hs578T but undetectable in MDA-MB-436 cells (Fig. 4 A).

We first investigated the dynamics of caveolae under mechanical stress by TIRF microscopy. In agreement with the disassembly of caveolae induced by higher membrane tension, we observed a rapid and significant decrease of Cav1 spots at the cell surface of Hs578T cells after exposure to a hypo-osmotic shock (Fig. 4 B). In contrast, the number of Cav1 spots remained identical in MDA-MB-436 cells (Fig. 4 C). However, when EHD2 was expressed in MDA-MB-436 cells, a strong decrease in cell surface Cav1 spot numbers was observed again under hypo-osmotic shock (Fig. 4 D).

We next addressed whether this defect in caveolae mechanosensing was also associated with defects in gene transcription regulation. MDA-MB-436 cells did not show any variation in the level of caveolae component transcription under mechanical stress, whereas the reexpression of EHD2, but not Cav1, restored this control (Fig. 4 E). Importantly, the restoration of this control required caveolae, as it was no longer observed when EHD2-transfected MDA-MB-436 cells were depleted of Cav1 (Fig. 4 E). Whereas cyclic stretch led to a decrease of caveolae component transcripts in Hs578T cells, EHD2 depletion suppressed this control (Fig. 4 F). Similar results were observed in cells depleted of Cav1. Altogether, these data confirm that

A

gene set names	Gene enrichment		
	Stretch	siEHD2	siEHD2 + stretch
ECM-receptor interaction	+		
AHR	+		
SRF	+		
Kras down	+		
TNFα signaling	+	+	+
Kras up		+	+
Hypoxia		+	+
Unfolded protein response		+	+
Apoptosis		+	+
STK33 up		+	+
E2F targets		-	-
E2F transcription factors			-
G2M checkpoints		-	-
Cell cycle		-	-
Cell division		-	
Beta catenin up		-	-

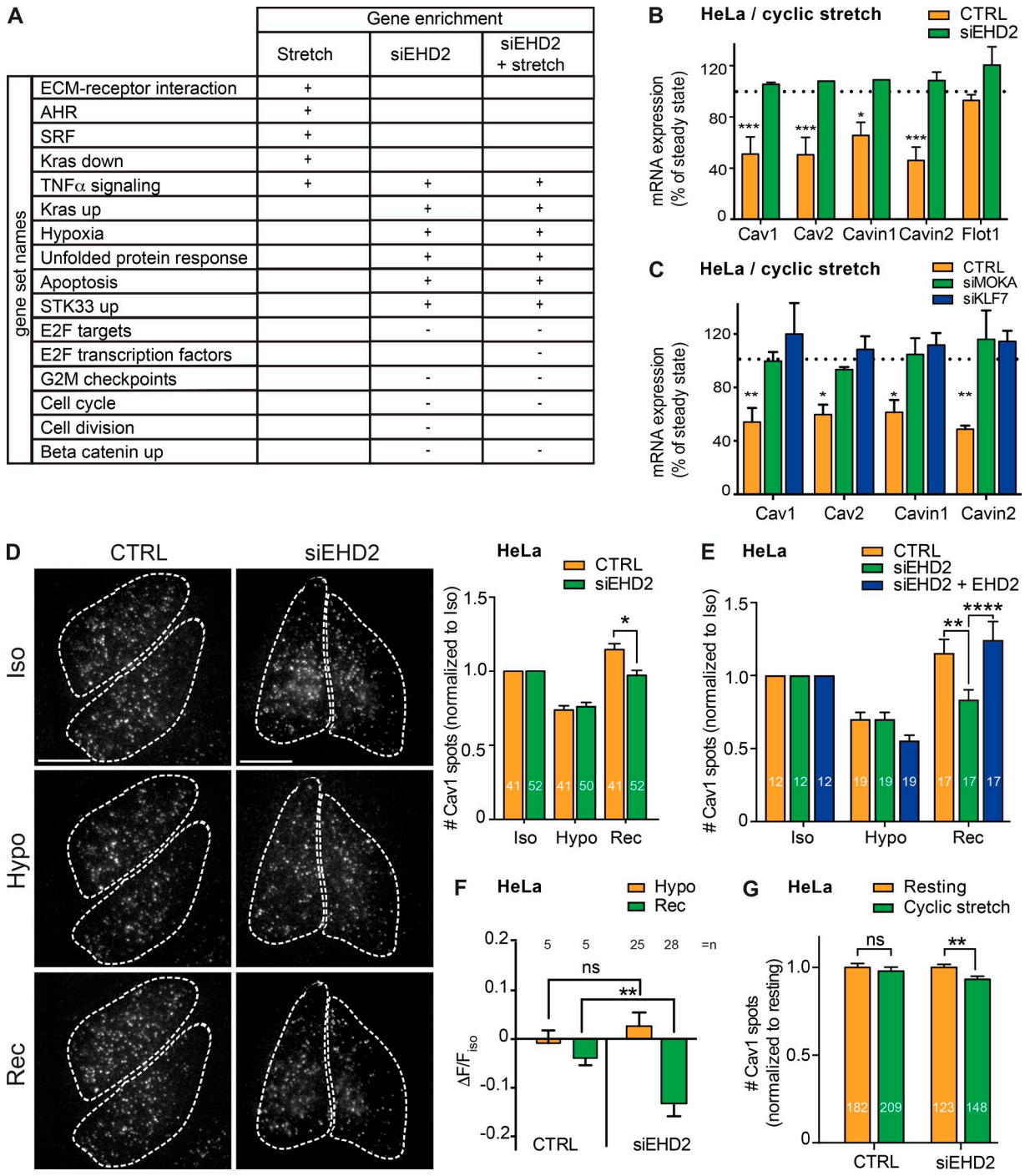

Figure 3. **EHD2 is required for the stabilization of caveolae and the control of gene transcription during tension variations at the plasma membrane. (A)** GSEA was performed to identify gene sets positively (+) or negatively (–) enriched by cyclic stretch in Hs578T cells depleted or not from EHD2. **(B)** Quantification of Cav1, Cav2, cavin1, cavin2, and flotillin-1 (Flot1) mRNA levels in HeLa cells transfected with control siRNA (CTRL) or siEHD2, after 30 min cyclic stretch. **(C)** Quantification of Cav1, Cav2, cavin1, and cavin2 mRNA levels in HeLa cells transfected with control siRNA (CTRL), siMOKA, or siKLF7 after 30 min cyclic stretch. **(D)** Representative TIRF images (left) and quantification (right) of changes in cell-surface Cav1 spot numbers in control siRNA (CTRL) or siEHD2-transfected Cav1-EGFP HeLa cells under resting (Iso), under hypo-osmotic (Hypo), and after return to iso-osmotic (Rec) conditions. Cells are delineated by dashes. **(E)** Quantification of changes in cell-surface endogenous Cav1 spot numbers in HeLa cells depleted (siEHD2) or not (CTRL) for EHD2 and transfected or not with EHD2-EGFP (+ EHD2) under Iso, Hypo, and Rec conditions. **(F)** Relative changes of the mean tether force under Hypo and Rec conditions in control siRNA (CTRL) and siEHD2 HeLa cells. **(G)** Quantification of cell surface Cav1 spot numbers at rest and after 30 min cyclic stretch in control siRNA (CTRL) or siEHD2 transfected HeLa cells. *, P < 0.05; **, P < 0.001; ***, P < 0.001; ****, P < 0.0001; two tailed *t* test. In B and C, Bonferroni's multiple comparison test; *n* = 3 independent experiments; in D–G, two-way ANOVA and Tukey's multiple comparisons test; *n* = 3; data are mean ± SEM. Numbers of cells are indicated on histogram bars. Scale bar = 10 µm.

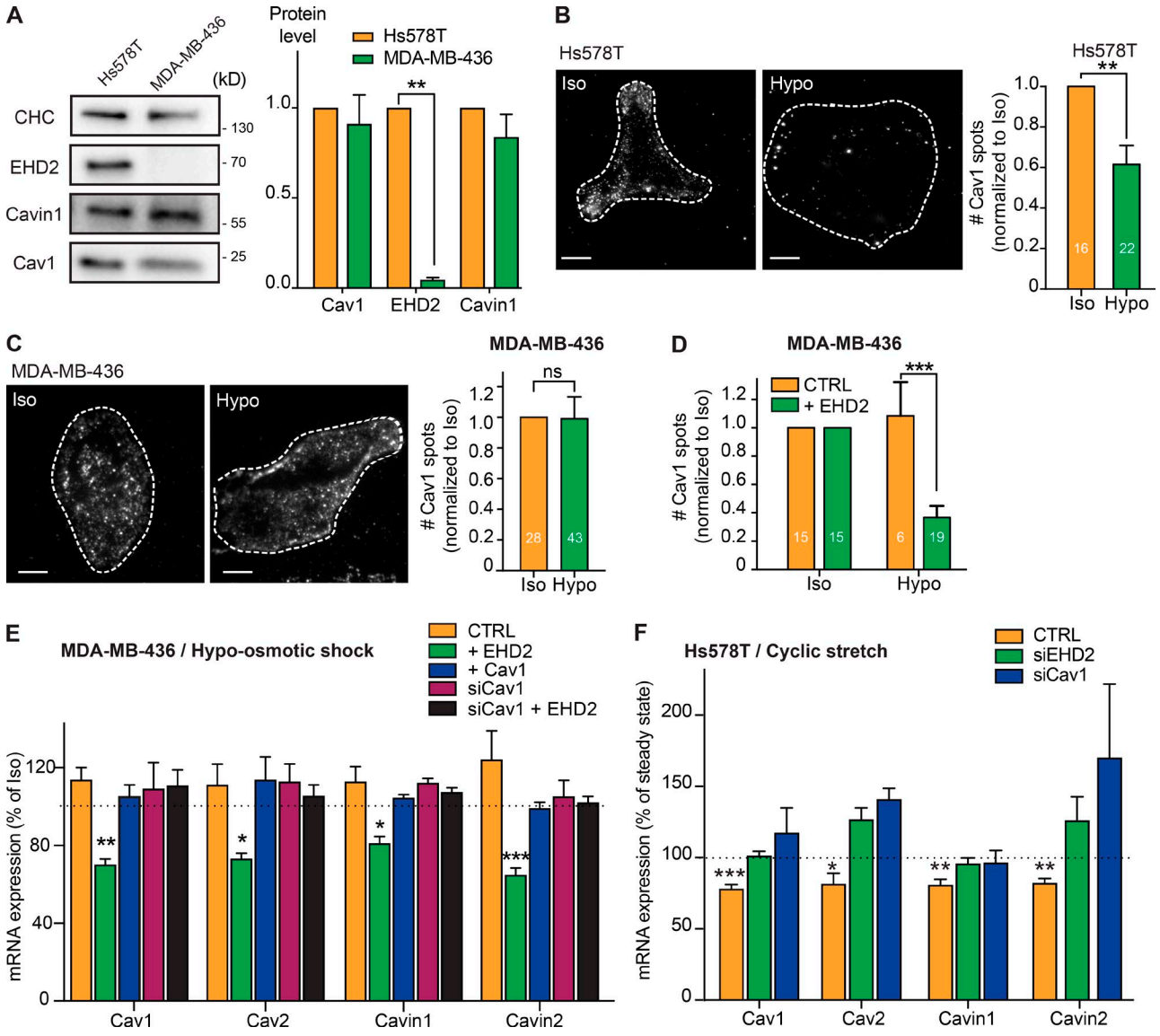

Figure 4. **Loss of EHD2 expression impairs caveolae mechanosensing and gene transcription in breast cancer cells. (A)** Immunoblot (left) and quantification (right) of EHD2, Cav1, and cavin1 protein levels normalized to CHC in Hs578T and MDA-MB-436 cells. **(B and C)** Representative TIRF images of changes in cell surface Cav1 spot numbers (left) and quantification (right) under resting (Iso) and hypo-osmotic (Hypo) conditions in Hs578T (B) or MDA-MB-436 (C) cells. Cells are delineated by dashes. Scale bar = 10 µm. **(D)** Quantification of changes in cell surface Cav1 spot numbers in MDA-MB-436 cells transfected or not (CTRL) with EHD2-EGFP under Iso and Hypo conditions. **(E)** Quantification of Cav1, Cav2, cavin1, and cavin2 mRNA levels in MDA-MB-436 cells transfected or not (CTRL) with EHD2 or Cav1 and in MDA-MB-436 cells depleted for Cav1 (siCav1) and transfected or not by EHD2 under hypo-osmotic conditions. **(F)** Quantification of Cav1, Cav2, cavin1, and cavin2 mRNA levels in Hs578T cells transfected with control siRNA (CTRL), siEHD2, or siCav1 after 30 min of cyclic stretch. For all panels, $n \geq 3$ independent experiments; mRNA levels are compared with resting conditions (dotted line); *, $P < 0.05$; **, $P < 0.01$; ***, $P < 0.001$; two tailed *t* test; data are mean ± SEM; numbers of cells are indicated on histogram bars.

functional caveolae are required for the mechanical control of gene transcription by EHD2.

To better understand how EHD2 controls the caveolae reservoir in breast cancer cells, we analyzed the ultrastructure of caveolae on unroofed cells using metal replica EM. Consistent with high Cav1 and EHD2 expression, Hs578T cells displayed numerous budded caveolae (Fig. 5, A–C). In contrast, MDA-MB-436 cells, which lack EHD2, presented very few caveolae, if any, and most membrane invaginations were clathrin-coated pits (Fig. 5, D–F). Cav1 immunogold labeling on standard transmission electron micrographs confirmed the absence of caveolar invaginations in MDA-MB-436 cells but revealed a significant amount of Cav1 proteins present at the plasma membrane (Fig. 5 J). In contrast, Cav1 proteins were always associated with bona fide caveolar invaginations in Hs578T cells. These results most likely explain the lack of caveolae disassembly observed in MDA-MB-436 cells (Fig. 4 C), because the Cav1 signal does not correspond to caveolar invaginations but to Cav1 clusters that are unlikely to flatten out under mechanical stress. Expressing EHD2 in MDA-MB-436 cells was sufficient to reconstitute the reservoir of caveolae at the plasma membrane (Fig. 5, G, H and I). EHD2 has not been involved in caveolae assembly (Morén et al., 2012; Stoeber et al.,

2012; Hoernke et al., 2017); therefore, it was unexpected that MDA-MB-436 breast cancer cells do not have caveolae, because their level of Cav1 and cavin1 expression is similar to that of Hs578T cells (Fig. 4 A). Our data strongly suggest that the absence of caveolae in breast cancer cells lacking EHD2 may represent a long-term consequence of the inability to stabilize the reservoir of caveolae under the changing mechanical environment experienced by cancer cells in the tumor mass. In this context, it is interesting that a recent study showed that EHD proteins (1, 2, and 4) are functionally redundant and that only the absence of all three EHDs results in loss of caveolae under mechanical stress (Yeow et al., 2017).

We and others have established caveolae as key mechanosensors (Gervásio et al., 2011; Sinha et al., 2011; Ariotti et al., 2014; Cheng et al., 2015; Lo et al., 2015). We reveal here that caveolae are also mechanotransducers, and that EHD2 is central to this new function. On the one hand, we show that ATP binding to EHD2 is required for assembling and stabilizing the reservoir of caveolae at the cell surface against the variations of membrane tension induced by mechanical stress. ATP binding allows EHD2 insertion into the plasma membrane, whereas ATP hydrolysis, possibly regulated by membrane curvature, is involved in EHD2 release (Hoernke et al., 2017). It is tempting to propose that caveolae flattening could trigger ATP hydrolysis by EHD2 and thereby its release from the plasma membrane. On the other hand, we show that the release of EHD2 from mechanically disassembled caveolae is rapidly followed by EHD2 nuclear translocation, where it regulates gene transcription. EHD2 SUMOylation, which is induced by mechanical stress, is a major regulator of EHD2 nucleocytoplasmic shuttling. Force-induced phosphorylation of Cav1 has been reported to regulate gene transcription of caveolae constituent biogenesis (Joshi et al., 2012). Our new results on EHD2 SUMOylation further illustrate the key role of posttranslational modifications in the caveolae response to mechanical stress. EHD2, which combines both mechanosensing and mechanotransducing activities, plays a central role in the mechanical cell response (Fig. 5 K).

Recent evidence shows that mechanical forces from both the tumor mass and its microenvironment can control cancer cells activity in vivo (DuFort et al., 2011; Fernández-Sánchez et al., 2015). Our study is the first report of a defect in caveolae mechanosensing and mechanotransduction in cancer cells and emphasizes the importance of revisiting the classic cellular functions of caveolae and their constituents through their new role in cell mechanics.

Materials and methods

Antibodies and reagents

The following commercially available antibodies were used for Western blotting: mouse monoclonal antibodies against clathrin heavy chain (CHC; BD Biosciences; 610500), lamin A/C (Santa Cruz Biotechnology; sc-7292), Hsp90 (Santa Cruz Biotechnology; sc-13119), EHD2 (Santa Cruz Biotechnology; sc-100724), dynamin (BD Biosciences; 610245), and filamin A (Chemicon; MAB1678); rabbit polyclonal antibodies against SUMO2/3 (Cell Signaling Technology; 4971), Cav1 (BD Biosciences; 610059), pacsin2 (Abgent; AP8088b); and cavin1 (Sigma; AV36965); for immunofluorescence, mouse monoclonal anti-cavin1 (BD Biosciences; 611258), goat polyclonal anti-EHD2 (Abcam; Ab23935), rabbit polyclonal anti-Cav1 (BD Biosciences; 610059), mouse monoclonal anti-lamin A/C (Santa Cruz Biotechnology; sc-7292), rabbit polyclonal anti-SUMO1 (Cell Signaling Technology; 4930), and rabbit polyclonal anti-SUMO2/3 (Cell Signaling Technology; 4971). Antibodies conjugated to Alexa Fluor 488, Cy3, Cy5, or HRP (Beckman Coulter and Invitrogen) were used as secondary antibodies. HaloTag dye JF635 was provided by L. Lavis (Janelia Research Campus, Howard Hughes Medical Institute, Ashburn, VA). Accutase was purchased from Sigma-Aldrich. Hepes, SDS, and Tris were purchased from Euromedex.

Plasmids

Cells were transfected using Lipofectamine 2000 (Invitrogen) according to the manufacturer's instructions. Experiments were performed 6–24 h after transfection. EHD2-mCherry, EHD2-EGFP, EHD2-I157Q-mCherry, and EHD2-T72A-mCherry were generously provided by A. Helenius (ETH Zurich, Zurich, Switzerland). EHD2-KK315-316AA-GFP was provided by M. Horowitz (Tel Aviv University, Tel Aviv, Israel). pmEmerald and Pacsin2-mCherry were purchased from Addgene. pCMV-HA-N was purchased from Clontech. EHD2-mEmerald was prepared by insertion of amplified EHD2 from EHD2-mCherry into pmEmerald plasmid using HindIII and BamHI restriction sites. Cav1-HaloTag was prepared by sequential insertion of Cav1 and HaloTag into pCMV-HA-N plasmid by EcoRI/BglII and XhoI/NotI restriction sites, respectively.

RNA interference

Cells were transfected with siRNAs using HiPerFect (Qiagen) according to the manufacturer's instructions and cultured for 72 h. Experiments were performed upon validation of depletion efficiency with immunoblot analysis using specific antibodies and normalization to the total level of CHC used as a loading control. Control siRNA (SI03650325, 5′-AAUUCUCCGAACGUG UCACGU-3′) was purchased from Qiagen and served as a reference point. The siRNA sequences were used at the final concentration of 20 nM: siEHD2 (Qiagen; SI04205271, 5′-AGCCCUUCC GCAAACUCAATT-3′, and SI04315108, 5′-CAUCCGUCAUUCAAA TT-3′), siPacsin2 (Qiagen; SI02224292, 5′-CCCUUAAUGUCCCGA GCAATT-3′, and SI02224299, 5′-AGCUUUACAUAGAACCUUATT-3′), siFilamin pool of 4 FlexiTube GeneSolution (Qiagen; GS2316, 5′-GGAAGAAGAUCCAGCAGAATT-3′, 5′-GUGGCGAUGGCAUGU ACAATT-3′, 5′-GGCCCAAACUGAACCCGAATT-3′, and 5′-CAG UCAACGAGGA-3′), siMOKA (GE Dharmacon; SMARTpool: ON-TARGETplus FBXO38 [81545] siRNA), siKLF7 (GE Dharmacon; SMARTpool: ON-TARGETplus KLF7 [8609] siRNA), and siCav1 (Eurogentec; 5′-CUAAACACCUCAACGAUGA-3′, 5′-GCAUCAACU UGCAGAAAGA-3′, 5′-GCAAAUACGUAGACUCGGA-3′, and 5′-GCA GUUGUACCAUGCAUUA-3′).

Cell culture

HeLa cells, Cav1-EGFP stably transfected HeLa cells (Sinha et al., 2011), and Hs578T cells were grown at 37°C under 5% CO_2 in DMEM GlutaMAX (GIBCO BRL Life Technologies) supple-

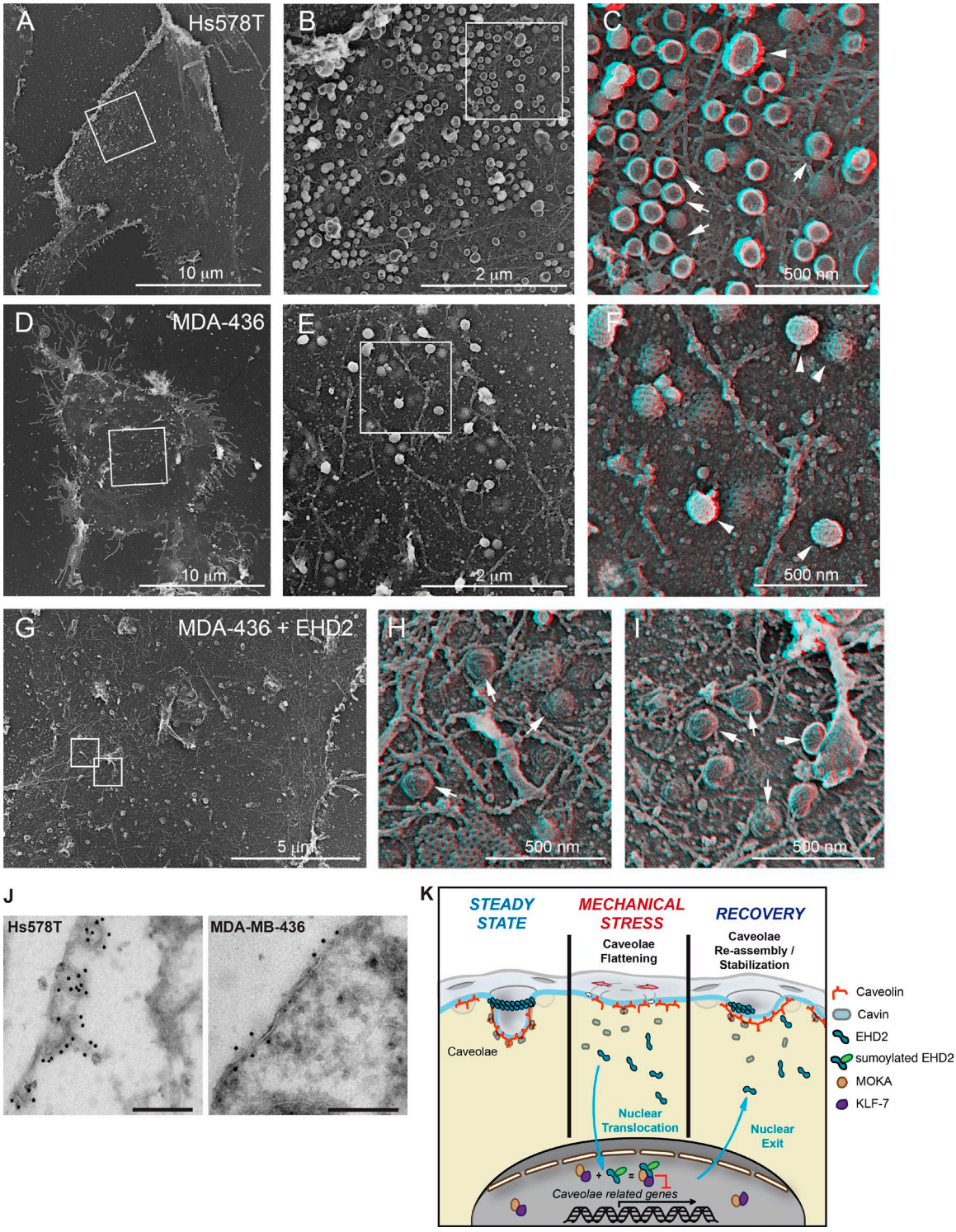

Figure 5. **EHD2 expression is required for the presence of caveolae at the plasma membrane of breast cancer cells. (A–I)** Survey view of the cytoplasmic surface of the plasma membrane in unroofed Hs578T cells (A–C), MDA-MB-436 (D–F) cells, and MDA-MB-436 cells transfected by EHD2-EGFP (G–I). For second inset (C, F, H, and I) use view glasses for 3D viewing of anaglyphs (left eye = red). Arrows indicate caveolae. Arrowheads indicate clathrin-coated pits. **(J)** Representative immunogold labeling of EM images of Cav1 protein localization in Hs578T and MDA-MB-436 cells. Scale bar = 200 nm. **(K)** Upon mechanical stress, Cav1, cavin1, and EHD2 are released from flattened caveolae. EHD2, but not cavin1 or Cav1, is SUMOylated and translocated to the nucleus where it controls gene transcription through interaction with MOKA and KLF-7. Upon stress release, EHD2 exits from the nucleus and is required for the stabilization of the caveolae reservoir at the plasma membrane.

mented with 10% FCS (GIBCO BRL Life Technologies), 5 mM pyruvate (GIBCO BRL Life Technologies), and 1% penicillin-streptomycin (GIBCO BRL Life Technologies). HeLa His-SUMO2 cells were grown as HeLa cells with 1 µg/ml puromycin (InvivoGen). MLECs (Sinha et al., 2011) were maintained in EGM-2 medium (Lonza) supplemented with 15% FBS (Hyclone; GE Healthcare), 4 mM L-glutamine (GIBCO BRL Life Technologies), 5 mM pyruvate, and 1% penicillin-streptomycin. MDA-MB-436 cells were grown at 37°C without CO_2 in Leibovitz's L-15 medium (GIBCO BRL Life Technologies) supplemented with 10% FCS (GIBCO BRL Life Technologies) and 1% penicillin-streptomycin (GIBCO BRL Life Technologies).

Generation of HeLa Cav1$^{-/-}$ cells

Single guide RNA (sgRNA) designed to target exon 3 of human caveolin-1 gene was selected and analyzed using online software Benchling. The selected guide (5′-GTATTTCGTCACAGTGAA GG-3′) was inserted into pSpCas9(BB)2A-Puro plasmid, which contains SpCas9 and sgRNA scaffold (px459 v2.0, Feng Zhang laboratory, Broad Institute of MIT and Harvard, Cambridge, MA; available from Addgene as plasmid 62988). 2 µg of plasmid was transfected using a single-cuvette Nucleofector device (Lonza) as per the manufacturer's protocol. In brief, 80% confluent HeLa cells were harvested, and 10^6 cells were resuspended in 100 µl complete solution R and transfected using Nucleofector program I-013. After transfection, cells were transferred to a 37°C, 5% CO_2 incubator, selected for puromycin for 72 h, and sorted as single cells into 96-well plates using a MoFlo Astrios cell sorter (Beckman Coulter). After clonal expansion, protein levels of clones were evaluated by Western immunoblotting.

Cyclic stretch

Cells were plated onto flexible-bottom plates (UniFlex plates; Flexcell International) coated with fibronectin (Sigma-Aldrich) and incubated at 37°C in a CO_2 incubator for 24 h before applying cyclic mechanical stretch. The cells were subjected to cyclic stretch at 0.5 Hz during 30 min using a computer-controlled vacuum stretch apparatus (FX-4000T Tension Plus System; FlexCell International) with a vacuum pressure sufficient to generate 10% mechanical stretch. Replicate control samples were maintained under static conditions with no applied cyclic stretch.

Hypo-osmotic shock

Hypo-osmotic shock was performed by diluting growth medium with deionized water (1:9 dilution for 30-mOsm hypo-osmotic shock and 1:1 for 150 mOsm hypo-osmotic shock).

Lysate preparation and immunoblot

Cells were lysed with sample buffer containing 2% SDS, 10% glycerol, 4 mM DTT, and Tris, pH 6.8. Lysates were analyzed by SDS-PAGE and immunoblotted with the indicated primary antibodies and HRP-conjugated secondary antibodies. Chemiluminescence signal was revealed using SuperSignal West Dura Extended Duration Substrate or SuperSignal West Femto Substrate (Thermo Fisher Scientific Life Technologies). Acquisition and quantification were performed on a ChemiDoc MP Imaging System (Bio-Rad).

Nuclear, cytosolic, and membrane extraction

Nuclear/cytoplasmic/membrane fractionation was conducted at resting conditions, at 2 and 5 min under hypo-osmotic shock (30 mOsm) as indicated, using the Subcellular Protein Fractionation Kit (Thermo Fisher Scientific) according to the manufacturer's protocol. The cytoplasmic fraction contains soluble cytoplasmic contents; the membrane fraction contains plasma, mitochondria, and ER/Golgi membranes; and the nuclear fraction contains the soluble nuclear extract and chromatin-bound nuclear proteins. Lysates were analyzed by SDS-PAGE and immunoblotted for lamin A/C as a marker of nuclear fraction, for Hsp90 as a marker of cytoplasmic fraction, and for CHC as a marker of membrane fraction. Fractions were quantified for protein content and normalized to the total cell lysate proteins.

GFP-trap

16 h after transfection, cells were treated with 100 nM leptomycin-B (Cell Signaling Technology; 9676) for 6 h. At resting conditions or after 5 min of hypo-osmotic shock, cells were harvested and lysed in 150 mM Tris-Cl, pH 6.7, 5% SDS, and 30% glycerol and then diluted 1:10 in PBS containing 0.5% NP-40 and protease inhibitor cocktail (Thermo Fisher Scientific). The lysates were then sonicated at 2× 10-s pulse (20 s in total) of 25% amplitude. Cleared lysates (13,200 rpm, 10 min, 4°C) were incubated overnight with GFPTrap-MA beads (Chromotek) at 4°C. Beads were washed three to five times with washing buffer (25 mM Tris-Cl, pH 7.4, 150 mM NaCl, 1 mM EDTA, and 5% glycerol) and eluted by boiling in 2× sample buffer at 95°C for 10 min. The eluted fractions were analyzed by Western blot and probed for GFP to determine the total EHD2-GFP pull-down level and for SUMO2/3 to measure SUMOylated EHD2.

Immunofluorescence and live-cell imaging

Cells were fixed for 15 min at room temperature with 4% PFA in PBS. After quenching with 50 mM NH_4Cl (Sigma-Aldrich) and permeabilization with 0.5% saponin (Sigma-Aldrich) or 1% Triton X-100, cells were blocked with 5% BSA (Sigma-Aldrich) and incubated sequentially with primary and secondary antibodies before being mounted in Fluoromount-G mounting medium (eBioscience). 2 µg/ml DAPI (Sigma-Aldrich) was used in mounting medium to counterstain nuclei. Images were acquired on a Leica DM 6000B inverted wide-field fluorescence microscope equipped with a HCX PL Apo 40× NA 1.25 oil-immersion objective and an EMCCD camera (Photometrics CoolSNAP HQ). Nuclear translocation was quantified with ImageJ software (National Institutes of Health) by calculating the nucleo-cytosolic ratio of EHD2 signal (nuclei masks were realized with the DAPI staining). TIRF images were acquired by TIRF video microscope (Nikon) equipped with a CFI Apo TIRF 100× NA 1.49 oil objective and an EMCCD camera (Photometrics HQ2). The quantification of surface Cav1 spots was realized by LabView as described in Sinha et al. (2011). In brief, caveolae were detected from TIRF images by first applying on the raw image a local intensity threshold of window size varying from 8 × 8 to 64 × 64 pixels, depending on the quality of the image. Pixels clustering together were detected as particles depending on their connectivity. Holes within particles, if any, were filled, connected particles were disconnected

by eroding boundaries, and finally particles were selected by size. For colocalization, images were analyzed with ImageJ and the JACoP plugin (Bolte and Cordelières, 2006). For live imaging, cells were maintained at 37°C and under 5% CO_2 throughout the acquisition.

Lattice light sheet microscopy (LLSM) imaging and intensity analysis

Cells expressing Cav1-HaloTag and EHD2-mEmerald were imaged using LLSM (Chen et al., 2014). Image volumes of Cav1-HaloTag– and EHD2-mEmerald–labeled cells were recorded every 2 s, using a 10-ms exposure in 30 mOsm hypo-osmotic environment for a total time of 5 min. All 3D datasets acquired were deskewed to account for the 31.8° angle of the detection objective (Nikon). After deskewing, deconvolution was performed using the Richardson–Lucy algorithm, and 4D visualization was performed using Vision 4D software (Arivis). Intensity analysis is based on a custom script written in Matlab, using Image Processing Toolbox. For the segmentation algorithm, nucleus and cell masks were defined based on Cav1 deconvolved images. The cell contour for each time point and z-plane was calculated using Otsu (Otsu, 1979) and Chan–Vese (Chan and Vese, 2001) algorithms implemented in Matlab Image Processing Toolbox. Similar analysis was performed to estimate the nucleus contour. Intensity for each time point was calculated by integrating the defined cell and nucleus area of the deskewed images for all planes of EHD2 labeling. The ratio between nucleus and whole-cell intensity was estimated for each time point and fitted to a sigmoid equation in Prism software.

PLA

The PLA kit was purchased from Sigma-Aldrich, and the assay was performed according to the manufacturer's protocol. Cells were fixed in 4% PFA for 10 min at room temperature, quenched in 50 mM NH_4Cl for 10 min, permeabilized with 0.2% Triton X-100 (wt/vol) for 10 min, and blocked in PBS/BSA. Cells were incubated with primary antibodies for 45 min in PBS/BSA. Coverslips were mounted in Fluoromount with DAPI to stain nuclei. PLA signals were visible as fluorescent dots and imaged using wide-field fluorescence inverted microscope Leica DM 6000B equipped with a HCX PL Apo 63× NA 1.32 oil-immersion objective and an EMCCD camera (Photometrics CoolSNAP HQ). Fluorescent dots were quantified using ImageJ. Cells and nuclei were delineated to create masks. After a maximum entropy threshold, the PLA dots were quantified in both masks with the ImageJ Analyze Particles plugin. Cytoplasmic and plasma membrane values were obtained by subtracting nuclear count from the cellular count. All counts were divided by the area in pixels.

qPCR

Cells were lysed using RNeasy Plus extraction kit from Qiagen at steady state or after 30 min of cyclic stretch. For hypo-osmotic shock experiments, cells were first exposed to 30 mOsm medium for 5 min, moved into iso-osmotic medium at 37°C during 1 h, and finally lysed using RNeasy Plus extraction kit. Reverse transcription reaction was performed with 1,000 ng total RNA per reaction using high-capacity cDNA reverse transcription kit (Applied Biosystems). qPCR was performed using 50 ng cDNA per 20-µl reaction. TaqMan Gene Expression Assays from Applied Biosystems were used: GAPDH (Hs02758991_g1), Cav1 (Hs00971716_m1), Cav2 (Hs00184597_m1), Cavin1 (Hs00396859_m1), Cavin2 (Hs00190538_m1), EHD2 (Hs00907482_m1), and Flot1 (Hs00195134_m1). Relative expression levels were calculated using ΔΔCT method with fold changes calculated as $2^{-\Delta\Delta CT}$. GAPDH served as the internal control.

DNA microarray

Total RNA was isolated using RNeasy Plus extraction kit after 30 min of cyclic stretch at 0.5 Hz. Gene expression profiling was performed using Affymetrix Human Gene ST 2.1 arrays. Cel files were preprocessed and annotated using the oligo and clariomshumanhttranscriptcluster.db packages. Normalization of expression across chips was performed using the RMA algorithm (rma() function from oligo package). No outlier was observed after visual inspection using the hist() and boxplot() functions. For each condition, the mean log2 fold change (logFC) compared with control was computed using the Limma R package. These logFC tables were then used to perform GSEA (Subramanian et al., 2005) with default parameters using the GSEA java application (v.2.2.1) and the gene set databases available on http://software.broadinstitute.org/gsea/msigdb/. Analysis was performed using the GseaPreranked tool. Enrichments were considered significant if the corresponding false discovery rate (FDR; BH correction) was lower than 5%. Data description, raw data files, and tables for logFC and FDR values have been deposited on http://microarrays.curie.fr/.

Force measurements

Plasma membrane tethers were extracted from cells with a bead (3 µm in diameter; Polysciences) coated with concanavalin A (Sigma-Aldrich) trapped in optical tweezers. The optical tweezers are made of a 1,064-nm laser beam (ytterbium fiber laser, λ = 1064 nm, TEM 00, 5 W; IPG Photonics) expanded and steered (optics by Elliot Scientific) in the back focal plane of the microscope objective (Apo-TIRF 100×, NA 1.45; Nikon). The whole setup was mounted on a Nikon Eclipse-Ti inverted microscope. The sample was illuminated by transmitted light, and videos were acquired at 10 Hz with an EMCCD camera (iXon 897; Andor) driven by Micro-Manager (Edelstein et al., 2014). The fine movements and particularly the translational movement necessary to pull the membrane tether were performed using a custom-made stage mounted on a piezoelectric element (P753; Physik Instrumente) driven by a servo controller (E665; Physik Instrumente) and a function generator (Tektronix AFG320; Sony).

Calibration was performed using an oscillatory modulation driven by a function generator (Tolić-Nørrelykke et al., 2006) and measuring the response of the bead to an oscillatory motion of the stage. We measured $k = 22P$ pN/(µm · W), where P is the laser power. This relationship is linear in the laser power range used for the experiments (0.5–2 W).

The membrane tether was held at constant length to measure the static force. For measuring membrane tension changes due to hypo-osmotic shock, the tether was held while the medium was diluted until the osmolarity reached 150 mOsm. For assessing the membrane tension change during recovery, medium osmolarity

was adjusted back to 300 mOsm with 10× MEM (GIBCO BRL Life Technologies). The medium changes were performed by slowly flowing in water or 10× MEM using a 2-ml surgical syringe. The position of the beads used to compute tether forces was detected from the images using a custom ImageJ macro.

EM

Cells were fixed at 37°C with 2% PFA in 0.1 M phosphate buffer. After several washes and quenching with glycine, cells were harvested in 10% gelatin, pelleted by mild centrifugation, and incubated on ice for 2 h. Afterward, pelleted cells were incubated overnight at 4°C in 2.3 M sucrose and mounted on nails in liquid nitrogen. 65-nm ultrathin cryosections were obtained using a Leica UCT ultracryomicrotome and collected on Cu/Pd-formvar-carbon–coated grids by picking up in a 1:1 mix of 2.3 M sucrose and methylcellulose. The sections were processed for immunogold labeling with an anti-Cav1 polyclonal antibody and Protein A conjugated to 10 nm gold (PAG10; https://www.cellbiology-utrecht.nl/) as reported previously (Sinha et al., 2011). After each labeling, grids were extensively washed with PBS and fixed again with 1% glutaraldehyde for 5 min at room temperature. Contrast was obtained by incubation with a 9:1 mix of methylcellulose and 4% uranyl acetate in water. Electron micrographs were acquired on a Tecnai Spirit electron microscope (FEI) equipped with a 4k CCD camera (EMSIS).

For unroofed metal replica EM, adherent plasma membranes from cultured cells grown on glass coverslips were disrupted by sonication as described previously (Heuser, 2000). Sample processing for platinum-replica EM of unroofed cells was performed as follows: glutaraldehyde/paraformaldehyde-fixed cells were further sequentially treated with osmium tetroxide, tannic acid, and uranyl acetate before ethanol dehydration and hexamethyldisilazane drying (Sigma-Aldrich). Dried samples were then rotary-shadowed with ∼2 nm platinum and 8 nm carbon. The resultant platinum replica was floated off the glass by angled immersion into hydrofluoric acid (5%), washed several times by flotation on distilled water, and picked up on 200-mesh formvar/carbon-coated EM grids. The grids were mounted in a eucentric side-entry goniometer stage of a transmission electron microscope operated at 80 kV (model CM120; Philips), replicas were viewed at ±10° tilt angles, and images were recorded with a Morada digital camera (Olympus). Images were processed in Adobe Photoshop to adjust brightness and contrast and presented in inverted contrast. Anaglyphs were made by converting the −10° tilt image to red and the +10° tilt image to cyan (blue/green), layering them on top of each other using the screen blending mode in Adobe Photoshop, and aligning them to each other.

Statistical analyses

All analyses were performed using GraphPad Prism v.6.0 and 7.0 for Windows (GraphPad Software). Two-tailed *t* test was used if comparing only two conditions. For comparing more than two conditions, one-way ANOVA was used with Bonferroni's multiple comparison test or Dunnett's multiple comparison test (if comparing all conditions to the control condition). Significance of mean comparison is marked on the graphs by asterisks. Error bars denote SEM or SD.

Online supplemental material

Fig. S1 shows imaging and quantification of EHD2 nuclear translocation under hypo-osmotic shock. Fig. S2 shows TIRF imaging and quantification of the dynamic colocalization of Cav1 and EHD2 during osmotic shock (A), EHD2-SUMO1 interaction by PLA (B), and EHD2-dependent gene regulation under hypo-osmotic conditions (C). Fig. S3 shows TIRF imaging and quantification of Cav1 spots after hypo-osmotic shock and recovery (A–C) and RNA silencing efficiency (D). Video 1 shows LLSM imaging EHD2 nuclear translocation under hypo-osmotic shock in a HeLa cell.

Acknowledgments

We thank Thierry Dubois for providing materials and expertise, Pierre Sens for analysis of membrane tension measurements, and Audrey Rapinat and David Gentien from the Genomics platform of the Institut Curie for the microarrays analysis. We are grateful to Michaël Trichet at the Electron Microscopy facility of the Institut de Biologie Paris-Seine (IBPS) for helpful advice and access to metal coaters.

The facilities as well as scientific and technical assistance from the PICT-IBiSA/Nikon Imaging Centre staff at Institut Curie-Centre National de la Recherche Scientifique and the France-BioImaging infrastructure (Agence Nationale de la Recherche [ANR], ANR-10-INSB-04) are acknowledged. LLSM was performed at the Advanced Imaging Center (AIC) at Howard Hughes Medical Institute Janelia Research Campus. The AIC is jointly supported by the Gordon and Betty Moore Foundation and Howard Hughes Medical Institute. The electron microscope facility was supported by the ANR through "Investments for the Future" program (France-BioImaging, ANR-10-INSB-04). This work was supported by institutional grants from the Institut Curie, Institut National de la Santé et de la Recherche Médicale, and Centre National de la Recherche Scientifique, and by specific grants from ANR (MECANOCAV, ANR-12-BSV2-0011; DECAV-RECAV, ANR-14-CE09-0008-03; and MOTICAV, ANR-17-CE-0013), Institut National du Cancer (INCa PLBIO12-203), Fondation de France, Marie Curie Actions—Networks for Initial Training (H2020-MSCA-ITN-2014), Association Française contre les Myopathies (15717 and 16754), and Program labellisé, Fondation ARC pour la Recherche sur le Cancer (PGA1 RF20170205456) to C. Lamaze, ANR (ANR-14-CE14-0002-02), Human Frontier Science Program (RGP0029-2014), and European Research Council (advanced grant 340485) to L. Johannes, ANR young researcher grant (EndoMechano ANR-14-CE12-0001-01) to S. Vassilopoulos. A. Grassart is supported by a Pasteur-Roux Fellowship. P. Pierobon is supported by grants from ANR (ANR-10-JCJC-1504-Immuphy) and PIC (Programme Incitatif et Collaboratif) Curie, "Cell polarity, division, growth and cancer." S. Torrino and W.-W. Shen were supported by a postdoctoral fellowship from Fondation ARC pour la Recherche sur le Cancer and Fondation de France, respectively. D. Köster and W.-W. Shen were supported by the Labex CelTisPhyBio Grants Program. The Johannes and Lamaze teams, the PICT-IBiSA/Nikon Imaging Centre at Institut Curie-Centre National de la Recherche Scientifique, and the France-BioImaging infrastructure are members of Labex CelTisPhyBio (ANR, ANR-

10-LBX-0038) and of Initiatives d'Excellence (IDEX) PSL (ANR, ANR-10-IDEX-0001-02 PSL).

The authors declare no competing financial interests.

Author contributions: S. Torrino and W.-W. Shen designed and performed the experiments, analyzed results and wrote the manuscript. C.M. Blouin, S.K. Mani, C. Viaris de Lesegno, P. Bost, D. Köst, C.A. Valades-Cruz, V. Chambon, and S. Vassilopoulos performed experiments or analysis. C.M. Blouin, A. Grassart, P. Pierobon, L. Johannes, V. Soumelis, C. Coirault, and S. Vassilopoulos provided technical support and conceptual advice. C. Lamaze supervised the project, designed experiments, and wrote the manuscript.

Submitted: 19 January 2018
Revised: 4 July 2018
Accepted: 27 September 2018

References

Ariotti, N., M.A. Fernández-Rojo, Y. Zhou, M.M. Hill, T.L. Rodkey, K.L. Inder, L.B. Tanner, M.R. Wenk, J.F. Hancock, and R.G. Parton. 2014. Caveolae regulate the nanoscale organization of the plasma membrane to remotely control Ras signaling. *J. Cell Biol.* 204:777–792. https://doi.org/10.1083/jcb.201307055

Bolte, S., and F.P. Cordelières. 2006. A guided tour into subcellular colocalization analysis in light microscopy. *J. Microsc.* 224:213–232. https://doi.org/10.1111/j.1365-2818.2006.01706.x

Chan, T.F., and L.A. Vese. 2001. Active contours without edges. *IEEE Trans. Image Process.* 10:266–277. https://doi.org/10.1109/83.902291

Chen, B.C., W.R. Legant, K. Wang, L. Shao, D.E. Milkie, M.W. Davidson, C. Janetopoulos, X.S. Wu, J.A. Hammer III, Z. Liu, et al. 2014. Lattice light-sheet microscopy: imaging molecules to embryos at high spatiotemporal resolution. *Science.* 346:1257998. https://doi.org/10.1126/science.1257998

Cheng, J.P., C. Mendoza-Topaz, G. Howard, J. Chadwick, E. Shvets, A.S. Cowburn, B.J. Dunmore, A. Crosby, N.W. Morrell, and B.J. Nichols. 2015. Caveolae protect endothelial cells from membrane rupture during increased cardiac output. *J. Cell Biol.* 211:53–61. https://doi.org/10.1083/jcb.201504042

DuFort, C.C., M.J. Paszek, and V.M. Weaver. 2011. Balancing forces: architectural control of mechanotransduction. *Nat. Rev. Mol. Cell Biol.* 12:308–319. https://doi.org/10.1038/nrm3112

Edelstein, A.D., M.A. Tsuchida, N. Amodaj, H. Pinkard, R.D. Vale, and N. Stuurman. 2014. Advanced methods of microscope control using μManager software. *J. Biol. Methods.* 1:e10. https://doi.org/10.14440/jbm.2014.36

Enserink, J.M. 2015. Sumo and the cellular stress response. *Cell Div.* 10:4. https://doi.org/10.1186/s13008-015-0010-1

Fernández-Sánchez, M.E., S. Barbier, J. Whitehead, G. Béalle, A. Michel, H. Latorre-Ossa, C. Rey, L. Fouassier, A. Claperon, L. Brullé, et al. 2015. Mechanical induction of the tumorigenic β-catenin pathway by tumour growth pressure. *Nature.* 523:92–95. https://doi.org/10.1038/nature14329

Gambin, Y., N. Ariotti, K.A. McMahon, M. Bastiani, E. Sierecki, O. Kovtun, M.E. Polinkovsky, A. Magenau, W. Jung, S. Okano, et al. 2013. Single-molecule analysis reveals self assembly and nanoscale segregation of two distinct cavin subcomplexes on caveolae. *eLife.* 3:e01434. https://doi.org/10.7554/eLife.01434

Garcia, J., J. Bagwell, B. Njaine, J. Norman, D.S. Levic, S. Wopat, S.E. Miller, X. Liu, J.W. Locasale, D.Y.R. Stainier, and M. Bagnat. 2017. Sheath cell invasion and trans-differentiation repair mechanical damage caused by loss of caveolae in the zebrafish notochord. *Curr. Biol.* 27:1982–1989.e3. https://doi.org/10.1016/j.cub.2017.05.035

Geiss-Friedlander, R., and F. Melchior. 2007. Concepts in sumoylation: a decade on. *Nat. Rev. Mol. Cell Biol.* 8:947–956. https://doi.org/10.1038/nrm2293

Gervásio, O.L., W.D. Phillips, L. Cole, and D.G. Allen. 2011. Caveolae respond to cell stretch and contribute to stretch-induced signaling. *J. Cell Sci.* 124:3581–3590. https://doi.org/10.1242/jcs.084376

Goetz, J.G., P. Lajoie, S.M. Wiseman, and I.R. Nabi. 2008. Caveolin-1 in tumor progression: the good, the bad and the ugly. *Cancer Metastasis Rev.* 27:715–735. https://doi.org/10.1007/s10555-008-9160-9

Heuser, J. 2000. The production of 'cell cortices' for light and electron microscopy. *Traffic.* 1:545–552. https://doi.org/10.1034/j.1600-0854.2000.010704.x

Hoernke, M., J. Mohan, E. Larsson, J. Blomberg, D. Kahra, S. Westenhoff, C. Schwieger, and R. Lundmark. 2017. EHD2 restrains dynamics of caveolae by an ATP-dependent, membrane-bound, open conformation. *Proc. Natl. Acad. Sci. USA.* 114:E4360–E4369. https://doi.org/10.1073/pnas.1614066114

Iskratsch, T., H. Wolfenson, and M.P. Sheetz. 2014. Appreciating force and shape—the rise of mechanotransduction in cell biology. *Nat. Rev. Mol. Cell Biol.* 15:825–833. https://doi.org/10.1038/nrm3903

Joshi, B., M. Bastiani, S.S. Strugnell, C. Boscher, R.G. Parton, and I.R. Nabi. 2012. Phosphocaveolin-1 is a mechanotransducer that induces caveola biogenesis via Egr1 transcriptional regulation. *J. Cell Biol.* 199:425–435. https://doi.org/10.1083/jcb.201207089

Kovtun, O., V.A. Tillu, W. Jung, N. Leneva, N. Ariotti, N. Chaudhary, R.A. Mandyam, C. Ferguson, G.P. Morgan, W.A. Johnston, et al. 2014. Structural insights into the organization of the cavin membrane coat complex. *Dev. Cell.* 31:405–419. https://doi.org/10.1016/j.devcel.2014.10.002

Lamaze, C., and S. Torrino. 2015. Caveolae and cancer: A new mechanical perspective. *Biomed. J.* 38:367–379. https://doi.org/10.4103/2319-4170.164229

Lamaze, C., N. Tardif, M. Dewulf, S. Vassilopoulos, and C.M. Blouin. 2017. The caveolae dress code: structure and signaling. *Curr. Opin. Cell Biol.* 47:117–125. https://doi.org/10.1016/j.ceb.2017.02.014

Li, M., X. Yang, J. Zhang, H. Shi, Q. Hang, X. Huang, G. Liu, J. Zhu, S. He, and H. Wang. 2013. Effects of EHD2 interference on migration of esophageal squamous cell carcinoma. *Med. Oncol.* 30:396. https://doi.org/10.1007/s12032-012-0396-4

Lim, Y.W., H.P. Lo, C. Ferguson, N. Martel, J. Giacomotto, G.A. Gomez, A.S. Yap, T.E. Hall, and R.G. Parton. 2017. Caveolae protect notochord cells against catastrophic mechanical failure during development. *Curr. Biol.* 27:1968–1981.e7. https://doi.org/10.1016/j.cub.2017.05.067

Liu, J., W. Ni, L. Qu, X. Cui, Z. Lin, Q. Liu, H. Zhou, and R. Ni. 2016. Decreased Expression of EHD2 Promotes Tumor Metastasis and Indicates Poor Prognosis in Hepatocellular Carcinoma. *Dig. Dis. Sci.* 61:2554–2567. https://doi.org/10.1007/s10620-016-4202-6

Lo, H.P., S.J. Nixon, T.E. Hall, B.S. Cowling, C. Ferguson, G.P. Morgan, N.L. Schieber, M.A. Fernandez-Rojo, M. Bastiani, M. Floetenmeyer, et al. 2015. The caveolin-cavin system plays a conserved and critical role in mechanoprotection of skeletal muscle. *J. Cell Biol.* 210:833–849. https://doi.org/10.1083/jcb.201501046

Ludwig, A., G. Howard, C. Mendoza-Topaz, T. Deerinck, M. Mackey, S. Sandin, M.H. Ellisman, and B.J. Nichols. 2013. Molecular composition and ultrastructure of the caveolar coat complex. *PLoS Biol.* 11:e1001640. https://doi.org/10.1371/journal.pbio.1001640

Morén, B., C. Shah, M.T. Howes, N.L. Schieber, H.T. McMahon, R.G. Parton, O. Daumke, and R. Lundmark. 2012. EHD2 regulates caveolar dynamics via ATP-driven targeting and oligomerization. *Mol. Biol. Cell.* 23:1316–1329. https://doi.org/10.1091/mbc.e11-09-0787

Nassar, Z.D., and M.O. Parat. 2015. Cavin Family: New Players in the Biology of Caveolae. *Int. Rev. Cell Mol. Biol.* 320:235–305. https://doi.org/10.1016/bs.ircmb.2015.07.009

Nassoy, P., and C. Lamaze. 2012. Stressing caveolae new role in cell mechanics. *Trends Cell Biol.* 22:381–389. https://doi.org/10.1016/j.tcb.2012.04.007

Otsu, N. 1979. Threshold Selection Method from Gray-Level Histograms. *IEEE Trans. Syst. Man Cybern.* 9:62–66. https://doi.org/10.1109/TSMC.1979.4310076

Palade, G.E. 1953. The fine structure of blood capillaries. *J. Appl. Phys.* 24:1424.

Pekar, O., S. Benjamin, H. Weidberg, S. Smaldone, F. Ramirez, and M. Horowitz. 2012. EHD2 shuttles to the nucleus and represses transcription. *Biochem. J.* 444:383–394. https://doi.org/10.1042/BJ20111268

Sheetz, M.P. 2001. Cell control by membrane-cytoskeleton adhesion. *Nat. Rev. Mol. Cell Biol.* 2:392–396. https://doi.org/10.1038/35073095

Shi, Y., X. Liu, Y. Sun, D. Wu, A. Qiu, H. Cheng, C. Wu, and X. Wang. 2015. Decreased expression and prognostic role of EHD2 in human breast carcinoma: correlation with E-cadherin. *J. Mol. Histol.* 46:221–231. https://doi.org/10.1007/s10735-015-9614-7

Sinha, B., D. Köster, R. Ruez, P. Gonnord, M. Bastiani, D. Abankwa, R.V. Stan, G. Butler-Browne, B. Vedie, L. Johannes, et al. 2011. Cells respond to mechanical stress by rapid disassembly of caveolae. *Cell.* 144:402–413. https://doi.org/10.1016/j.cell.2010.12.031

Söderberg, O., M. Gullberg, M. Jarvius, K. Ridderstråle, K.J. Leuchowius, J. Jarvius, K. Wester, P. Hydbring, F. Bahram, L.G. Larsson, and U. Landegren. 2006. Direct observation of individual endogenous protein complexes in situ by proximity ligation. *Nat. Methods.* 3:995–1000. https://doi.org/10.1038/nmeth947

Stoeber, M., I.K. Stoeck, C. Hänni, C.K. Bleck, G. Balistreri, and A. Helenius. 2012. Oligomers of the ATPase EHD2 confine caveolae to the plasma membrane through association with actin. *EMBO J.* 31:2350–2364. https://doi.org/10.1038/emboj.2012.98

Stoeber, M., P. Schellenberger, C.A. Siebert, C. Leyrat, A. Helenius, and K. Grünewald. 2016. Model for the architecture of caveolae based on a flexible, net-like assembly of Cavin1 and Caveolin discs. *Proc. Natl. Acad. Sci. USA.* 113:E8069–E8078. https://doi.org/10.1073/pnas.1616838113

Subramanian, A., P. Tamayo, V.K. Mootha, S. Mukherjee, B.L. Ebert, M.A. Gillette, A. Paulovich, S.L. Pomeroy, T.R. Golub, E.S. Lander, and J.P. Mesirov. 2005. Gene set enrichment analysis: a knowledge-based approach for interpreting genome-wide expression profiles. *Proc. Natl. Acad. Sci. USA.* 102:15545–15550. https://doi.org/10.1073/pnas.0506580102

Tolić-Nørrelykke, S.F., M.B. Rasmussen, F.S. Pavone, K. Berg-Sørensen, and L.B. Oddershede. 2006. Stepwise bending of DNA by a single TATA-box binding protein. *Biophys. J.* 90:3694–3703. https://doi.org/10.1529/biophysj.105.074856

Yamada, E. 1955. The fine structure of the gall bladder epithelium of the mouse. *J. Biophys. Biochem. Cytol.* 1:445–458. https://doi.org/10.1083/jcb.1.5.445

Yang, X., H. Ren, L. Yao, X. Chen, and A. He. 2015. Role of EHD2 in migration and invasion of human breast cancer cells. *Tumour Biol.* 36:3717–3726. https://doi.org/10.1007/s13277-014-3011-9

Yeow, I., G. Howard, J. Chadwick, C. Mendoza-Topaz, C.G. Hansen, B.J. Nichols, and E. Shvets. 2017. EHD Proteins Cooperate to Generate Caveolar Clusters and to Maintain Caveolae during Repeated Mechanical Stress. *Curr. Biol.* 27:2951–2962.e5. https://doi.org/10.1016/j.cub.2017.07.047

REFERENCES:

Aboulaich, N., Vainonen, J. P., Strålfors, P., & Vener, A. V. (2004). Vectorial proteomics reveal targeting, phosphorylation and specific fragmentation of polymerase I and transcript release factor (PTRF) at the surface of caveolae in human adipocytes. *Biochemical Journal*, *383*(2), 237-248.

Aboulaich, N., Chui, P. C., Asara, J. M., Flier, J. S., & Maratos-Flier, E. (2011). Polymerase I and transcript release factor regulates lipolysis via a phosphorylation-dependent mechanism. *Diabetes*, *60*(3), 757-765.

Ainsworth, C. (2008). Cell biology: Stretching the imagination. *Nature News*, *456*(7223), 696-699.

Akabayov SR, Biron Z, Lamken P, Piehler J, Anglister J. NMR mapping of the IFNAR1-EC binding site on IFNalpha2 reveals allosteric changes in the IFNAR2-EC binding site. Biochemistry. 2010 Feb 2;49(4):687-95.

Al-Shali, K. Z., & Hegele, R. A. (2004). Laminopathies and atherosclerosis. *Arteriosclerosis, thrombosis, and vascular biology*, *24*(9), 1591-1595.

Altschuler, L., Wook, J. O., Gurari, D., Chebath, J., & Revel, M. (1999). Involvement of receptor-bound protein methyltransferase PRMT1 in antiviral and antiproliferative effects of type I interferons. *Journal of interferon & cytokine research*, *19*(2), 189-195.

Anderson, R. G. (1991). Molecular motors that shape endocytic. *Intracellular trafficking of proteins*, *5*, 13.

Andreone, B. J., Chow, B. W., Tata, A., Lacoste, B., Ben-Zvi, A., Bullock, K., ... & Gu, C. (2017). Blood-brain barrier permeability is regulated by lipid transport-dependent suppression of caveolae-mediated transcytosis. *Neuron*, *94*(3), 581-594.

Alessandri, K., B.R. Sarangi, V.V. Gurchenkov, B. Sinha, T.R. Kiessling, L. Fetler, F. Rico, S. Scheuring, C. Lamaze, A. Simon, S. Geraldo, D. Vignjevic, H. Domejean, L. Rolland, A. Funfak, J. Bibette, N. Bremond, and P. Nassoy. 2013. Cellular capsules as a tool for multicellular spheroid production and for investigating the mechanics of tumor progression in vitro. *Proc Natl Acad Sci U S A*. 110 :14843-14848.

Alspach, E., Lussier, D. M., & Schreiber, R. D. (2019). Interferon γ and its important roles in promoting and inhibiting spontaneous and therapeutic cancer immunity. *Cold Spring Harbor perspectives in biology*, *11*(3), a028480.

Aoki, S., & Epand, R. M. (2012). Caveolin-1 hydrophobic segment peptides insertion into membrane mimetic systems: role of proline residue. *Biochimica et Biophysica Acta (BBA)-Biomembranes*, *1818*(1), 12-18.

Ariotti, N., Fernández-Rojo, M. A., Zhou, Y., Hill, M. M., Rodkey, T. L., Inder, K. L., ... & Parton, R. G. (2014). Caveolae regulate the nanoscale organization of the plasma membrane to remotely control Ras signaling. *Journal of Cell Biology*, *204*(5), 777-792.

Ariotti, N., Rae, J., Leneva, N., Ferguson, C., Loo, D., Okano, S., ... & Parton, R. G. (2015). Molecular characterization of caveolin-induced membrane curvature. *Journal of Biological Chemistry*, *290*(41), 24875-24890.

Arora, T., Liu, B., He, H., Kim, J., Murphy, T. L., Murphy, K. M., ... & Shuai, K. (2003). PIASx is a transcriptional co-repressor of signal transducer and activator of transcription 4. *Journal of Biological Chemistry*, *278*(24), 21327-21330.

Babon, J. J., Lucet, I. S., Murphy, J. M., Nicola, N. A., & Varghese, L. N. (2014). The molecular regulation of Janus kinase (JAK) activation. *Biochemical Journal*, *462*(1), 1-13.

Bach, E. A., Aguet, M., & Schreiber, R. D. (1997). The IFNγ receptor: a paradigm for cytokine receptor signaling. *Annual review of immunology*, *15*(1), 563-591.

Bae, C., Gottlieb, P. A., & Sachs, F. (2013). Human PIEZO1: removing inactivation. *Biophysical journal*, *105*(4), 880-886.

Bai, X., Yang, X., Jia, X., Rong, Y., Chen, L., Zeng, T., ... & Jin, S. (2020). CAV1-CAVIN1-LC3B-mediated autophagy regulates high glucose-stimulated LDL transcytosis. Autophagy, 16(6), 1111-1129.

Barry, S. P., Davidson, S. M., & Townsend, P. A. (2008). Molecular regulation of cardiac hypertrophy. *The international journal of biochemistry & cell biology*, *40*(10), 2023-2039.

Bastiani, M., Liu, L., Hill, M. M., Jedrychowski, M. P., Nixon, S. J., Lo, H. P., ... & Parton, R. G. (2009). MURC/Cavin-4 and cavin family members form tissue-specific caveolar complexes. *Journal of Cell Biology*, *185*(7), 1259-1273.

Bates, I. R., Wiseman, P. W., & Hanrahan, J. W. (2006). Investigating membrane protein dynamics in living cells. Biochemistry and cell biology, 84(6), 825-831.

Bendayan, M., & Rasio, E. A. (1996). Transport of insulin and albumin by the microvascular endothelium of the rete mirabile. *Journal of Cell Science*, *109*(7), 1857-1864.

Behrmann, I., Smyczek, T., Heinrich, P. C., Schmitz-Van de Leur, H., Komyod, W., Giese, B., ... & Haan, C. (2004). Janus kinase (Jak) subcellular localization revisited: the exclusive membrane localization of endogenous Janus kinase 1 by cytokine receptor interaction uncovers the Jak· receptor complex to be equivalent to a receptor tyrosine kinase. *Journal of Biological Chemistry*, *279*(34), 35486-35493.

Bernatchez P. Endothelial caveolin and its scaffolding domain in cancer. Cancer Metastasis Rev. 2020 Jun;39(2):471-483.

Betz, R. C., Schoser, B. G., Kasper, D., Ricker, K., Ramírez, A., Stein, V., ... & Kubisch, C. (2001). Mutations in CAV3 cause mechanical hyperirritability of skeletal muscle in rippling muscle disease. *Nature genetics*, *28*(3), 218-219.

Betzig, E., Patterson, G. H., Sougrat, R., Lindwasser, O. W., Olenych, S., Bonifacino, J. S., ... & Hess, H. F. (2006). Imaging intracellular fluorescent proteins at nanometer resolution. Science, 313(5793), 1642-1645.

Bonilla, E., Fischbeck, K., & Schotland, D. L. (1981). Freeze-fracture studies of muscle caveolae in human muscular dystrophy. *The American journal of pathology*, *104*(2), 167.

Bousoik E, Montazeri Aliabadi H. "Do We Know Jack" About JAK? A Closer Look at JAK/STAT Signaling Pathway. Front Oncol. 2018 Jul 31; 8:287.

Breen, M. R., Camps, M., Carvalho-Simoes, F., Zorzano, A., & Pilch, P. F. (2012). Cholesterol depletion in adipocytes causes caveolae collapse concomitant with proteosomal degradation of cavin-2 in a switch-like fashion. *PloS one*, *7*(4), e34516.

Bretscher, M. S., & Whytock, S. (1977). Membrane-associated vesicles in fibroblasts. *Journal of ultrastructure research*, *61*(2), 215-217.

Bruns, R. R., & Palade, G. E. (1968). Studies on blood capillaries: I. General organization of blood capillaries in muscle. *The Journal of cell biology*, *37*(2), 244-276.

Bruns, R. R., & Palade, G. E. (1968). Studies on blood capillaries: II. Transport of ferritin molecules across the wall of muscle capillaries. *The Journal of cell biology*, *37*(2), 277-299.

Brugnera, E., Haney, L., Grimsley, C., Lu, M., Walk, S. F., Tosello-Trampont, A. C., ... & Ravichandran, K. S. (2002). Unconventional Rac-GEF activity is mediated through the Dock180–ELMO complex. *Nature cell biology*, *4*(8), 574-582.

Bugaj, L. J., Choksi, A. T., Mesuda, C. K., Kane, R. S. & Schaffer, D. V. Optogenetic protein clustering and signaling activation in mammalian cells. Nature Methods 10, 249–252 (2013)

Burgener, R., Wolf, M., Ganz, T., & Baggiolini, M. (1990). Purification and characterization of a major phosphatidylserine-binding phosphoprotein from human platelets. *Biochemical Journal*, *269*(3), 729-734.

Burridge, K., & Wennerberg, K. (2004). Rho and Rac take center stage. *Cell*, *116*(2), 167-179.

Burridge K, Guilluy C. Focal adhesions, stress fibers and mechanical tension. Exp Cell Res. 2016 Apr 10;343(1):14-20. doi: 10.1016/j.yexcr.2015.10.029. Epub 2015 Oct 28.

Bursac, P., Fabry, B., Trepat, X., Lenormand, G., Butler, J. P., Wang, N., ... & An, S. S. (2007). Cytoskeleton dynamics: fluctuations within the network. *Biochemical and biophysical research communications*, *355*(2), 324-330.

Busija AR, Patel HH, Insel PA. Caveolins and cavins in the trafficking, maturation, and degradation of caveolae: implications for cell physiology. Am J Physiol Cell Physiol. 2017 Apr 1;312(4):C459-C477.

Byrne, D. P., Dart, C., & Rigden, D. J. (2012). Evaluating caveolin interactions: do proteins interact with the caveolin scaffolding domain through a widespread aromatic residue-rich motif?

Capell, B. C., Collins, F. S., & Nabel, E. G. (2007). Mechanisms of cardiovascular disease in accelerated aging syndromes. *Circulation Research*, *101*(1), 13-26.

Carman, C. V., Lisanti, M. P., & Benovic, J. L. (1999). Regulation of G protein-coupled receptor kinases by caveolin. *Journal of Biological Chemistry*, *274*(13), 8858-8864.

Carozzi, A. J., Ikonen, E., Lindsay, M. R., & Parton, R. G. (2000). Role of cholesterol in developing T-tubules: analogous mechanisms for T-tubule and caveolae biogenesis. *Traffic*, *1*(4), 326-341.

Chaudhary, N., Gomez, G. A., Howes, M. T., Lo, H. P., McMahon, K. A., Rae, J. A., ... & Parton, R. G. (2014). Endocytic crosstalk: cavins, caveolins, and caveolae regulate clathrin-independent endocytosis. *PLoS biology*, *12*(4), e1001832.

Chen, C. S., Mrksich, M., Huang, S., Whitesides, G. M., & Ingber, D. E. (1997). Geometric control of cell life and death. *Science*, *276*(5317), 1425-1428.

Chen, M., Cheng, A., Candotti, F., Zhou, Y. J., Hymel, A., Fasth, A., ... & O'Shea, J. J. (2000). Complex effects of naturally occurring mutations in the JAK3 pseudokinase domain: evidence for interactions between the kinase and pseudokinase domains. *Molecular and Cellular Biology*, *20*(3), 947-956.

Chen, Y., Wen, R., Yang, S., Schuman, J., Zhang, E. E., Yi, T., ... & Wang, D. (2003). Identification of Shp-2 as a Stat5A phosphatase. *Journal of Biological Chemistry*, *278*(19), 16520-16527.

Chen, W., Daines, M. O., & Hershey, G. K. K. (2004). Turning off signal transducer and activator of transcription (STAT): the negative regulation of STAT signaling. *Journal of Allergy and Clinical Immunology*, *114*(3), 476-489.

Chen, J., Baig, E., & Fish, E. N. (2004). Diversity and relatedness among the type I interferons. *Journal of interferon & cytokine research*, *24*(12), 687-698.

Chen, C. S. (2008). Mechanotransduction–a field pulling together? *Journal of cell science*, *121*(20), 3285-3292.

Chen, Z. H., Lam, H. C., Jin, Y., Kim, H. P., Cao, J., Lee, S. J., ... & Choi, A. M. (2010). Autophagy protein microtubule-associated protein 1 light chain-3B (LC3B) activates extrinsic apoptosis during cigarette smoke-induced emphysema. *Proceedings of the National Academy of Sciences*, *107*(44), 18880-18885.

Cheng, J. P., Mendoza-Topaz, C., Howard, G., Chadwick, J., Shvets, E., Cowburn, A. S., ... & Nichols, B. J. (2015). Caveolae protect endothelial cells from membrane rupture during increased cardiac output. *Journal of Cell Biology*, *211*(1), 53-61.

Chill, J. H., Quadt, S. R., Levy, R., Schreiber, G., & Anglister, J. (2003). The human type I interferon receptor: NMR structure reveals the molecular basis of ligand binding. *Structure*, *11*(7), 791-802.

Cho, H. J., Park, J. H., Nam, J. H., Chang, Y. C., Park, B., & Hoe, H. S. (2018). Ascochlorin suppresses MMP-2-mediated migration and invasion by targeting FAK and JAK-STAT signaling cascades. *Journal of cellular biochemistry*, *119*(1), 300-313.

Chung, C. D., Liao, J., Liu, B., Rao, X., Jay, P., Berta, P., & Shuai, K. (1997). Specific inhibition of Stat3 signal transduction by PIAS3. *Science*, *278*(5344), 1803-1805.

Claflin, D. R., & Brooks, S. V. (2008). Direct observation of failing fibers in muscles of dystrophic mice provides mechanistic insight into muscular dystrophy. *American Journal of Physiology-Cell Physiology*, *294*(2), C651-C658.

Clark, E. A., Golub, T. R., Lander, E. S., & Hynes, R. O. (2000). Genomic analysis of metastasis reveals an essential role for RhoC. *Nature*, *406*(6795), 532-535.

Collins, B. M., Davis, M. J., Hancock, J. F., & Parton, R. G. (2012). Structure-based reassessment of the caveolin signaling model: do caveolae regulate signaling through caveolin-protein interactions? *Developmental cell*, *23*(1), 11-20.

Coste B, Mathur J, Schmidt M, Earley TJ, Ranade S, Petrus MJ, Dubin AE, Patapoutian A. Piezo1 and Piezo2 are essential components of distinct mechanically activated cation channels. Science. 2010 Oct 1;330(6000):55-60.

Coste B, Xiao B, Santos JS, Syeda R, Grandl J, Spencer KS, Kim SE, Schmidt M, Mathur J, Dubin AE, Montal M, Patapoutian A. Piezo proteins are pore-forming subunits of mechanically activated channels. Nature. 2012 Feb 19;483(7388):176-81.

Couet, J., Shengwen, L., Okamoto, T., Scherer, P. E., & Lisanti, M. P. (1997). Molecular and cellular biology of caveolae: paradoxes and plasticities. *Trends in cardiovascular medicine*, *7*(4), 103-110.

Cross, S. E., Jin, Y. S., Rao, J., & Gimzewski, J. K. (2007). Nanomechanical analysis of cells from cancer patients. *Nature nanotechnology*, *2*(12), 780-783.

Darnell, J. E., Kerr, I. M., & Stark, G. R. (1994). Jak-STAT pathways and transcriptional activation in response to IFNs and other extracellular signaling proteins. *Science*, *264*(5164), 1415-1421.

Daumke, O., Lundmark, R., Vallis, Y., Martens, S., Butler, P. J. G., & McMahon, H. T. (2007). Architectural and mechanistic insights into an EHD ATPase involved in membrane remodelling. *Nature*, *449*(7164), 923-927.

Deb, D. K., Sassano, A., Lekmine, F., Majchrzak, B., Verma, A., Kambhampati, S., ... & Platanias, L. C. (2003). Activation of protein kinase Cδ by IFN-γ. *The Journal of Immunology*, *171*(1), 267-273.

Decker, T., & Kovarik, P. (2000). Serine phosphorylation of STATs. Oncogene, 19(21), 2628-2637.

Deville SS, Cordes N. The Extracellular, Cellular, and Nuclear Stiffness, a Trinity in the Cancer Resistome-A Review. Front Oncol. 2019 Dec 6;9:1376.

Dietzen, D. J., Hastings, W. R., & Lublin, D. M. (1995). Caveolin Is Palmitoylated on Multiple Cysteine Residues: Palmitoylation is not necessary for localization of caveolin to caveolae. *Journal of Biological Chemistry*, *270*(12), 6838-6842.

Doherty, G. J., & McMahon, H. T. (2009). Mechanisms of endocytosis. Annual review of biochemistry, 78, 857-902.

Drab, M., Verkade, P., Elger, M., Kasper, M., Lohn, M., Lauterbach, B., ... & Kurzchalia, T. V. (2001). Loss of caveolae, vascular dysfunction, and pulmonary defects in caveolin-1 gene-disrupted mice. *Science*, *293*(5539), 2449-2452.

Dulhunty, A. F., & Franzini-Armstrong, C. (1975). The relative contributions of the folds and caveolae to the surface membrane of frog skeletal muscle fibres at different sarcomere lengths. *The Journal of physiology*, *250*(3), 513-539.

Dupree, P., Parton, R. G., Raposo, G., Kurzchalia, T. V., & Simons, K. (1993). Caveolae and sorting in the trans-Golgi network of epithelial cells. *The EMBO journal*, *12*(4), 1597-1605.

Ealick, S. E., Cook, W. J., Vijay-Kumar, S., Carson, M., Nagabhushan, T. L., Trotta, P. P., & Bugg, C. E. (1991). Three-dimensional structure of recombinant human interferon-gamma. *Science*, *252*(5006), 698-702.

Echarri, A., Pavón, D. M., Sánchez, S., García-García, M., Calvo, E., Huerta-López, C., ... & Del Pozo, M. A. (2019). An Abl-FBP17 mechanosensing system couples local plasma membrane curvature and stress fiber remodeling during mechanoadaptation. Nature communications, 10(1), 1-16.

Elliott, M. H., Ashpole, N. E., Gu, X., Herrnberger, L., McClellan, M. E., Griffith, G. L., ... & Stamer, W. D. (2016). Caveolin-1 modulates intraocular pressure: implications for caveolae mechanoprotection in glaucoma. *Scientific reports*, *6*(1), 1-12.

Engelman, J. A., Zhang, X. L., & Lisanti, M. P. (1998). Genes encoding human caveolin-1 and-2 are co-localized to the D7S522 locus (7q31. 1), a known fragile site (FRA7G) that is frequently deleted in human cancers. *FEBS letters*, *436*(3), 403-410.

Enyedi, P., & Czirják, G. (2010). Molecular background of leak K+ currents: two-pore domain potassium channels. *Physiological reviews*, *90*(2), 559-605.

Fairn, G. D., Schieber, N. L., Ariotti, N., Murphy, S., Kuerschner, L., Webb, R. I., ... & Parton, R. G. (2011). High-resolution mapping reveals topologically distinct cellular pools of phosphatidylserine. Journal of Cell Biology, 194(2), 257-275.

Fernandez, I., Ying, Y., Albanesi, J., & Anderson, R. G. (2002). Mechanism of caveolin filament assembly. *Proceedings of the National Academy of Sciences*, *99*(17), 11193-11198.

Fernandez, A., Bautista, M., Stanciauskas, R., Chung, T., & Pinaud, F. (2017). Cell-shaping micropatterns for quantitative super-resolution microscopy imaging of membrane mechanosensing proteins. ACS applied materials & interfaces, 9(33), 27575-27586.

Fernández-Pérez, L., Borja-Guerra, C., Diaz-Chico, J. C., & Flores-Morales, A. (2013). Estrogens regulate the hepatic effects of growth hormone, a hormonal interplay with multiple fates. *Frontiers in endocrinology*, *4*, 66.

Fiala GJ, Minguet S. Caveolin-1: The Unnoticed Player in TCR and BCR Signaling. Adv Immunol. 2018;137:83-133.

Firmbach-Kraft, I., Byers, M., Shows, T., Dalla-Favera, R., & Krolewski, J. J. (1990). tyk2, prototype of a novel class of non-receptor tyrosine kinase genes. *Oncogene*, *5*(9), 1329-1336.

Fiucci, G., Ravid, D., Reich, R., & Liscovitch, M. (2002). Caveolin-1 inhibits anchorage-independent growth, anoikis and invasiveness in MCF-7 human breast cancer cells. *Oncogene*, *21*(15), 2365-2375.

Forbes, M. S., Rennels, M. L., & Nelson, E. (1979). Caveolar systems and sarcoplasmic reticulum in coronary smooth muscle cells of the mouse. *Journal of ultrastructure research*, *67*(3), 325-339.

Fra, A. M., Williamson, E., Simons, K., & Parton, R. G. (1994). Detergent-insoluble glycolipid microdomains in lymphocytes in the absence of caveolae. *Journal of Biological Chemistry*, *269*(49), 30745-30748.

Fra, A. M., Williamson, E., Simons, K., & Parton, R. G. (1995). De novo formation of caveolae in lymphocytes by expression of VIP21-caveolin. *Proceedings of the National Academy of Sciences*, *92*(19), 8655-8659.

Fujita, A., Cheng, J., Tauchi-Sato, K., Takenawa, T., & Fujimoto, T. (2009). A distinct pool of phosphatidylinositol 4, 5-bisphosphate in caveolae revealed by a nanoscale labeling technique. *Proceedings of the National Academy of Sciences*, *106*(23), 9256-9261.

Gabella G, Blundell D. Effect of stretch and contraction on caveolae of smooth muscle cells. Cell Tissue Res. 1978 Jul 5;190(2):255-71.

Gabor, K. A., Stevens, C. R., Pietraszewski, M. J., Gould, T. J., Shim, J., Yoder, J. A., ... & Kim, C. H. (2013). Super resolution microscopy reveals that caveolin-1 is required for spatial organization of CRFB1 and subsequent antiviral signaling in zebrafish. PloS one, 8(7), e68759.

Gadina, M., Chisolm, D. A., Philips, R. L., McInness, I. B., Changelian, P. S., & O'Shea, J. J. (2020). Translating JAKs to jakinibs. The Journal of Immunology, 204(8), 2011-2020.

Galbiati, F., Volonté, D., Minetti, C., Chu, J. B., & Lisanti, M. P. (1999). Phenotypic behavior of caveolin-3 mutations that cause autosomal dominant limb girdle muscular dystrophy (LGMD-1C): retention of LGMD-1C caveolin-3 mutants within the Golgi complex. *Journal of Biological Chemistry*, *274*(36), 25632-25641.

Galbiati, F., Volonté, D., Minetti, C., Bregman, D. B., & Lisanti, M. P. (2000). Limb-girdle muscular dystrophy (LGMD-1C) mutants of caveolin-3 undergo ubiquitination and proteasomal degradation: treatment with proteasomal inhibitors blocks the dominant negative effect of LGMD-1C mutants and rescues wild-type caveolin-3. *Journal of Biological Chemistry*, *275*(48), 37702-37711.

Galbiati, F., Razani, B., & Lisanti, M. P. (2001). Emerging themes in lipid rafts and caveolae. *Cell*, *106*(4), 403-411.

Gambin, Y., Ariotti, N., McMahon, K. A., Bastiani, M., Sierecki, E., Kovtun, O., ... & Parton, R. G. (2014). Single-molecule analysis reveals self assembly and nanoscale segregation of two distinct cavin subcomplexes on caveolae. *elife*, *3*, e01434.

García-Cardeña, G., Martasek, P., Masters, B. S. S., Skidd, P. M., Couet, J., Li, S., ... & Sessa, W. C. (1997). Dissecting the interaction between nitric oxide synthase (NOS) and caveolin: Functional significance of the NOS caveolin binding domainin vivo. *Journal of Biological Chemistry*, *272*(41), 25437-25440.

Garcia-Parajo MF, Cambi A, Torreno-Pina JA, Thompson N, Jacobson K. Nanoclustering as a dominant feature of plasma membrane organization. J Cell Sci. 2014 Dec 1;127(Pt 23):4995-5005.

Gardel, M. L., Shin, J. H., MacKintosh, F. C., Mahadevan, L., Matsudaira, P., & Weitz, D. A. (2004). Elastic behavior of cross-linked and bundled actin networks. *Science*, *304*(5675), 1301-1305.

Gaus, K., Le Lay, S., Balasubramanian, N., & Schwartz, M. A. (2006). Integrin-mediated adhesion regulates membrane order. *The Journal of cell biology*, *174*(5), 725-734.

Gehler, S., Baldassarre, M., Lad, Y., Leight, J. L., Wozniak, M. A., Riching, K. M., ... & Keely, P. J. (2009). Filamin A–β1 integrin complex tunes epithelial cell response to matrix tension. *Molecular biology of the cell*, *20*(14), 3224-3238.

Geiger, B., Spatz, J. P., & Bershadsky, A. D. (2009). Environmental sensing through focal adhesions. *Nature reviews Molecular cell biology*, *10*(1), 21-33.

Geiger, B., & Yamada, K. M. (2011). Molecular architecture and function of matrix adhesions. *Cold Spring Harbor perspectives in biology*, *3*(5), a005033.

Ghitescu, L., Fixman, A., Simionescu, M., & Simionescu, N. (1986). Specific binding sites for albumin restricted to plasmalemmal vesicles of continuous capillary endothelium: receptor-mediated transcytosis. *The Journal of cell biology*, *102*(4), 1304-1311.

Ghoreschi K, Laurence A, O'Shea JJ. Janus kinases in immune cell signaling. Immunol Rev. 2009 Mar;228(1):273-87.

Giancotti, F. G., & Ruoslahti, E. (1999). Integrin signaling. *science*, *285*(5430), 1028-1033.

Glenney, J. R. (1989). Tyrosine phosphorylation of a 22-kDa protein is correlated with transformation by Rous sarcoma virus. *Journal of Biological Chemistry*, *264*(34), 20163-20166.

Glenney Jr, J. R. (1992). The sequence of human caveolin reveals identity with VIP21, a component of transport vesicles. *FEBS letters*, *314*(1), 45-48.

Glogauer, M., Arora, P., Chou, D., Janmey, P. A., Downey, G. P., & McCulloch, C. A. (1998). The role of actin-binding protein 280 in integrin-dependent mechanoprotection. *Journal of Biological Chemistry*, *273*(3), 1689-1698.

Gough, D. J., Levy, D. E., Johnstone, R. W., & Clarke, C. J. (2008). IFNγ signaling—Does it mean JAK–STAT? *Cytokine & growth factor reviews*, *19*(5-6), 383-394.

Greenberg MJ, Arpağ G, Tüzel E, Ostap EM. A Perspective on the Role of Myosins as Mechanosensors. Biophys J. 2016 Jun 21;110(12):2568-2576.

Greenhalgh, C. J., & Hilton, D. J. (2001). Negative regulation of cytokine signaling. *Journal of leukocyte biology*, *70*(3), 348-356.

Griffoni, C., Spisni, E., Santi, S., Riccio, M., Guarnieri, T., & Tomasi, V. (2000). Knockdown of caveolin-1 by antisense oligonucleotides impairs angiogenesis in vitro and in vivo. *Biochemical and biophysical research communications*, *276*(2), 756-761.

Guck, J., Schinkinger, S., Lincoln, B., Wottawah, F., Ebert, S., Romeyke, M., ... & Bilby, C. (2005). Optical deformability as an inherent cell marker for testing malignant transformation and metastatic competence. *Biophysical journal*, *88*(5), 3689-3698.

Gustavsson, A., Yuan, M., & Fällman, M. (2004). Temporal dissection of β1-integrin signaling indicates a role for p130Cas-Crk in filopodia formation. *Journal of Biological Chemistry*, *279*(22), 22893-22901.

Gustincich, S., & Schneider, C. (1993). Serum deprivation response gene is induced by serum starvation but not by contact inhibition. *Cell growth and differentiation*, *4*, 753-753.

Gustincich, S., Vatta, P., Goruppi, S., Wolf, M., Saccone, S., Della Valle, G., ... & Schneider, C. (1999). The humanserum deprivation responsegene (sdpr) maps to 2q32–q33 and codes for a phosphatidylserine-binding protein. *Genomics*, *57*(1), 120-129.

Hailstones, D., Sleer, L. S., Parton, R. G., & Stanley, K. K. (1998). Regulation of caveolin and caveolae by cholesterol in MDCK cells. *Journal of lipid research*, *39*(2), 369-379.

Hale, C. M., Sun, S. X., & Wirtz, D. (2009). Resolving the role of actoymyosin contractility in cell microrheology. *PloS one*, *4*(9), e7054.

Hanahan D, Weinberg RA. Hallmarks of cancer: the next generation. Cell. 2011 Mar 4;144(5):646-74.

Hansen CG, Bright NA, Howard G, Nichols BJ. SDPR induces membrane curvature and functions in the formation of caveolae. Nat Cell Biol. 2009 Jul;11(7):807-14.

Hansen, C. G., Howard, G., & Nichols, B. J. (2011). Pacsin 2 is recruited to caveolae and functions in caveolar biogenesis. *Journal of cell science*, *124*(16), 2777-2785.

Hansen, C. G., Shvets, E., Howard, G., Riento, K., & Nichols, B. J. (2013). Deletion of cavin genes reveals tissue-specific mechanisms for morphogenesis of endothelial caveolae. *Nature communications*, *4*(1), 1-13.

Hassan, G. S., Jasmin, J. F., Schubert, W., Frank, P. G., & Lisanti, M. P. (2004). Caveolin-1 deficiency stimulates neointima formation during vascular injury. *Biochemistry*, *43*(26), 8312-8321.

Hayashi, K., Matsuda, S., Machida, K., Yamamoto, T., Fukuda, Y., Nimura, Y., ... & Hamaguchi, M. (2001). Invasion activating caveolin-1 mutation in human scirrhous breast cancers. *Cancer research*, *61*(6), 2361-2364.

Hayer, A., Stoeber, M., Bissig, C., & Helenius, A. (2010). Biogenesis of caveolae: stepwise assembly of large caveolin and cavin complexes. *Traffic*, *11*(3), 361-382.

Heilemann, M., Van De Linde, S., Schüttpelz, M., Kasper, R., Seefeldt, B., Mukherjee, A., ... & Sauer, M. (2008). Subdiffraction-resolution fluorescence imaging with conventional fluorescent probes. Angewandte Chemie International Edition, 47(33), 6172-6176.

Heineke, J., & Molkentin, J. D. (2006). Regulation of cardiac hypertrophy by intracellular signalling pathways. *Nature reviews Molecular cell biology*, *7*(8), 589-600.

Hell, S. W., and Jan Wichmann. "Breaking the diffraction resolution limit by stimulated emission: stimulated-emission-depletion fluorescence microscopy." Optics letters 19.11 (1994): 780-782.

Hell, S. W. (2005). Fluorescence nanoscopy: breaking the diffraction barrier by the RESOLFT concept. In 2005 IEEE LEOS Annual Meeting Conference Proceedings (p. 42). IEEE.

Hell, S. W., Sahl, S. J., Bates, M., Zhuang, X., Heintzmann, R., Booth, M. J., ... & Cordes, T. (2015). The 2015 super-resolution microscopy roadmap. Journal of Physics D: Applied Physics, 48(44), 443001.

Heltianu, C., Dobrila, L., Antohe, F., & Simionescu, M. (1989). Evidence for thyroxine transport by the lung and heart capillary endothelium. *Microvascular research*, *37*(2), 188-203.

Henley, J. R., Krueger, E. W., Oswald, B. J., & McNiven, M. A. (1998). Dynamin-mediated internalization of caveolae. *The Journal of cell biology*, *141*(1), 85-99.

Hertzog, M., Monteiro, P., Le Dez, G., & Chavrier, P. (2012). Exo70 subunit of the exocyst complex is involved in adhesion-dependent trafficking of caveolin-1. PloS one, 7(12), e52627.

Hervy, M., Hoffman, L., & Beckerle, M. C. (2006). From the membrane to the nucleus and back again: bifunctional focal adhesion proteins. *Current opinion in cell biology*, *18*(5), 524-532.

Hess, S. T., Girirajan, T. P., & Mason, M. D. (2006). Ultra-high resolution imaging by fluorescence photoactivation localization microscopy. Biophysical journal, 91(11), 4258-4272.

Heydemann, A., Doherty, K. R., & McNally, E. M. (2007). Genetic modifiers of muscular dystrophy: implications for therapy. *Biochimica et Biophysica Acta (BBA)-Molecular Basis of Disease*, *1772*(2), 216-228.

Hill, M. M., Bastiani, M., Luetterforst, R., Kirkham, M., Kirkham, A., Nixon, S. J., ... & Parton, R. G. (2008). PTRF-Cavin, a conserved cytoplasmic protein required for caveola formation and function. *Cell*, *132*(1), 113-124.

Hilton, D. J., Richardson, R. T., Alexander, W. S., Viney, E. M., Willson, T. A., Sprigg, N. S., ... & Nicola, N. A. (1998). Twenty proteins containing a C-terminal SOCS box form five structural classes. *Proceedings of the National Academy of Sciences*, *95*(1), 114-119.

Hilton, D. J. (1999). Negative regulators of cytokine signal transduction. *Cellular and Molecular Life Sciences CMLS*, *55*(12), 1568-1577.

Hirama, T., Das, R., Yang, Y., Ferguson, C., Won, A., Yip, C. M., ... & Fairn, G. D. (2017). Phosphatidylserine dictates the assembly and dynamics of caveolae in the plasma membrane. *Journal of Biological Chemistry*, *292*(34), 14292-14307.

Hirama, T., Lu, S. M., Kay, J. G., Maekawa, M., Kozlov, M. M., Grinstein, S., & Fairn, G. D. (2017). Membrane curvature induced by proximity of anionic phospholipids can initiate endocytosis. Nature communications, 8(1), 1-14.

Hoernke, M., Mohan, J., Larsson, E., Blomberg, J., Kahra, D., Westenhoff, S., ... & Lundmark, R. (2017). EHD2 restrains dynamics of caveolae by an ATP-dependent, membrane-bound, open conformation. Proceedings of the National Academy of Sciences, 114(22), E4360-E4369.

Hoffman, E. P., & Kunkel, L. M. (1989). Dystrophin abnormalities in Duchenne/Becker muscular dystrophy. *Neuron*, *2*(1), 1019-1029.

Hofmann, S. R., Lam, A. Q., Frank, S., Zhou, Y. J., Ramos, H. L., Kanno, Y., ... & O'Shea, J. J. (2004). Jak3-independent trafficking of the common γ chain receptor subunit: chaperone function of Jaks revisited. *Molecular and cellular biology*, *24*(11), 5039-5049.

Hoffmann, C., Berking, A., Agerer, F., Buntru, A., Neske, F., Chhatwal, G. S., ... & Hauck, C. R. (2010). Caveolin limits membrane microdomain mobility and integrin-mediated uptake of fibronectin-binding pathogens. *Journal of cell science*, *123*(24), 4280-4291.

Hoop, C. L., Sivanandam, V. N., Kodali, R., Srnec, M. N., & van der Wel, P. C. (2012). Structural characterization of the caveolin scaffolding domain in association with cholesterol-rich membranes. Biochemistry, 51(1), 90-99.

Honoré, E. (2007). The neuronal background K 2P channels: focus on TREK1. *Nature reviews neuroscience*, *8*(4), 251-261.

Horiuchi, H., Kawamata, H., Fujimori, T., & Kuroda, Y. (2003). A MEK inhibitor (U0126) prolongs survival in nude mice bearing human gallbladder cancer cells with K-ras mutation: analysis in a novel orthotopic inoculation model. *International journal of oncology*, *23*(4), 957-963.

Hoshijima, M. (2006). Mechanical stress-strain sensors embedded in cardiac cytoskeleton: Z disk, titin, and associated structures. *American Journal of Physiology-Heart and Circulatory Physiology*, *290*(4), H1313-H1325.

Hove, J. R., Köster, R. W., Forouhar, A. S., Acevedo-Bolton, G., Fraser, S. E., & Gharib, M. (2003). Intracardiac fluid forces are an essential epigenetic factor for embryonic cardiogenesis. *Nature*, *421*(6919), 172-177.

Hu, P., & Luo, B. H. (2013). Integrin bi-directional signaling across the plasma membrane. *Journal of cellular physiology*, *228*(2), 306-312.

Hu Y, Chen M, Wang M, Li X. Flow-mediated vasodilation through mechanosensitive G protein-coupled receptors in endothelial cells. Trends Cardiovasc Med. 2021 Jan 3:S1050-1738(21)00001-3.

Huang, S., & Ingber, D. E. (1999). The structural and mechanical complexity of cell-growth control. *Nature cell biology*, *1*(5), E131-E138.

Huang, S., & Ingber, D. E. (2005). Cell tension, matrix mechanics, and cancer development. *Cancer cell*, *8*(3), 175-176.

Hülsmann, B. B., Labokha, A. A., & Görlich, D. (2012). The permeability of reconstituted nuclear pores provides direct evidence for the selective phase model. *Cell*, *150*(4), 738-751.

Igaz, P., Toth, S., & Falus, A. (2001). Biological and clinical significance of the JAK-STAT pathway; lessons from knockout mice. *Inflammation Research*, *50*(9), 435-441.

Ihle, J. N., & Kerr, I. M. (1995). Jaks and Stats in signaling by the cytokine receptor superfamily. *Trends in Genetics*, *11*(2), 69-74.

Ikonen, E., & Parton, R. G. (2000). Caveolins and cellular cholesterol balance. *Traffic*, *1*(3), 212-217.

Ingber, D. E. (1993). Cellular tensegrity: defining new rules of biological design that govern the cytoskeleton. *Journal of cell science*, *104*(3), 613-627.

Ingber, D. E. (2003). Tensegrity II. How structural networks influence cellular information processing networks. *Journal of cell science*, *116*(8), 1397-1408.

Irie-Sasaki, J., Sasaki, T., Matsumoto, W., Opavsky, A., Cheng, M., Welstead, G., ... & Penninger, J. M. (2001). CD45 is a JAK phosphatase and negatively regulates cytokine receptor signalling. *Nature*, *409*(6818), 349-354.

Isaacs, A., & Lindenmann, J. (1957). Virus interference. I. The interferon. *Proceedings of the Royal Society of London. Series B-Biological Sciences*, *147*(927), 258-267.

Isaacs, A., Lindenmann, J., & Valentine, R. C. (1957). Virus interference. II. Some properties of interferon. *Proceedings of the Royal Society of London. Series B-Biological Sciences*, *147*(927), 268-273.

Itoh, T., Erdmann, K. S., Roux, A., Habermann, B., Werner, H., & De Camilli, P. (2005). Dynamin and the actin cytoskeleton cooperatively regulate plasma membrane invagination by BAR and F-BAR proteins. *Developmental cell*, *9*(6), 791-804.

Ivashkiv, L. B. (2018). IFNγ: signalling, epigenetics and roles in immunity, metabolism, disease and cancer immunotherapy. *Nature Reviews Immunology*, *18*(9), 545-558.

Izumi, T., Shibata, Y., & Yamamoto, T. (1989). The cytoplasmic surface structures of uncoated vesicles in various tissues of rat as revealed by quick-freeze, deep-etching replicas. *Microscopy*, *38*(1), 47-53.

Izumi, Y., Hirai, S. I., Tamai, Y., Fujise-Matsuoka, A., Nishimura, Y., & Ohno, S. (1997). A protein kinase Cδ-binding protein SRBC whose expression is induced by serum starvation. *Journal of Biological Chemistry*, *272*(11), 7381-7389.

Jansa, P., Mason, S. W., Hoffmann-Rohrer, U., & Grummt, I. (1998). Cloning and functional characterization of PTRF, a novel protein which induces dissociation of paused ternary transcription complexes. *The EMBO journal*, *17*(10), 2855-2864.

Jasmin, J. F., Mercier, I., Sotgia, F., & Lisanti, M. P. (2006). SOCS proteins and caveolin-1 as negative regulators of endocrine signaling. Trends in Endocrinology & Metabolism, 17(4), 150-158.

Jones, C. J., Kuo, L., Davis, M. J., & Chilian, W. M. (1995). Regulation of coronary blood flow: coordination of heterogeneous control mechanisms in vascular microdomains. *Cardiovascular research*, *29*(5), 585-596.

Jones, B. C., Logsdon, N. J., & Walter, M. R. (2008). Structure of IL-22 bound to its high-affinity IL-22R1 chain. *Structure*, *16*(9), 1333-1344.

Ju, H., Zou, R., Venema, V. J., & Venema, R. C. (1997). Direct interaction of endothelial nitric-oxide synthase and caveolin-1 inhibits synthase activity. *Journal of Biological Chemistry*, *272*(30), 18522-18525.

Kamura, T., Sato, S., Haque, D., Liu, L., Kaelin, W. G., Conaway, R. C., & Conaway, J. W. (1998). The Elongin BC complex interacts with the conserved SOCS-box motif present in members of the SOCS, ras, WD-40 repeat, and ankyrin repeat families. *Genes & development*, *12*(24), 3872-3881.

Karpusas, M., Nolte, M., Benton, C. B., Meier, W., Lipscomb, W. N., & Goelz, S. (1997). The crystal structure of human interferon β at 2.2-Å resolution. *Proceedings of the National Academy of Sciences*, *94*(22), 11813-11818.

Kennedy, M. J. et al. Rapid blue-light-mediated induction of protein interactions in living cells. Nature Methods 7, 973–975 (2010).

Kim, T. K., & Maniatis, T. (1996). Regulation of interferon-γ-activated STAT1 by the ubiquitin-proteasome pathway. *Science*, *273*(5282), 1717-1719.

Kim, C. A., Delépine, M., Boutet, E., El Mourabit, H., Le Lay, S., Meier, M., ... & Magré, J. (2008). Association of a homozygous nonsense caveolin-1 mutation with Berardinelli-Seip congenital lipodystrophy. *The Journal of Clinical Endocrinology & Metabolism*, *93*(4), 1129-1134.

Kim, J. H., Schlebach, J. P., Lu, Z., Peng, D., Reasoner, K. C., & Sanders, C. R. (2016). A pH-mediated topological switch within the N-terminal domain of human caveolin-3. *Biophysical journal*, *110*(11), 2475-2485.

Kirkham, M., Nixon, S. J., Howes, M. T., Abi-Rached, L., Wakeham, D. E., Hanzal-Bayer, M., ... & Parton, R. G. (2008). Evolutionary analysis and molecular dissection of caveola biogenesis. *Journal of cell science*, *121*(12), 2075-2086.

Kisseleva, T., Bhattacharya, S., Braunstein, J., & Schindler, C. W. (2002). Signaling through the JAK/STAT pathway, recent advances and future challenges. *Gene*, *285*(1-2), 1-24.

Khan, S., & Sheetz, M. P. (1997). Force effects on biochemical kinetics. *Annual review of biochemistry*, *66*(1), 785-805.

Khater, I. M., Meng, F., Wong, T. H., Nabi, I. R., & Hamarneh, G. (2018). Super resolution network analysis defines the molecular architecture of caveolae and caveolin-1 scaffolds. Scientific reports, 8(1), 1-15.

Khater, I. M., Liu, Q., Chou, K. C., Hamarneh, G., & Nabi, I. R. (2019). Super-resolution modularity analysis shows polyhedral caveolin-1 oligomers combine to form scaffolds and caveolae. Scientific reports, 9(1), 1-10.

Kile, B. T., Schulman, B. A., Alexander, W. S., Nicola, N. A., Martin, H. M., & Hilton, D. J. (2002). The SOCS box: a tale of destruction and degradation. *Trends in biochemical sciences*, *27*(5), 235-241.

Klingmüller, U., Lorenz, U., Cantley, L. C., Neel, B. G., & Lodish, H. F. (1995). Specific recruitment of SH-PTP1 to the erythropoietin receptor causes inactivation of JAK2 and termination of proliferative signals. *Cell*, *80*(5), 729-738.

Koch D, Westermann M, Kessels MM, Qualmann B. Ultrastructural freeze-fracture immunolabeling identifies plasma membrane-localized syndapin II as a crucial factor in shaping caveolae. Histochem Cell Biol. 2012 Aug;138(2):215-30.

Koenderink, G. H., Dogic, Z., Nakamura, F., Bendix, P. M., MacKintosh, F. C., Hartwig, J. H., ... & Weitz, D. A. (2009). An active biopolymer network controlled by molecular motors. *Proceedings of the National Academy of Sciences*, *106*(36), 15192-15197.

Kolluru, G. K., Siamwala, J. H., & Chatterjee, S. (2010). eNOS phosphorylation in health and disease. *Biochimie*, *92*(9), 1186-1198.

Kontzias, A., Kotlyar, A., Laurence, A., Changelian, P., & O'Shea, J. J. (2012). Jakinibs: a new class of kinase inhibitors in cancer and autoimmune disease. Current opinion in pharmacology, 12(4), 464-470.

Kotenko, S. V., Gallagher, G., Baurin, V. V., Lewis-Antes, A., Shen, M., Shah, N. K., ... & Donnelly, R. P. (2003). IFN-λs mediate antiviral protection through a distinct class II cytokine receptor complex. *Nature immunology*, *4*(1), 69-77.

Kovtun, O., Tillu, V. A., Jung, W., Leneva, N., Ariotti, N., Chaudhary, N., ... & Collins, B. M. (2014). Structural insights into the organization of the cavin membrane coat complex. *Developmental cell*, *31*(4), 405-419.

Kovtun O, Tillu VA, Ariotti N, Parton RG, Collins BM. Cavin family proteins and the assembly of caveolae. J Cell Sci. 2015 Apr 1;128(7):1269-78.

Kristof, A. S., Marks-Konczalik, J., Billings, E., & Moss, J. (2003). Stimulation of signal transducer and activator of transcription-1 (STAT1)-dependent gene transcription by lipopolysaccharide and interferon-

γ is regulated by mammalian target of rapamycin. *Journal of Biological Chemistry*, *278*(36), 33637-33644.

Kuipers, A. J., Middelbeek, J., & van Leeuwen, F. N. (2012). Mechanoregulation of cytoskeletal dynamics by TRP channels. *European journal of cell biology*, *91*(11-12), 834-846.

Kumar, A., & Boriek, A. M. (2003). Mechanical stress activates the nuclear factor-kappaB pathway in skeletal muscle fibers: a possible role in Duchenne muscular dystrophy. *The FASEB Journal*, *17*(3), 386-396.

Krieg, M., Arboleda-Estudillo, Y., Puech, P. H., Käfer, J., Graner, F., Müller, D. J., & Heisenberg, C. P. (2008). Tensile forces govern germ-layer organization in zebrafish. *Nature cell biology*, *10*(4), 429-436.

Kwon, H., Lee, J., Jeong, K., Jang, D., & Pak, Y. (2015). Fatty acylated caveolin-2 is a substrate of insulin receptor tyrosine kinase for insulin receptor substrate-1-directed signaling activation. *Biochimica et Biophysica Acta (BBA)-Molecular Cell Research*, *1853*(5), 1022-1034.

LaFave, L. M., & Levine, R. L. (2012). JAK2 the future: therapeutic strategies for JAK-dependent malignancies. *Trends in pharmacological sciences*, *33*(11), 574-582.

Lahtinen, U., Honsho, M., Parton, R. G., Simons, K., & Verkade, P. (2003). Involvement of caveolin-2 in caveolar biogenesis in MDCK cells. *FEBS letters*, *538*(1-3), 85-88.

Lamaze, C., Tardif, N., Dewulf, M., Vassilopoulos, S., & Blouin, C. M. (2017). The caveolae dress code: structure and signaling. *Current opinion in cell biology*, *47*, 117-125.

Lamaze, C., & Blouin, C. M. (2013). Interferon gamma receptor: the beginning of the journey. Frontiers in immunology, 4, 267.

Lammerding, J., Schulze, P. C., Takahashi, T., Kozlov, S., Sullivan, T., Kamm, R. D., ... & Lee, R. T. (2004). Lamin A/C deficiency causes defective nuclear mechanics and mechanotransduction. *The Journal of clinical investigation*, *113*(3), 370-378.

Landar, A., Curry, B., Parker, M. H., DiGiacomo, R., Indelicato, S. R., Nagabhushan, T. L., ... & Walter, M. R. (2000). Design, characterization, and structure of a biologically active single-chain mutant of human IFN-γ. *Journal of molecular biology*, *299*(1), 169-179.

Le, P. U., Guay, G., Altschuler, Y., & Nabi, I. R. (2002). Caveolin-1 is a negative regulator of caveolae-mediated endocytosis to the endoplasmic reticulum. *Journal of Biological Chemistry*, *277*(5), 3371-3379.

Lecuit, T., & Lenne, P. F. (2007). Cell surface mechanics and the control of cell shape, tissue patterns and morphogenesis. *Nature reviews Molecular cell biology*, *8*(8), 633-644.

Lee, H., Volonte', D., Galbiati, F., Iyengar, P., Lublin, D. M., Bregman, D. B., ... & Lisanti, M. P. (2000). Constitutive and growth factor-regulated phosphorylation of caveolin-1 occurs at the same site (Tyr-14) in vivo: identification of a c-Src/Cav-1/Grb7 signaling cassette. *Molecular Endocrinology*, *14*(11), 1750-1775.

Lee, J., & Glover, K. J. (2012). The transmembrane domain of caveolin-1 exhibits a helix–break–helix structure. *Biochimica et Biophysica Acta (BBA)-Biomembranes*, *1818*(5), 1158-1164.

Lelek, M., Gyparaki, M.T., Beliu, G. et al. Single-molecule localization microscopy. Nat Rev Methods Primers 1, 39 (2021).

Levy, D. E., & Lee, C. K. (2002). What does Stat3 do? *The Journal of clinical investigation*, *109*(9), 1143-1148.

Liao, J., Fu, Y., & Shuai, K. (2000). Distinct roles of the NH2-and COOH-terminal domains of the protein inhibitor of activated signal transducer and activator of transcription (STAT) 1 (PIAS1) in cytokine-induced PIAS1–Stat1 interaction. *Proceedings of the National Academy of Sciences*, *97*(10), 5267-5272.

Li, S., Lisanti, M. P., & Seitz, R. (1996). Phosphorylation of Caveolin by Src Tyrosine Kinases: The α-isoform of caveolin is selectively phosphorylated by v-Src in vivo. *Journal of Biological Chemistry*, *271*(7), 3863-3868.

Li, Z., Strunk, J. J., Lamken, P., Piehler, J., & Walz, T. (2008). The EM structure of a type I interferon–receptor complex reveals a novel mechanism for cytokine signaling. *Journal of molecular biology*, *377*(3), 715-724.

Li J, Hou B, Tumova S, Muraki K, Bruns A, Ludlow MJ, Sedo A, Hyman AJ, McKeown L, Young RS, Yuldasheva NY, Majeed Y, Wilson LA, Rode B, Bailey MA, Kim HR, Fu Z, Carter DA, Bilton J, Imrie H, Ajuh P, Dear TN, Cubbon RM, Kearney MT, Prasad RK, Evans PC, Ainscough JF, Beech DJ. Piezo1 integration of vascular architecture with physiological force. Nature. 2014 Nov 13;515(7526):279-282.

Lipardi, C., Mora, R., Colomer, V., Paladino, S., Nitsch, L., Rodriguez-Boulan, E., & Zurzolo, C. (1998). Caveolin transfection results in caveolae formation but not apical sorting of glycosylphosphatidylinositol (GPI)-anchored proteins in epithelial cells. *The Journal of cell biology*, *140*(3), 617-626.

Lisanti, M. P., Scherer, P. E., Tang, Z., & Sargiacomo, M. (1994). Caveolae, caveolin and caveolin-rich membrane domains: a signalling hypothesis. *Trends in cell biology*, *4*(7), 231-235.

Liu, B., Liao, J., Rao, X., Kushner, S. A., Chung, C. D., Chang, D. D., & Shuai, K. (1998). Inhibition of Stat1-mediated gene activation by PIAS1. *Proceedings of the National Academy of Sciences*, *95*(18), 10626-10631.

Liu, B., Gross, M., ten Hoeve, J., & Shuai, K. (2001). A transcriptional corepressor of Stat1 with an essential LXXLL signature motif. *Proceedings of the National Academy of Sciences*, *98*(6), 3203-3207.

Liu, J., Wang, X. B., Park, D. S., & Lisanti, M. P. (2002). Caveolin-1 expression enhances endothelial capillary tubule formation. *Journal of Biological Chemistry*, *277*(12), 10661-10668.

Liu, L., Brown, D., McKee, M., LeBrasseur, N. K., Yang, D., Albrecht, K. H., ... & Pilch, P. F. (2008). Deletion of Cavin/PTRF causes global loss of caveolae, dyslipidemia, and glucose intolerance. *Cell metabolism*, *8*(4), 310-317.

Liu L, Pilch PF. A critical role of cavin (polymerase I and transcript release factor) in caveolae formation and organization. J Biol Chem. 2008 Feb 15;283(7):4314-22.

Liu, L., & Pilch, P. F. (2016). PTRF/Cavin-1 promotes efficient ribosomal RNA transcription in response to metabolic challenges. *Elife*, *5*, e17508.

Liu Q, Tucker CL. Engineering genetically-encoded tools for optogenetic control of protein activity. Curr Opin Chem Biol. 2017 Oct;40:17-23.

Liu J, Ni W, Qu L, Cui X, Lin Z, Liu Q, Zhou H, Ni R. Decreased Expression of EHD2 Promotes Tumor Metastasis and Indicates Poor Prognosis in Hepatocellular Carcinoma. Dig Dis Sci. 2016 Sep;61(9):2554-67.

Lo, H. P., Hall, T. E., & Parton, R. G. (2016). Mechanoprotection by skeletal muscle caveolae. *Bioarchitecture*, *6*(1), 22-27.

Loufrani, L., Dubroca, C., You, D., Li, Z., Levy, B., Paulin, D., & Henrion, D. (2004). Absence of dystrophin in mice reduces NO-dependent vascular function and vascular density: total recovery after a treatment with the aminoglycoside gentamicin. *Arteriosclerosis, thrombosis, and vascular biology*, *24*(4), 671-676.

Lozano, J., Xing, R., Cai, Z., Jensen, H. L., Trempus, C., Mark, W., ... & Kolesnick, R. (2003). Deficiency of kinase suppressor of Ras1 prevents oncogenic ras signaling in mice. *Cancer research*, *63*(14), 4232-4238.

Ludwig, A., Howard, G., Mendoza-Topaz, C., Deerinck, T., Mackey, M., Sandin, S., ... & Nichols, B. J. (2013). Molecular composition and ultrastructure of the caveolar coat complex. *PLoS biology*, *11*(8), e1001640.

Machleidt, T., Li, W. P., Liu, P., & Anderson, R. G. (2000). Multiple domains in caveolin-1 control its intracellular traffic. *The Journal of cell biology*, *148*(1), 17-28.

Maksimovic S, Nakatani M, Baba Y, Nelson AM, Marshall KL, Wellnitz SA, Firozi P, Woo SH, Ranade S, Patapoutian A, Lumpkin EA. Epidermal Merkel cells are mechanosensory cells that tune mammalian touch receptors. Nature. 2014 May 29;509(7502):617-21.

Manning, G., Whyte, D. B., Martinez, R., Hunter, T., & Sudarsanam, S. (2002). The protein kinase complement of the human genome. *Science*, *298*(5600), 1912-1934.

Martinez-Outschoorn, U.E., F. Sotgia, and M.P. Lisanti. 2015. Caveolae and signalling in cancer. *Nature reviews. Cancer*. 15:225-237.

Mas, P., Devlin, P. F., Panda, S. & Kay, S. A. Functional interaction of phytochrome B and cryptochrome 2. Nature 408, 207–211 (2000).

Matsuda, C., Hayashi, Y. K., Ogawa, M., Aoki, M., Murayama, K., Nishino, I., ... & Jr, R. H. B. (2001). The sarcolemmal proteins dysferlin and caveolin-3 interact in skeletal muscle. *Human molecular genetics*, *10*(17), 1761-1766.

Matthews, B. D., Overby, D. R., Mannix, R., & Ingber, D. E. (2006). Cellular adaptation to mechanical stress: role of integrins, Rho, cytoskeletal tension and mechanosensitive ion channels. *Journal of cell science*, *119*(3), 508-518.

Mazzoccoli, G., Carughi, S., De Cata, A., Giuliani, A., Masciale, N., La Viola, M., ... & Balzanelli, M. (2003). Interstitial lung diseases. *Recenti progressi in medicina*, *94*(5), 227-237.

McBride, K. M., McDonald, C., & Reich, N. C. (2000). Nuclear export signal located within the DNA-binding domain of the STAT1transcription factor. *The EMBO journal*, *19*(22), 6196-6206.

McMahon, H. T., & Boucrot, E. (2015). Membrane curvature at a glance. Journal of cell science, 128(6), 1065-1070.

McMullen JR, Jennings GL. Differences between pathological and physiological cardiac hypertrophy: novel therapeutic strategies to treat heart failure. Clin Exp Pharmacol Physiol. 2007 Apr;34(4):255-62.

McNally, E. M., de Sá Moreira, E., Duggan, D. J., Bönnemann, C. G., Lisanti, M. P., Lidov, H. G., ... & Kunkel, L. M. (1998). Caveolin-3 in muscular dystrophy. *Human molecular genetics*, *7*(5), 871-877.

Mederos y Schnitzler, M., Storch, U., Meibers, S., Nurwakagari, P., Breit, A., Essin, K., ... & Gudermann, T. (2008). Gq-coupled receptors as mechanosensors mediating myogenic vasoconstriction. *The EMBO journal*, *27*(23), 3092-3103.

Mendoza, J. L., Escalante, N. K., Jude, K. M., Bellon, J. S., Su, L., Horton, T. M., ... & Garcia, K. C. (2019). Structure of the IFNγ receptor complex guides design of biased agonists. *Nature*, *567*(7746), 56-60.

Mertens, C., Zhong, M., Krishnaraj, R., Zou, W., Chen, X., & Darnell, J. E. (2006). Dephosphorylation of phosphotyrosine on STAT1 dimers requires extensive spatial reorientation of the monomers facilitated by the N-terminal domain. *Genes & development*, *20*(24), 3372-3381.

Messal HA, Alt S, Ferreira RMM, Gribben C, Wang VM, Cotoi CG, Salbreux G, Behrens A. Tissue curvature and apicobasal mechanical tension imbalance instruct cancer morphogenesis. Nature. 2019 Feb;566(7742):126-130.

Meyer, T., Marg, A., Lemke, P., Wiesner, B., & Vinkemeier, U. (2003). DNA binding controls inactivation and nuclear accumulation of the transcription factor Stat1. *Genes & development*, *17*(16), 1992-2005.

Michel, J. B., Feron, O., Sase, K., Prabhakar, P., & Michel, T. (1997). Caveolin versus calmodulin: counterbalancing allosteric modulators of endothelial nitric oxide synthase. *Journal of Biological Chemistry*, *272*(41), 25907-25912.

Mierke CT. The matrix environmental and cell mechanical properties regulate cell migration and contribute to the invasive phenotype of cancer cells. Rep Prog Phys. 2019 Jun;82(6):064602.

Minetti, C., Bado, M., Broda, P., Sotgia, F., Bruno, C., Galbiati, F., ... & Cordone, G. (2002). Impairment of caveolae formation and T-system disorganization in human muscular dystrophy with caveolin-3 deficiency. *The American journal of pathology*, *160*(1), 265-270.

Mir, K. D., Parr, R. D., Schroeder, F., & Ball, J. M. (2007). Rotavirus NSP4 interacts with both the amino- and carboxyl-termini of caveolin-1. *Virus research*, *126*(1-2), 106-115.

Mirkovic, K., Palmersheim, J., Lesage, F., & Wickman, K. (2012). Behavioral characterization of mice lacking Trek channels. *Frontiers in behavioral neuroscience*, *6*, 60.

Miyamoto T, Mochizuki T, Nakagomi H, Kira S, Watanabe M, Takayama Y, Suzuki Y, Koizumi S, Takeda M, Tominaga M. Functional role for Piezo1 in stretch-evoked Ca^{2+} influx and ATP release in urothelial cell cultures. J Biol Chem. 2014 Jun 6;289(23):16565-75.

Modregger, J., Ritter, B., Witter, B., Paulsson, M., & Plomann, M. (2000). All three PACSIN isoforms bind to endocytic proteins and inhibit endocytosis. *Journal of cell science*, *113*(24), 4511-4521.

Monier, S., Parton, R. G., Vogel, F., Behlke, J., Henske, A., & Kurzchalia, T. V. (1995). VIP21-caveolin, a membrane protein constituent of the caveolar coat, oligomerizes in vivo and in vitro. *Molecular biology of the cell*, *6*(7), 911-927.

Montesano, R., Roth, J., Robert, A., & Orci, L. (1982). Non-coated membrane invaginations are involved in binding and internalization of cholera and tetanus toxins. *Nature*, *296*(5858), 651-653.

Moore, K. A., Polte, T., Huang, S., Shi, B., Alsberg, E., Sunday, M. E., & Ingber, D. E. (2005). Control of basement membrane remodeling and epithelial branching morphogenesis in embryonic lung by Rho and cytoskeletal tension. *Developmental dynamics: an official publication of the American Association of Anatomists*, *232*(2), 268-281.

Morén, B., Shah, C., Howes, M. T., Schieber, N. L., McMahon, H. T., Parton, R. G., ... & Lundmark, R. (2012). EHD2 regulates caveolar dynamics via ATP-driven targeting and oligomerization. *Molecular biology of the cell*, *23*(7), 1316-1329.

Morris R, Kershaw NJ, Babon JJ. The molecular details of cytokine signaling via the JAK/STAT pathway. Protein Sci. 2018;27(12):1984-2009. doi:10.1002/pro.3519

Motta-Mena, L. B. et al. An optogenetic gene expression system with rapid activation and deactivation kinetics. Nature Chem. Biol. 10, 196–202 (2014).

Mowen, K. A., Tang, J., Zhu, W., Schurter, B. T., Shuai, K., Herschman, H. R., & David, M. (2001). Arginine methylation of STAT1 modulates IFNα/β-induced transcription. *Cell*, *104*(5), 731-741.

Muhammad, H., Rais, Y., Miosge, N., & Ornan, E. M. (2012). The primary cilium as a dual sensor of mechanochemical signals in chondrocytes. *Cellular and Molecular Life Sciences*, *69*(13), 2101-2107.

Mundy, D. I., Machleidt, T., Ying, Y. S., Anderson, R. G., & Bloom, G. S. (2002). Dual control of caveolar membrane traffic by microtubules and the actin cytoskeleton. *Journal of cell science*, *115*(22), 4327-4339.

Murata, M., Peränen, J., Schreiner, R., Wieland, F., Kurzchalia, T. V., & Simons, K. A. I. (1995). VIP21/caveolin is a cholesterol-binding protein. *Proceedings of the National Academy of Sciences*, *92*(22), 10339-10343.

Muriel, O., Echarri, A., Hellriegel, C., Pavón, D. M., Beccari, L., & Del Pozo, M. A. (2011). Phosphorylated filamin A regulates actin-linked caveolae dynamics. Journal of cell science, 124(16), 2763-2776.

Myers, M. P., Andersen, J. N., Cheng, A., Tremblay, M. L., Horvath, C. M., Parisien, J. P., ... & Tonks, N. K. (2001). TYK2 and JAK2 are substrates of protein-tyrosine phosphatase 1B. *Journal of Biological Chemistry*, *276*(51), 47771-47774.

Nagel G, Ollig D, Fuhrmann M, Kateriya S, Musti AM, Bamberg E, Hegemann P. Channelrhodopsin-1: a light-gated proton channel in green algae. Science. 2002 Jun 28;296(5577):2395-8.

Nagel G, Szellas T, Huhn W, Kateriya S, Adeishvili N, Berthold P, Ollig D, Hegemann P, Bamberg E. Channelrhodopsin-2, a directly light-gated cation-selective membrane channel. Proc Natl Acad Sci U S A. 2003 Nov 25;100(24):13940-5.

Nakamura, F., Osborn, T. M., Hartemink, C. A., Hartwig, J. H., & Stossel, T. P. (2007). Structural basis of filamin A functions. *The Journal of cell biology*, *179*(5), 1011-1025.

Nakamura, F., Stossel, T. P., & Hartwig, J. H. (2011). The filamins: organizers of cell structure and function. *Cell adhesion & migration*, *5*(2), 160-169.

Nassoy, P., & Lamaze, C. (2012). Stressing caveolae new role in cell mechanics. *Trends in cell biology*, *22*(7), 381-389.

Neel, B. G. (1993, December). Structure and function of SH2-domain containing tyrosine phosphatases. In *Seminars in cell biology* (Vol. 4, No. 6, pp. 419-432). Academic Press.

Nelson, C. M., & Chen, C. S. (2003). VE-cadherin simultaneously stimulates and inhibits cell proliferation by altering cytoskeletal structure and tension. *Journal of cell science*, *116*(17), 3571-3581.

Neophytou CM, Panagi M, Stylianopoulos T, Papageorgis P. The Role of Tumor Microenvironment in Cancer Metastasis: Molecular Mechanisms and Therapeutic Opportunities. Cancers (Basel). 2021 Apr 23;13(9):2053.

Nguyen, A. M., & Jacobs, C. R. (2013). Emerging role of primary cilia as mechanosensors in osteocytes. *Bone*, *54*(2), 196-204.

Nicholson, S. E., Willson, T. A., Farley, A., Starr, R., Zhang, J. G., Baca, M., ... & Nicola, N. A. (1999). Mutational analyses of the SOCS proteins suggest a dual domain requirement but distinct mechanisms for inhibition of LIF and IL-6 signal transduction. *The EMBO journal*, *18*(2), 375-385.

Nilius, B., & Owsianik, G. (2011). The transient receptor potential family of ion channels. *Genome biology*, *12*(3), 1-11.

Nistor, A., & Simionescu, M. (1986). Uptake of low density lipoproteins by the hamster lung: interactions with capillary endothelium. *American Review of Respiratory Disease*, *134*(5), 1266-1272.

Nix, D. A., & Beckerle, M. C. (1997). Nuclear–cytoplasmic shuttling of the focal contact protein, zyxin: a potential mechanism for communication between sites of cell adhesion and the nucleus. *The Journal of cell biology*, *138*(5), 1139-1147.

Nixon, S. J., Carter, A., Wegner, J., Ferguson, C., Floetenmeyer, M., Riches, J., ... & Parton, R. G. (2007). Caveolin-1 is required for lateral line neuromast and notochord development. *Journal of cell science*, *120*(13), 2151-2161.

Northcott JM, Northey JJ, Barnes JM, Weaver VM. Fighting the force: Potential of homeobox genes for tumor microenvironment regulation. Biochim Biophys Acta. 2015 Apr;1855(2):248-53. doi: 10.1016/j.bbcan.2015.03.004.

Nystrom, F. H., Chen, H., Cong, L. N., Li, Y., & Quon, M. J. (1999). Caveolin-1 interacts with the insulin receptor and can differentially modulate insulin signaling in transfected Cos-7 cells and rat adipose cells. *Molecular endocrinology*, *13*(12), 2013-2024.

O'Brien, T. R., Prokunina-Olsson, L., & Donnelly, R. P. (2014). IFN-λ4: the paradoxical new member of the interferon lambda family. *Journal of Interferon & Cytokine Research*, *34*(11), 829-838.

Ogata, T., Ueyama, T., Isodono, K., Tagawa, M., Takehara, N., Kawashima, T., ... & Oh, H. (2008). MURC, a muscle-restricted coiled-coil protein that modulates the Rho/ROCK pathway, induces cardiac dysfunction and conduction disturbance. *Molecular and cellular biology*, *28*(10), 3424-3436.

Oh, P., McIntosh, D. P., & Schnitzer, J. E. (1998). Dynamin at the neck of caveolae mediates their budding to form transport vesicles by GTP-driven fission from the plasma membrane of endothelium. *The Journal of cell biology*, *141*(1), 101-114.

Oh, P., Borgström, P., Witkiewicz, H., Li, Y., Borgström, B. J., Chrastina, A., ... & Schnitzer, J. E. (2007). Live dynamic imaging of caveolae pumping targeted antibody rapidly and specifically across endothelium in the lung. *Nature biotechnology*, *25*(3), 327-337.

Oh, P., Testa, J. E., Borgstrom, P., Witkiewicz, H., Li, Y., & Schnitzer, J. E. (2014). In vivo proteomic imaging analysis of caveolae reveals pumping system to penetrate solid tumors. *Nature Medicine*, *20*(9), 1062-1068.

Okamoto, T., Schlegel, A., Scherer, P. E., & Lisanti, M. P. (1998). Caveolins, a family of scaffolding proteins for organizing "preassembled signaling complexes" at the plasma membrane. *Journal of Biological Chemistry*, *273*(10), 5419-5422.

Örtegren, U., Karlsson, M., Blazic, N., Blomqvist, M., Nystrom, F. H., Gustavsson, J., ... & Strålfors, P. (2004). Lipids and glycosphingolipids in caveolae and surrounding plasma membrane of primary rat adipocytes. *European Journal of Biochemistry*, *271*(10), 2028-2036.

O'Shea, J. J., Gadina, M., & Schreiber, R. D. (2002). Cytokine signaling in 2002: new surprises in the Jak/Stat pathway. *Cell*, *109*(2), S121-S131.

Palade, G. E. (1953). The fine structure of blood capillaries. *J Appl phys*, *24*, 1424.

Palmer, B. M. (2005). Thick filament proteins and performance in human heart failure. *Heart failure reviews*, *10*(3), 187-197.

Parmar, S., & Platanias, L. C. (2003). Interferons: mechanisms of action and clinical applications. *Current opinion in oncology*, *15*(6), 431-439.

Parr, R. D., Martin, G. G., Hostetler, H. A., Schroeder, M. E., Mir, K. D., Kier, A. B., ... & Schroeder, F. (2007). A new N-terminal recognition domain in caveolin-1 interacts with sterol carrier protein-2 (SCP-2). *Biochemistry*, *46*(28), 8301-8314.

Parton, R. G., & Del Pozo, M. A. (2013). Caveolae as plasma membrane sensors, protectors and organizers. *Nature reviews Molecular cell biology*, *14*(2), 98-112.

Parton, R. G., Del Pozo, M. A., Vassilopoulos, S., Nabi, I. R., Le Lay, S., Lundmark, R., ... & Lamaze, C. (2020). Caveolae: The FAQs. Traffic, 21(1), 181-185.

Parton, R. G., Hanzal-Bayer, M., & Hancock, J. F. (2006). Biogenesis of caveolae: a structural model for caveolin-induced domain formation. *Journal of cell science*, *119*(5), 787-796.

Parton, R. G., & Simons, K. (2007). The multiple faces of caveolae. *Nature reviews Molecular cell biology*, *8*(3), 185-194.

Parton RG, Del Pozo MA, Vassilopoulos S, Nabi IR, Le Lay S, Lundmark R, Kenworthy AK, Camus A, Blouin CM, Sessa WC, Lamaze C. Caveolae: The FAQs. Traffic. 2020 Jan;21(1):181-185. doi: 10.1111/tra.12689.

Paszek, M. J., & Weaver, V. M. (2004). The tension mounts: mechanics meets morphogenesis and malignancy. *Journal of mammary gland biology and neoplasia*, *9*(4), 325-342.

Paszek, M. J., Zahir, N., Johnson, K. R., Lakins, J. N., Rozenberg, G. I., Gefen, A., ... & Weaver, V. M. (2005). Tensional homeostasis and the malignant phenotype. *Cancer cell*, *8*(3), 241-254.

Patel, A. J., Honoré, E., Maingret, F., Lesage, F., Fink, M., Duprat, F., & Lazdunski, M. (1998). A mammalian two pore domain mechano-gated S-like K+ channel. *The EMBO journal*, *17*(15), 4283-4290.

Patel, A. J., & Honoré, E. (2001). Properties and modulation of mammalian 2P domain K+ channels. *Trends in neurosciences*, *24*(6), 339-346.

Patel HH, Murray F, Insel PA. Caveolae as organizers of pharmacologically relevant signal transduction molecules. *Annu Rev Pharmacol Toxicol*. 2008;48:359-391.

Pelkmans, L., Püntener, D., & Helenius, A. (2002). Local actin polymerization and dynamin recruitment in SV40-induced internalization of caveolae. *science*, *296*(5567), 535-539.

Pelkmans, L., Bürli, T., Zerial, M., & Helenius, A. (2004). Caveolin-stabilized membrane domains as multifunctional transport and sorting devices in endocytic membrane traffic. *Cell*, *118*(6), 767-780.

Perestrelo AR, Silva AC, Oliver-De La Cruz J, Martino F, Horváth V, Caluori G, Polanský O, Vinarský V, Azzato G, de Marco G, Žampachová V, Skládal P, Pagliari S, Rainer A, Pinto-do-Ó P, Caravella A, Koci K, Nascimento DS, Forte G. Multiscale Analysis of Extracellular Matrix Remodeling in the Failing Heart. Circ Res. 2021 Jan 8;128(1):24-38.

Pestka, S., Langer, J. A., Zoon, K. C., & Samuel, C. E. (1987). Interferons and their actions. *Annual review of biochemistry*, *56*(1), 727-777.

Pestka, S., Kotenko, S. V., Muthukumaran, G., Izotova, L. S., Cook, J. R., & Garotta, G. (1997). The interferon gamma (IFN-γ) receptor: a paradigm for the multichain cytokine receptor. *Cytokine & growth factor reviews*, *8*(3), 189-206.

Pestka, S., Krause, C. D., & Walter, M. R. (2004). Interferons, interferon-like cytokines, and their receptors. *Immunological reviews*, *202*(1), 8-32.

Peters, K. R., Carley, W. W., & Palade, G. E. (1985). Endothelial plasmalemmal vesicles have a characteristic striped bipolar surface structure. *The Journal of Cell Biology*, *101*(6), 2233-2238.

Peyronnet R, Martins JR, Duprat F, Demolombe S, Arhatte M, Jodar M, Tauc M, Duranton C, Paulais M, Teulon J, Honoré E, Patel A. Piezo1-dependent stretch-activated channels are inhibited by Polycystin-2 in renal tubular epithelial cells. EMBO Rep. 2013 Dec;14(12):1143-8.

Piehler, J., Thomas, C., Garcia, K. C., & Schreiber, G. (2012). Structural and dynamic determinants of type I interferon receptor assembly and their functional interpretation. Immunological reviews, 250(1), 317-334

Piganis, R. A., De Weerd, N. A., Gould, J. A., Schindler, C. W., Mansell, A., Nicholson, S. E., & Hertzog, P. J. (2011). Suppressor of cytokine signaling (SOCS) 1 inhibits type I interferon (IFN) signaling via the

interferon α receptor (IFNAR1)-associated tyrosine kinase Tyk2. Journal of biological chemistry, 286(39), 33811-33818.

Pita-Thomas, Wolfgang, et al. "Promoting filopodial elongation in neurons by membrane-bound magnetic nanoparticles." Nanomedicine: Nanotechnology, Biology and Medicine 11.3 (2015): 559-567.

Platanias, L. C. (2005). Mechanisms of Type-I-and Type-II-interferon-mediated signaling. *Nature Reviews Immunology*, *5*(5), 375-386.

Plucinsky, S. M., & Glover, K. J. (2015). Secondary structure analysis of a functional construct of caveolin-1 reveals a long C-terminal helix. *Biophysical journal*, *109*(8), 1686-1688.

Polte, T. R., Eichler, G. S., Wang, N., & Ingber, D. E. (2004). Extracellular matrix controls myosin light chain phosphorylation and cell contractility through modulation of cell shape and cytoskeletal prestress. *American Journal of Physiology-Cell Physiology*, *286*(3), C518-C528.

Poole, C. A., Jensen, C. G., Snyder, J. A., Gray, C. G., Hermanutz, V. L., & Wheatley, D. N. (1997). Confocal analysis of primary cilia structure and colocalization with the Golgi apparatus in chondrocytes and aortic smooth muscle cells. *Cell biology international*, *21*(8), 483-494.

Praetorius, H. A., & Spring, K. R. (2003). The renal cell primary cilium functions as a flow sensor. *Current opinion in nephrology and hypertension*, *12*(5), 517-520.

Predescu, S. A., Predescu, D. N., Timblin, B. K., Stan, R. V., & Malik, A. B. (2003). Intersectin regulates fission and internalization of caveolae in endothelial cells. *Molecular biology of the cell*, *14*(12), 4997-5010.

Prescott L, Brightman MW. The sarcolemma of Aplysia smooth muscle in freeze-fracture preparations. Tissue Cell. 1976;8(2):241-58.

Prinetti, A., Aureli, M., Illuzzi, G., Prioni, S., Nocco, V., Scandroglio, F., ... & Sonnino, S. (2010). GM3 synthase overexpression results in reduced cell motility and in caveolin-1 upregulation in human ovarian carcinoma cells. *Glycobiology*, *20*(1), 62-77.

Prior, I. A., Muncke, C., Parton, R. G., & Hancock, J. F. (2003). Direct visualization of Ras proteins in spatially distinct cell surface microdomains. *The Journal of cell biology*, *160*(2), 165-170.

Prokunina-Olsson, L., Muchmore, B., Tang, W., Pfeiffer, R. M., Park, H., Dickensheets, H., ... & O'Brien, T. R. (2013). A variant upstream of IFNL3 (IL28B) creating a new interferon gene IFNL4 is associated with impaired clearance of hepatitis C virus. *Nature genetics*, *45*(2), 164-171.

Qualmann, B., Roos, J., DiGregorio, P. J., & Kelly, R. B. (1999). Syndapin I, a synaptic dynamin-binding protein that associates with the neural Wiskott-Aldrich syndrome protein. *Molecular biology of the cell*, *10*(2), 501-513.

Radha, V., Mitra, A., Dayma, K., & Sasikumar, K. (2011). Signalling to actin: role of C3G, a multitasking guanine-nucleotide-exchange factor. *Bioscience reports*, *31*(4), 231-244.

Radhakrishnan, R., Walter, L. J., Hruza, A., Reichert, P., Trotta, P. P., Nagabhushan, T. L., & Walter, M. R. (1996). Zinc mediated dimer of human interferon-α2b revealed by X-ray crystallography. *Structure*, *4*(12), 1453-1463.

Ragimbeau, J., Dondi, E., Alcover, A., Eid, P., Uzé, G., & Pellegrini, S. (2003). The tyrosine kinase Tyk2 controls IFNAR1 cell surface expression. *The EMBO journal*, *22*(3), 537-547.

Rajab, A., Straub, V., McCann, L. J., Seelow, D., Varon, R., Barresi, R., ... & Schuelke, M. (2010). Fatal cardiac arrhythmia and long-QT syndrome in a new form of congenital generalized lipodystrophy with muscle rippling (CGL4) due to PTRF-CAVIN mutations. *PLoS genetics*, *6*(3), e1000874.

Ramírez, C. M., Zhang, X., Bandyopadhyay, C., Rotllan, N., Sugiyama, M. G., Aryal, B., ... & Fernández-Hernando, C. (2019). Caveolin-1 regulates atherogenesis by attenuating low-density lipoprotein transcytosis and vascular inflammation independently of endothelial nitric oxide synthase activation. Circulation, 140(3), 225-239.

Ranade SS, Qiu Z, Woo SH, Hur SS, Murthy SE, Cahalan SM, Xu J, Mathur J, Bandell M, Coste B, Li YS, Chien S, Patapoutian A. Piezo1, a mechanically activated ion channel, is required for vascular development in mice. Proc Natl Acad Sci U S A. 2014 Jul 15;111(28):10347-52.

Ranade SS, Woo SH, Dubin AE, Moshourab RA, Wetzel C, Petrus M, Mathur J, Bégay V, Coste B, Mainquist J, Wilson AJ, Francisco AG, Reddy K, Qiu Z, Wood JN, Lewin GR, Patapoutian A. Piezo2 is the major transducer of mechanical forces for touch sensation in mice. Nature. 2014 Dec 4;516(7529):121-5.

Randal, M., & Kossiakoff, A. A. (2001). The structure and activity of a monomeric interferon-γ: α-chain receptor signaling complex. *Structure*, *9*(2), 155-163.

Rausch V, Bostrom JR, Park J, Bravo IR, Feng Y, Hay DC, Link BA, Hansen CG. The Hippo Pathway Regulates Caveolae Expression and Mediates Flow Response via Caveolae. Curr Biol. 2019 Jan 21;29(2):242-255.e6.

Rawlings JS, Rosler KM, Harrison DA. The JAK/STAT signaling pathway. J Cell Sci. 2004 Mar 15;117(Pt 8):1281-3.

Razani, B., Engelman, J. A., Wang, X. B., Schubert, W., Zhang, X. L., Marks, C. B., ... & Lisanti, M. P. (2001). Caveolin-1 null mice are viable but show evidence of hyperproliferative and vascular abnormalities. *Journal of Biological Chemistry*, *276*(41), 38121-38138.

Razani, B., & Lisanti, M. P. (2001). Caveolin-deficient mice: insights into caveolar function human disease. *The Journal of clinical investigation*, *108*(11), 1553-1561.

Razani, B., Wang, X. B., Engelman, J. A., Battista, M., Lagaud, G., Zhang, X. L., ... & Lisanti, M. P. (2002). Caveolin-2-deficient mice show evidence of severe pulmonary dysfunction without disruption of caveolae. *Molecular and cellular biology*, *22*(7), 2329-2344.

Razani, B., Woodman, S. E., & Lisanti, M. P. (2002). Caveolae: from cell biology to animal physiology. *Pharmacological reviews*, *54*(3), 431-467.

Razinia, Z., Mäkelä, T., Ylänne, J., & Calderwood, D. A. (2012). Filamins in mechanosensing and signaling. *Annual review of biophysics*, *41*, 227-246.

Reese C, Dyer S, Perry B, Bonner M, Oates J, Hofbauer A, Sessa W, Bernatchez P, Visconti RP, Zhang J, Hatfield CM, Silver RM, Hoffman S, Tourkina E. Differential regulation of cell functions by CSD peptide subdomains. Respir Res. 2013 Sep 8;14(1):90.

Repetto, S., Bado, M., Broda, P., Lucania, G., Masetti, E., Sotgia, F., ... & Minetti, C. (1999). Increased number of caveolae and caveolin-3 overexpression in Duchenne muscular dystrophy. *Biochemical and biophysical research communications*, *261*(3), 547-550.

Richter, T., Floetenmeyer, M., Ferguson, C., Galea, J., Goh, J., Lindsay, M. R., ... & Parton, R. G. (2008). High-resolution 3D quantitative analysis of caveolar ultrastructure and caveola–cytoskeleton interactions. *Traffic*, *9*(6), 893-909.

Rizzo V, Sung A, Oh P, Schnitzer JE. Rapid mechanotransduction in situ at the luminal cell surface of vascular endothelium and its caveolae. J Biol Chem. 1998 Oct 9;273(41):26323-9.

Rizzo V, Morton C, DePaola N, Schnitzer JE, Davies PF. Recruitment of endothelial caveolae into mechanotransduction pathways by flow conditioning in vitro. Am J Physiol Heart Circ Physiol. 2003 Oct;285(4):H1720-9.

Rogers, R. S., Horvath, C. M., & Matunis, M. J. (2003). SUMO modification of STAT1 and its role in PIAS-mediated inhibition of gene activation. *Journal of Biological Chemistry*, *278*(32), 30091-30097.

Roisman LC, Jaitin DA, Baker DP, Schreiber G. Mutational analysis of the IFNAR1 binding site on IFNalpha2 reveals the architecture of a weak ligand-receptor binding-site. J Mol Biol. 2005 Oct 21;353(2):271-81.

Root, K. T., Julien, J. A., & Glover, K. J. (2019). Secondary structure of caveolins: a mini review. *Biochemical Society Transactions*, *47*(5), 1489-1498.

Rosengren, B. I., Rippe, A., Rippe, C., Venturoli, D., Swärd, K., & Rippe, B. (2006). Transvascular protein transport in mice lacking endothelial caveolae. *American Journal of Physiology-Heart and Circulatory Physiology*, *291*(3), H1371-H1377.

Rothberg, K. G., Heuser, J. E., Donzell, W. C., Ying, Y. S., Glenney, J. R., & Anderson, R. G. (1992). Caveolin, a protein component of caveolae membrane coats. *Cell*, *68*(4), 673-682.

Roy, S., Luetterforst, R., Harding, A., Apolloni, A., Etheridge, M., Stang, E., ... & Parton, R. G. (1999). Dominant-negative caveolin inhibits H-Ras function by disrupting cholesterol-rich plasma membrane domains. *Nature cell biology*, *1*(2), 98-105.

Rui, H., Root, K. T., Lee, J., Glover, K. J., & Im, W. (2014). Probing the U-shaped conformation of caveolin-1 in a bilayer. *Biophysical journal*, *106*(6), 1371-1380.

Sahai, E., & Marshall, C. J. (2002). RHO–GTPases and cancer. *Nature Reviews Cancer*, *2*(2), 133-142.

Sahai, E., & Marshall, C. J. (2003). Differing modes of tumour cell invasion have distinct requirements for Rho/ROCK signalling and extracellular proteolysis. *Nature cell biology*, *5*(8), 711-719.

Saharinen, P., Takaluoma, K., & Silvennoinen, O. (2000). Regulation of the Jak2 tyrosine kinase by its pseudokinase domain. *Molecular and cellular biology*, *20*(10), 3387-3395.

Sargiacomo, M., Sudol, M., Tang, Z., & Lisanti, M. P. (1993). Signal transducing molecules and glycosyl-phosphatidylinositol-linked proteins form a caveolin-rich insoluble complex in MDCK cells. *Journal of Cell Biology*, *122*(4), 789-807.

Sargiacomo, M., Scherer, P. E., Tang, Z., Kübler, E., Song, K. S., Sanders, M. C., & Lisanti, M. P. (1995). Oligomeric structure of caveolin: implications for caveolae membrane organization. *Proceedings of the National Academy of Sciences*, *92*(20), 9407-9411.

Sarntinoranont, M., Rooney, F., & Ferrari, M. (2003). Interstitial stress and fluid pressure within a growing tumor. *Annals of biomedical engineering*, *31*(3), 327-335.

Sasaki, A., Yasukawa, H., Shouda, T., Kitamura, T., Dikic, I., & Yoshimura, A. (2000). CIS3/SOCS-3 suppresses erythropoietin (EPO) signaling by binding the EPO receptor and JAK2. *Journal of Biological Chemistry*, *275*(38), 29338-29347.

Sawada, Y., Tamada, M., Dubin-Thaler, B. J., Cherniavskaya, O., Sakai, R., Tanaka, S., & Sheetz, M. P. (2006). Force sensing by mechanical extension of the Src family kinase substrate p130Cas. *Cell*, *127*(5), 1015-1026.

Schiller, H. B., Hermann, M. R., Polleux, J., Vignaud, T., Zanivan, S., Friedel, C. C., ... & Fässler, R. (2013). β 1-and α v-class integrins cooperate to regulate myosin II during rigidity sensing of fibronectin-based microenvironments. *Nature cell biology*, *15*(6), 625-636.

Schindler, C., Shuai, K., Prezioso, V. R., & Darnell, J. E. (1992). Interferon-dependent tyrosine phosphorylation of a latent cytoplasmic transcription factor. *Science*, *257*(5071), 809-813.

Schlegel, A., & Lisanti, M. P. (2000). A molecular dissection of caveolin-1 membrane attachment and oligomerization: two separate regions of the caveolin-1 C-terminal domain mediate membrane binding and oligomer/oligomer interactions in vivo. *Journal of Biological Chemistry*, *275*(28), 21605-21617.

Schlegel, A., Arvan, P., & Lisanti, M. P. (2001). Caveolin-1 binding to endoplasmic reticulum membranes and entry into the regulated secretory pathway are regulated by serine phosphorylation: protein sorting at the level of the endoplasmic reticulum. *Journal of Biological Chemistry*, *276*(6), 4398-4408.

Schlörmann, W., Steiniger, F., Richter, W., Kaufmann, R., Hause, G., Lemke, C., & Westermann, M. (2010). The shape of caveolae is omega-like after glutaraldehyde fixation and cup-like after cryofixation. *Histochemistry and cell biology*, *133*(2), 223-228.

Schmeichel, K. L., & Beckerle, M. C. (1997). Molecular dissection of a LIM domain. *Molecular biology of the cell*, *8*(2), 219-230.

Schoenborn, J. R., & Wilson, C. B. (2007). Regulation of interferon-γ during innate and adaptive immune responses. *Advances in immunology*, *96*, 41-101.

Schroeder, M. E., Hostetler, H. A., Schroeder, F., & Ball, J. M. (2012). Elucidation of the rotavirus NSP4-caveolin-1 and-cholesterol interactions using synthetic peptides. *Journal of amino acids*, *2012*.

Schubert, A. L., Schubert, W., Spray, D. C., & Lisanti, M. P. (2002). Connexin family members target to lipid raft domains and interact with caveolin-1. *Biochemistry*, *41*(18), 5754-5764.

Schubert, W., Frank, P. G., Woodman, S. E., Hyogo, H., Cohen, D. E., Chow, C. W., & Lisanti, M. P. (2002). Microvascular hyperpermeability in caveolin-1 (−/−) knock-out mice: Treatment with a specific nitric-oxide synthase inhibitor, L-NAME, restores normal microvascular permeability in Cav-1 null mice. *Journal of Biological Chemistry*, *277*(42), 40091-40098.

Schwartz, M. A., & Ginsberg, M. H. (2002). Networks and crosstalk: integrin signalling spreads. *Nature cell biology*, *4*(4), E65-E68.

Sciandra, F., Bozzi, M., Bianchi, M., Pavoni, E., Giardina, B., & Brancaccio, A. (2003). Dystroglycan and muscolar dystrophies related to the dystrophin-glycoprotein complex. *Annali-istituto superiore di sanita*, *39*(2), 173-182.

Seemann, E., Sun, M., Krueger, S., Tröger, J., Hou, W., Haag, N., ... & Qualmann, B. (2017). Deciphering caveolar functions by syndapin III KO-mediated impairment of caveolar invagination. *Elife*, *6*, e29854.

Senda, T., Saitoh, S. I., & Mitsui, Y. (1995). Refined crystal structure of recombinant murine interferon-β at 2.15 Å resolution. *Journal of molecular biology*, *253*(1), 187-207.

Senju, Y., Itoh, Y., Takano, K., Hamada, S., & Suetsugu, S. (2011). Essential role of PACSIN2/syndapin-II in caveolae membrane sculpting. *Journal of cell science*, *124*(12), 2032-2040.

Sharma, D. K., Brown, J. C., Choudhury, A., Peterson, T. E., Holicky, E., Marks, D. L., ... & Pagano, R. E. (2004). Selective stimulation of caveolar endocytosis by glycosphingolipids and cholesterol. *Molecular biology of the cell*, *15*(7), 3114-3122.

Shen, W. W., Bièche, I., Fuhrmann, L., Vacher, S., Vincent-Salomon, A., Torrino, S., & Lamaze, C. (2020). EHD2 is a predictive biomarker of chemotherapy efficacy in triple negative breast carcinoma. *Scientific reports*, *10*(1), 1-12.

Shimizu-Sato S, Huq E, Tepperman JM, Quail PH. A light-switchable gene promoter system. Nat Biotechnol. 2002 Oct;20(10):1041-4.

Shivanandan, A., Radenovic, A., & Sbalzarini, I. F. (2013). MosaicIA: an ImageJ/Fiji plugin for spatial pattern and interaction analysis. BMC bioinformatics, 14(1), 1-10.

Shrestha, A., Pinaud, F., & Haselwandter, C. A. (2021). Mechanics of cup-shaped caveolae. Physical Review E, 104(2), L022401.

Shuai, K., Schindler, C., Prezioso, V. R., & Darnell, J. E. (1992). Activation of transcription by IFN-gamma: tyrosine phosphorylation of a 91-kD DNA binding protein. *Science*, *258*(5089), 1808-1812.

Shuai K, Liu B. Regulation of JAK-STAT signalling in the immune system. Nat Rev Immunol. 2003 Nov;3(11):900-11.

Shvets, E., Bitsikas, V., Howard, G., Hansen, C. G., & Nichols, B. J. (2015). Dynamic caveolae exclude bulk membrane proteins and are required for sorting of excess glycosphingolipids. *Nature communications*, *6*(1), 1-16.

Simionescu, N., Simionescu, M., & Palade, G. E. (1972). Permeability of intestinal capillaries: pathway followed by dextrans and glycogens. *The Journal of cell biology*, *53*(2), 365-392.

Simionescu, M., Simionescu, N., & Palade, G. E. (1975). Segmental differentiations of cell junctions in the vascular endothelium. The microvasculature. *Journal of Cell Biology*, *67*(3), 863-885.

Simoncic, P. D., Lee-Loy, A., Barber, D. L., Tremblay, M. L., & McGlade, C. J. (2002). The T cell protein tyrosine phosphatase is a negative regulator of janus family kinases 1 and 3. *Current biology*, *12*(6), 446-453.

Simone, L. C., Caplan, S., & Naslavsky, N. (2013). Role of phosphatidylinositol 4, 5-bisphosphate in regulating EHD2 plasma membrane localization. *PloS one*, *8*(9), e74519.

Singh, R. D., Puri, V., Valiyaveettil, J. T., Marks, D. L., Bittman, R., & Pagano, R. E. (2003). Selective caveolin-1–dependent endocytosis of glycosphingolipids. *Molecular biology of the cell*, *14*(8), 3254-3265.

Singh, R. D., Marks, D. L., Holicky, E. L., Wheatley, C. L., Kaptzan, T., Sato, S. B., ... & Pagano, R. E. (2010). Gangliosides and β1-Integrin Are Required for Caveolae and Membrane Domains. *Traffic*, *11*(3), 348-360.

Sinha, B., Köster, D., Ruez, R., Gonnord, P., Bastiani, M., Abankwa, D., ... & Nassoy, P. (2011). Cells respond to mechanical stress by rapid disassembly of caveolae. *Cell*, *144*(3), 402-413.

Smith, S., Tripathi, R., Goodings, C., Cleveland, S., Mathias, E., Hardaway, J. A., ... & Davé, U. P. (2014). LIM domain only-2 (LMO2) induces T-cell leukemia by two distinct pathways. *PloS one*, *9*(1), e85883.

Somlyo, A. P., Devine, C. E., Somlyo, A. V., & North, S. R. (1971). Sarcoplasmic reticulum and the temperature-dependent contraction of smooth muscle in calcium-free solutions. *The Journal of cell biology*, *51*(3), 722-741.

Song, K. S., Scherer, P. E., Tang, Z., Okamoto, T., Li, S., Chafel, M., ... & Lisanti, M. P. (1996). Expression of caveolin-3 in skeletal, cardiac, and smooth muscle cells: caveolin-3 is a component of the sarcolemma and co-fractionates with dystrophin and dystrophin-associated glycoproteins. *Journal of Biological Chemistry*, *271*(25), 15160-15165.

Song, K. S., Tang, Z., Li, S., & Lisanti, M. P. (1997). Mutational analysis of the properties of caveolin-1: a novel role for the C-terminal domain in mediating homo-typic caveolin-caveolin interactions. *Journal of Biological Chemistry*, *272*(7), 4398-4403.

Song, L., Bhattacharya, S., Yunus, A. A., Lima, C. D., & Schindler, C. (2006). Stat1 and SUMO modification. Blood, 108(10), 3237-3244.

Sonnino, S., & Prinetti, A. (2009). Sphingolipids and membrane environments for caveolin. *FEBS letters*, *583*(4), 597-606.

Sowa, G., Pypaert, M., & Sessa, W. C. (2001). Distinction between signaling mechanisms in lipid rafts vs. caveolae. *Proceedings of the National Academy of Sciences*, *98*(24), 14072-14077

Sowa, G., Pypaert, M., Fulton, D., & Sessa, W. C. (2003). The phosphorylation of caveolin-2 on serines 23 and 36 modulates caveolin-1-dependent caveolae formation. *Proceedings of the National Academy of Sciences*, *100*(11), 6511-6516.

Spisni, E., Tomasi, V., Cestaro, A., & Tosatto, S. C. (2005). Structural insights into the function of human caveolin 1. *Biochemical and biophysical research communications*, *338*(3), 1383-1390.

Spolski, R., & Leonard, W. J. (2014). Interleukin-21: a double-edged sword with therapeutic potential. *Nature reviews Drug discovery*, *13*(5), 379-395.

Stan, R. V., Tkachenko, E., & Niesman, I. R. (2004). PV1 is a key structural component for the formation of the stomatal and fenestral diaphragms. *Molecular biology of the cell*, *15*(8), 3615-3630.

Stan, R. V. (2005). Structure of caveolae. *Biochimica et Biophysica Acta (BBA)-Molecular Cell Research*, *1746*(3), 334-348.

Stehbens, W. E., Delahunt, B., Shozawa, T., & Gilbert-Barness, E. (2001). Smooth muscle cell depletion and collagen types in progeric arteries. *Cardiovascular Pathology*, *10*(3), 133-136.

Stoeber, M., Stoeck, I. K., Hänni, C., Bleck, C. K. E., Balistreri, G., & Helenius, A. (2012). Oligomers of the ATPase EHD2 confine caveolae to the plasma membrane through association with actin. *The EMBO journal*, *31*(10), 2350-2364.

Stoeber, M., Schellenberger, P., Siebert, C. A., Leyrat, C., Helenius, A., & Grünewald, K. (2016). Model for the architecture of caveolae based on a flexible, net-like assembly of Cavin1 and Caveolin discs. *Proceedings of the National Academy of Sciences*, *113*(50), E8069-E8078.

Storm, C., Pastore, J. J., MacKintosh, F. C., Lubensky, T. C., & Janmey, P. A. (2005). Nonlinear elasticity in biological gels. *Nature*, *435*(7039), 191-194.

Stossel, T. P., Condeelis, J., Cooley, L., Hartwig, J. H., Noegel, A., Schleicher, M., & Shapiro, S. S. (2001). Filamins as integrators of cell mechanics and signalling. *Nature reviews Molecular cell biology*, *2*(2), 138-145.

Strickland, D. et al. TULIPs: tunable, light-controlled interacting protein tags for cell biology. Nature Methods 9, 379–384 (2012).

Subramaniam, P. S., Torres, B. A., & Johnson, H. M. (2001). So many ligands, so few transcription factors: a new paradigm for signaling through the STAT transcription factors. *Cytokine*, *15*(4), 175-187.

Suresh, S. (2007). Elastic clues in cancer detection. *Nature Nanotechnology*, *2*(12), 748-749.

Sun X, Phua DYZ, Axiotakis L Jr, Smith MA, Blankman E, Gong R, Cail RC, Espinosa de Los Reyes S, Beckerle MC, Waterman CM, Alushin GM. Mechanosensing through Direct Binding of Tensed F-Actin by LIM Domains. Dev Cell. 2020 Nov 23;55(4):468-482.e7.

Swiatek-Machado, K., Mieczkowski, J., Ellert-Miklaszewska, A., Swierk, P., Fokt, I., Szymanski, S., ... & Kaminska, B. (2012). Novel small molecular inhibitors disrupt the JAK/STAT3 and FAK signaling pathways and exhibit a potent antitumor activity in glioma cells. *Cancer biology & therapy*, *13*(8), 657-670.

Tagawa, A., Mezzacasa, A., Hayer, A., Longatti, A., Pelkmans, L., & Helenius, A. (2005). Assembly and trafficking of caveolar domains in the cell: caveolae as stable, cargo-triggered, vesicular transporters. *The Journal of cell biology*, *170*(5), 769-779.

Tahir, S. A., Yang, G., Ebara, S., Timme, T. L., Satoh, T., Li, L., ... & Thompson, T. C. (2001). Secreted caveolin-1 stimulates cell survival/clonal growth and contributes to metastasis in androgen-insensitive prostate cancer. *Cancer research*, *61*(10), 3882-3885.

Tang, Z., Scherer, P. E., Okamoto, T., Song, K., Chu, C., Kohtz, D. S., ... & Lisanti, M. P. (1996). Molecular Cloning of Caveolin-3, a Novel Member of the Caveolin Gene Family Expressed Predominantly in Muscle. *Journal of Biological Chemistry*, *271*(4), 2255-2261.

Taslimi A, Vrana JD, Chen D, Borinskaya S, Mayer BJ, Kennedy MJ, Tucker CL. An optimized optogenetic clustering tool for probing protein interaction and function. Nat Commun. 2014 Sep 18;5:4925.

Tee, Y. H., Shemesh, T., Thiagarajan, V., Hariadi, R. F., Anderson, K. L., Page, C., ... & Bershadsky, A. D. (2015). Cellular chirality arising from the self-organization of the actin cytoskeleton. *Nature cell biology*, *17*(4), 445-457.

ten Hoeve, J., de Jesus Ibarra-Sanchez, M., Fu, Y., Zhu, W., Tremblay, M., David, M., & Shuai, K. (2002). Identification of a nuclear Stat1 protein tyrosine phosphatase. *Molecular and cellular biology*, *22*(16), 5662-5668.

Thomas, C., Moraga, I., Levin, D., Krutzik, P. O., Podoplelova, Y., Trejo, A., ... & Garcia, K. C. (2011). Structural linkage between ligand discrimination and receptor activation by type I interferons. *Cell*, *146*(4), 621-632.

Thompson d'Arcy, W. (1917). On growth and form. *Cambridge: Cambridge University Press*, *16*, 794.

Tillu, V. A., Kovtun, O., McMahon, K. A., Collins, B. M., & Parton, R. G. (2015). A phosphoinositide-binding cluster in cavin1 acts as a molecular sensor for cavin1 degradation. *Molecular biology of the cell*, *26*(20), 3561-3569.

Tillu VA, Lim YW, Kovtun O, Mureev S, Ferguson C, Bastiani M, McMahon KA, Lo HP, Hall TE, Alexandrov K, Collins BM, Parton RG. A variable undecad repeat domain in cavin1 regulates caveola formation and stability. EMBO Rep. 2018 Sep;19(9):e45775.

Tillu VA, Rae J, Gao Y, Ariotti N, Floetenmeyer M, Kovtun O, McMahon KA, Chaudhary N, Parton RG, Collins BM. Cavin1 intrinsically disordered domains are essential for fuzzy electrostatic interactions and caveola formation. Nat Commun. 2021 Feb 10;12(1):931.

Tiruppathi, C., Song, W., Bergenfeldt, M., Sass, P., & Malik, A. B. (1997). Gp60 activation mediates albumin transcytosis in endothelial cells by tyrosine kinase-dependent pathway. *Journal of Biological Chemistry*, *272*(41), 25968-25975.

Tischer D, Weiner OD. Illuminating cell signalling with optogenetic tools. Nat Rev Mol Cell Biol. 2014 Aug;15(8):551-8.

Tran RDH, Siemens M, Nguyen CHH, Ochs AR, Zaragoza MV, Grosberg A. The Effect of Cyclic Strain on Human Fibroblasts With Lamin A/C Mutations and Its Relation to Heart Disease. J Biomech Eng. 2020 Jun 1;142(6):0610021–9.

Trushina, E., Du Charme, J., Parisi, J., & McMurray, C. T. (2006). Neurological abnormalities in caveolin-1 knock out mice. *Behavioural brain research*, *172*(1), 24-32.

Tsujita, K., Suetsugu, S., Sasaki, N., Furutani, M., Oikawa, T., & Takenawa, T. (2006). Coordination between the actin cytoskeleton and membrane deformation by a novel membrane tubulation domain of PCH proteins is involved in endocytosis. *The Journal of cell biology*, *172*(2), 269-279.

Uddin, S., Sassano, A., Deb, D. K., Verma, A., Majchrzak, B., Rahman, A., ... & Platanias, L. C. (2002). Protein kinase C-δ (PKC-δ) is activated by type I interferons and mediates phosphorylation of Stat1 on serine 727. *Journal of Biological Chemistry*, *277*(17), 14408-14416.

Uddin, S., & Platanias, L. C. (2004). Mechanisms of Type-I interferon signal transduction. *BMB Reports*, *37*(6), 635-641.

Uittenbogaard, A., & Smart, E. J. (2000). Palmitoylation of caveolin-1 is required for cholesterol binding, chaperone complex formation, and rapid transport of cholesterol to caveolae. *Journal of Biological Chemistry*, *275*(33), 25595-25599.

Vainonen, J. P., Aboulaich, N., Turkina, M. V., Strålfors, P., & Vener, A. V. (2004). N-terminal processing and modifications of caveolin-1 in caveolae from human adipocytes. *Biochemical and biophysical research communications*, *320*(2), 480-486.

van der Pijl R, Strom J, Conijn S, Lindqvist J, Labeit S, Granzier H, Ottenheijm C. Titin-based mechanosensing modulates muscle hypertrophy. J Cachexia Sarcopenia Muscle. 2018 Oct;9(5):947-961.

Van Deurs, B., Roepstorff, K., Hommelgaard, A. M., & Sandvig, K. (2003). Caveolae: anchored, multifunctional platforms in the lipid ocean. *Trends in cell biology*, *13*(2), 92-100.

Vandorpe, D. H., Xu, C., Shmukler, B. E., Otterbein, L. E., Trudel, M., Sachs, F., ... & Alper, S. L. (2010). Hypoxia activates a Ca2+-permeable cation conductance sensitive to carbon monoxide and to GsMTx-4 in human and mouse sickle erythrocytes. *PloS one*, *5*(1), e8732.

VanSaun, M. N. (2013). Molecular pathways: adiponectin and leptin signaling in cancer. *Clinical Cancer Research*, *19*(8), 1926-1932.

Vasile, E., Simionescu, M., & Simionescu, N. (1983). Visualization of the binding, endocytosis, and transcytosis of low-density lipoprotein in the arterial endothelium in situ. *The Journal of cell biology*, *96*(6), 1677-1689.

Velazquez, L., Fellous, M., Stark, G. R., & Pellegrini, S. (1992). A protein tyrosine kinase in the interferon αβ signaling pathway. *Cell*, *70*(2), 313-322.

Verstraeten, V. L., Ji, J. Y., Cummings, K. S., Lee, R. T., & Lammerding, J. (2008). Increased mechanosensitivity and nuclear stiffness in Hutchinson–Gilford progeria cells: effects of farnesyltransferase inhibitors. *Aging cell*, *7*(3), 383-393.

Villarino, A. V., Kanno, Y., & O'Shea, J. J. (2017). Mechanisms and consequences of Jak–STAT signaling in the immune system. *Nature immunology*, *18*(4), 374-384.

Voets, T., & Nilius, B. (2009). TRPCs, GPCRs and the Bayliss effect. *The EMBO Journal*, *28*(1), 4-5.

Vogel, V. (2006). Mechanotransduction involving multimodular proteins: converting force into biochemical signals. *Annu. Rev. Biophys. Biomol. Struct.*, *35*, 459-488.

Vogel, V., & Sheetz, M. (2006). Local force and geometry sensing regulate cell functions. *Nature reviews Molecular cell biology*, *7*(4), 265-275.

Volkers, L., Mechioukhi, Y., & Coste, B. (2015). Piezo channels: from structure to function. *Pflügers Archiv-European Journal of Physiology*, *467*(1), 95-99.

Wallweber, H. J., Tam, C., Franke, Y., Starovasnik, M. A., & Lupardus, P. J. (2014). Structural basis of recognition of interferon-α receptor by tyrosine kinase 2. *Nature structural & molecular biology*, *21*(5), 443-448.

Walser, P. J., Ariotti, N., Howes, M., Ferguson, C., Webb, R., Schwudke, D., ... & Parton, R. G. (2012). Constitutive formation of caveolae in a bacterium. *Cell*, *150*(4), 752-763.

Walter, M. R. (2004). Structural analysis of IL-10 and Type I interferon family members and their complexes with receptor. *Advances in protein chemistry*, *68*, 171-223.

Walter, M. R. (2020). The role of structure in the biology of interferon signaling. Frontiers in Immunology, 11, 2943.

Wanaski, S. P., Ng, B. K., & Glaser, M. (2003). Caveolin scaffolding region and the membrane binding region of SRC form lateral membrane domains. *Biochemistry*, *42*(1), 42-56.

Wang, X., Chen, X. & Yang, Y. Spatiotemporal control of gene expression by a light-switchable transgene system. Nature Methods 9, 266–269 (2012).

Wang H, Vilela M, Winkler A, Tarnawski M, Schlichting I, Yumerefendi H, Kuhlman B, Liu R, Danuser G, Hahn KM. LOVTRAP: an optogenetic system for photoinduced protein dissociation. Nat Methods. 2016 Sep;13(9):755-8.

Wang YX, Wang DY, Guo YC, Guo J. Zyxin: a mechanotransductor to regulate gene expression. Eur Rev Med Pharmacol Sci. 2019 Jan;23(1):413-425.

Wang H, Vilela M, Winkler A, Tarnawski M, Schlichting I, Yumerefendi H, Kuhlman B, Liu R, Danuser G, Hahn KM. LOVTRAP: an optogenetic system for photoinduced protein dissociation. Nat Methods. 2016 Sep;13(9):755-8.

Way, M., & Parton, R. G. (1995). M-caveolin, a muscle-specific caveolin-related protein. *FEBS letters*, *376*(1-2), 108-112.

Wen, Z., Zhong, Z., & Darnell Jr, J. E. (1995). Maximal activation of transcription by Statl and Stat3 requires both tyrosine and serine phosphorylation. *Cell*, *82*(2), 241-250.

Wen, Z., & Darnell Jr, J. E. (1997). Mapping of Stat3 serine phosphorylation to a single residue (727) and evidence that serine phosphorylation has no influence on DNA binding of Stat1 and Stat3. *Nucleic acids research*, *25*(11), 2062-2067.

Wilks, A. F. (1989). Two putative protein-tyrosine kinases identified by application of the polymerase chain reaction. *Proceedings of the National Academy of Sciences*, *86*(5), 1603-1607.

Williams, J. J., Alotaiq, N., Mullen, W., Burchmore, R., Liu, L., Baillie, G. S., ... & Palmer, T. M. (2018). Interaction of suppressor of cytokine signalling 3 with cavin-1 links SOCS3 function and cavin-1 stability. Nature communications, 9(1), 1-17.

Witte, K., Witte, E., Sabat, R., & Wolk, K. (2010). IL-28A, IL-28B, and IL-29: promising cytokines with type I interferon-like properties. *Cytokine & growth factor reviews*, *21*(4), 237-251.

Wolf, K., Wu, Y. I., Liu, Y., Geiger, J., Tam, E., Overall, C., ... & Friedl, P. (2007). Multi-step pericellular proteolysis controls the transition from individual to collective cancer cell invasion. *Nature cell biology*, *9*(8), 893-904.

Wong, J., Baddeley, D., Bushong, E. A., Yu, Z., Ellisman, M. H., Hoshijima, M., & Soeller, C. (2013). Nanoscale distribution of ryanodine receptors and caveolin-3 in mouse ventricular myocytes: dilation of t-tubules near junctions. Biophysical journal, 104(11), L22-L24.

Wong, T. H., Khater, I. M., Joshi, B., Shahsavari, M., Hamarneh, G., & Nabi, I. R. (2021). Single molecule network analysis identifies structural changes to caveolae and scaffolds due to mutation of the caveolin-1 scaffolding domain. Scientific reports, 11(1), 1-14;

Woo SH, Ranade S, Weyer AD, Dubin AE, Baba Y, Qiu Z, Petrus M, Miyamoto T, Reddy K, Lumpkin EA, Stucky CL, Patapoutian A. Piezo2 is required for Merkel-cell mechanotransduction. Nature. 2014 May 29;509(7502):622-6.

Woodman, S. E., Ashton, A. W., Schubert, W., Lee, H., Williams, T. M., Medina, F. A., ... & Lisanti, M. P. (2003). Caveolin-1 knockout mice show an impaired angiogenic response to exogenous stimuli. *The American journal of pathology*, *162*(6), 2059-2068.

Woods, A., Wang, G., & Beier, F. (2007). Regulation of chondrocyte differentiation by the actin cytoskeleton and adhesive interactions. *Journal of cellular physiology*, *213*(1), 1-8.

Wu, T. R., Hong, Y. K., Wang, X. D., Ling, M. Y., Dragoi, A. M., Chung, A. S., ... & Chin, Y. E. (2002). SHP-2 is a dual-specificity phosphatase involved in Stat1 dephosphorylation at both tyrosine and serine residues in nuclei. *Journal of Biological Chemistry*, *277*(49), 47572-47580.

Wu, D., & Terrian, D. M. (2002). Regulation of caveolin-1 expression and secretion by a protein kinase Cε signaling pathway in human prostate cancer cells. *Journal of Biological Chemistry*, *277*(43), 40449-40455.

Wu, Y. I. et al. A genetically encoded photoactivatable Rac controls the motility of living cells. Nature 461, 104–108 (2009).

Wu M, Frieboes HB, McDougall SR, Chaplain MA, Cristini V, Lowengrub J. The effect of interstitial pressure on tumor growth: coupling with the blood and lymphatic vascular systems. J Theor Biol. 2013 Mar 7;320:131-51.

www.mechanobio.info - Figure 1: Models for force-induced modulation of cytoskeletal stiffness.

www.abbelight.com – Figure 14: Principle of single molecule localization microscopy.

Xiao, R., & Xu, X. S. (2010). Mechanosensitive channels: in touch with Piezo. *Current Biology*, *20*(21), R936-R938.

Xiao LL, Yan WW, Liu Y, Chen S, Fu BM. Modeling Cell Adhesion and Extravasation in Microvascular System. Adv Exp Med Biol. 2018;1097:219-234.

Yamada, E. (1955). The fine structure of the gall bladder epithelium of the mouse. *The Journal of Cell Biology*, *1*(5), 445-458.

Yamaguchi, T., Lu, C., Ida, L., Yanagisawa, K., Usukura, J., Cheng, J., ... & Takahashi, T. (2016). ROR1 sustains caveolae and survival signalling as a scaffold of cavin-1 and caveolin-1. *Nature communications*, *7*(1), 1-13.

Yang, G., Truong, L. D., Timme, T. L., Ren, C., Wheeler, T. M., Park, S. H., ... & Thompson, T. C. (1998). Elevated expression of caveolin is associated with prostate and breast cancer. *Clinical Cancer Research*, *4*(8), 1873-1880.

Yang, L., & Scarlata, S. (2017). Super-resolution visualization of caveola deformation in response to osmotic stress. Journal of Biological Chemistry, 292(9), 3779-3788.

Yang, L., & Scarlata, S. (2017). Super-resolution visualization of caveola deformation in response to osmotic stress. Journal of Biological Chemistry, 292(9), 3779-3788. Le Lan, C., Neumann, J.-M., and Jamin, N. (2006). Role of the membrane interface on the conformation of the caveolin scaffolding domain: a CD and NMR study. FEBS Lett. *580*, 5301–5305.

Yang X, Ren H, Yao L, Chen X, He A. Role of EHD2 in migration and invasion of human breast cancer cells. Tumour Biol. 2015 May;36(5):3717-26.

Yeow, I., Howard, G., Chadwick, J., Mendoza-Topaz, C., Hansen, C. G., Nichols, B. J., & Shvets, E. (2017). EHD proteins cooperate to generate caveolar clusters and to maintain caveolae during repeated mechanical stress. Current Biology, 27(19), 2951-2962.

Yoshimura, A. (1998). The CIS family: negative regulators of JAK–STAT signaling. *Cytokine & growth factor reviews*, *9*(3-4), 197-204.

You C, Marquez-Lago TT, Richter CP, et al. Receptor dimer stabilization by hierarchical plasma membrane microcompartments regulates cytokine signaling. Sci Adv. 2016;2(12):e1600452. Published 2016 Dec 2. doi:10.1126/sciadv.1600452

Yu J, Bergaya S, Murata T, Alp IF, Bauer MP, Lin MI, Drab M, Kurzchalia TV, Stan RV, Sessa WC. Direct evidence for the role of caveolin-1 and caveolae in mechanotransduction and remodeling of blood vessels. J Clin Invest. 2006 May;116(5):1284-91.

Yu H, Mouw JK, Weaver VM. Forcing form and function: biomechanical regulation of tumor evolution. *Trends Cell Biol*. 2011;21(1):47-56.

Zanin N, Viaris de Lesegno C, Lamaze C, Blouin CM. Interferon Receptor Trafficking and Signaling: Journey to the Cross Roads. Front Immunol. 2021 Jan 20; 11:615603.

Zemel, A., Bischofs, I. B., & Safran, S. A. (2006). Active elasticity of gels with contractile cells. *Physical review letters*, *97*(12), 128103.

Zemel, A., Rehfeldt, F., Brown, A. E. X., Discher, D. E., & Safran, S. A. (2010). Cell shape, spreading symmetry, and the polarization of stress-fibers in cells. *Journal of Physics: Condensed Matter*, *22*(19), 194110.

Zhang, J. G., Farley, A., Nicholson, S. E., Willson, T. A., Zugaro, L. M., Simpson, R. J., ... & Baca, M. (1999). The conserved SOCS box motif in suppressors of cytokine signaling binds to elongins B and C and may couple bound proteins to proteasomal degradation. *Proceedings of the National Academy of Sciences*, *96*(5), 2071-2076.

Zhang, S. Y., Boisson-Dupuis, S., Chapgier, A., Yang, K., Bustamante, J., Puel, A., ... & Casanova, J. L. (2008). Inborn errors of interferon (IFN)-mediated immunity in humans: insights into the respective roles of IFN-α/β, IFN-γ, and IFN-λ in host defense. *Immunological reviews*, *226*(1), 29-40.

Zhao, Y. Y., Liu, Y., Stan, R. V., Fan, L., Gu, Y., Dalton, N., ... & Chien, K. R. (2002). Defects in caveolin-1 cause dilated cardiomyopathy and pulmonary hypertension in knockout mice. *Proceedings of the National Academy of Sciences*, *99*(17), 11375-11380.

Zheng, Q., Han, L., Dong, Y., Tian, J., Huang, W., Liu, Z., ... & Ren, H. (2014). JAK2/STAT3 targeted therapy suppresses tumor invasion via disruption of the EGFRvIII/JAK2/STAT3 axis and associated focal adhesion in EGFRvIII-expressing glioblastoma. *Neuro-oncology*, *16*(9), 1229-1243.

Zhou, Y. J., Chen, M., Cusack, N. A., Kimmel, L. H., Magnuson, K. S., Boyd, J. G., ... & O'Shea, J. J. (2001). Unexpected effects of FERM domain mutations on catalytic activity of Jak3: structural implication for Janus kinases. *Molecular cell*, *8*(5), 959-969.

Zhou J, Li YS, Chien S. Shear stress-initiated signaling and its regulation of endothelial function. Arterioscler Thromb Vasc Biol. 2014 Oct;34(10):2191-8.

Zhu, T., Goh, E. L., & Lobie, P. E. (1998). Growth hormone stimulates the tyrosine phosphorylation and association of p125 focal adhesion kinase (FAK) with JAK2: FAK is not required for STAT-mediated transcription. *Journal of Biological Chemistry*, *273*(17), 10682-10689.

Zhu, C., Bao, G., & Wang, N. (2000). Cell mechanics: mechanical response, cell adhesion, and molecular deformation. *Annual review of biomedical engineering*, *2*(1), 189-226.

Zimmerberg, J., & Kozlov, M. M. (2006). How proteins produce cellular membrane curvature. *Nature reviews Molecular cell biology*, *7*(1), 9-19.

Zou, Y., Akazawa, H., Qin, Y., Sano, M., Takano, H., Minamino, T., ... & Komuro, I. (2004). Mechanical stress activates angiotensin II type 1 receptor without the involvement of angiotensin II. *Nature cell biology*, *6*(6), 499-506.

université PARIS-SACLAY

ÉCOLE DOCTORALE
Signalisations et réseaux intégratifs en biologie (BIOSIGNE)

Titre : Contrôle à distance de la mechano-signalisation JAK-STAT par les cavéoles

Mots clés : cavéoles, JAK/STAT, signalisation, mechanotransduction, cancer

Résumé : La membrane plasmique de la plupart des cellules eucaryotes possède des nanodomaines lipidiques invaginés spécialisés appelés cavéoles. Comme les puits recouverts de clathrine, les cavéoles possèdent un manteau caractéristique composé de protéines essentielles comprenant les cavéolines et les cavines [Parton et Simons 2007, Parton et del Pozo 2013, Lamaze et. al 2017]. En plus d'être impliquées dans des fonctions cellulaires importantes telles que la transcytose, l'homéostasie lipidique, l'endocytose et la signalisation, le rôle protecteur des cavéoles dans le maintien de l'intégrité de la membrane plasmique dans des conditions de stress mécanique a récemment été démontré [Sinha et al. 2011]. Les cavéoles agissent comme des « réservoirs membranaires » qui peuvent s'aplatir en démantelant leur manteau protéique et ainsi amortir les variations de tension membranaire résultant des contraintes mécaniques. Après l'aplatissement des cavéoles, cavéolines et leurs protéines d'enveloppe sont libérées et cet événement a été supposé être impliqué dans la transduction du signal en aval [Nassoy et Lamaze 2012]. Le but de mon travail de thèse était de décrypter le contrôle précis de la signalisation par la mécanique des cavéoles.

Nous avons donc essayé de disséquer la mécanotransduction cavéolaire en élucidant les événements moléculaires sous-jacents au contrôle de la signalisation JAK-STAT par le désassemblage des cavéoles. En combinant l'imagerie à super résolution à l'analyse de réseaux par apprentissage automatique (machine learning), nous montrons qu'en réponse à un stress mécanique, les cavéoles se fragmentent en assemblages plus petits (également appelés cavéoline-1 (Cav1) non cavéolaires) qui présentent une augmentation de leur mobilité au niveau de la membrane plasmique. En outre, nous avons constaté que Cav-1 régule négativement la phosphorylation de STAT3 dépendante de la kinase JAK1. De plus, nous avons observé l'interaction entre Cav1 et JAK1 qui augmente lors d'un stress mécanique plus important et qui est médiée par le domaine d'échafaudage de la cavéoline (CSD). L'ensemble de nos résultats démontrent que les cavéoles peuvent agir comme des organites de mécano-signalisation avec la capacité de contrôler à distance la transduction du signal en aval de la membrane plasmique.

Title : Remote control of JAK/STAT signaling through caveolae mechanics

Keywords : caveolae, JAK/STAT, signaling, mechanotransduction, cancer

Abstract : The plasma membrane of most eukaryotic cells possess specialized invaginated lipid nanodomains called caveolae. Like clathrin coated pits, caveolae possess a characteristic coat composed of a suite of essential proteins including caveolins and cavins [Parton and Simons 2007, Parton and del Pozo 2013, Lamaze et al. 2017]. In addition to being implicated in important cellular functions such as transcytosis, lipid homeostasis, endocytosis and signaling, caveolae have been recently shown to demonstrate a protective role in maintaining the integrity of the plasma membrane under conditions of mechanical stress [Sinha et al. 2011]. The caveolar pits act as 'membrane reservoirs' that can flatten out by disassembling their coat and thereby buffer the membrane tension variations resulting from mechanical stress. Following caveolae flattening, caveolins and the caveolar coat proteins are released and this event has been hypothesized to be involved in downstream signal transduction [Nassoy and Lamaze 2012]. The goal of my thesis work was to unravel the precise control of signaling by caveolae mechanics.

Here we tried to dissect mechanotransduction through caveolae by elucidating the molecular events underlying the control of JAK-STAT signaling through disassembly of caveolae. Using state-of-the-art super resolution imaging combined with machine-learning network analysis, we show that in response to mechanical stress, caveolae disassemble into so-called smaller scaffolds (also known as non-caveolar caveolin-1 (Cav1) which display increased mobility at the plasma membrane. In addition, we found that Cav-1 negatively regulates JAK1 kinase dependent STAT3 phosphorylation. Furthermore, we revealed the interaction between Cav1 and JAK1 which increases upon an increase in mechanical stress and is mediated by the caveolin scaffolding domain (CSD). Taken together, our results demonstrate that caveolae can act as mechano-signaling organelles with an ability to remotely control downstream signal transduction from the PM.

Maison du doctorat de l'Université Paris-Saclay
2ème étage aile ouest, Ecole normale supérieure Paris-Saclay
4 avenue des Sciences,
91190 Gif sur Yvette, France